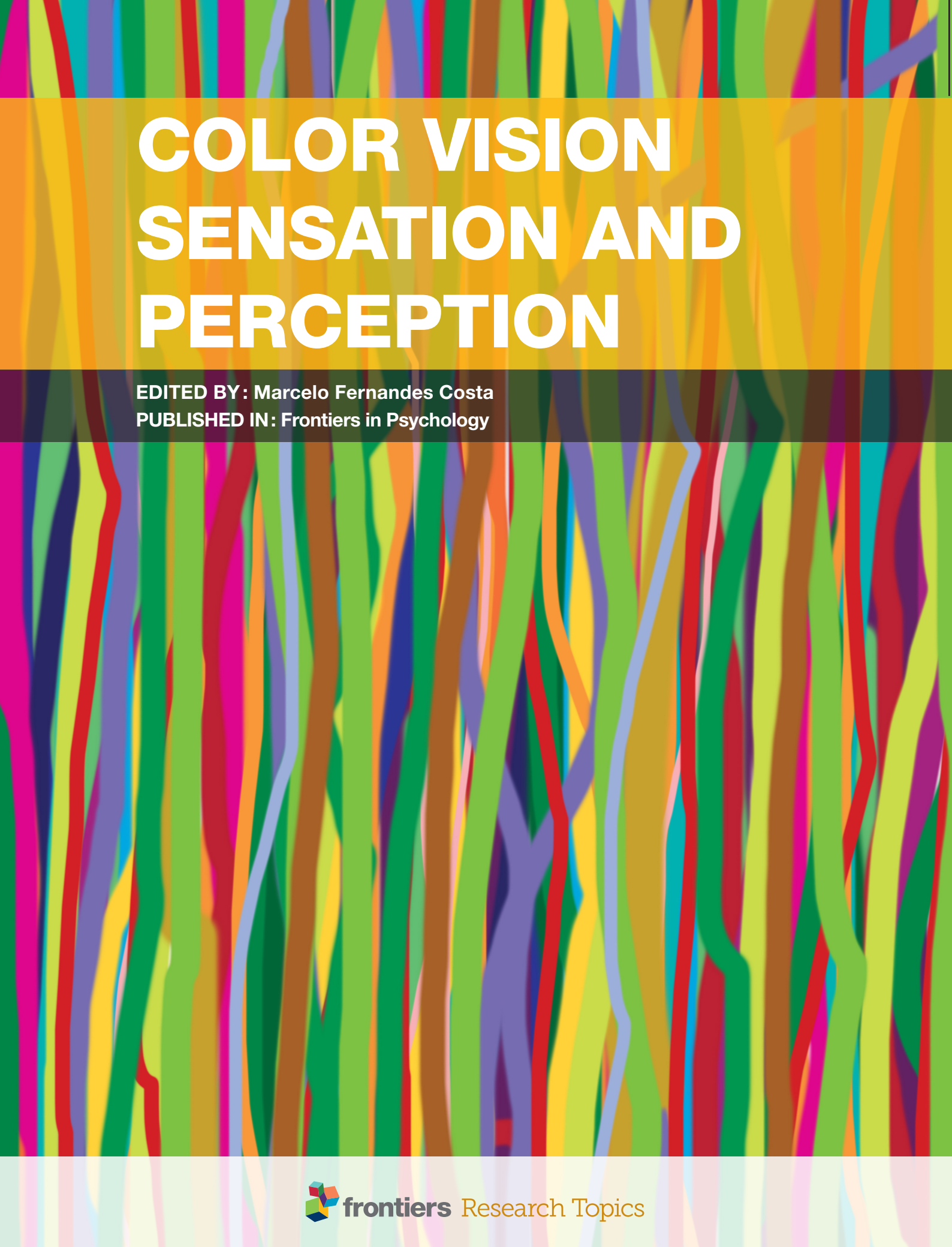

COLOR VISION SENSATION AND PERCEPTION

EDITED BY: Marcelo Fernandes Costa
PUBLISHED IN: Frontiers in Psychology

frontiers Research Topics

frontiers

ISSN 1664-8714
ISBN 978-2-88919-960-0
DOI 10.3389/978-2-88919-960-0

About Frontiers

Frontiers is more than just an open-access publisher of scholarly articles: it is a pioneering approach to the world of academia, radically improving the way scholarly research is managed. The grand vision of Frontiers is a world where all people have an equal opportunity to seek, share and generate knowledge. Frontiers provides immediate and permanent online open access to all its publications, but this alone is not enough to realize our grand goals.

Frontiers Journal Series

The Frontiers Journal Series is a multi-tier and interdisciplinary set of open-access, online journals, promising a paradigm shift from the current review, selection and dissemination processes in academic publishing. All Frontiers journals are driven by researchers for researchers; therefore, they constitute a service to the scholarly community. At the same time, the Frontiers Journal Series operates on a revolutionary invention, the tiered publishing system, initially addressing specific communities of scholars, and gradually climbing up to broader public understanding, thus serving the interests of the lay society, too.

Dedication to Quality

Each Frontiers article is a landmark of the highest quality, thanks to genuinely collaborative interactions between authors and review editors, who include some of the world's best academicians. Research must be certified by peers before entering a stream of knowledge that may eventually reach the public - and shape society; therefore, Frontiers only applies the most rigorous and unbiased reviews.
Frontiers revolutionizes research publishing by freely delivering the most outstanding research, evaluated with no bias from both the academic and social point of view.
By applying the most advanced information technologies, Frontiers is catapulting scholarly publishing into a new generation.

What are Frontiers Research Topics?

Frontiers Research Topics are very popular trademarks of the Frontiers Journals Series: they are collections of at least ten articles, all centered on a particular subject. With their unique mix of varied contributions from Original Research to Review Articles, Frontiers Research Topics unify the most influential researchers, the latest key findings and historical advances in a hot research area! Find out more on how to host your own Frontiers Research Topic or contribute to one as an author by contacting the Frontiers Editorial Office: **researchtopics@frontiersin.org**

COLOR VISION SENSATION AND PERCEPTION

Topic Editor:
Marcelo Fernandes Costa, Universidade de São Paulo, Brazil

The Rainbow Lines II. Digital Painting using blind layers technique by Marcelo F. Costa, 2104. Original size 50x80 inches

Color vision is considered a microcosm of the visual science. Special physiological and psychological processes make this scientific topic an intriguing and complex research field that can aggregates around molecular biologists, neurophysiologists, physicists, psychophysicists and cognitive neuroscientists. Our purpose is to present the frontier knowledge of this area of visual science, showing, in the end, the future prospects of application and basic studies of color perception.

Citation: Costa, M. F., ed. (2016). Color Vision Sensation and Perception. Lausanne: Frontiers Media. doi: 10.3389/978-2-88919-960-0

Table of Contents

Section Color Naming and Gender

frontiers in Psychology

EDITORIAL
published: 19 July 2016
doi: 10.3389/fpsyg.2016.01084

Editorial: Color Vision Sensation and Perception

Marcelo F. Costa[1,2]*

[1] Departamento de Psicologia Experimental, Instituto de Psicologia, Universidade de São Paulo, São Paulo, Brasil, [2] Núcleo de Neurociências e Comportamento e Neurociências Aplicada, Universidade de São Paulo, São Paulo, Brasil

Keywords: color discrimination, congenital color blindness, luminance, mesopic vision, scotopic vision, clinical psychophysics, perceptual organization, color naming

The Editorial on the Research Topic

Color Vision Sensation and Perception

Color vision is one of the most intriguing phenomena of the visual experience and has been the object of study from vision scientists to philosophers of perception. The wavelengths, their intensity and purity are experienced as hue, brightness and saturation based on complex information processing of the light entering the eyes. This special research topic is devoted to covering from basic aspects based on light and retinal processes to perceptual and cognitive mechanisms and their respective applications in clinical settings.

The reader will find a series of papers organized in two chapters, one devoted to the more basic phenomena and processing, the other focused on the more cognitive and cultural aspects.

The integrative aspect of luminance in color vision starts our journey. Reduction in number of levels of luminance in pseudoisochromatic stimulations affects the chromaticity thresholds measured psychophysically, suggesting interactions between luminance and color in those stimuli with luminance steps lower than seven (Souza et al.). Color sensation was also investigated under low-light levels. Mesopic and scotopic conditions could be considered an interference zone for color vision since rods activities generate physiological interferences in cone-driven retinal chromatic pathways. This review paper keeps us up to date regarding the range and impact of rod–cone interactions on human visual function and performance (Zele and Cao).

Clinical applications centered on congenital color blindness end the first chapter. Sensory psychophysical thresholds on the tritanopic color confusion axis were investigated in protanomalous and deuteranomalous subjects (Costa et al.). Reduction in discrimination was found for both types of congenital color blindness, protanomalous and deuteranomalous, but subjects in the latter group showed worse results. Electrophysiological assessments regarding luminance and compound stimuli (luminance plus red-green stimulus) were also evaluated in congenital color blindness subjects. Since compound stimuli elicited small or no response in red-green congenital color blinds, this finding could indicate that the cortical response for compound stimuli in the present experiment was dominated by chromatic contribution (Risuenho et al.).

A search for discrimination thresholds addressed using the pseudoisochromatic plates configures a new psychophysical application for the traditional and widely used color test (Jurasevska et al.).

Basic perceptual phenomena of Gestalt theories regarding color vision were addressed using figure-ground perception on saturation and contrast polarity modulations. The study conducted by Dresp-Langley and Reeves investigated the lightness dependency of the achromatic loci in color space. The results pointed toward a hitherto undocumented functional role of color saturation in the genesis of form, and in particular figure-ground percepts. Two experiments conducted by

OPEN ACCESS

Edited and reviewed by:
Rufin VanRullen, Centre de Recherche Cerveau et Cognition, France

***Correspondence:**
Marcelo F. Costa
costamf@usp.br

Specialty section:
This article was submitted to Perception Science, a section of the journal Frontiers in Psychology

Received: *20 April 2016*
Accepted: *04 July 2016*
Published: *19 July 2016*

Citation:
Costa MF (2016) Editorial: Color Vision Sensation and Perception. Front. Psychol. 7:1084. doi: 10.3389/fpsyg.2016.01084

Kuriki showed that first, a color-appearance space normalized to daylight may be defined for the human visual system and second, that color space could reduce the discrepancy between the achromatic loci and the lightness axis of the color appearance models. The last study of the perceptual mechanism section relates retinal image quality for the display red and blue pixel radiation with the chromostereopsis retinal disparity achieved (Ozolinsh and Muizniece).

Color is also important from an anthropological view in which a long debate regarding the existence of natural categories of hue and their universality has been addressed by ethological, electrophysiological, behavioral and psychophysical perspectives. The color naming and gender section presents contributions regarding the variations in color naming occurring in congenital color blindness subjects and the gender and cultural aspects related to color preferences. The study of Nagy et al. shows that dichromatic subjects involve the brightness properties of the different spectral stimuli when judging their chromatic content and that at the shorter wavelengths the signal of the intact tritos photoreceptor dominates the decision making in color naming tasks, even for the anopes. Al-Rasheed provides evidence that both sex differences and cultural differences are relevant in hue preference in terms of how stimulus-background cone-contrast was weighted summarizing color preference quantitatively rather than using subjective color names.

The question of how we see colors and how we can discuss their impact in many dimensions of our life is an actual and multidiscipline inquiry to which we hope to contribute with this special research topic.

Enjoy this special topic on color vision.

AUTHOR CONTRIBUTIONS

The author confirms being the sole contributor of this work and approved it for publication.

FUNDING

Supported by Conselho Nacional de Desenvolvimento Científico Edital Universal 440357/2014-4. MFC is a level 2 research fellow.

ACKNOWLEDGMENTS

I would like to thank Professors Dora Fix Ventura and Luiz Carlos de Lima Silveira for their support and encouragement to carry out this Special Topic in Color Vision.

Conflict of Interest Statement: The author declares that the research was conducted in the absence of any commercial or financial relationships that could be construed as a potential conflict of interest.

frontiers in
PSYCHOLOGY

ORIGINAL RESEARCH ARTICLE
published: 23 December 2014
doi: 10.3389/fpsyg.2014.01291

Low number of luminance levels in the luminance noise increases color discrimination thresholds estimated with pseudoisochromatic stimuli

Givago S. Souza[1,2], Felecia L. Malone[3], Teera L. Crawford[4], Letícia Miquilini[1], Raílson C. Salomão[1], Diego L. Guimarães[1], Dora F. Ventura[5], Malinda E. C. Fitzgerald[3,6] and Luiz Carlos L. Silveira[1,2]*

[1] Instituto de Ciências Biológicas, Universidade Federal do Pará, Belém, Brazil
[2] Núcleo de Medicina Tropical, Universidade Federal do Pará, Belém, Brazil
[3] Department of Biology, University of Memphis, Memphis, TN, USA
[4] College of Medicine, University of Tennessee Health Science Center, Memphis, TN, USA
[5] Instituto de Psicologia, Universidade de São Paulo, São Paulo, Brazil
[6] Department of Anatomy and Neurobiology, University of Tennessee Health Science Center, Memphis, TN, USA

Edited by:
Laurence T. Maloney, Stanford University, USA

Reviewed by:
Rocco Palumbo, Schepens Eye Research Institute – Harvard Medical School, USA
Mirella Telles Salgueiro Barboni, University of São Paulo, Brazil

***Correspondence:**
Luiz Carlos L. Silveira, Núcleo de Medicina Tropical, Universidade Federal do Pará, Avenida Generalíssimo Deodoro 92 (Umarizal), 66055-240 Belém, PA, Brazil
e-mail: luiz@ufpa.br

In pseudoisochromatic stimuli the presence of spatial and luminance noise forces the subject to discriminate the target from the background solely on the basis of chromaticity difference. Color-blind subjects may show difficulty to identify the target due to the elimination of borders and brightness clues caused by the luminance and spatial noise. Few studies have fully described the features of pseudoisochromatic stimuli. Fewer investigators have focused their studies in the effects of specific pseudoisochromatic parameters on color discrimination. We used the Cambridge Color Test (CCT) to investigate the influence on color discrimination thresholds due to the number of luminance levels present in the luminance noise. The CCT default has six luminance steps; however, in our investigation a total of eight different conditions were tested from 2 to 16 luminance steps. It was found that the CCT provided very robust values for color discrimination thresholds, which were degraded only for very small number of luminance steps. When the number of steps was increased, the color discrimination thresholds improved from 2 to 6 luminance steps and gradually reached a plateau for 10 or more luminance steps. The area of color discrimination ellipses as a function of luminance steps matches the relative proportion of ineffective contrasts between mosaic patches as a function of luminance steps, assuming that contrast becomes ineffective for values 18.6% or less. The lower number of color and luminance interactions in these conditions could explain the measured increase of color discrimination thresholds. The primary conclusion from this investigation was that results from pseudoisochromatic tests should have their parameters described in more detail. This type of description would allow a better understanding of the results provided, interpretations, and therefore cross study comparison of results obtained from different laboratories.

Keywords: pseudoisochromatic stimulus, compound stimulus, color-luminance interaction, Cambridge Color Test, color vision, P pathway

INTRODUCTION

Deficiencies in color vision decrease the ability to discriminate certain colors under specific circumstances. The inability to discriminate colors can result in visual problems in daily life. Full characterization of color vision deficiency would allow subjects with decreased color discrimination to potentially conduct necessary adjustments to their visual deficiencies and live a more normal life. Testing for color vision deficiencies may identify the existence, type, and severity of defects, providing a basis for the evaluation of the defect's impact on personal and professional performance (Dain, 2004).

Multiple types of visual testing exist that are used to measure the level of color perception, including pseudoisochromatic plate tests (Birch, 2001). Pseudoisochromatic plates employ targets broken into patches of a given chromaticity embedded in a background of patches of different chromaticity, but the two sets of patches – those that compose the target and those that compose the background – vary in size and luminance, to isolate and measure the subject's color discrimination performance (Mollon, 2003).

The pseudoisochromatic tests were developed based on the suggestions of Jakob Stilling (1842–1915) to eliminate the edges between target and background by breaking the stimulus into a mosaic with patches of different sizes (spatial noise) and brightness (luminance noise). One major aspect of pseudoisochromatic stimuli is that the presence of spatial and luminance noise requires the subject to heavily rely on chromatic signals to differentiate the target from its background (Mollon and Reffin, 1989; Regan et al., 1994).

The first pseudoisochromatic test to become largely used, named for Shinobu Ishihara (1879–1963), was introduced in the early 1900s to identify deficiencies in red–green color vision (Heidary and Gharebaghi, 2013). Although the Ishihara test is still widely used, it failed to properly categorize many defects of color vision, especially those of tritan category (Aarnisalo, 1979). The American Optical Hardy-Rand-Rittler (AOHRR) test was produced in several versions during the mid and late 1900s due to issues with the saturation of red and green plates. This test distinguished between protans and deutans with difficulties, because it did not contain a sufficiently large range of weak and strong stimuli to correctly identify the specific color vision defect (Walls, 1959). The Standard Pseudoisochromatic Plates (SPP) test is presented either in a version for congenital visual defects (SPP-C) or another version for acquired visual defects (SPP-A), but it is more affected by the duration per test item and viewing distance than other pseudoisochromatic tests such as the Ishiara test and the City University Color Vision Test (CUCVT; Somerfield et al., 1989; Dain, 2004).

Although there is wide use of pseudoisochromatic stimuli in color vision investigation, few studies have focused on how the features of the stimuli themselves could influence the visual perception. Most studies focused on the test conditions such as illuminance of the stimulus plates, viewing distance, and exposure time (Long et al., 1984; Somerfield et al., 1989). These conditions have been found to significantly affect individual performance on visual screening tests. The administration of multiple and/or different plate tests may require viewing conditions within certain standards in order to ensure test validity and comparability (Long et al., 1985). It has been observed that patients with low visual acuity had a high rate of recognition with utilization of the Ishihara plates in color discrimination tests (Gordon and Field, 1978). These authors suggested that the elimination of high spatial frequency information, by the low visual acuity, might explain the better performance of the subjects (Gordon and Field, 1978). Taylor and Woodhouse showed that blurring could also improve the recognition and therefore discrimination performance using pseudoisochromatic plates in deutans (Taylor and Woodhouse, 1979).

Examples of studies that investigated how specific features of the pseudoisochromatic stimuli could potentially influence visual perception were those that provided the basis for the development of Cambridge Color Test (CCT; Mollon and Reffin, 1989; Reffin et al., 1991; Regan et al., 1994). Mollon and Reffin (1989) used pseudoisochromatic stimuli and modulated the target chromaticity along several axes of the chromaticity diagram using a staircase method. The procedure allowed them to estimate several color discrimination thresholds around a given chromaticity locus and to plot the corresponding MacAdam ellipse. They observed that color discrimination ellipses of trichromats and dichromats corresponded well to the color vision genotype of the subjects. Normal data for color discrimination using the CCT have been published by Ventura et al. (2003), Paramei (2012), and Paramei and Oakley (2014). Other investigatiors have applied similar paradigms to investigate color discrimination in both children and non-human primates (Mancuso et al., 2006; Goulart et al., 2008, 2013).

The amount of luminance noise represents an important parameter to characterize a pseudoisochromatic stimulus. Changes in the composition of the luminance noise might influence the visual perception of the target, because it can change the interaction of luminance and chromatic information in the visual scene (Switkes et al., 1988; Ingling and Grigsby, 1990; Logothetis et al., 1990; Gur and Akri, 1992; Clery et al., 2013). In the current study we investigated how the number of luminance levels in the luminance noise of pseudoisochromatic stimuli influenced the color discrimination ellipses.

MATERIALS AND METHODS

SUBJECTS

Nine subjects (25.67 ± 3.24 years old) were included in the current study. All subjects gave written consent to participate in the study. This study agreed with the tenets of the Declaration of Helsinki and it was approved by the Ethical Committee for Research in Humans, Tropical Medicine Nucleus, Federal University of Pará (Report #570.434) and the IRB at UTHSC. None of subjects had any history of ophthalmological, neurological, or systemic diseases that could affect visual performance. Verification of visual function was performed by an ophthalmologist that conducted the following initial examinations: ophthalmoscopic and retinoscopic exam, slit lamp exam of the eye media, refractive state measurement, Snellen visual acuity test, and Ishihara plate test. All subjects were monocularly tested and the eye with the highest Snellen visual acuity, based on prior initial ophthalmological examination, was the eye used for the pseudoisochromatic stimuli examination. All the subjects were normal regarding the results of ophthalmological exam, had normal or corrected to 20/20 visual acuity, and performed with no mistakes in the Ishihara's plate test.

STIMULATION

The stimuli were generated in a ViSaGe system (Cambridge Research System, CRS, Rochester, England, UK) and exhibited in a 21″ CRT display with high spatial, temporal, and chromatic resolution (1600 × 1200 pixels, 125 Hz, 14 bits, Mitsubishi, Tokyo, Japan). Luminance and chromaticity were measured and gamma-correction was performed to calibrate the monitor using a colorimeter ColorCal (CRS).

We used the CCT software (CCT, CRS) to estimate color discrimination ellipses around coordinates ($u' = 0.1977$, $v' = 0.4689$) of the CIE 1976 Color Space. Each stimulus was comprised of an assortment of discrete circular patches with their own random size and luminance. The minimum and maximum luminance values of the luminance noise were 8 and 18 cd/m^2, respectively. Embedded in this field of spatial and luminance noise there was a target with the shape of a Landolt's "C" formed by its own assortment of patches differing in chromaticity from those of the background (Regan et al., 1994). Subjects were placed 3.25 meters away from the monitor in a dark room. At this distance, the Landolt's "C" gap, outer diameter, and inner diameter measured 1, 4.3, and 2.2° of visual angle, respectively. The stimulus was shown for 3 sec. The target chromaticity was modulated along eight chromatic vectors radiating from the background chromaticity.

PSYCHOPHYSICAL PROCEDURES

The CCT uses a four-alternative forced choice staircase to estimate color discrimination thresholds along each chromatic vector. The subject's task was to identify the orientation of the Landolt's "C" gap (up, down, left, or right). The subject's response was recorded using a four-button response box (CB6, CRS). Each correct response resulted in a decrease of the chromatic vector and an error resulted in an increase of the chromatic vector.

The determination of the color discrimination ellipse was performed under eight different luminance step conditions: 2, 4, 6, 8, 10, 12, 14, and 16 (**Figure 1**). The luminance steps refer to the number of equally spaced luminance levels randomly distributed in the luminance noise range of the CCT stimulation. For all participants, eight different stimulus conditions were shown, each one with a different number of luminance levels in the luminance noise. For every stimulus condition, we estimated the color discrimination thresholds along eight different chromatic axes. The tests were performed twice with sections occurring separately in three different days. The stimulus conditions testing always started in the luminance step 2 and ended with luminance step 16.

DATA ANALYSIS

An ellipse function was fitted to the eight color discrimination thresholds using the Khachiyan Ellipsoid Method (Khachiyan, 1979) implemented with Matlab R2013a routines (Mathworks, Natick, MA, USA). We calculated the area, major axis, and minor axis of the ellipses, and lengths of protan, deutan, and tritan vectors. These values were taken as parameters to compare color discrimination across different stimulus conditions. Subjects sequentially repeated the whole test twice and the results were averaged for each subject along the eight vectors. All the results were analyzed and presented as "grand means" for the group of nine subjects altogether.

For each subject, data of each parameter were divided by the maximum value to normalize the results across all testing conditions. The one-way ANOVA followed by Tukey *post hoc* test was used to compare the results ($\alpha = 0.05$).

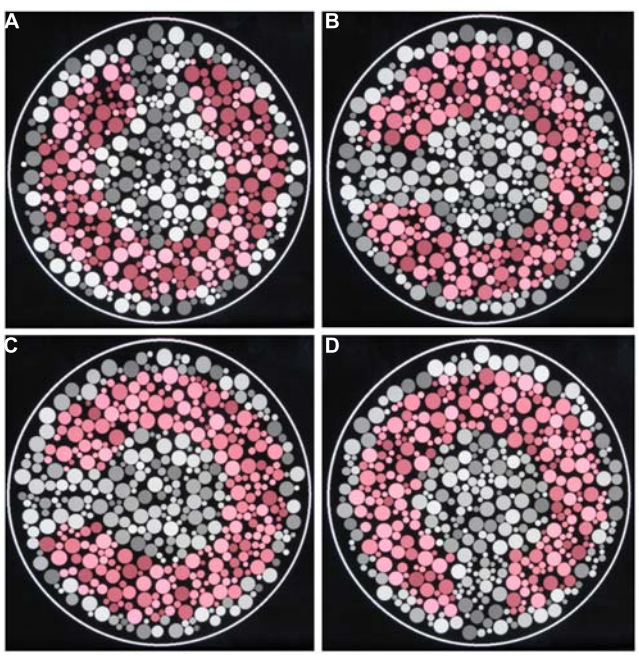

FIGURE 1 | Pseudoisochromatic stimuli used in this work. (A–D) Four different categories of luminance levels in the luminance noise: 2, 6, 10, and 16 luminance levels.

RESULTS

Figure 2 shows the mean color discrimination ellipses in the CIE1976 Color Space for test conditions with 2, 6, 10, and 16 luminance levels in the luminance noise. Visual inspection reveals that the mean ellipse estimated with two luminance levels in the luminance noise (**Figure 2A**) had a larger area than the mean ellipses estimated with 6, 10, or 16 luminance levels on the luminance noise (**Figures 2B–D**).

Figure 3 summarizes all the statistical comparisons between the parameters for each test condition. All the parameters for ellipses obtained with two luminance levels in the luminance noise were larger than those for other seven combinations of luminance levels. However, statistical significance was reached only in few comparisons for one-dimensional parameters. There were no statistically significant differences for the comparisons between major semi-axis lengths estimated from the eight-luminance step conditions.

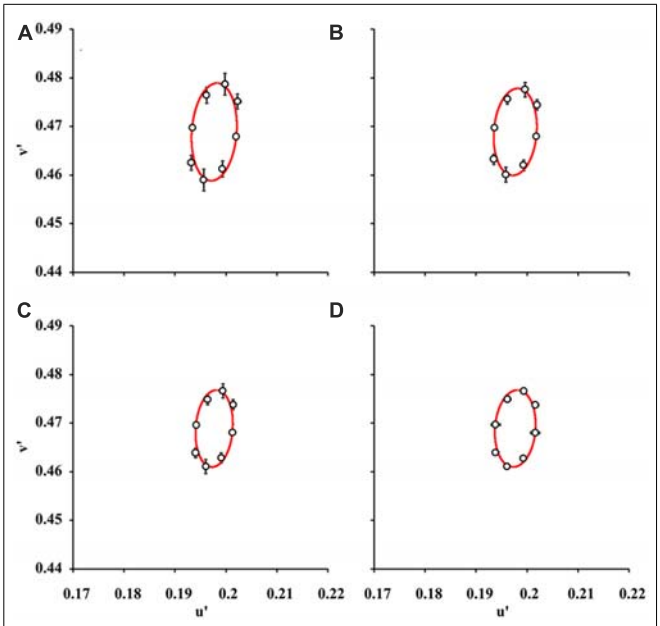

FIGURE 2 | Mean color discrimination ellipses for various degrees of luminance noise. The data points and bars represent "grand means" and standard deviations for color discrimination thresholds in the CIE 1976 Color Space from nine subjects. Data points were fitted by ellipses estimated by using pseudoisochromatic stimuli with 2 **(A)**, 6 **(B)**, 10 **(C)**, and 16 **(D)** luminance levels in the luminance noise. The color discrimination thresholds obtained with two luminance levels in the luminance noise were higher than in any other conditions ($p < 0.05$, one-way ANOVA followed by Tukey *post hoc* test) and consequently the ellipse in **(A)** is larger than all other ellipses.

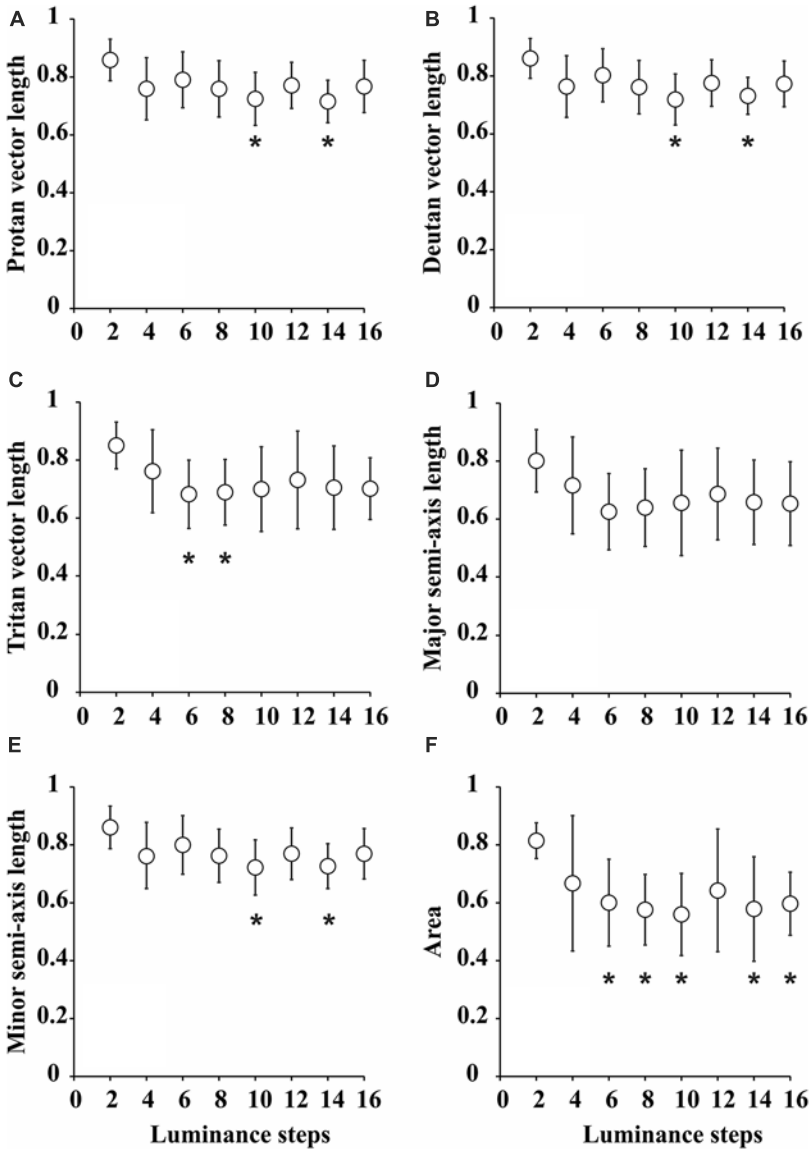

FIGURE 3 | Statistical comparisons between the parameters of color discrimination ellipses for various degrees of luminance noise. (A) Protan vector length. **(B)** Deutan vector length. **(C)** Tritan vector length. **(D)** Major semi-axis length. **(E)** Minor semi-axis length. **(F)** Ellipse area. Values were "grand-means" for nine subjects that performed the tests twice and were averaged for each individual. Generally, all the parameters were larger for pseudoisochromatic tests performed with two luminance levels in the luminance noise, but only attained statistical significance level in a few comparisons for protan vector length [$F(7,136) = 2.2$, $p < 0.05$, $\eta^2 = 0.69$], deutan vector length [$F(7,136) = 2.3$, $p < 0.05$, $\eta^2 = 0.7$], tritan vector length [$F(7,136) = 2.43$, $p < 0.05$, $\eta^2 = 0.71$], and minor semi-axis length [$F(7,136) = 2.1$, $p < 0.05$, $\eta^2 = 0.77$]. For ellipses areas, most of comparisons were statistically significant. *$p < 0.05$, one-way ANOVA followed by Tukey *post hoc* test.

The comparisons between the minor semi-axis lengths, protan vector lengths, deutan vector lengths, and tritan vector lengths resulted in statistically significant differences only in a few cases identified with asterisks in the plots.

We found that ellipse area was the best parameter that discriminated between different the test conditions. The ellipses for two luminance levels in the luminance noise had areas (0.81 ± 0.06) larger than for all other conditions and it was statistically significant larger [$F(7,136) = 3.29$, $p < 0.05$, $\eta^2 = 0.69$] in the comparison with ellipses for 6 (0.60 ± 0.15), 8 (0.58 ± 0.12), 10 (0.56 ± 0.14), 14 (0.58 ± 0.18), and 16 (0.60 ± 0.11) luminance levels in the luminance noise.

DISCUSSION

The luminance noise is an important feature of pseudoisochromatic tests. It is used to avoid borders and contrast between contiguous regions of the stimulus that would base the discrimination between target and background on cues other than chromatic differences. We found that decreasing the number of luminance levels composing the luminance noise impaired the

color discrimination of trichromats, especially for very low numbers: two luminance levels resulted in larger ellipse areas; longer major semi-axes; longer minor semi-axes; and longer protan, deutan, and tritan vectors. That is, worse color discrimination thresholds were observed when compared to conditions with more luminance levels in the luminance noise.

The discrimination between target and background in pseudoisochromatic stimuli might be influenced by interaction between luminance and color information. Natural scenes are composed of both spatial and temporal mixture of color and luminance information, raising an interest in determining how these aspects are processed and discriminated within the visual system. Some authors suggested that the visual system performs an independent (orthogonal) and parallel processing of color and luminance (Livingstone and Hubel, 1987). This is supported by a scope of psychophysical and physiological data that showing distinct spatial and temporal properties of both the luminance and color channels (Wilson and Wilkinson, 2004; Solomon and Lennie, 2007). Others have suggested that the luminance and chromatic contribution for a perceptual task are summed at higher levels of the visual cortex (Switkes et al., 1988; Ingling and Grigsby, 1990; Logothetis et al., 1990; Gur and Akri, 1992).

The luminance and chromatic contrast processing might not be totally independent and they might in fact exert an influence upon each other. It is possible that independent processing of luminance and color information occurs only at the very early stages of the visual processing; however, it has been shown that many types of cells in the retina, lateral geniculate nucleus, and V1 respond to color and luminance contrast with varied degrees of sensitivities (Kaplan et al., 1988; Lee et al., 1989a,b, 1990, 2011; Johnson et al., 2001; Horwitz and Albright, 2005; Nassi and Callaway, 2009; Li et al., 2014).

The color information seems to potentiate the luminance contrast perception. Improvement in the spatial contrast sensitivity, wavelength discrimination, reaction times, and stereo-vision due the interaction of both chromatic and luminance information have been previously reported (Ueno and Swanson, 1989; Jordan et al., 1990; Logothetis et al., 1990; Gur and Akri, 1992). Gur and Akri (1992) investigated human contrast sensitivity that was estimated by luminance, chromatic, and compound luminance plus chromatic sinusoidal gratings. They observed that the luminance contrast sensitivity was enhanced by the addition of color information and *vice versa*. These investigators suggested that there was an additive mechanism that supported the enhancement of the contrast detection. Troscianko et al. (1996) conducted studies on color discrimination of two achromatopsic subjects using both static and dynamic (25 Hz) chromatic stimuli with luminance noise. They observed that subjects had the color discrimination impaired with static noise, but had normal performance with dynamic noise. These authors suggested that color discrimination estimated by static luminance would be relied by a conscious and color opponent mechanism reflecting probably the activity of both parvo- and magnocellular pathways. The color discrimination estimated using dynamic luminance noise would be performed by an unconscious and non-opponent mechanism that could be represented by the activation of the either the magnocellular or koniocellular pathways.

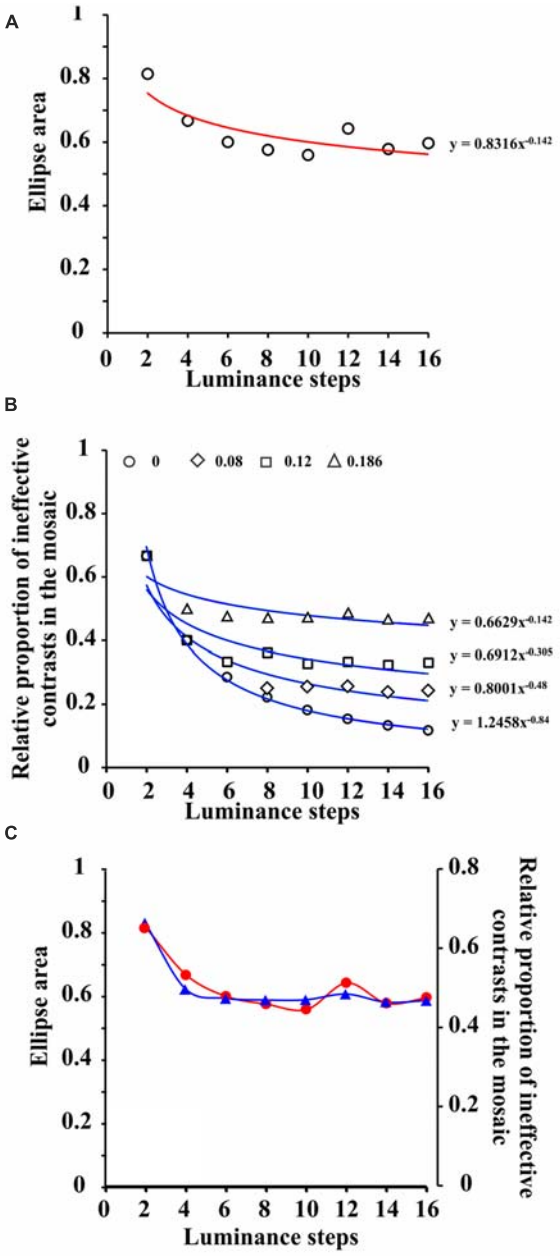

FIGURE 4 | Co-variation of the color discrimination ellipse areas and relative proportion of ineffective contrasts present in the mosaic. (A) Area of color discrimination ellipses measured with pseudoisochromatic stimuli bearing progressive number of luminance steps in the luminance noise. Data points represent grand means (nine subjects, two measurements averaged for each individual) and were fitted with a power function. **(B)** Relative proportion of ineffective contrasts present in the mosaic of pseudoisochromatic stimuli as a function of number of luminance steps in the luminance noise. From top to bottom, the different groups of data points represent different values of Weber contrast threshold, and they were also fitted with power functions. Contrast threshold equal to 0.186 was fitted with a power function with the same exponent as the one for ellipses areas illustrated in **(A)**. **(C)** Data points for relative proportion of ineffective contrasts in the mosaic of pseudoisochromatic stimuli were vertically adjusted to fit the data points for color discrimination ellipse areas. The two sets of data points were connected with spline functions. (see text for further details).

The current study, the number of possible combinations of luminance contrasts between two neighbor circular patches in the pseudoisochromatic stimuli varied according to the number of luminance steps. In the pseudoisochromatic stimuli of this study, two neighboring circular patches could vary from presenting the same luminance levels (0 contrast) to presenting the minimum and maximum luminance levels for that particular condition (highest contrast). In this study, the highest contrast was obtained between patches with 8 and 18 cd/m^2 (Weber's contrast = 0.55). The higher the number of luminance levels in the noise, the higher the number of possible luminance contrasts between two circular patches within the mosaic.

It was hypothesized in the current study that not all possible luminance contrasts present within the mosaic could affect chromatic detection in the same amount and would explain the change in color discrimination threshold as a function of number of luminance steps in the luminance noise (**Figure 4A**). Low luminance contrasts do not have the same effect as high luminance contrasts to increase target chromatic integration since low contrasts may contribute little to the luminance noise. In order to find which luminance contrast could be the minimally effective contrast to modulate target integration, we estimated the relative proportion of ineffective luminance contrasts, present in each stimulus condition, assuming different contrast thresholds (**Figure 4B**). A Weber contrast threshold of 0.186 generates a relative proportion of ineffective contrasts, present in the mosaic, as a function of number of luminance steps in the luminance noise, which matches the color discrimination threshold as a function of number of luminance steps in the luminance noise (**Figure 4C**).

A Weber luminance contrast threshold equal to 0.186 is relatively high compared to the peak of human luminance contrast sensitivity, but it is compatible with a pathway of low luminance contrast sensitivity, such as the P cell pathway. P cell pathway could be an adequate candidate to integrate luminance contrast information and color contrast information in the perception of pseudoisochromatic stimuli, such as those used in the current study, since P cells are very sensitive to color contrast and relatively insensitive to luminance contrast (Kaplan and Shapley, 1986; Lee et al., 1989a,b, 1990, 2011).

CONCLUSION

The CCT is a robust color discrimination test, since the values it provides for color discrimination thresholds are relatively insensitive to luminance noise. We suggest that stimulus conditions with six or more luminance levels would be more appropriate to test and characterize vision disabilities with pseudoisochromatic stimuli such the one used in the CCT. A pathway with high chromatic contrast sensitivity and low luminance contrast sensitivity seems to mediate the subject response to CCT. Pseudoisochromatic tests should have all the parameters fully described to allow for better interpretation of the results they provide and a more straightforward comparison of obtained results in different laboratories under different conditions.

ACKNOWLEDGMENTS

This research was supported by the following grants: CNPq #486545/2012-1; FAPESP Thematic Project 08/58731-2; 2T37 MD 1378-13 NIH; and FINEP IBN Net #1723. Diego L. Guimarães received CNPq fellowship for non-graduate students. Letícia Miquilini received CAPES fellowship for graduate students. Luiz Carlos L. Silveira and Dora F. Ventura are CNPq research fellows.

REFERENCES

Aarnisalo, E. (1979). Screening of red-green defects of colour vision with pseudoisochromatic tests. *Acta Ophthalmol.* (*Copenh.*) 57, 397–408. doi: 10.1111/j.1755-3768.1979.tb01822.x

Birch, J. (2001). "Design of pseudoisochromatic plates," in *Diagnosis of Defective Colour Vision*, ed. J. Birch (Oxford: Butterworth-Heinemann), 41–44.

Clery, S., Bloj, M., and Harris, J. M. (2013). Interactions between luminance and color signals: effects on shape. *J. Vis.* 13, 16, 1–23, doi: 10.1167/13.5.16

Dain, S. (2004). Clinical colour vision tests. *Clin. Exp. Optom.* 87, 276–293. doi: 10.1111/j.1444-0938.2004.tb05057.x

Gordon, I., and Field, D. (1978). A possible explanation as to why the newly sighted commonly perform well on pseudoisochromatic colour vision tests. *Perception* 7, 119–122. doi: 10.1068/p070119

Goulart, P. R., Bandeira, M. L., Tsubota, D., Oiwa, N. N., Costa, M. F., and Ventura, D. F. (2008). A computer-controlled color vision test for children based on the Cambridge Colour Test. *Vis. Neurosci.* 25, 445–450. doi: 10.1017/S0952523808080589

Goulart, P. R., Bonci, D. M., Galvão, O. F., Silveira, L. C. L., and Ventura, D. F. (2013). Color discrimination in the tufted capuchin monkey, *Sapajus* spp. *PLoS ONE* 88:e62255. doi: 10.1371/journal.pone.0062255

Gur, M., and Akri, V. (1992). Isoluminant stimuli may not expose the full contribution of color to visual functioning: spatial contrast sensitivity measurements indicate interaction between color and luminance processing. *Vision Res.* 32, 1253–1262. doi: 10.1016/0042-6989(92)90220-D

Heidary, F., and Gharebaghi, R. (2013). A modified pseudoisochromatic Ishihara colour vision test based on eastern Arabic numerals. *Med. Hypothesis Discov. Innov. Ophthalmol.* 2, 83–85.

Horwitz, G. D., and Albright, T. D. (2005). Paucity of chromatic linear motion detectors in macaque V1. *J. Vis.* 5, 525–533.

Ingling, C. R., and Grigsby, S. S. (1990). Perceptual correlates of magnocellular and parvocellular channels: seeing form and depth in afterimages. *Vision Res.* 30, 823–828. doi: 10.1016/0042-6989(90)90051-L

Johnson, E. N., Hawken, M. J., and Shapley, R. (2001). The spatial transformation of color in the primary visual cortex of the macaque monkey. *Nat. Neurosci.* 4, 409–416. doi: 10.1038/86061

Jordan, J. R., Geisler, W. S., and Bovik, A. C. (1990). Color as a source of information in the stereo correspondence process. *Vision Res.* 30, 1955–1970. doi: 10.1016/0042-6989(90)90015-D

Kaplan, E., and Shapley, R. M. (1986). The primate retina contains two types of ganglion cells, with high and low contrast sensitivity. *Proc. Natl. Acad. Sci. U.S.A.* 83, 2755–2757. doi: 10.1073/pnas.83.8.2755

Kaplan, E., Shapley, R. M., and Purpura, K. (1988). Color and luminance contrast as tools for probing the primate retina. *Neurosci. Res. Suppl.* 8, S151–S165. doi: 10.1016/0921-8696(88)90014-X

Khachiyan, L. G. (1979). A polynomial algorithm in linear programming. *Sov. Math. Dokl.* 20, 191–194.

Lee, B. B., Martin, P. R., and Valberg, A. (1989a). Sensitivity of macaque retinal ganglion cells to chromatic and luminance flicker. *J. Physiol.* (*Lond.*) 414, 223–243.

Lee, B. B., Martin, P. R., and Valberg, A. (1989b). Nonlinear summation of M- and L-cone inputs to phasic retinal ganglion cells of the macaque. *J. Neurosci.* 9, 1433–1442.

Lee, B. B., Pokorny, J., Smith, V. C., Martin, P. R., and Valberg, A. (1990). Luminance and chromatic modulation sensitivity of macaque ganglion cells and human observers. *J. Opt. Soc. Am. A* 7, 2223–2236. doi: 10.1364/JOSAA.7.002223

Lee, B. B., Sun, H., and Valberg, A. (2011). Segregation of chromatic and luminance signals using a novel grating stimulus. *J. Physiol.* (*Lond.*) 589, 59–73. doi: 10.1113/jphysiol.2010.188862

Li, X., Chen, Y., Lashgari, R., Bereshpolova, Y., Swadlow, H. A., Lee, B. B., et al. (2014). Mixing of chromatic and luminance retinal signals in primate area V1. *Cereb. Cortex* doi: 10.1093/cercor/bhu002 [Epub ahead of print].

Livingstone, M. S., and Hubel, D. H. (1987). Psychophysical evidence for separate channels for the perception of form, color, movement, and depth. *J. Neurosci.* 7, 3416–3468.

Logothetis, N. K., Schiller, P. H., Charles, E. R., and Hurlbert, A. C. (1990). Perceptual deficits and the activity of the color-opponent and broad-band pathways at isoluminance. *Science* 247, 214–217. doi: 10.1126/science.2294602

Long, G., Lyman, B., Monaghan, E., Penn, D., Brochin, H., and Morano, E. (1984). Further investigation of viewing conditions on standard pseudoisochromatic tests. *Bull. Psychonom. Soc.* 22, 525–528. doi: 10.3758/BF03333897

Long, G., Lyman, B., and Tuck, J. (1985). Distance, duration, and blur effects on the perception of pseudoisochromatic stimuli. *Opthalmic Physiol. Opt.* 5, 185–194. doi: 10.1111/j.1475-1313.1985.tb00655.x

Mancuso, K., Neitz, M., and Neitz, J. (2006). An adaptation of the Cambridge Colour Test for use with animals. *Vis. Neurosci.* 23, 695–701. doi: 10.1017/S0952523806233364

Mollon, J. D. (2003). "The origins of modern color science," in *Color Science*, ed. S. Shevell (Washington, DC: Optical Society of America), 1–39.

Mollon, J. D., and Reffin, J. P. (1989). A computer-controlled colour vision test that combines the principles of Chibret and Stilling. *J. Physiol.* 414, 5P.

Nassi, J. J., and Callaway, E. M. (2009). Parallel processing strategies of the primate visual system. *Nat. Rev. Neurosci.* 10, 360–372. doi: 10.1038/nrn2619

Paramei, G. V. (2012). Color discrimination across four life decades assessed by the Cambridge Colour Test. *J. Opt. Soc. Am. A* 29, A290–A297. doi: 10.1364/JOSAA.29.00A290

Paramei, G. V., and Oakley, B. (2014). Variation of color discrimination across the life span. *J. Opt. Soc. Am. A* 31, A375–A384. doi: 10.1364/JOSAA.31.00A375

Reffin, J., Astell, S., and Mollon, J. D. (1991). "Trials of a computer-controlled colour vision test that preserves the advantages of pseudoisochromatic plates," in *Colour Vision Deficiencies X*, eds B. Drum and A. Serra (Dordrecht: Kluwer), 67–76.

Regan, B. C., Reffin, J. P., and Mollon, J. D. (1994). Luminance noise and the rapid determination of discrimination ellipses in colour deficiency. *Vision Res.* 34, 1279–1299. doi: 10.1016/0042-6989(94)90203-8

Solomon, S. G., and Lennie, P. (2007). The machinery of colour vision. *Nat. Rev. Neurosci.* 8, 276–286. doi: 10.1038/nrn2094

Somerfield, M. R., Long, G. M., Tuck, J. P., and Gillard, E. T. (1989). Effects of viewing conditions on standard measures of acquired and congenital color defects. *Optom. Vis. Sci.* 66, 29–33. doi: 10.1097/00006324-198901000-00011

Switkes, E., Bradley, A., and De Valois, K. K. (1988). Contrast dependence and mechanisms of masking interactions among chromatic and luminance gratings. *J. Opt. Soc. Am. A.* 5, 1149–1162. doi: 10.1364/JOSAA.5.001149

Taylor, S., and Woodhouse, J. (1979). Blur and pseudoisochromatic colour vision tests. *Perception* 8, 351–353. doi: 10.1068/p080351

Troscianko, T., Davidoff, J., Humphreys, G., Landis, T., Fahle, M., Greenlee, M., et al. (1996). Human colour discrimination based on a non-parvocellular pathway. *Curr. Biol.* 6, 200–210. doi: 10.1016/S0960-9822(02)00453-0

Ueno, T., and Swanson, W. H. (1989). Response pooling between chromatic and luminance systems. *Vision Res.* 29, 325–333. doi: 10.1016/0042-6989(89)90081-3

Ventura, D. F., Silveira, L. C. L., Rodrigues, A. R., Nishi, M., de Souza, J. M., Gualtieri, M., et al. (2003). "Preliminary norms for the Cambridge Colour Test," in *Normal and Defective Colour Vision*, eds J. D. Mollon, J. Pokorny, and K. Knoblauch (Oxford: Oxford University Press), 331–339. doi: 10.1093/acprof:oso/9780198525301.003.0034

Walls, G. L. (1959). How good is the HHR test for color blindness? *Am. J. Optom. Physiol. Opt.* 36, 169–193. doi: 10.1097/00006324-195904000-00001

Wilson, H. R., and Wilkinson, F. (2004). "Spatial channels in vision and spatial pooling," in *The Visual Neuroscience*, eds L. M. Chalupa and J. S. Werner (Cambridge, MA: MIT Press), 1060–1068.

Conflict of Interest Statement: The Reviewer Dr. Mirella Telles Salgueiro Barboni declares that, despite being affiliated with the same institution as author Dr. Dora Fix Ventura, the review process was handled objectively and no conflict of interest exists. The authors declare that the research was conducted in the absence of any commercial or financial relationships that could be construed as a potential conflict of interest.

Received: 28 August 2014; accepted: 24 October 2014; published online: 23 December 2014.

Citation: Souza GS, Malone FL, Crawford TL, Miquilini L, Salomão RC, Guimarães DL, Ventura DF, Fitzgerald MEC and Silveira LCL (2014) Low number of luminance levels in the luminance noise increases color discrimination thresholds estimated with pseudoisochromatic stimuli. Front. Psychol. ***5****:1291. doi: 10.3389/fpsyg.2014.01291*

This article was submitted to Perception Science, a section of the journal Frontiers in Psychology.

frontiers in
PSYCHOLOGY

REVIEW ARTICLE
published: 22 January 2015
doi: 10.3389/fpsyg.2014.01594

Vision under mesopic and scotopic illumination

Andrew J. Zele[1]* and Dingcai Cao[2]*

[1] *Visual Science Laboratory, School of Optometry and Vision Science & Institute of Health and Biomedical Innovation, Queensland University of Technology, Brisbane, QLD, Australia*
[2] *Visual Perception Laboratory, Department of Ophthalmology and Visual Sciences, University of Illinois at Chicago, Chicago, IL, USA*

Edited by:
Marcelo Fernandes Costa, Universidade de São Paulo, Brazil

Reviewed by:
John L. Barbur, City University London, UK
Arthur Gilman Shapiro, American University, USA

****Correspondence:***
Andrew J. Zele, Visual Science Laboratory, School of Optometry and Vision Science & Institute of Health and Biomedical Innovation, Queensland University of Technology, 60 Musk Avenue, Brisbane 4051, QLD, Australia
e-mail: andrew.zele@qut.edu.au;
Dingcai Cao, Visual Perception Laboratory, Department of Ophthalmology and Visual Sciences, University of Illinois at Chicago, Room 149, 1905 West Taylor Street, Chicago, IL 60612, USA
e-mail: dcao98@uic.edu

Evidence has accumulated that rod activation under mesopic and scotopic light levels alters visual perception and performance. Here we review the most recent developments in the measurement of rod and cone contributions to mesopic color perception and temporal processing, with a focus on data measured using a four-primary photostimulator method that independently controls rod and cone excitations. We discuss the findings in the context of rod inputs to the three primary retinogeniculate pathways to understand rod contributions to mesopic vision. Additionally, we present evidence that hue perception is possible under scotopic, pure rod-mediated conditions that involves cortical mechanisms.

Keywords: vision, rods, cones, scotopic, mesopic, photopic, color, temporal

INTRODUCTION

The visual system is responsive to continual changes in the spectral, spatial, and temporal properties of the illuminant across ∼10 log units of dynamic range (Hood and Finkelstein, 1986). This is accomplished, in part, by switching operations between two photoreceptor classes in the retina, rods and cones, which have partially overlapping operating light ranges. Under high illuminations, rods are in saturation and photopic vision (Maxwell, 1860; Helmholtz, 1924; Hurvich and Jameson, 1957; Hering, 1964; DeValois and DeValois, 1993) is initiated by the outputs of three cone photoreceptor classes (L-, M-, and S-cones) with overlapping spectral sensitivities (Smith and Pokorny, 1975) to provide trichromatic color perception. With intermediate, mesopic illuminations when rods gradually become sensitive and cones are still active, there are subtle changes and a reduction in both the perceptual quality and gamut of perceivable colors (Nagel, 1924). Under dim, scotopic illuminations, only rods are active and color perception is still possible by different physiological computations than the trichromatic system (Pokorny et al., 2006, 2008; Elliott and Cao, 2013).

Photoreceptor outputs are transmitted from retina to brain for image forming vision via three major classes of retinal ganglion cells in primates that process distinct aspects of visual information (Dacey, 2000; Kaplan, 2004; Lee et al., 2010). The first class, known as parasol ganglion cells, project to the magnocellular (MC) layer of the LGN. The parasol ganglion cells display ON-center, OFF-surround antagonistic receptive field structures, with L- and M-cones contributing to both the centers and surrounds (spatial opponency; Rodieck, 1991). There are two subtypes of parasol ganglion cells based on the sign of the center response, including +(L+M) for ON-center cells and −(L+M) for OFF-center cells. The MC-pathway is believed to the physiological substrate of the luminous efficiency function (Lennie et al., 1993). The second class, known as midget ganglion cells, receives differential L- and M-cone inputs in the receptive field center and surround. There are four subtypes of midget ganglion cells, depending on the type and sign of cone input in the center, including +L/−M (ON response to L-cone input but OFF-response to M-cone input in the center), –L/+M, +M/−L, and −M/+L. The surround of midget ganglion cells, however, can receive mixed inputs from both L- and M-cones instead of only one type of cone input (Lee et al., 2012). Therefore midget ganglion cells display both "spatial opponency" and "chromatic opponency" to signal both spatial and chromatic (red–green) information. The notion that spatial and chromatic information is conveyed by two separate channels ("two-channel hypothesis" proposed by Rodieck, 1991) has now been dismissed. The midget ganglion cells project to the parvocellular (PC) layer in the LGN and mediate the "red–green" chromatic opponency signal and spatial acuity. The third class, known as small bistratified ganglion cells, has a spatially coextensive center and surround receptive field structure that receives excitatory S-cone input and inhibitory L+M input. These cells

project to the koniocellular (KC) layer of the LGN and are believed to mediate blue–yellow chromatic processing. Because the spectral signatures of the primary retinogeniculate neurons differ from human color perception (DeValois and DeValois, 1993), cortical transformations of these retinal projections (Calkins, 2004) and small populations of LGN cells with circuitry matching hue perception (Tailby et al., 2008) is necessary (Neitz and Neitz, 2008). Rod contribution to visual perception under mesopic illuminations is believed to be mediated via rod and cone inputs to the three pathways (Lee et al., 1997; Crook et al., 2009; Field et al., 2009; Cao et al., 2010), with rod signals merging into the cone pathway in the retina either through the rod–cone gap junctions or through rod bipolars and AII amacrines to cone bipolars (Daw et al., 1990; Sharpe and Stockman, 1999). This paper reviews current progress in understanding rod contributions to chromatic and temporal aspects of vision.

The original determinations of the Duplicity Theory of Vision (Schultze, 1866; von Kries, 1896; Müller, 1930; Saugstad and Saugstad, 1959; Stabell and Stabell, 2009) proposed separate and independent rod and cone functions, but the anatomical and physiological reality is that rods and cones share neural pathways in the retina (Polyak, 1941; Daw et al., 1990; Wassle et al., 1995; Sharpe and Stockman, 1999). The study of mesopic vision within a range of 3-4 log units of illumination (CIE, 1989, 1994) when there is a dual processing of rod and cone signals, is about revealing the nature of interactions between rod and cone photoreceptor signals. Between daylight and darkness (namely, dawn and dusk), as well as in many modern indoor lighting settings and most nighttime outdoor and traffic lighting environments, the visual system combines rod and cone signals and rod–cone interactions can modify perceptual experience and alter almost every aspect of visual processing, including visual detection (Buck et al., 1997; Sun et al., 2001b) and discrimination (Knight et al., 1998; Cao et al., 2008b), hue perception (Willmer, 1949; Lie, 1963; Trezona, 1970; Stabell and Stabell, 1971; Buck et al., 1998), color vision (Cao et al., 2005, 2008a; Pokorny et al., 2006), temporal vision (Kremers and Meierkord, 1999; Sun et al., 2001c; Cao et al., 2006; Zele et al., 2008; Cao and Lu, 2012; Zele et al., 2012, 2013), and spatial vision (Lange et al., 1997). Buck (2004, 2014) has comprehensively reviewed the effects of rod and cone interactions on human vision.

Determining the physiological substrates and mechanisms of rod–cone interaction, and how these give rise to the altered perceptual experience under mesopic illumination are largely unresolved problems in visual neuroscience. Historically, many estimates of sensitivity, magnitude, and timing of the interaction are limited by methodological approaches that inadvertently alter the relative excitation of rods and three cone classes in an undesirable manner with variation in the stimulus parameters. A central challenge in the study of mesopic vision is therefore to develop methodologies to measure rod and cone signal contributions separately and during rod–cone interaction.

CLASSICAL EXPERIMENTAL METHODS FOR THE STUDY OF MESOPIC VISION

The methodologies developed to differentiate outer retina signaling are typically based on known functional differences between the rod and cone systems (**Figure 1**), and apply these methods to study rod–cone interactions arising between the stimulus area and surround (lateral interactions) or within the stimulus area (local interactions). In one method, measurements are obtained during adaptation to darkness after exposure to a bleaching light; first for the initial cone plateau adaptation phase during which only cones are sensitive, and then during the full dark-adapted phase in which both rods and cones are sensitive, but when rods are more sensitive than cones (Hecht and Hsia, 1945). As fully sensitive cones are functional during the later dark adaptation phase, rod responses can be affected by cone involvement and so there may be incomplete rod isolation. The adaptation state of rods and cones affects their relative sensitivities such that short wavelength adaptation decreases the slope of the scotopic threshold versus intensity (TvI) curve [0.72–0.78; Sharpe et al., 1992; Shapiro et al., 1996b; although S-cone signals do not appear to regulate rod sensitivity (Shapiro, 2002)] whereas L-cone excitation desensitizes the rods and steepens the TvI slope from 0.80 to 0.98 (Shapiro, 2002). The scotopic TvI function is more sensitive at higher illumination levels (Sharpe et al., 1992; Shapiro et al., 1996b; Shapiro, 2002) and rods remain active at higher illuminances (Shapiro, 2002; Kremers et al., 2009) than reported initially by Aguilar and Stiles (1954), meaning that the effect of rod intrusions may be underestimated in many experiments. Although the rod system has lower contrast sensitivity ($\Delta L/L = \sim 0.14$ vs. ~ 0.015), its higher amplification enables single photon responses (Hecht et al., 1942). The visual resolution of the two systems varies by some 1200:1 between dim scotopic illuminations ($\sim$10 min arc) and bright photopic illuminations ($\sim$5 s arc; Hecht and Mintz, 1939). Note that thresholds for acuity and contrast sensitivity are more complex than simple TVI curves for the rod and cone systems (Barbur and Stockman, 2010). Importantly, because rod activity is optimized for low illumination and cones for high illumination, mesopic rod–cone interactions reflect signal processing at the extremes of the photoreceptor operating ranges.

Foveal and parafoveal measurements have been used to compare cone and rod function because cones are the predominant photoreceptor class in the fovea and rods are most prevalent in the parafovea (Curcio et al., 1990). This approach is limited by eccentric variations in the relative rod and cone densities, the temporal properties of rod vision (Raninen and Rovamo, 1986) and chromatic properties of cone vision (Moreland and Cruz, 1959). Moreover, rod–cone interactions may be affecting measurements and foveal and parafoveal stimuli may not truly reflect isolated cone or rod function. There is also no single eccentricity with only rod photoreceptors, unlike that for cones. The receptive fields sizes of the rod and cone system also differ. Compared to the spatial integration properties of the cone system, the rod system has larger areal summation (up to 0.4 vs. 0.025 deg^2; Barlow, 1958), a lower peak spatial contrast sensitivity (0.5 c/° vs. $\sim$4.0 c/°) and cut-off frequency ($\sim$6 c/° vs. $\sim$60 c/°; Campbell and Green, 1965; Hess and Nordby, 1986), and so the differential responsivities of the two systems to the spatial frequency characteristics of the stimulus (e.g., area, edges, and borders; Barbur and Stockman, 2010) must be carefully balanced within the experimental design and in the interpretation of the data.

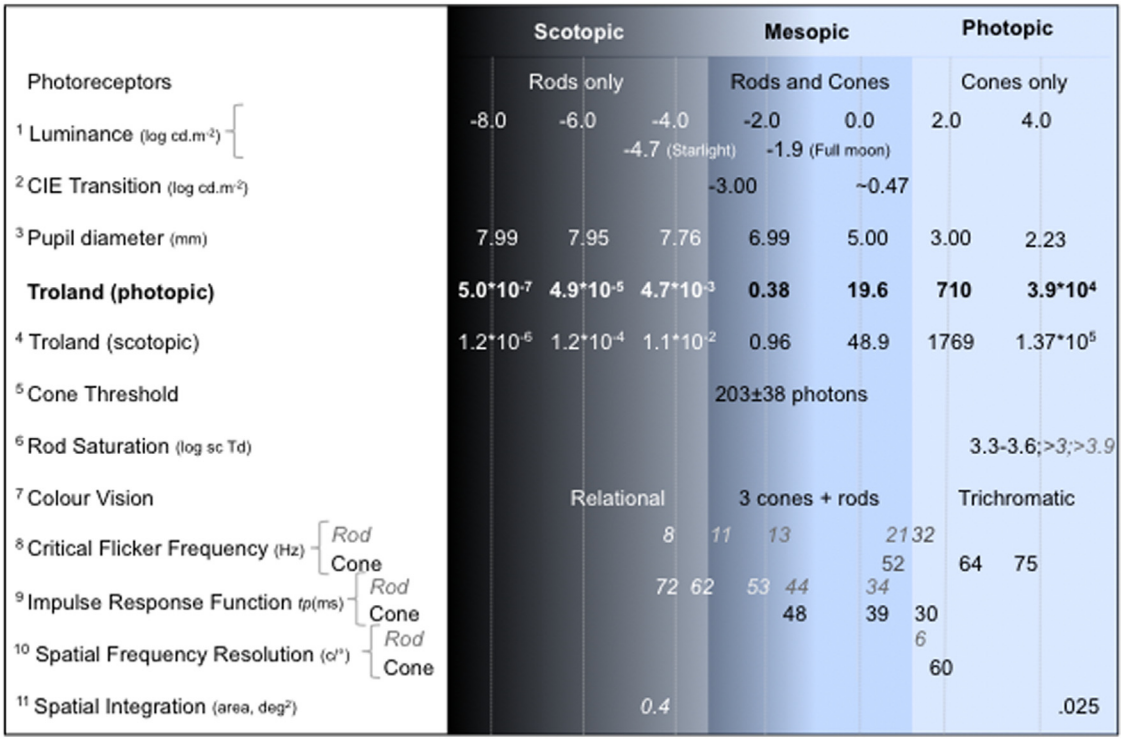

FIGURE 1 | Visual functions under scotopic, mesopic and photopic illumination. The luminance level (log cd.m^{-2}) is the reference for estimating pupil diameter using the empirical relation between pupil diameter (mm) and field luminance (Crawford, 1936; Pokorny and Smith, 1997). The reported values align approximately with the photopic retinal illuminance (photopic Troland is shown in bold) of the measurement conditions in the referenced study. When rod and cone values are both reported, *rod values are italicized*. Note that the reported values can vary with the observer, stimulus and measurement condition; see References for details of the experimental conditions: [1]Estimate of the light level under starlight and full moon from Smith et al. (1994); [2]CIE (1994): the transition values are complexly dependent on the viewing conditions (for example, see estimates of the rod saturation range); [3]Crawford (1936), Pokorny and Smith (1997); [4]$Km_{sc}/Km_{ph} = 2.49$; [5]Cone threshold estimated at the cornea (Koenig and Hofer, 2011); [6]Aguilar and Stiles (1954), Shapiro (2002), Kremers et al. (2009). [7]Pokorny et al. (2006); [8]Rod data from Conner and MacLeod (1977), Hess and Nordby (1986), Sun et al. (2001a); cone data from de Lange (1954), Kelly (1961); [9]Time to peak (tp ms) of the impulse response function from Cao et al. (2007); [10]Campbell and Green (1965), Hess and Nordby (1986); [11]Barlow (1958).

The different spectral sensitivities of the two systems provide basis for isolating their responses. Long-wavelength adapting lights have been used to preferentially desensitize cones, but complete rod isolation is not achieved because rods and cones have roughly the same sensitivity at long wavelengths in the dark-adapted eye, and short-wavelength (S) and middle-wavelength (M) cones are not completely desensitized by long wavelength adapting lights (Crawford and Palmer, 1985). Another method is to use high temporal frequencies to bias detection to cones (Coletta and Adams, 1984). Rod system temporal integration is longer than the cone system (100 ms to ∼1s vs. ∼10-50 ms; Barlow, 1958) and both the scotopic peak temporal contrast sensitivity (5–9 Hz vs. 8–10 Hz) and maximum critical frequency is lower (20–28 Hz) than photopic vision (50–60Hz; de Lange, 1954; Conner and MacLeod, 1977; Sun et al., 2001a). Rod and cone temporal sensitivities may be more similar, however, depending on the mesopic adaptation level, spectral properties of the illuminant and stimulus eccentricity, and complete cone isolation may not be achieved. Another approach is to take advantage of the Stiles–Crawford effect and focus the light from the test field near the edge of a fully dilated pupil, which reduces the quantal efficiency of the cones, but not rods (Aguilar and Stiles, 1954). Taken together, the aim is to develop a method that controls for the distinct functional response properties of the rod and cone systems, in addition to differences in their retinal distributions, spectral sensitivities, sensitivity regulation, retinogeniculate, and higher order processing, factors that underlie the challenges and complexities encountered in the study of mesopic visual function.

INDEPENDENT CONTROL OF ROD AND CONE SIGNALING WITH A FOUR-PRIMARY PHOTOSTIMULATING METHOD

Standard signal generators with three-primary lights are sufficient to achieve independent control of rods and two cone photoreceptor classes in dichromatic observers (Knoblauch, 1995; Kremers and Meierkord, 1999), but not the rods and three cone photoreceptors in trichromats to study rod–cone interactions. To do this, isoscotopic lines can define the combination of three primary lights with a constant scotopic luminance (fixed level of rod activity) within the domain of combinations with a constant photopic luminance, but even so it is not possible to control both scotopic and photopic luminance using three primaries in trichromats (Shapiro et al., 1996a). To achieve independent control, the

number of primary lights must be no less than the number of active photoreceptors.

The four-primary method overcomes limitations of traditional methods to allow independent control of the excitation of the rod and three cone photoreceptors at the same chromaticity, adaptation level and retinal locus (Sun et al., 2001a; Pokorny et al., 2004). The theoretical basis for four-primary photostimulating methodology is silent substitution, as defined by Shapiro et al. (1996a). Effectively, the four-primary wavelengths are carefully chosen to maintain the excitation levels of some photoreceptor classes while varying the excitation of specific photoreceptor classes using silent substitution (Estévez and Spekreijse, 1982).

Considering silent substitution in color matching provides an example of independent control of rod and cones experimentally. In color matching, the chromaticity of an equal-energy spectrum light can be metamerically matched using a combination of three primary lights of different wavelengths (e.g., 460, 516, and 660 nm). The same chromaticity can also be matched using a different set of primary lights (e.g., 460, 558, and 660 nm). When a metameric match is determined for each of the sets of primaries, the L-, M-, and S-cone excitations will be equal for both matches. In this example, the two stimuli differ in only one primary (either 516 or 558 nm) while the other two primaries (460 and 660 nm) are the same in both stimuli. Since rods are more sensitive to 516 nm light than 558 nm light, switching these two sets of metameric primaries over time produces rod modulation while maintaining constant cone excitations. A similar approach can be applied to isolate L-, M-, or S-cones.

The four-primary photostimulating method offers several advantages in the study of mesopic vision. First, it can modulate one photoreceptor class while keeping the excitations of the other three photoreceptors constant, thereby allowing analysis of the contribution of only one photoreceptor to visual perception. Second, the four-primary colorimeter can maintain the same mean cone chromaticity and luminance level, while changing rod or cone excitations. Third, since the four-primary method can modulate L-, M-, and S-cone excitation independently, the independent control of postreceptoral signals, defined in MacLeod and Boynton cone chromaticity space as L/(L+M) and S/(L+M), can be easily achieved, which is not the case with other methodologies.

The four-primary photostimulating method is a better method for studying mesopic vision because direct measurements of isolated rod and cone functions and their interactions can be achieved, whereas other methods infer rod and cone functions from a comparison of measurements obtained under different conditions. Finally, the colorimeter calibration process can compensate for individual differences in pre-receptoral filtering (e.g., lens and macular pigment) to reduce errors associated with absorption of the primary lights by these filters at the plane of the retina (Pokorny et al., 2004).

NEURAL PATHWAYS RELATED TO MESOPIC VISION

Since mesopic vision is a transitional stage between *photopic* and *scotopic* vision, it would be expected that both rod and cone signals would be sent to the cortex in mesopic conditions. The neural circuitry of the retina has been shown to allow both cone and rod signals to be transmitted to the pathways that carry information to the lateral geniculate nuclei (LGN) and then to the cortex. Physiological studies have demonstrated that, in addition to cone input, rods contribute to all three major retinogeniculate pathways. At mesopic and scotopic illuminations, physiological recordings from macaque retina indicate that parasol cells of the MC-pathway are the primary transmitter of rod signals (Gouras and Link, 1966; Virsu and Lee, 1983; Virsu et al., 1987; Purpura et al., 1988; Lee et al., 1997; Cao et al., 2010), with evidence for rod and cone signaling via small bistratified ganglion cells of the KC-pathway (Crook et al., 2009; Field et al., 2009) and midget ganglion cells of the PC-pathway (Grünert, 1997; Lee et al., 1997; Dunn et al., 2007). The analysis of natural image statistics also indicates that rods provide input to all of the three major pathways (Barrionuevo and Cao, 2014). The sharing of neural pathways allows for rod and cone signal interactions in visual system processing and provides the neural basis for rod contribution to color vision.

Figure 2 shows a schematic of the two primary retinal rod pathways conveying visual information to the MC-, PC-, and KC-pathway ganglion cells that mediate different aspects of visual perception. The *rod bipolar pathway* (rods → rod bipolars → AII amacrine cells → ON/OFF cone bipolars) is a slower pathway that has been hypothesized to be active at scotopic light levels (Verweij et al., 1999). The *rod–cone gap junction pathway* (rods → cones → ON/OFF cone bipolars) is a faster pathway that has been hypothesized to be active at scotopic and mesopic light levels (Schneeweis and Schnapf, 1995; Verweij et al., 1999; Hornstein et al., 2005). However, studies have shown that, at certain light levels, both retinal rod pathways are active simultaneously in mesopic vision (Sharpe et al., 1989; Stockman et al., 1991). Therefore, the visual system has potentially a transitional stage from the *rod bipolar pathway* to the *rod–cone gap junction pathway*. The transitional range during which both retinal rod pathways are potentially functioning is thought to occur at high scotopic and low mesopic light levels.

ROD CONTRIBUTIONS TO MESOPIC COLOR VISION

When both rods and cones are operational, rods influence all aspects of color vision (Lythgoe, 1931; Gilbert, 1950; Trezona, 1970; Stabell and Stabell, 1975a,b, 1976, 1979, 1994; Smith and Pokorny, 1977; Montag and Boynton, 1987; Buck, 1997; Cao et al., 2005). In trichromatic observers, large field and peripherally viewed lights stimulate four different photoreceptor classes at mesopic light levels and as light level decreases, large field color matches made with three primaries do not obey Grassman's laws (Shapiro et al., 1994). Conversely, the dichromatic retina behaves similarly to the trichromatic retina with large or peripherally viewed mesopic stimuli when rods operate as the third photoreceptor class (Smith and Pokorny, 1977). Rods have been consistently shown to enhance brightness (Ikeda and Shimozono, 1981; Benimoff et al., 1982), produce brightness contrast (induction) in a central cone detected test field (Sun et al., 2001b), decrease saturation of spectral lights (Lythgoe, 1931; Gilbert, 1950; Buck et al., 1998), and improve discrimination at long-wavelengths (Stabell and Stabell, 1977). On the FM-100 hue test, rod intrusion causes discrimination loss and increased errors on the tritan axis (Knight

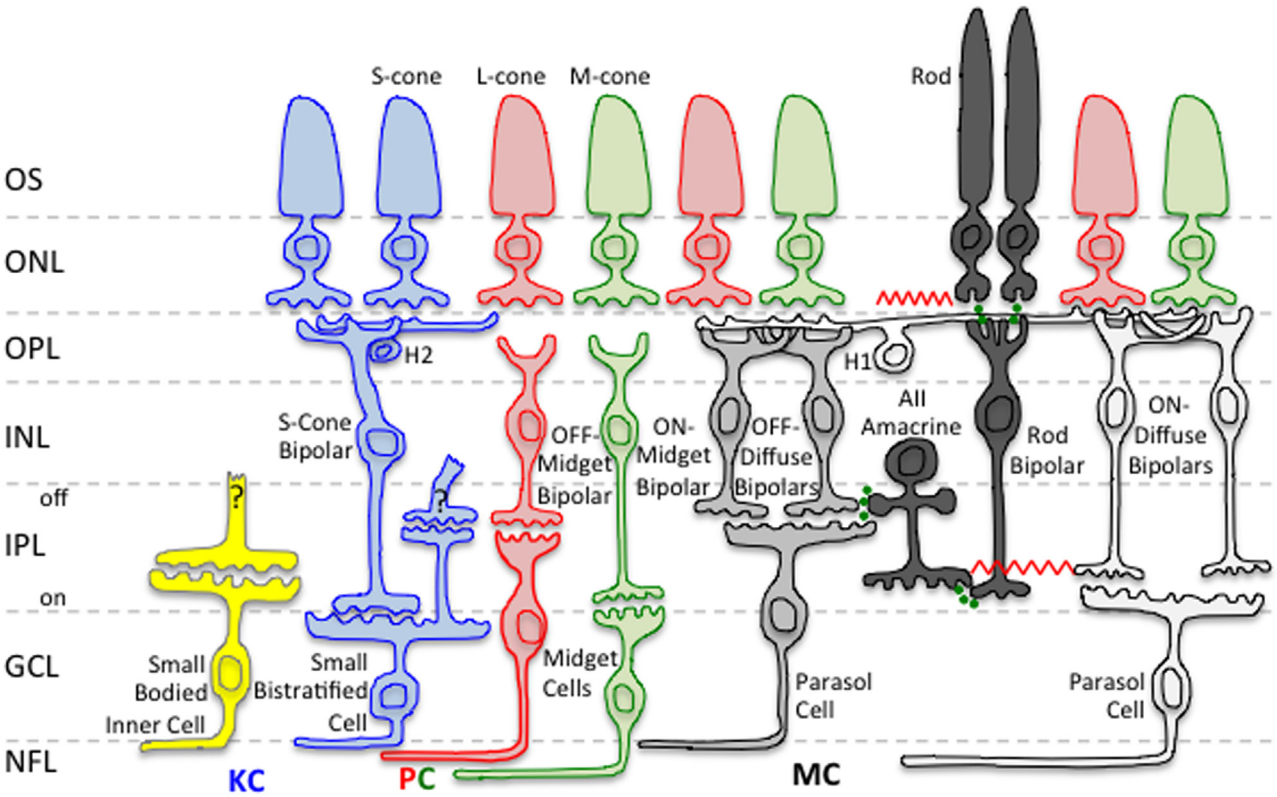

FIGURE 2 | Neural pathways related to mesopic vision. Rod signals input to all three primary retinogeniculate pathways, namely the magnocellular (MC), parvocellular (PC), and koniocellular (KC) pathways. Only rod inputs to the MC pathway are shown in this schematic. Green circles indicate chemical synapses. The red zig–zags indicate electrical synapses. Retinal layers are indicated on the left: OS, Outer Segment; ONL, Outer Nuclear Layer; OPL, Outer Plexiform Layer; INL, Inner Nuclear Layer; IPL, Inner Plexiform Layer; GCL, Ganglion Cell Layer; NFL, Nerve Fiber Layer.

et al., 1998). The degradation in cone chromatic discrimination that occurs in the presence of rod activity was attributed initially to rods weakening the cone signal to produce a desaturation effect (Lythgoe, 1931; Gilbert, 1950).

Color percepts associated with rod activations have been studied using unique hue measurements and hue scaling (Nerger et al., 1995; Buck et al., 1998; Nerger et al., 2003), color matching at low light levels (Trezona, 1970), scotopic color contrast (Willmer, 1949; Stabell and Stabell, 1994; Buck, 1997), by comparing measurements in foveal and parafoveal retinal locations and between dark-adapted and cone-plateau conditions (Ambler, 1974; Nagy and Doyal, 1993) and under full moon-light (Smith et al., 1994). Reports indicate that the rod percept is bluish, with evidence for multiple hue percepts (e.g., Nagel, 1924; Middleton and Mayo, 1952; Ambler, 1974; Smith et al., 1994; Stabell and Stabell, 1994; Buck et al., 1998; Nerger et al., 1998; Buck, 2001; Ishida, 2002; Shin et al., 2004). Rod activity also causes a shift (or bias) in perceived hue as demonstrated by Buck et al. (1998, 2006, 2008, 2012), Buck (2001), Knight and Buck (2002), Thomas and Buck (2004), Buck and DeLawyer (2014), and Foote and Buck (2014) in a comprehensive series of investigations that quantified three predominant hue shifts (1) the shift of unique yellow to longer wavelengths to enhance the red–green balance toward green (rod green bias), (2) the shift of unique blue to longer wavelengths (rod red bias), and (3) the shift of unique green to longer wavelengths to enhance the blue–yellow balance toward blue (rod blue bias). The critical area up to which there are no further perceived changes in hue or saturation at a given eccentricity, increases with rod activity (Pitts et al., 2005; Troup et al., 2005; Volbrecht et al., 2009). These experimental designs, however, do not yield results easily interpretable in terms of the underlying physiological mechanisms, and may be methodology dependent; for a discussion see Volbrecht et al. (2010) and Buck (2014). One reason is that a single hue sensation may not be associated with a given cone class (Knoblauch and Shevell, 2001). The most unambiguous approach is to measure the appearance of a rod signals in terms of cone activation at the same retinal location under the same adaptation conditions as achieved with a four-primary colorimeter. This negates the problems associated with a change in rod–cone excitation resulting from differences in a retinal eccentricity, illumination, or stimulus wavelength. When the four photoreceptor excitations are independently controlled (Pokorny et al., 2004), it was demonstrated that rod signals cause chromaticity shifts in directions other than toward white, demonstrating that rod activity does not lead to a purely weakened cone signal (Cao et al., 2005; **Figure 3**).

To characterize the color of rod signaling in terms of cone excitations [L/(L+M), S/(L+M), (L+M)], Cao et al. (2005, 2008a,b)

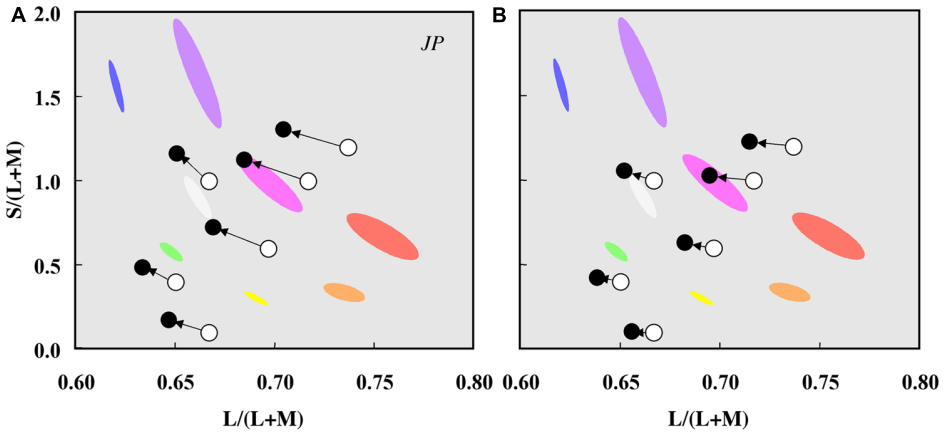

FIGURE 3 | Chromaticity shifts in the color appearance of cone signals due to rod excitation. Data for one observer (JP) plotted in a relative cone Troland space at 2 photopic Td **(A)** and 10 photopic Td **(B)**. The arrows indicate the effect of increased rod excitation on the direction of the color shift from the stimulus chromaticities (unfilled circles) to the matching chromaticities (filled circles). Ellipses show the chromaticities of eight non-dark appearing basic colors. Adapted from Cao et al. (2005).

used a four-primary photostimulator (Pokorny et al., 2004) and developed a perceptual matching technique that equates rod percepts with cone percepts. Because post-receptoral pathways have no information about the photoreceptor class (rod or cone) initiating the signal, rod percepts matched to cone-mediated percepts can be linked to PC-, MC-, and KC- pathway signaling. With this methodology, an incremental change in rod excitation generates a blue–greenish percept, equivalent to a decrease in L/(L+M) excitation, and increases in both S/(L+M) and (L+M) excitation (Cao et al., 2005, 2008a,b). Conversely, a decremental change in the rod excitation generates a reddish percept, equivalent to an increase in L/(L+M) excitation, a decrease in (L+M) excitation and little or no change in S/(L+M) (Cao et al., 2008b).

Rod contributions to mesopic color perception involve differential rod signal weightings in the PC-, MC- and KC-pathways as a function of illumination level and rod contrast. The relationship between the incremental rod contrast signal (up to 80% rod contrast) and the level of PC-, MC-, and KC-pathway excitation is approximately linear (Cao et al., 2008a), consistent with physiological recordings from primate PC cells showing a linear relationship with cone contrast at all light levels, and MC cells showing a linear response at light levels less than 30 Td (Purpura et al., 1988). The rod signal strength decreases with increasing retinal illuminance in a non-linear pattern across pathways (**Figure 4**; Cao et al., 2008a) that can be described by a physiologically plausible model based on primate retinal ganglion cell responses (Smith et al., 2000; Zele et al., 2006; Cao et al., 2008a,c) with rod contributions to the cone pathways via rod–cone gap junctions at mesopic levels (Cao et al., 2008a).

In addition to affecting the perceived hue, brightness, and saturation, rod activity can alter cone-mediated chromatic discrimination (Stabell and Stabell, 1977; Nagy and Doyal, 1993; Knight et al., 1998, 2001; Cao et al., 2008b; Shepherd and Wyatt, 2008; Volbrecht et al., 2011). In comparison to measurements under photopic illumination, chromatic sensitivity measured under mesopic illuminations is differentially altered in the areas of the protan, deutan, and tritan confusion lines, with the greatest sensitivity loss near the tritan axis, but in general, the magnitude of the rod intrusion is small when measured with luminance contrast masking techniques (Walkey et al., 2001). When cone-mediated chromatic discrimination is affected by rod activity, it causes asymmetric changes for conditions where L-cone relative to M-cone excitation increases (L/M increment) and S-cone excitation decreases (S-decrement), without altering discrimination for other cone excitations (Cao et al., 2008b). Rod incremental signals degrade chromatic discrimination and rod decremental signals improve chromatic discrimination, with rod activity causing a shift in the ellipse origin and a change in the length of the minor axes (Cao et al., 2008b). Rod and cone signals combine differently in determining chromatic discrimination for different post-receptoral luminance and chromatic pathways such that the effects of rod pedestals are similar to chromatic L/(L+M) cone pedestals for L/M increment discrimination (rod contribution to the inferred PC pathway), but similar to luminance (L+M) cone pedestals for S-decrement discrimination (rod contribution to the inferred MC-pathway; Cao et al., 2008b).

ROD CONTRIBUTIONS TO SCOTOPIC COLOR VISION

Textbook descriptions of rod contributions to color vision often state that rods signal only achromatic percepts, yet vision in twilight illumination is not always colorless (e.g., Nagel, 1924; Willmer, 1949; Thomson and Trezona, 1951; Middleton and Mayo, 1952; Lie, 1963; Ambler, 1974; Smith et al., 1994; Stabell and Stabell, 1994; Nerger et al., 1998; Buck, 2001; Ishida, 2002; Shin et al., 2004). The viewing conditions used in these studies, however, may not exclusively involve rods. Nagel (1924) noted that for illumination levels below cone threshold, many observers perceive short-wavelength reflective paper samples as blue, although he suggested that such observations do not contradict the notion of color blindness under scotopic light levels, but rather the impossibility of discriminating colors as qualities that are different

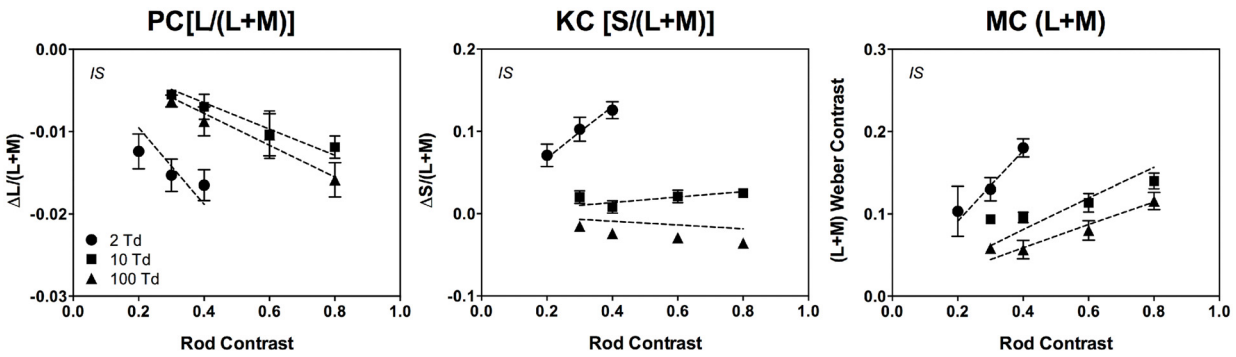

FIGURE 4 | The cone contrasts that perceptually match a rod signal are linear as a function of rod contrast. The data were measured at 2, 10, and 100 Td (observer IS). The dashed lines are fits based on a physiologically plausible model. Adapted from Cao et al. (2008a).

from one another. Recent evidence in trichromats and dichromats brings this view into question (Pokorny et al., 2006, 2008).

With photopic illumination, cones dominate vision; the rod system is in saturation for all but the longest visible wavelengths, and their contribution to visual perception is minimal as rods in saturation do not signal stimulus change. Rod–cone coupling can, however, extend the range of rod signaling (Hornstein et al., 2005; Seeliger et al., 2011), regulate light adaptation (Cameron and Lucas, 2009) and the coupling strength may be controlled by a retinal circadian clock which increases cone receptive field size and slow the kinetics of the cone response at nighttime (Ribelayga et al., 2008). At high illuminations, rods make significant contributions to non-image forming functions via the melanopsin pathway to the circadian system (Altimus et al., 2008) and the pupil control pathway (for review Feigl and Zele, 2014). With reductions in light level from daylight to twilight, both rods and cones contribute to visual perception and further reductions lead to a selective loss in S-cone sensitivity and a progressive increase in rod sensitivity (Brown, 1951; Verriest, 1963; Walkey et al., 2001). Whilst L- and M-cones remain active, rods and L-cones primarily mediate percepts since rods are more sensitive than M-cones to mid- and short-wavelength light under twilight illumination (Pokorny et al., 2006). As rods gradually become dominant during dark-adaptation, the peak of visual sensitivity shifts toward shorter wavelengths so that objects predominantly reflecting mid- and short-wavelength light appear relatively brighter than objects reflecting long-wavelength light (Purkinje, 1825). For wavelengths greater than 650 nm, the photochromatic interval approaches zero and the rods and cones have about equal dark-adapted thresholds (Hecht and Hsia, 1945; Wald, 1945). Thus, with reductions in light level and long-wavelength stimuli, there is no situation where rods alone merdiate vision. With progressively shorter wavelengths, however, rod sensitivity increases by a factor of 1000 or greater than cones in the mid- and short-wavelength regions of the visible spectrum (Kohlrausch, 1931).

McCann and Benton (1969) observed multi-colored percepts in complex scenes illuminated with a red appearing light (656 nm) set just above L-cone threshold and superimposed with a monochromatic light (546 or 450 nm) set below cone threshold (scotopic). Such percepts were also present with Mondrian patterns (McCann, 1972). The rod contribution to this effect was determined by setting the threshold level for perception of faint blue–green, red, or yellow hues to each of 10 monochromatic lights (420–600 nm) in the presence of the 656 nm light (set just above L-cone threshold); the scotopic luminosity function matched the threshold levels of the 10 monochromatic lights (McKee et al., 1977). When the 656 nm light was increased by 1.2 log units and each of the 10 monochromatic lights were re-adjusted to find a criterion called the optimum color (that was neither too blue–green nor too red), the observers reported a wide range of hue percepts and the data again matched the scotopic luminosity function, indicating that the optimum color involved the same mechanisms. Finally, the criterion optimum color was similar irrespective of whether a 510 nm light was imaged in the pupil center or pupil periphery; rod function was implicated by an absence of the Stiles–Crawford effect. The Stiles–Crawford effect for cones was found only when the irradiance of the 656 nm light was further increased and the irradiance of the 510 nm light at the criterion optimum color needed to be set at a level above cone threshold (McKee et al., 1977). The percepts appear brighter, sharper, and slightly more saturated under photopic conditions. Taken together, these studies clearly demonstrate that multicolored percepts can be generated through interaction of L-cone and rod signals whereas independently, only (achromatic) lightness percepts are signaled. See McCann et al. (2004) for a review of rod and L-cone color.

Pokorny et al. (2006) demonstrated that rods mediate variegated, scotopic hue percepts when multiple stimuli are present in the field of view. When observers are presented with an array of reflective paper samples under scotopic illumination, trichromatic participants perceive brighter appearing stimuli as blue–green–gray, and darker appearing stimuli as reddish-orange, irrespective of the photopically assigned color names. This rod color was termed *relational* because the color appearance of a paper samples changed depending on the lightness of other paper samples in view (Pokorny et al., 2006). When the samples were viewed in isolation they were perceived as blue-green, consistent with Nagel's (1924) description. Pokorny et al. (2006) hypothesized that the visual system estimates probable color based on prior experience of viewing color in the natural environment

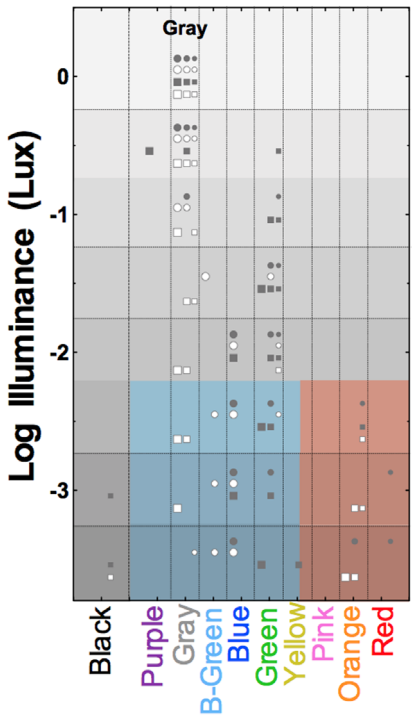

FIGURE 5 | Surface color perception under scotopic illumination reveals relational hue percepts mediated exclusively via the rod pathway. Symbols show the reported color names from four trichromatic observers of the gray OSA-UCS color sample as a function of photopic illuminance. Symbol size refers to the lightness of the OSA-UCS sample, with lightness increasing with increasing symbol size. Light levels below about −2.25 log Lux are solely mediated by rods; the colored shaded areas demarcate the blue–green–gray and red–orange color categories used by the observers (samples below threshold were black). Adapted from Pokorny et al. (2006).

under dim viewing conditions. **Figure 5** shows that a sample that appears gray at photopic illumination (i.e., has no chromatic information) invokes variegated color sensations at mesopic and scotopic illuminations. Such scotopic color perceptions are not restricted to trichromats; congenital dichromats have a rich color gamut under scotopic viewing conditions (Pokorny et al., 2008). Although dichromats can name color in fair agreement with color normal observers under photopic conditions (Scheibner and Boynton, 1968; Nagy and Boynton, 1979), the assigned color names under scotopic illuminations are not consistent with the scotopic lightness of the samples as were the names assigned by deuteranomalous trichromats and color normals. Pokorny et al. (2008) proposed that the limited color gamut experienced by a dichromat at photopic light levels leads to a limited association of rod color perception with objects differing in scotopic reflectance.

To understand rod color vision in complex viewing environments, Elliott and Cao (2013) investigated perceived hue in natural scene images under scotopic light levels. They showed that when a test patch had low variation in the luminance distribution and was a decrement in luminance compared to the surrounding area, reddish or orangish percepts were more likely to be reported compared to all other percepts. In contrast, when a test patch had high variation and was an increment in luminance, the probability of perceiving blue, green, or yellow hues increased. In addition, when observers had a strong, but singular daylight hue association for the test patch, color percepts were reported more often and hues appeared more saturated compared to patches with no daylight hue association. This suggests that some cortical mechanisms, which integrate experience in daylight conditions with the bottom–up rod signal processing under scotopic illumination, can modulate scotopic color perception.

ROD–CONE INTERACTIONS IN TEMPORAL PROCESSING

Rod–cone interactions are best illustrated with stimuli that change overtime because these conditions exploit the different temporal response properties of rods and cones. While it has been demonstrated that both rods and cones contribute signals to the retinogeniculate pathways, the relative contributions of rods and cones to each of the pathways are not known. To understand how rod and cone signals are combined in different post-receptoral pathways, summation paradigms were developed to measure threshold changes as a function of the phase, contrast, and adaptation state of rods and cones (Ikeda and Urakubo, 1969; van den Berg and Spekreijse, 1977; Benimoff et al., 1982; Drum, 1982; Buck and Knight, 1994; Naarendorp et al., 1996; Kremers and Meierkord, 1999). A linear vector sum model demonstrates that a temporal combination of rod and cone signals may mediate flicker detection (MacLeod, 1972; van den Berg and Spekreijse, 1977). A non-linear combination of rod and cone signals has been shown to mediate other tasks (Buck and Knight, 1994). Because the cone pathway temporal response is faster than the rod pathway, temporal frequency dependent destructive interference between rod and cone signals causes cancelation when the signals are 180° out of phase (MacLeod, 1972; van den Berg and Spekreijse, 1977) as can occur for the putative fast and slow rod pathways (Conner, 1982; Sharpe et al., 1989; Stockman et al., 1991), but such interactions occur when the rods and cones have different sensitivities to the test stimuli and are in different states of adaptation. This is not a major factor for incremental or decremental stimuli, however, as the faster signal is processed before the slower signal (Cao et al., 2007). The type of summation also depends on the pathways mediating detection. Using a four-primary colorimetery to measure thresholds for mixed rod and L-cone (or M-cone) modulations as a function of their relative phase and frequency (2 or 10 Hz), Sun et al. (2001c) showed that probability summation occurred when rod and cone signals were mediated separately via the MC and PC pathway, and linear summation (addition or cancelation) when rods and cone signals were both mediated via the MC pathway (Sun et al., 2001c). Consistent with this observation, physiological recordings of sinusoidal stimulation of macaque parasol cells show linear summation of rod and cone signals (Cao et al., 2010).

Mesopic vision can change depending on whether signaling involves both the faster *rod–cone gap junction pathway* and the slower *rod bipolar pathway,* or when signaling shifts between these pathways. If cones are more light adapted than rods, or there is higher cone contrast, cancelation occurs at a temporal frequency where there is a 180° phase shift between the fast and

slow pathways (van den Berg and Spekreijse, 1977; Conner, 1982; Sharpe et al., 1989; Stockman et al., 1991, 1995). When higher cone light adaption promotes cone signaling via the faster pathway and rod signaling via the slower pathway, cone signaling is 60–80 ms faster than rod signaling (MacLeod, 1972; van den Berg and Spekreijse, 1977; Barbur, 1982; Sharpe et al., 1989). On the contrary, when cone and rod latencies are estimated under conditions of comparable mesopic light adaptation and all photoreceptor signals are transmitted via the faster *rod–cone gap junction pathway,* the cone–rod latency difference is reduced to 8–20 ms (Sun et al., 2001b; Cao et al., 2007), in agreement with physiological estimates (Schneeweis and Schnapf, 1995; Verweij et al., 1999). The transition from the slower to the faster pathways also changes the system gain, which has been noted in rod reaction time models during the transition from high scotopic to low mesopic light levels (Cao et al., 2007).

When rods are dark-adapted in the region surrounding a cone-detected target (lateral interaction), rods suppress cone flicker detection (Lythgoe and Tansley, 1929; MacLeod, 1972; van den Berg and Spekreijse, 1977; Goldberg et al., 1983; Alexander and Fishman, 1984; Coletta and Adams, 1984; Stockman et al., 1991; Anderson and Vingrys, 2001; Cao et al., 2006; Zele and Vingrys, 2007). The mechanism and physiological substrates of lateral rod–cone interaction has been the subject of considerable debate. It was initially inferred from psychophysical studies that rods primarily interacted with L-cones when flicker sensitivity measured using stimulus conditions that caused rod excitation to vary with the wavelength of the test light (Coletta and Adams, 1984, 1985; Frumkes et al., 1988); such interpretations are not reconcilable with retinal physiology. Although early physiological reports in amphibians indicated that horizontal cells were the neural locus (Frumkes and Eysteinsson, 1988), horizontal cell inputs in primates are additive and synapse primarily with cones (Dacey et al., 1996). Using a four-primary colorimeter, it was demonstrated that lateral suppressive rod–cone interactions occur at low surround illuminances ($\leq$0.5 Td) and are specific to receptoral (L-cone, M-cone) and postreceptoral [L+M+S] and [L+M+S+Rod] modulations containing luminance variation (Cao et al., 2006). The lateral rod–cone interaction decrease cone critical fusion frequency (CFF) by about 6 Hz (Cao et al., 2006) and reduce temporal contrast sensitivity for frequencies >6–8 Hz (Zele et al., 2008). This suppression of temporally modulated sinusoidal stimuli seems to occur in a spatial frequency range of 1–2 c/° (Lange et al., 1997). The mesopic L- and M-cone CFFs in trichromatic observers (Cao et al., 2006) are also consistent with differences in *CFF* between protanopes and deuteranopes (Smith and Pokorny, 1972; Lutze et al., 1989). That cone CFF at high mesopic light levels is suppressed by dim equiluminant surrounds ($\leq$0.2 Td) that promote rod activity is consistent with the involvement of inhibitory signals from the AII amacrine cell directly to either cone bipolar cells or ganglion cells (Cao and Lu, 2012) and is strong in the MC-pathway (Cao et al., 2006). MC-pathway units respond vigorously to all of these modulation patterns used in the psychophysical investigation [L−, M−, L+M+S, L+M+S+Rod] (Yeh et al., 1995) and rod inputs to the retinogeniculate pathways are predominant in MC-cells (Lee et al., 1997).

Suppressive rod–cone interactions with cone isolating flicker stimuli on dim backgrounds are not significant for S-cone modulations (Cao et al., 2006) but interactions do occur when S-cones and rods are simultaneously temporally modulated (Zele et al., 2012). Interactions between rods and S-cones might be more complex, with evidence from four-primary colorimetry for linear summation of the two signals in the KC pathway which produces antagonistic, phase dependent threshold changes (Zele et al., 2012). These rod and S-cone interactions depend on the relative photoreceptor contrast ratios and a mutual, non-linear reinforcement, possibly originating at the photoreceptor level, that acts to decrease threshold (supra-additivity) with increasing contrast ratios (Zele et al., 2012). It is known from physiological studies that KC-pathway units respond vigorously to S-cone and luminance containing modulations (Yeh et al., 1995) with mesopic rod inputs to small bistratified ganglion cells in the macaque retina (Crook et al., 2009; Field et al., 2009) and with high contrast incremental stimuli in lateral geniculate nucleus of rhesus (Virsu and Lee, 1983), however, another study detected no physiologically measurable rod input to KC-ganglion units in macaque with temporal modulation (Lee et al., 1997). Physiological recording in ganglion cells have indicated that the PC-units have weak inputs from rods (Lee et al., 1997), consistent with a weak suppression of chromatic L/(L+M) signals (Cao et al., 2006). Chromatic L/(L+M) flicker detection has a different pattern of suppression and is reduced relative to that found for luminance-containing modulations, with a peak suppression at about 5 Td (Cao et al., 2006).

The relative rod contributions to the three pathways depends on the rod temporal profile. Rods produce luminance signals transmitted via the MC pathway at all measured pulse durations from 25 to 1000 ms, but only produce chromatic signals transmitted by the PC and PC pathways when the pulse duration is >75 ms (**Figure 6**; Zele et al., 2013). The implication is that the nature of the rod–cone interaction changes with the relative weighting of the rod and cone signals in the three pathways (Zele et al., 2013). The perception of motion of peripherally fixated, small circular stimuli at photopic illuminances are distorted such that the circle takes on a comet like appearance, yet long temporal responses are not typically associated with photopic vision (Barbur et al., 1986). Interestingly, the spectral response of the comet effect is consistent with rod–cone interactions, the implication being that rods in saturations can inhibit cone signaling (Barbur et al., 1986). Rod–cone interactions produce large transient sensitivity reductions at stimulus onset and offset (Buck et al., 1984; Buck, 1985; Pokorny et al., 2003; Zele and Vingrys, 2007) but the sensitivity loss due to rod–cone interactions can be less than that observed for mesopic cone–cone interactions (Zele et al., 2013). The temporal adaptation response for non-opponent cone–cone interactions is monophasic whereas opponent cone–cone interactions are biphasic (Zele et al., 2013). In contrast, different adaptation processes regulate rod and cone vision (He and MacLeod, 2000) and so an increase in the local rod adaptation level facilities rod signaling through temporal summation, pointing to some intrinsic difference in the processing of rod and cone signals in post-receptoral pathways (Zele et al., 2013).

An examination of the relationship between rod–cone interactions for stimuli that are temporally modulated (periodic) or

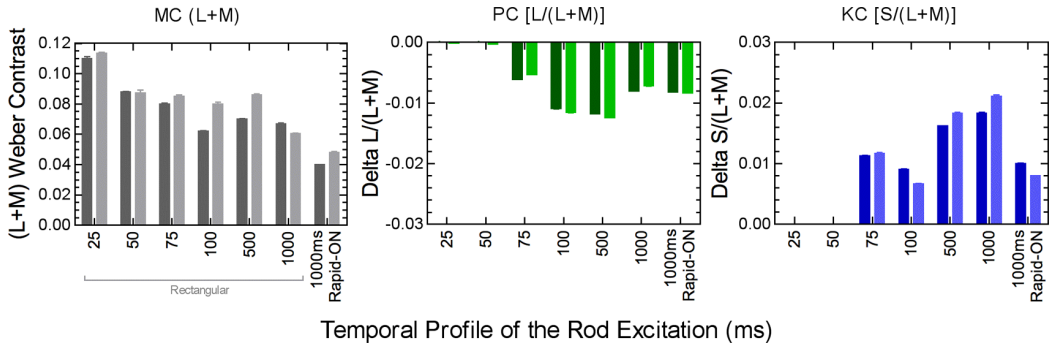

FIGURE 6 | Post-receptoral rod signaling weights in the MC, PC, and KC pathways depend on the temporal properties of the rod signal. Data were measured using a perceptual matching paradigm at 5 photopic Td (two observers; darker and lighter columns). Adapted from Zele et al. (2013).

pulsed (aperiodic) found the interactions are a general visual phenomenon affecting both periodic and aperiodic stimuli, causing the cone pathway temporal impulse response function (IRF) amplitude to decrease and the time-to peak to be delayed (Zele et al., 2008). This suppressive effect is analogous to reducing cone system contrast sensitivity and increasing the integration time (Zele et al., 2008). In the absence of an interaction, rod–cone latency differences at mesopic light levels are ∼20 ms (Schneeweis and Schnapf, 1995; Verweij et al., 1999; Sun et al., 2001c; Cao et al., 2007) and rod–cone interactions reduce this latency difference by ∼7 ms, potentially improving temporal processing under conditions where both rods and cones contribute to vision (Zele et al., 2008). Rod–cone coupling may be important for these processes.

Simple reaction times for rod or cone stimuli with various contrasts and retinal illuminances were measured (Cao et al., 2007; Zele et al., 2007) and reaction times to cone stimuli were always shorter. These measured reaction times can be modeled by rod and cone IRFs (Cao et al., 2007; Cao and Pokorny, 2010). In a separate investigation, the effects of rod–cone interaction on reaction time mediated by chromatic and luminance pathways were studied. Lateral rod–cone interactions increase cone-mediated RTs with the strongest rod–cone interactions in a dark surround (Zele et al., 2014). Reaction time has been explored as a basis for developing a real world, performance based mesopic luminous efficiency functions (He et al., 1997, 1998; Walkey et al., 2005, 2006a,b) with the assumption that reaction time is signaled via the MC pathway (He et al., 1998). Recent evidence, however, indicates there is an involvement of chromatic pathways (Walkey et al., 2006b) and rod–cone interactions alter cone mediated reaction times mediated via the chromatic and luminance pathways (Zele et al., 2014). Further developments are required to evaluate the mesopic reaction time conditions under which Abney's law holds, as required for photopic and scotopic luminous efficiency (Lennie et al., 1993) and to ensure that the laboratory derivations of mesopic luminous efficiency are not affected by rod–cone interaction in practical real world conditions, and are robust to, or can easily accommodate, changes in relative rod and cone sensitivity that occur with changes in the viewing conditions so that its applicable in the broadest range of lighting environments.

CONCLUSION AND FUTURE DIRECTIONS

At present there are numerous outstanding problems in the study of the dual processing of rod and cone signals. The range and impact of rod–cone interactions on human visual function and performance is only becoming known, and the subtlety and significance of these effects is becoming apparent. The cortical mechanisms for scotopic color vision are still to be defined (Pokorny et al., 2006; Elliott and Cao, 2013) and there are significant gaps in understanding the interactions between rods and S-cones for temporal processing and their roles in mesopic color perception. The quantification of the effects of rod–cone interaction on motion processing is also incomplete. To fully understand these processes under conditions best able to control for the differences between the rod and cone systems, the four-primary colorimetric method will be central. The generality of this methodology is becoming clear with new applications beyond psychophysics in the areas of physiology (Cao et al., 2010), electroretinography (Cao et al., 2011) and pupillometry (Barrionuevo et al., 2014). Combinations of these techniques will be critical for determining the physiological substrates, both in the retina and cortex, in addition to answering questions about the mechanisms of rod–cone interaction including how the relative rod and cone weights change in the post-receptoral pathways and their affects on visual function and performance.

Computational descriptions of mesopic vision derived from functional data in humans will be important for industrial applications that require optimal lighting conditions. The effects of rod–cone interaction in visual function and performance are directly applicable to many occupational environments, including transportation (i.e., aviation, maritime, rail, and road) and medicine. There are well-accepted luminosity functions for photopic and scotopic lighting conditions that are often used in science and industry, but complex nature of rod and cone contributions in mesopic illuminations means there is currently no accepted mesopic luminous efficiency function (CIE, 1989; Stockman and Sharpe, 2006). It will be important to determine general mesopic luminous efficiency functions (CIE, 1989), whether they be performance based (He et al., 1998; Walkey et al., 2006b), use minimum motion photometry (Raphael and MacLeod, 2011) or equivalent luminance (CIE, 2001), or a new method. The use of an

inappropriate spectral luminous efficiency function in the mesopic region has energy efficiency and economic consequences, not to mention safety issues in, for example, lighting for nighttime transportation. Future developments in this area will include practical lighting standards for mesopic illuminations that are energy efficient and optimize visual performance. Advances in the study of mesopic vision should provide needed information for solutions to many industrial application problems. The development of a widely applicable, mesopic luminous efficiency function will be one of the most challenging problems encountered in this area of research.

We anticipate that the development of new tests for the study of rod–cone interaction in normal eyes will have great potential for translation to applied investigations (Alexander and Fishman, 1984; Arden and Hogg, 1985; Alexander et al., 1988; Falcao-Reis et al., 1991) for the development of non-invasive tests for the early detection of retinal eye disease with four-primary methodology (Feigl and Zele, 2010; Feigl et al., 2011), and for understanding the progression of retinal eye diseases that affect both rods and cones (e.g., age-related macular degeneration, diabetes, cone–rod dystrophy). New developments of clinical mesopic vision tests will be important because most acquired retinal diseases involve both the rod and cone systems. Moreover, impaired vision in the mesopic range is probably the most sensitive and earliest sign of a range of retinal diseases (Petzold and Plant, 2006). The number of complaints about disturbances in mesopic and scotopic vision after corneal refractive surgery is also increasing, indicating the importance of developing new measures of these visual disturbances (Fan-Paul et al., 2002).

In general, decision processing in perceptual detection or action tasks is cortically mediated and, therefore, the photoreceptor source of information in these tasks should not be a salient factor at the level of the cortex. In mesopic decision processing, rod and cone signals should be considered as largely interchangeable in terms of postreceptoral visual processing and decision processing for final perception (Cao and Pokorny, 2010). However, if a retinal disease preferentially affects a particular photoreceptor class, thereby affecting rod and cone contributions to the retinogeniculate pathways and rod and cone interactions, visual perception may be affected. Therefore, the study of changes in rod and cone contributions and interactions in neural pathways in diseases may be helpful in understanding the mechanisms of visual loss. Expanding the study of retinal diseases by examining visual perception under mesopic conditions may prove to be illuminating.

AUTHOR CONTRIBUTIONS

The Authors made equal intellectual contributions to the paper and are accountable for all intellectual aspects of the work.

ACKNOWLEDGMENTS

Supported by the Australian Research Council ARC-DP140100333 (Andrew J. Zele), NIH National Eye Institute R01EY019651 (Dingcai Cao), UIC core grant for vision research P30-EY01792 and an Unrestricted Departmental Grant from the Research to Prevent Blindness.

REFERENCES

Aguilar, M., and Stiles, W. S. (1954). Saturation of the rod mechanism of the retina at high levels of illumination. *Opt. Acta* 1, 59–65. doi: 10.1080/713818657

Alexander, K. R., and Fishman, G. A. (1984). Rod-cone interaction in flicker perimetry. *Br. J. Ophthalmol.* 68, 303–309. doi: 10.1136/bjo.68.5.303

Alexander, K. R., Fishman, G. A., and Derlacki, D. J. (1988). Mechanisms of rod-cone interaction: evidence from congenital stationary nightblindness. *Vision Res.* 28, 575–583. doi: 10.1016/0042-6989(88)90107-1

Altimus, C. M., Guler, A. D., Villa, K. L., McNeill, D. S., Legates, T. A., and Hattar, S. (2008). Rods-cones and melanopsin detect light and dark to modulate sleep independent of image formation. *Proc. Natl. Acad. Sci. U.S.A.* 105, 19998–20003. doi: 10.1073/pnas.0808312105

Ambler, B. A. (1974). Hue discrimination in peripheral vision under conditions of dark and light adaptation. *Percept. Psychophys.* 15, 586–590. doi: 10.3758/BF03199306

Anderson, A. J., and Vingrys, A. J. (2001). Multiple processes mediate flicker sensitivity. *Vision Res.* 41, 2449–2455. doi: 10.1016/S0042-6989(01)00139-0

Arden, G. B., and Hogg, C. R. (1985). Rod-cone interactions and analysis of retinal disease. *Br. J. Ophthalmol.* 69, 404–415. doi: 10.1136/bjo.69.6.404

Barbur, J. L. (1982). Reaction-time determination of the latency between visual signals generated by rods and cones. *Ophthalmic Physiol. Opt.* 2, 179–185. doi: 10.1111/j.1475-1313.1982.tb00175.x

Barbur, J. L., Dunn, G. M., and Wilson, J. A. (1986). The perception of moving comets at high retinal illuminance levels: a rod-cone interaction effect. *Biol. Cybern.* 55, 145–158. doi: 10.1007/BF00341930

Barbur, J. L., and Stockman, A. (2010). "Photopic, mesopic and scotopic vision and changes in visual performance," in: *Encyclopedia of the Eye*, eds D. E. Dartt, J. C. Besharse, and R. Dana (Oxford: Elsevier), 323–331. doi: 10.1016/B978-0-12-374203-2.00233-5

Barlow, H. B. (1958). Temporal and spatial summation in human vision at different background intensities. *J. Physiol.* 141, 337–350. doi: 10.1113/jphysiol.1958.sp005978

Barrionuevo, P. A., and Cao, D. (2014). Contributions of rhodopsin, cone opsins, and melanopsin to postreceptoral pathways inferred from natural image statistics. *J. Opt. Soc. Am. A Opt. Image Sci. Vis.* 31, A131–A139. doi: 10.1364/JOSAA.31.00A131

Barrionuevo, P. A., Nicandro, N., McAnany, J. J., Zele, A. J., Gamlin, P., and Cao, D. (2014). Assessing rod, cone, and melanopsin contributions to human pupil flicker responses. *Invest. Ophthalmol. Vis. Sci.* 55, 719–727. doi: 10.1167/iovs.13-13252

Benimoff, N., Schneider, S., and Hood, D. C. (1982). Interactions between rod and cone channels above threshold: a test of various models. *Vision Res.* 22, 1133–1140. doi: 10.1016/0042-6989(82)90078-5

Brown, W. R. J. (1951). The influence of luminance level on visual sensitivity to color differences. *J. Opt. Soc. Am.* 41, 684–688. doi: 10.1364/JOSA.41.000684

Buck, S. L. (1985). Cone-rod interaction over time and space. *Vision Res.* 25, 907–916. doi: 10.1016/0042-6989(85)90201-9

Buck, S. L. (1997). Influence of rod signals on hue perception: evidence from successive scotopic contrast. *Vision Res.* 37, 1295–1301. doi: 10.1016/S0042-6989(96)00276-3

Buck, S. L. (2001). What is the hue of rod vision? *Color Res. Appl.* 26, S57–S59. doi: 10.1002/1520-6378(2001)26:1+<::AID-COL13>3.0.CO;2-J

Buck, S. L. (2004). "Rod-cone interactions in human vision," in *The Visual Neurosciences*, eds L. M. Chalupa and J. Werner (Cambridge, MA: MIT Press), 863–878.

Buck, S. L. (2014). "The interaction of rod and cone signals: Pathways and psychophysics," in *The New Visual Neurosciences*, eds L. M. Chalupa and J. Werner (Cambridge, MA: MIT Press), 485–499.

Buck, S. L., and DeLawyer, T. (2014). Dark versus bright equilibrium hues: rod and cone biases. *J. Opt. Soc. Am. A Opt. Image Sci. Vis.* 31, A75–A81. doi: 10.1364/JOSAA.31.000A75

Buck, S. L., Juve, R., Wisner, D., and Concepcion, A. (2012). Rod hue biases produced on CRT displays. *J. Opt. Soc. Am. A Opt. Image Sci. Vis.* 29, A36–A43. doi: 10.1364/JOSAA.29.000A36

Buck, S. L., and Knight, R. (1994). Partial additivity of rod signals with M- and L-cone signals in increment detection. *Vision Res.* 34, 2537–2545. doi: 10.1016/0042-6989(94)90240-2

Buck, S. L., Knight, R., Fowler, G., and Hunt, B. (1998). Rod influence on hue-scaling functions. *Vision Res.* 38, 3259–3263. doi: 10.1016/S0042-6989(97)00436-7

Buck, S. L., Sanocki, E., and Knight, R. (1997). "Do rod signals add with S cone signals in increment detection," in *Colour Vision Deficiencies*, ed. C. Cavonius (Dordrecht: Kluwer), 451–458.

Buck, S. L., Stefurak, D. L., Moss, C., and Regal, D. (1984). The time-course of rod-cone interaction. *Vision Res.* 24, 543–548. doi: 10.1016/0042-6989(84)90108-1

Buck, S. L., Thomas, L. P., Connor, C. R., Green, K. B., and Quintana, T. (2008). Time course of rod influences on hue perception. *Vis. Neurosci.* 25, 517–520. doi: 10.1017/S0952523808080279

Buck, S. L., Thomas, L. P., Hillyer, N., and Samuelson, E. M. (2006). Do rods influence the hue of foveal stimuli? *Vis. Neurosci.* 23, 519–523. doi: 10.1017/S0952523806233510

Calkins, D. J. (2004). "Linking retinal circuits to color opponency," in *The Visual Neurosciences*, eds L. M. Chalupa and J. Werner (Cambridge, MA: MIT Press), 989–1002.

Cameron, M. A., and Lucas, R. J. (2009). Influence of the rod photoresponse on light adaptation and circadian rhythmicity in the cone ERG. *Mol. Vis.* 15, 2209–2216.

Campbell, F. W., and Green, D. G. (1965). Optical and retinal factors affecting visual resolution. *J. Physiol.* 181, 576–593. doi: 10.1113/jphysiol.1965.sp007784

Cao, D., Lee, B. B., and Sun, H. (2010). Combination of rod and cone inputs in parasol ganglion cells of the magnocellular pathway. *J. Vis.* 10, 1–15. doi: 10.1167/10.11.4

Cao, D., and Lu, Y. H. (2012). Lateral suppression of mesopic rod and cone flicker detection. *J Opt Soc Am A Opt. Image Sci. Vis.* 29, A188–A193. doi: 10.1364/JOSAA.29.00A188

Cao, D., and Pokorny, J. (2010). Rod and cone contrast gains derived from reaction time distribution modeling. *J. Vis.* 10, 1–15. doi: 10.1167/10.2.11

Cao, D., Pokorny, J., and Grassi, M. A. (2011). Isolated mesopic rod and cone electroretinograms realized with a four-primary method. *Doc. Ophthalmol.* 123, 29–41. doi: 10.1007/s10633-011-9279-9

Cao, D., Pokorny, J., and Smith, V. C. (2005). Matching rod percepts with cone stimuli. *Vision Res.* 45, 2119–2128. doi: 10.1016/j.visres.2005.01.034.

Cao, D., Pokorny, J., Smith, V. C., and Zele, A. J. (2008a). Rod contributions to color perception: linear with rod contrast. *Vision Res.* 48, 2586–2592. doi: 10.1016/j.visres.2008.05.001

Cao, D., Zele, A. J., and Pokorny, J. (2008b). Chromatic discrimination in the presence of incremental and decremental rod pedestals. *Vis. Neurosci.* 25, 399–404. doi: 10.1017/S0952523808080425

Cao, D., Zele, A. J., Smith, V. C., and Pokorny, J. (2008c). S-cone discrimination for stimuli with spatial and temporal chromatic contrast. *Vis. Neurosci.* 25, 349–354. doi: 10.1017/S095252380808022X

Cao, D., Zele, A. J., and Pokorny, J. (2006). Dark-adapted rod suppression of cone flicker detection: evaluation of receptoral and postreceptoral interactions. *Vis. Neurosci.* 23, 531–537. doi: 10.1017/S0952523806233376

Cao, D., Zele, A. J., and Pokorny, J. (2007). Linking impulse response functions to reaction time: rod and cone reaction time data and a computational model. *Vision Res.* 47, 1060–1074. doi: 10.1016/j.visres.2006.11.027

CIE. (1989). *Mesopic Photometry: History, Special Problems, and Practical Solutions.* Publication CIE No. 81. Paris: Bureau Central de la CIE, TC 1–01.

CIE. (1994). *Light as a True Visual Quantity: Principles of Measurement.* Publication CIE No. 41. 1st Edn 1978/Reprint 1994 Edn. Paris: Bureau Central de la CIE.

CIE. (2001). *Testing of Supplementary Systems of Photometry.* Vienna: Bureau of the Commission Internationale de l'Eclairage, CIE Publication No. 141.

Coletta, N. J., and Adams, A. J. (1984). Rod cone interaction in flicker detection. *Vision Res.* 24, 1333–1340. doi: 10.1016/0042-6989(84)90188-3

Coletta, N. J., and Adams, A. J. (1985). Loss of flicker sensitivity on dim backgrounds in normal and dichromatic observers. *Invest. Ophthomol. Vis. Sci.* 26, 187.

Conner, J. D. (1982). The temporal properties of rod vision. *J. Physiol.* 332, 139–155. doi: 10.1113/jphysiol.1982.sp014406

Conner, J. D., and MacLeod, D. I. (1977). Rod photoreceptors detect rapid flicker. *Science* 195, 698–699. doi: 10.1126/science.841308

Crawford, B. H. (1936). The dependence of pupil size upon external light stimulus under static and variable conditions. *Proc. R. Soc. Lon. Ser. B Biol. Sci.* 121, 376–395.

Crawford, B. H., and Palmer, D. A. (1985). The scotopic visibility curve and cone intrusion. *Vision Res.* 25, 863–866. doi: 10.1016/0042-6989(85)90194-4

Crook, J. D., Davenport, C. M., Peterson, B. B., Packer, O. S., Detwiler, P. B., and Dacey, D. M. (2009). Parallel ON and OFF cone bipolar inputs establish spatially coextensive receptive field structure of blue-yellow ganglion cells in primate retina. *J. Neurosci.* 29, 8372–8387. doi: 10.1523/JNEUROSCI.1218-09.2009

Curcio, C. A., Sloan, K. R., Kalina, R. E., and Hendrickson, A. E. (1990). Human photoreceptor topography. *J. Comp. Neurol.* 292, 497–523. doi: 10.1002/cne.902920402

Dacey, D. M. (2000). Parallel pathways for spectral coding in primate retina. *Annu. Rev. Neurosci.* 23, 743–775. doi: 10.1146/annurev.neuro.23.1.743

Dacey, D. M., Lee, B., Stafford, B. D., Pokorny, K. J., and Smith, V. C. (1996). Horizontal cells of the primate retina: cone specificity without spectral opponency. *Science* 271, 656–659. doi: 10.1126/science.271.5249.656

Daw, N. W., Jensen, E. J., and Bunken, W. J. (1990). Rod pathways in the mammalian retinae. *Trends Neurosci.* 13, 110–115. doi: 10.1016/0166-2236(90)90187-F

de Lange, H. (1954). Experiments on flicker and some calculations on an electrical analogue of the foveal systems. *Physica* 8, 935–950.

DeValois, R. L., and DeValois, K. K. (1993). A multi-stage color model. *Vision Res.* 33, 1053–1065. doi: 10.1016/0042-6989(93)90240-W

Drum, B. (1982). Summation of rod and cone responses at absolute threshold. *Vision Res.* 22, 823–826. doi: 10.1016/0042-6989(82)90014-1

Dunn, F. A., Lankheet, M. J., and Rieke, F. (2007). Light adaptation in cone vision involves switching between receptor and post-receptor sites. *Nature* 449, 603–606. doi: 10.1038/nature06150

Elliott, S. L., and Cao, D. (2013). Scotopic hue percepts in natural scenes. *J. Vis.* 13, 15. doi: 10.1167/13.13.15

Estévez, O., and Spekreijse, H. (1982). The silent substitution method in visual research. *Vision Res.* 22, 681–691. doi: 10.1016/0042-6989(82)90104-3

Falcao-Reis, F. M., Hogg, C. R., Frumkes, T. E., and Arden, G. B. (1991). Nyctalopia with normal rod function: a suppression of cones by rods. *Eye* 5, 138–144. doi: 10.1038/eye.1991.25

Fan-Paul, N. I., Li, J., Miller, J. S., and Florakis, G. J. (2002). Night vision disturbances after corneal refractive surgery. *Surv. Ophthalmol.* 47, 533–546. doi: 10.1016/S0039-6257(02)00350-8

Feigl, B., Cao, D., Morris, C. P., and Zele, A. J. (2011). Persons with age-related maculopathy risk genotypes and clinically normal eyes have reduced mesopic vision. *Invest. Ophthomol. Vis. Sci.* 52, 1145–1150. doi: 10.1167/iovs.10-5967

Feigl, B., and Zele, A. J. (2010). Macular function in tilted disc syndrome. *Doc. Ophthalmol.* 120, 201–203. doi: 10.1007/s10633-010-9215-4

Feigl, B., and Zele, A. J. (2014). Melanopsin-expressing intrinsically photosensitive retinal ganglion cells in retinal disease. *Optometry Vis. Sci.* 91, 894–903. doi: 10.1097/OPX.0000000000000284

Field, G. D., Greschner, M., Gauthier, J. L., Rangel, C., Shlens, J., Sher, A., et al. (2009). High-sensitivity rod photoreceptor input to the blue-yellow color opponent pathway in macaque retina. *Nat. Neurosci.* 12, 1159–1164. doi: 10.1038/nn.2353

Foote, K. G., and Buck, S. L. (2014). Rod hue biases for foveal stimuli on CRT displays. *J. Opt. Soc. Am. A Opt. Image Sci. Vis.* 31, A23–A26. doi: 10.1364/JOSAA.31.000A23

Frumkes, T. E., and Eysteinsson, T. (1988). The cellular basis for suppressive rod cone interaction. *Vis. Neurosci.* 1, 263–273. doi: 10.1017/S0952523800001929

Frumkes, T. E., Naarendorp, F., and Goldberg, S. H. (1988). Abnormalities in retinal neurocircuitry in protanopes: evidence provided by psychophysical investigation of temporal-spatial interaction. *Invest. Ophthomol. Vis. Sci.* 29, 163.

Gilbert, M. (1950). Colour perception in parafoveal vision. *Proc. Physical. Soc. B* 63, 83–89. doi: 10.1088/0370-1301/63/2/303

Goldberg, S. H., Frumkes, T. E., and Nygaard, R. W. (1983). Inhibitory influence of unstimulated rods in the human retina: evidence provided by examining cone flicker. *Science* 221, 180–182. doi: 10.1126/science.6857279

Gouras, P., and Link, K. (1966). Rod and cone interaction in dark-adapted monkey ganglion cells. *J. Physiol.* 184, 499–510. doi: 10.1113/jphysiol.1966.sp007928

Grünert, U. (1997). Anatomical evidence for rod input to the parvocellular pathway in the visual system of the primate. *Eur. J. Neurosci.* 9, 617–621. doi: 10.1111/j.1460-9568.1997.tb01638.x

He, S., and MacLeod, D. I. (2000). Spatial and temporal properties of light adaptation in the rod system. *Vision Res.* 40, 3073–3081. doi: 10.1016/S0042-6989(00)00141-3

He, Y., Bierman, A., and Rea, M. S. (1998). A system of mesopic photometry. *Light. Res. Technol.* 30, 175–181. doi: 10.1177/096032719803000407

He, Y., Rea, M., Bierman, A., and Bullough, J. (1997). Evaluating light source efficacy under mesopic conditions using reaction times. *J. Illum. Eng. Soc.* 26, 125–138. doi: 10.1080/00994480.1997.10748173

Hecht, S., and Hsia, Y. (1945). Dark adaptation following light adaptation to red and white lights. *J. Opt. Soc. Am.* 35, 261–267. doi: 10.1364/JOSA.35.000261

Hecht, S., and Mintz, E. U. (1939). The visibility of single lines at various illuminations and the retinal basis of visual resolution. *J. Gen. Physiol.* 22, 593–612. doi: 10.1085/jgp.22.5.593

Hecht, S., Shlaer, S., and Pirenne, M. H. (1942). Energy, quanta and vision. *J. Gen. Physiol.* 224, 665–699.

Helmholtz, H. (1924). *Physiological Optics*, Third German Edn, Vol. 3, ed. J. P. C. Southall (Rochester, New York: Optical Society of America).

Hering, E. (1964). *Outlines of a Theory of the Light Sense*, trans. L. M. Hurvich and D. Jameson (Cambridge, MA: Harvard University Press).

Hess, R. F., and Nordby, K. (1986). Spatial and temporal properties of human rod vision in the achromat. *J. Physiol.* 371, 387–406. doi: 10.1113/jphysiol.1986.sp015982

Hood, D. C., and Finkelstein, M. A. (1986). "Sensitivity to Light," in *Handbook of Perception and Human Performance, Sensory Processes and Perception*, Vol. 1, ed. K. Boff, R. L. Kaufman, and J. Thomas (New York: John Wiley & Sons).

Hornstein, E. P., Verweij, J., Li, P. H., and Schnapf, J. L. (2005). Gap-junctional coupling and absolute sensitivity of photoreceptors in macaque retina. *J. Neurosci.* 25, 11201–11209. doi: 10.1523/JNEUROSCI.3416-05.2005

Hurvich, L. M., and Jameson, D. (1957). An opponent-process theory of color vision. *Psychol. Rev.* 6, 384–404. doi: 10.1037/h0041403

Ikeda, M., and Shimozono, H. (1981). Mesopic luminous-efficiency functions. *J. Opt. Soc. Am.* 71, 280–284. doi: 10.1364/JOSA.71.000280

Ikeda, M., and Urakubo, M. (1969). Rod-cone interrelation. *J. Opt. Soc. Am.* 59, 217–222. doi: 10.1364/JOSA.59.000217

Ishida, T. (2002). Color identification data obtained from photopic to mesopic illuminance levels. *Color Res. Appl.* 27, 252–259. doi: 10.1002/col.10065

Kaplan, E. (2004). "The M, P, and K pathways of the primate visual system," in *The Visual Neurosciences*, eds L. M. Chalupa and J. Werner (Cambridge, MA: MIT Press), 481–493.

Kelly, D. H. (1961). Visual responses to time-dependent stimuli: I. Amplitude sensitivity measurements. *J. Opt. Soc. Am.* 51, 422–429. doi: 10.1364/JOSA.51.000422

Knight, R., and Buck, S. L. (2002). Time-dependent changes of rod influence on hue perception. *Vision Res.* 42, 1651–1662. doi: 10.1016/S0042-6989(02)00087-1

Knight, R., Buck, S. L., Fowler, G. A., and Nguyen, A. (1998). Rods affect S-cone discrimination on the Farnsworth-Munsell 100-hue test. *Vision Res.* 38, 3477–3481. doi: 10.1016/S0042-6989(97)00414-8

Knight, R., Buck, S. L., and Pereverzeva, M. (2001). Stimulus size affects rod influence on tritan chromatic discrimination. *Color Res. Appl.* 26, S65–S68. doi: 10.1002/1520-6378(2001)26:1+<::AID-COL15>3.0.CO;2-D

Knoblauch, K. (1995). "Duel bases in dichromatic color space," in *Colour Vision Deficiencies XII*, ed. B. Drum (Dordrecht: Kluwer Academic Publishers), 165–176.

Knoblauch, K., and Shevell, S. K. (2001). Relating cone signals to color appearance: failure of monotonicity in yellow/blue. *Vis. Neurosci.* 18, 901–906. doi: 10.1017/S0952523801186062

Koenig, D., and Hofer, H. (2011). The absolute threshold of cone vision. *J. Vis.* 11, 1–24. doi: 10.1167/11.1.21

Kohlrausch, A. (1931). "Tagesehen, dämmersehen, adaptation," in *Handbuch der Normalen und Pathologischen Physiologie*, eds A. Bethe, G. Bergmann, V. G. Embden, and A. Ellinger (Berlin: Springer), 1499–1594.

Kremers, J., Czop, D., and Link, B. (2009). Rod and S-cone driven ERG signals at high retinal illuminances. *Doc. Ophthalmol.* 118, 205–216. doi: 10.1007/s10633-008-9159-0

Kremers, J., and Meierkord, S. (1999). Rod-cone-interactions in deuteranopic observers: models and dynamics. *Vision Res.* 39, 3372–3385. doi: 10.1016/S0042-6989(99)00027-9

Lange, G., Denny, N., and Frumkes, T. E. (1997). Suppressive rod-cone interactions: evidence for separate retinal (temporal) and extraretinal (spatial) mechanisms in achromatic vision. *J. Opt. Soc. Am. A Opt. Image Sci. Vis.* 14, 2487–2498. doi: 10.1364/JOSAA.14.002487

Lee, B. B., Martin, P. R., and Uünert, G. R. (2010). Retinal connectivity and primate vision. *Prog. Ret. Eye Res.* 29, 622–639. doi: 10.1016/j.preteyeres.2010.08.004

Lee, B. B., Shapley, R. M., Hawken, M. J., and Sun, H. (2012). Spatial distributions of cone inputs to cells of the parvocellular pathway investigated with cone-isolating gratings. *J. Opt. Soc. Am. A Opt. Image Sci. Vis.* 29, A223–A232. doi: 10.1364/JOSAA.29.00A223

Lee, B. B., Smith, V., Pokorny, C. J., and Kremers, J. (1997). Rod inputs to macaque ganglion cells. *Vision Res.* 37, 2813–2828. doi: 10.1016/S0042-6989(97)00108-9

Lennie, P., Pokorny, J., and Smith, V. C. (1993). Luminance. *J. Opt. Soc. Am. A Opt. Image Sci. Vis.* 10, 1283–1293. doi: 10.1364/JOSAA.10.001283

Lie, I. (1963). Dark adaptation and the photochromatic interval. *Doc. Ophthalmol.* 17, 411–510. doi: 10.1007/BF00573528

Lutze, M., Smith, V. C., and Pokorny, J. (1989). Critical flicker frequency in X-chromosome linked dichromats. *Doc. Opthalmol. Proc. Ser.* 52, 69–77.

Lythgoe, R. (1931). Dark-adaptation and the peripheral colour sensations of normal subjects. *Br. J. Ophthalmol.* 15, 193–210. doi: 10.1136/bjo.15.4.193

Lythgoe, R. J., and Tansley, K. (1929). The relation of the critical frequency of flicker to the adaptation of the eye. *Proc. R. Soc. Lon. Ser. B* 105B, 60–92.

MacLeod, D. I. (1972). Rods cancel cones in flicker. *Nature* 235, 173–174. doi: 10.1038/235173a0

Maxwell, J. C. (1860). On the theory of compound colors and relations of the colors of the spectrum (Reprinted with commentary by Qasim Zaidi. *Color Res. Appl.* 18, 270–287, 1993). *Philos. Trans.* 150, 57–84. doi: 10.1098/rstl.1860.0005

McCann, J. J. (1972). Rod-cone interactions: different color sensations from identical stimuli. *Science* 176, 1255–1257. doi: 10.1126/science.176.4040.1255

McCann, J. J., and Benton, J. L. (1969). Interaction of the long-wave cones and the rods to produce color sensations. *J. Opt. Soc. Am.* 59, 103–107. doi: 10.1364/JOSA.59.000103

McCann, J. J., Benton, J. L., and McKee, S. P. (2004). Red/white projections and rod/long-wave cone color: an annotated bibliography. *J. Electron. Imag.* 13, 8–14. doi: 10.1117/1.1635830

McKee, S. P., McCann, J. J., and Benton, J. L. (1977). Color vision from rod and long-wave cone interactions: conditions in which rods contribute to multicolored images. *Vision Res.* 17, 175–185. doi: 10.1016/0042-6989(77)90080-3

Middleton, W. E. K., and Mayo, E. G. (1952). The appearance of colors in twilight. *J. Opt. Soc. Am. A Opt. Image Sci. Vis.* 42, 116–121.

Montag, E. D., and Boynton, R. M. (1987). Rod influence in dichromatic surface color perception. *Vision Res.* 27, 2153–2162. doi: 10.1016/0042-6989(87)90129-5

Moreland, J. D., and Cruz, A. (1959). Colour perception with the peripheral retina. *Opt. Acta* 6, 117–151. doi: 10.1080/713826278

Müller, G. E. (1930). Über die Farbenempfindungen. *Z. Psychol. Physiol. Sinnesorg. Ergänzung.* 17, 1–434.

Naarendorp, F., Rice, K. S., and Sieving, P. A. (1996). Summation of rod and S cone signals at threshold in human observers. *Vision Res.* 36, 2681–2688. doi: 10.1016/0042-6989(96)00023-5

Nagel, W. (1924). "Appendix: adaptation, twilight vision and the duplicity theory," in *Helmholtz's Treatise on Physiological Optics*, transl. J. P. Southall, 3rd German Edition (Rochester, NY: Optical Society of America), 313–343.

Nagy, A. L., and Boynton, R. M. (1979). Large-field color naming of dichromats with rods bleached. *J. Opt. Soc. Am.* 69, 1259–1265. doi: 10.1364/JOSA.69.001259

Nagy, A. L., and Doyal, J. A. (1993). Red-green color discrimination as a function of stimulus field size in peripheral vision. *J. Opt. Soc. Am. A Opt. Image Sci. Vis.* 10, 1147–1156. doi: 10.1364/JOSAA.10.001147

Neitz, J., and Neitz, M. (2008). Colour vision: the wonder of hue. *Curr. Biol.* 18, R700–R702. doi: 10.1016/j.cub.2008.06.062

Nerger, J. L., Volbrecht, V. J., and Ayde, C. J. (1995). Unique hue judgments as a function of test size in the fovea and at 20-deg temporal eccentricity. *J. Opt. Soc. Am. A Opt. Image Sci. Vis.* 12, 1225–1232. doi: 10.1364/JOSAA.12.001225

Nerger, J. L., Volbrecht, V. J., Ayde, C. J., and Imhoff, S. M. (1998). Effect of the S-cone mosaic and rods on red/green equilibria. *J. Opt. Soc. Am. A Opt. Image Sci. Vis.* 15, 2816–2826. doi: 10.1364/JOSAA.15.002816

Nerger, J. L., Volbrecht, V. J., and Haase, K. A. (2003). "The influence of rods on colour naming during dark adaptation," in *Normal and Defective Colour Vision*, ed. J. Mollon, J. Pokorny, and K. Knoblauch (Oxford: Oxford University Press), 173–178.

Petzold, A., and Plant, G. T. (2006). Clinical disorders affecting mesopic vision. *Ophthalmic. Physiol. Opt.* 26, 326–341. doi: 10.1111/j.1475-1313.2006.00417.x

Pitts, M. A., Troup, L. J., Volbrecht, V. J., and Nerger, J. L. (2005). Chromatic perceptive field sizes change with retinal illuminance. *J. Vis.* 5, 435–443. doi: 10.1167/5.5.4

Pokorny, J., Lutze, M., Cao, D., and Zele, A. J. (2006). The color of night: surface color perception under dim illuminations. *Vis. Neurosci.* 23, 525–530. doi: 10.1017/S0952523806233492

Pokorny, J., Lutze, M., Cao, D., and Zele, A. J. (2008). The color of night: surface color categorization by color defective observers under dim illuminations. *Vis. Neurosci.* 25, 475–480. doi: 10.1017/S0952523808080486

Pokorny, J., and Smith, V. C. (1997). "How much light reaches the retina?," in *Documenta Ophthalmologica Proceedings Series; Colour Vision Deficiencies XIII*, ed. C. Cavonius, (Great Britain: Kluwer Academic Publishers), 491–511.

Pokorny, J., Smithson, H., and Quinlan, J. (2004). Photostimulator allowing independent control of rods and the three cone types. *Vis. Neurosci.* 21, 263–267. doi: 10.1017/S0952523804213207

Pokorny, J., Sun, V. C. W., and Smith, V. C. (2003). Temporal dynamics of early light adaptation. *J. Vis.* 3, 423–431. doi: 10.1167/3.6.3

Polyak, S. L. (1941). *The Retina*. Chicago: University of Chicago Press.

Purkinje, J. (1825). *Beobachtungen und Versuche zur Physiologie der Sinne. Neue Beiträge zur Kenntniss des Sehens in subjectiver Hinsicht*. Berlin: Reimer.

Purpura, K., Kaplan, E., and Shapley, R. M. (1988). Background light and the contrast gain of primate P and M retinal ganglion cells. *Proc. Natl. Acad. Sci. U.S.A.* 85, 4534–4537. doi: 10.1073/pnas.85.12.4534

Raninen, A., and Rovamo, J. (1986). Perimetry of critical flicker frequency in human rod and cone vision. *Vision Res.* 26, 1249–1255. doi: 10.1016/0042-6989(86)90105-7

Raphael, S., and MacLeod, D. I. (2011). Mesopic luminance assessed with minimum motion photometry. *J. Vis.* 11, 1–21. doi: 10.1167/11.9.14

Ribelayga, C., Cao, Y., and Mangel, S. C. (2008). The circadian clock in the retina controls rod-cone coupling. *Neuron* 59, 790–801. doi: 10.1016/j.neuron.2008.07.017

Rodieck, R. W. (1991). "Which cells code for color?," in: *Pigments to Perception*, eds A. Valberg and B. B. Lee (New York: Plenum), 83–93. doi: 10.1007/978-1-4615-3718-2_10

Saugstad, P., and Saugstad, A. (1959). The duplicity theory. An evaluation. *Adv. Ophthalmol.* 9, 1–51.

Scheibner, H. M., and Boynton, R. M. (1968). Residual red-green discrimination in dichromats. *J. Opt. Soc. Am. A Opt. Image Sci. Vis.* 58, 1151–1158.

Schneeweis, D. M., and Schnapf, J. L. (1995). Photovoltage of rods and cones in the macaque retina. *Science* 268, 1053–1056. doi: 10.1126/science.7754386

Schultze, M. (1866). Zur anatomie und physiologie der retina. *Arch. Mikr. Anat. Entwicklungsmech* 2, 175–286. doi: 10.1007/BF02962033

Seeliger, M. W., Brombas, A., Weiler, R., Humphries, P., Knop, G., Tanimoto, N., et al. (2011). Modulation of rod photoreceptor output by HCN1 channels is essential for regular mesopic cone vision. *Nat. Commun.* 2:532. doi: 10.1038/ncomms1540

Shapiro, A. G. (2002). Cone-specific mediation of rod sensitivity in trichromatic observers. *Invest. Ophthamol. Vis. Sci.* 43, 898–905.

Shapiro, A. G., Pokorny, J., and Smith, V. C. (1994). Rod contribution to large field color-matching. *Color Res. Appl.* 19, 236–245. doi: 10.1002/col.5080190404

Shapiro, A. G., Pokorny, J., and Smith, V. C. (1996a). Cone-Rod receptor spaces, with illustrations that use CRT phosphor and light-emitting-diode spectra. *J. Opt. Soc. Am. A Opt. Image Sci. Vis.* 13, 2319–2328. doi: 10.1364/JOSAA.13.002319

Shapiro, A. G., Pokorny, J., and Smith, V. C. (1996b). An investigation of scotopic threshold-versus-illuminance curves for the analysis of color-matching data. *Color. Res. Appl.* 21, 80–86. doi: 10.1002/(SICI)1520-6378(199604)21:2<80::AID-COL1>3.0.CO;2-0

Sharpe, L. T., Fach, C., and Stockman, A. (1992). The field adaptation of the human rod visual system. *J. Physiol.* 445, 319–343. doi: 10.1113/jphysiol.1992.sp018926

Sharpe, L. T., and Stockman, A. (1999). Rod pathways: the importance of seeing nothing. *Trends in Neurosci.* 22, 497–504. doi: 10.1016/S0166-2236(99)01458-7

Sharpe, L. T., Stockman, A., and MacLeod, D. I. (1989). Rod flicker perception: scotopic duality, phase lags and destructive interference. *Vision Res.* 29, 1539–1559. doi: 10.1016/0042-6989(89)90137-5

Shepherd, A. J., and Wyatt, G. (2008). Changes in induced hues at low luminance and following dark adaptation suggest rod-cone interactions may differ for luminance increments and decrements. *Vis. Neurosci.* 25, 387–394. doi: 10.1017/S0952523808080358

Shin, J. C., Yaguchi, H., and Shioiri, S. (2004). Change of color appearance in photopic, mesopic and scotopic vision. *Opt. Rev.* 11, 265–271. doi: 10.1007/s10043-004-0265-2

Smith, G., Vingrys, A. J., Maddocks, J. D., and Hely, C. P. (1994). Color recognition and discrimination under full moonlight. *Appl. Optics* 33, 4741–4748. doi: 10.1364/AO.33.004741

Smith, V. C., and Pokorny, J. (1972). Spectral sensitivity of color-blind observers and the human cone photopigments. *Vision Res.* 12, 2059. doi: 10.1016/0042-6989(72)90058-2

Smith, V. C., and Pokorny, J. (1975). Spectral sensitivity of the foveal cone photopigments between 400 and 500 nm. *Vision Res.* 15, 161–171. doi: 10.1016/0042-6989(75)90203-5

Smith, V. C., and Pokorny, J. (1977). Large-field trichromacy in protanopes and deuteranopes. *J. Opt. Soc. Am.* 67, 213–220. doi: 10.1364/JOSA.67.000213

Smith, V. C., Pokorny, J., and Sun, H. (2000). Chromatic contrast discrimination: data and prediction for stimuli varying in L and M cone excitation. *Color Res. Appl.* 25, 105–115. doi: 10.1002/(SICI)1520-6378(200004)25:2<105::AID-COL5>3.0.CO;2-G

Stabell, B., and Stabell, U. (1976). Effects of rod activity on colour threshold. *Vision Res.* 16, 1105–1110. doi: 10.1016/0042-6989(76)90250-9

Stabell, B., and Stabell, U. (1979). Rod and cone contributions to change in hue with eccentricity. *Vision Res.* 19, 1121–1125. doi: 10.1016/0042-6989(79)90007-5

Stabell, B., and Stabell, U. (2009). *The Duplicity Theory of Vision: From Newton to the Present.* Cambridge: Cambridge University Press. doi: 10.1017/CBO9780511605413

Stabell, U., and Stabell, B. (1971). Chromatic rod vision. II. Wavelength of pre-stimulation varied. *Scand. J. Psychol.* 12, 282–288. doi: 10.1111/j.1467-9450.1971.tb00631.x

Stabell, U., and Stabell, B. (1975a). The effect of rod activity on colour matching functions. *Vision Res.* 15, 1119–1123. doi: 10.1016/0042-6989(75)90010-3

Stabell, U., and Stabell, B. (1975b). Scotopic contrast hues triggered by rod activity. *Vision Res* 15, 1119–1123. doi: 10.1016/0042-6989(75)90009-7

Stabell, U., and Stabell, B. (1977). Wavelength discrimination of peripheral cones and its change with rod intrusion. *Vision Res.* 17, 423–426. doi: 10.1016/0042-6989(77)90034-7

Stabell, U., and Stabell, B. (1994). Mechanisms of chromatic rod vision in scotopic illumination. *Vision Res.* 34, 1019–1027. doi: 10.1016/0042-6989(94)90006-X

Stockman, A., and Sharpe, L. T. (2006). Into the twilight zone: the complexities of mesopic vision and luminous efficiency. *Ophthal. Physl. Opt.* 26, 225–239. doi: 10.1111/j.1475-1313.2006.00325.x

Stockman, A., Sharpe, L. T., Ruther, K., and Nordby, K. (1995). Two signals in the human rod visual system: a model based on electrophysiological data. *Vis. Neurosci.* 12, 951–970. doi: 10.1017/S0952523800009500

Stockman, A., Sharpe, L. T., Zrenner, E., and Nordby, K. (1991). Slow and fast pathways in the human rod visual system: electrophysiology and psychophysics. *J. Opt. Soc. Am. A Opt. Image Sci. Vis.* 8, 1657–1665. doi: 10.1364/JOSAA.8.001657

Sun, H., Pokorny, J., and Smith, V. C. (2001a). Control of the modulation of human photoreceptors. *Color Res. Appl.* 26, S69–S75. doi: 10.1002/1520-6378(2001)26:1+<::AID-COL16>3.0.CO;2-A

Sun, H., Pokorny, J., and Smith, V. C. (2001b). Brightness Induction from rods. *J. Vision* 1, 32–41. doi: 10.1167/1.1.4

Sun, H., Pokorny, J., and Smith, V. C. (2001c). Rod-cone interaction assessed in inferred magnocellular and parvocellular postreceptoral pathways. *J. Vision* 1, 42–54. doi: 10.1167/1.1.5

Tailby, C., Solomon, S. G., and Lennie, P. (2008). Functional asymmetries in visual pathways carrying S-cone signals in macaque. *J. Neurosci.* 28, 4078–4087. doi: 10.1523/JNEUROSCI.5338-07.2008

Thomas, L. P., and Buck, S. L. (2004). Generality of rod hue biases with smaller, brighter, and photopically specified stimuli. *Vis. Neurosci* 21, 257–262.

Thomson, L. C., and Trezona, P. W. (1951). The variations of hue discrimination with change of luminance level. *J. Physiol.* 114, 98–106. doi: 10.1113/jphysiol.1951.sp004606

Trezona, P. W. (1970). Rod participation in the 'blue' mechanism and its effect on colour matching. *Vision Res.* 10, 317–332. doi: 10.1016/0042-6989(70)90103-3

Troup, L. J., Pitts, M. A., Volbrecht, V. J., and Nerger, J. L. (2005). Effect of stimulus intensity on the sizes of chromatic perceptive fields. *J. Opt. Soc. Am. A Opt. Image Sci. Vis.* 22, 2137–2142. doi: 10.1364/JOSAA.22.002137

van den Berg, T. J. T. P., and Spekreijse, H. (1977). Interaction between rod and cone signals studied with temporal sine wave stimulation. *J. Opt. Soc. Am.* 67, 1210–1217. doi: 10.1364/JOSA.67.001210

Verriest, G. (1963). Further studies on acquired deficiency of color discrimination. *J. Opt. Soc. Am.* 53, 185–195. doi: 10.1364/JOSA.53.000185

Verweij, J. B., Peterson, B., Dacey, D. M., and Buck, S. L. (1999). Sensitivity and dynamics of rod signals in H1 horizontal cells of the macaque monkey retina. *Vision Res.* 39, 3662–3672. doi: 10.1016/S0042-6989(99)00093-0

Virsu, V., and Lee, B. B. (1983). Light adaptation in cells of macaque lateral geniculate nucleus and its relation to human light adaptation. *J. Neurophysiol.* 50, 864–878.

Virsu, V., Lee, B. B., and Creutzfeldt, O. D. (1987). Mesopic spectral responses and the Purkinje shift of macaque lateral geniculate cells. *Vision Res.* 27, 191–200. doi: 10.1016/0042-6989(87)90181-7

Volbrecht, V. J., Clark, C. L., Nerger, J. L., and Randell, C. E. (2009). Chromatic perceptive field sizes measured at 10 degrees eccentricity along the horizontal and vertical meridians. *J. Opt. Soc. Am. A Opt. Image Sci. Vis.* 26, 1167–1177. doi: 10.1364/JOSAA.26.001167

Volbrecht, V. J., Nerger, J. L., Baker, L. S., Trujillo, A. R., and Youngpeter, K. (2010). Unique hue loci differ with methodology. *Ophthal. Physl. Opt.* 30, 545–552. doi: 10.1111/j.1475-1313.2010.00727.x

Volbrecht, V. J., Nerger, J. L., and Trujillo, A. R. (2011). Middle- and long-wavelength discrimination declines with rod photopigment regeneration. *J. Opt. Soc. Am. A Opt. Image Sci. Vis.* 28, 2600–2606. doi: 10.1364/JOSAA.28.002600

von Kries, J. (1896). Uber die Funktion der Netzhautstabchen. *Z. Psychol. Physiol. Sinnesorg.* 9, 81–123.

Wald, G. (1945). Human vision and spectrum. *Science* 101, 653–658. doi: 10.1126/science.101.2635.653

Walkey, H. C., Barbur, J. L., Harlow, J. A., Hurden, A., Moorhead, I. R., and Taylor, J. A. (2005). Effective contrast of colored stimuli in the mesopic range: a metric for perceived contrast based on achromatic luminance contrast. *J. Opt. Soc. Am. A Opt. Image Sci. Vis.* 22, 17–28. doi: 10.1364/JOSAA.22.000017

Walkey, H. C., Barbur, J. L., Harlow, J. A., and Makous, W. (2001). Measurements of chromatic sensitivity in the mesopic range. *Color Res. Appl.* 26, S36–S42. doi: 10.1002/1520-6378(2001)26:1+<::AID-COL9>3.0.CO;2-S

Walkey, H. C., Harlow, J. A., and Barbur, J. L. (2006a). Changes in reaction time and search time with background luminance in the mesopic range. *Ophthal. Physl. Opt.* 26, 288–299. doi: 10.1111/j.1475-1313.2006.00412.x

Walkey, H. C., Harlow, J. A., and Barbur, J. L. (2006b). Characterising mesopic spectral sensitivity from reaction times. *Vision Res.* 46, 4232–4243. doi: 10.1016/j.visres.2006.08.002

Wassle, H., Grünert, U., Chun, M. H., and Boycott, B. B. (1995). The rod pathway of the macaque monkey retina: identification of AII-amacrine cells with antibodies against calretinin. *J. Comp. Neurol.* 361, 537–551. doi: 10.1002/cne.903610315

Willmer, E. N. (1949). Low threshold rods and the perception of blue. *J. Physiol. (London)* 111, 17.

Yeh, T., Lee, B. B., and Kremers, J. (1995). The temporal response of ganglion cells of the macaque retina to cone-specific modulation. *J. Opt. Soc. Am. A Opt. Image Sci. Vis.* 12, 456–464. doi: 10.1364/JOSAA.12.000456

Zele, A. J., Cao, D., and Pokorny, J. (2007). Threshold units: a correct metric for reaction time? *Vision Res.* 47, 608–611. doi: 10.1016/j.visres.2006.12.003

Zele, A. J., Cao, D., and Pokorny, J. (2008). Rod-cone interactions and the temporal impulse response of the cone pathway. *Vision Res.* 48, 2593–2598. doi: 10.1016/j.visres.2008.04.003

Zele, A. J., Kremers, J., and Feigl, B. (2012). Mesopic rod and S-cone interactions revealed by modulation thresholds. *J Opt Soc Am A Opt. Image Sci. Vis.* 29, A19–A26. doi: 10.1364/JOSAA.29.000A19

Zele, A. J., Maynard, M. L., and Feigl, B. (2013). Rod and cone pathway signaling and interaction under mesopic illumination. *J. Vision* 13, 1–19. doi: 10.1167/13.1.21

Zele, A. J., Maynard, M. L., Joyce, D. S., and Cao, D. (2014). Effect of rod-cone interactions on mesopic visual performance mediated by chromatic and luminance pathways. *J. Opt. Soc. Am. A Opt. Image Sci. Vis.* 31, A7–A14. doi: 10.1364/JOSAA.31.0000A7

Zele, A. J., Smith, V. C., and Pokorny, J. (2006). Spatial and temporal chromatic contrast: effects on chromatic discrimination for stimuli varying in L- and M-cone excitation. *Vis. Neurosci.* 23, 495–501. doi: 10.1017/S0952523806232012

Zele, A. J., and Vingrys, A. J. (2007). Defining the detection mechanisms for symmetric and rectified flicker stimuli. *Vision Res.* 47, 2700–2713. doi: 10.1016/j.visres.2007.05.005

Conflict of Interest Statement: The authors declare that the research was conducted in the absence of any commercial or financial relationships that could be construed as a potential conflict of interest.

Received: 14 October 2014; accepted: 28 December 2014; published online: 22 January 2015.

*Citation: Zele AJ and Cao D (2015) Vision under mesopic and scotopic illumination. Front. Psychol. **5**:1594. doi: 10.3389/fpsyg.2014.01594*

This article was submitted to Perception Science, a section of the journal Frontiers in Psychology.

frontiers in
PSYCHOLOGY

ORIGINAL RESEARCH ARTICLE
published: 28 January 2015
doi: 10.3389/fpsyg.2015.00053

Cortical responses elicited by luminance and compound stimuli modulated by pseudo-random sequences: comparison between normal trichromats and congenital red-green color blinds

Bárbara B. O. Risuenho[1], Letícia Miquilini[1], Eliza Maria C. B. Lacerda[1], Luiz Carlos L. Silveira[1,2,3] and Givago S. Souza[1,2] *

[1] *Instituto de Ciências Biológicas – Universidade Federal do Pará, Belém, Brazil*
[2] *Núcleo de Medicina Tropical – Universidade Federal do Pará, Belém, Brazil*
[3] *Universidade Ceuma, São Luís, Brazil*

Edited by:
Marcelo Fernandes Costa, Universidade de São Paulo, Brazil

Reviewed by:
Sophie Wuerger, University of Liverpool, UK
Thomas Wachtler, Ludwig-Maximilians-Universität München, Germany

***Correspondence:**
Givago S. Souza, Núcleo de Medicina Tropical – Universidade Federal do Pará, Av. Generalíssimo Deodoro 92 Umarizal 66055-240, Belém, Pará, Brazil
e-mail: givagosouza@ufpa.br

Conventional pattern-reversal visual evoked cortical potential (VECP) shows positivity for luminance and chromatic equiluminant stimuli while conventional pattern-onset VECP shows positivity for luminance pattern-onset and negativity for chromatic pattern-onset. We evaluated how the presentation mode affects VECPs elicited by luminance and compound (luminance plus chromatic) pseudo-random stimulation. Eleven normal trichromats and 17 red-green color-blinds were studied. Pattern-reversal and pattern-onset luminance and compound (luminance plus red-green) gratings were temporally modulated by m-sequence. We used a cross-correlation routine to extract the first order kernel (K1) and the first and second slices of the second order kernel (K2.1 and K2.2, respectively) from the VECP response. We integrated the amplitude of VECP components as a function of time in order to estimate its magnitude for each stimulus condition. We also used a normalized cross-correlation method in order to test the similarity of the VECP components. The VECP components varied with the presentation mode and the presence of red-green contrast in the stimuli. In trichromats, for compound conditions, pattern-onset K1, K2.1, and K2.2, and pattern-reversal K2.1 and K2.2 had negative-dominated waveforms at 100 ms. Small negativity or small positivity were observed in dichromats. Trichromats had larger VECP magnitude than color-blinds for compound pattern-onset K1 (with large variability across subjects), compound pattern-onset and pattern-reversal K2.1, and compound pattern-reversal K2.2. Trichromats and color-blinds had similar VECP amplitude for compound pattern-reversal K1 and compound pattern-onset K2.2, as well as for all luminance conditions. The cross-correlation analysis showed high similarity between waveforms of compound pattern-onset K2.1 and pattern-reversal K2.2 as well as pattern-reversal K2.1 and K2.2. We suggest that compound pattern-reversal K2.1 is an appropriate response to study red-green color-opponent activity.

Keywords: evoked potential, pseudo-random VECP, pattern-onset VECP, pattern-reversal VECP, color vision, trichromacy, daltonism

INTRODUCTION

Using pseudo-random stimulation it was possible to elicit negative-dominated visual evoked cortical potentials (VECP) for chromatic equiluminant contrast using both pattern-onset and pattern-reversal stimuli (Gerth et al., 2003). These findings differed from those obtained with conventional periodical stimulation (Carden et al., 1985; Suttle and Harding, 1999). When conventional periodical stimuli are used, such as sinusoidal gratings, luminance, and chromatic equiluminant pattern-reversal as well as luminance pattern-onset stimulation elicited positive-dominated VECP at around 100 ms while chromatic equiluminant pattern-onset stimulation elicited negative-dominated VECP at the same latency (Carden et al., 1985; Kulikowski and Parry, 1987; Murray et al., 1987; Kulikowski et al., 1989). Since the chromatic equiluminant pattern-onset VECP usually shows higher signal-to-noise ratio compared to chromatic equiluminant pattern-reversal VECP and also exhibit inverse polarity compared to luminance pattern-onset VECP, many have used this stimulation mode to study the mechanism of chromatic equiluminant transient VECPs (Carden et al., 1985; Kulikowski and Parry, 1987; Murray et al., 1987; Berninger et al., 1989; Kulikowski et al., 1989, 1996; Rabin et al., 1994; Porciatti and Sartucci, 1999; Gomes et al., 2006, 2008, 2010; Souza et al., 2008).

McKeefry et al. (1996) discussed about the activation of chromatic and achromatic mechanisms by pattern reversal and pattern onset–offset stimulations. They based their suggestions in the features of response from tonic and phasic cells in the visual system (Gouras, 1968; Dreher et al., 1976; Kaplan and Shapley,

1982, 1986; Hicks et al., 1983). They consider that for some stimulus selective condition the dichotomy between tonic/sustained cells and phasic/transient cells overlap with magnocellular (luminance) and parvocellular (chromatic) activity, respectively. Tonic cells has larger responses for the onset of the stimulus than for its offset due the sustained response is longer as long as the stimulus is on, and it has low responsivity to contrast reversal modulated by temporal square-wave function due its sustained nature of their response. Phasic cells had similar responses for the stimulus onset and offset due their transient response, but they has higher responses for contrast reversal with square-wave temporal modulation. McKeefry et al. (1996) found that the chromatic onset–offset VECP is dominated by a fundamental component, while the achromatic onset–offset VECP had a second harmonic additionally to the fundamental component. For pattern reversal VECPs, both chromatic and achromatic responses, had high second harmonic, which peaked at the achromatic stimulus condition and was minimum at the chromatic isoluminance.

Until now, only homogenous fields or complex patterns were used to compose pseudo-random stimuli to investigate chromatic cortical responses in different visual field sectors (Baseler and Sutter, 1997; Gerth et al., 2003). For spatial vision, additionally to dartboard stimulus (Baseler and Sutter, 1997), a stimulus composed by a matrix of triangles was also used to elicit cortical activity in multifocal VECP studies (Gerth et al., 2003). Triangle patterns were used to reduce the high spatial frequency components present in other forms of stimulation. However, it is difficult to make a straightforward association between the spatial properties of triangle patterns or dartboard patterns and those of sinusoidal gratings that are relevant for the recorded cortical responses. Sinusoidal gratings are the simplest stimuli used to study spatial vision and they were widely used in intracellular and extracellular single-unit electrophysiology, non-invasive electrophysiology, and psychophysics (e.g., Carden et al., 1985; Mullen, 1985; Lee et al., 1989).

Gerth et al. (2003) showed that chromatic pseudo-random VECP had the same polarity nevertheless the presentation mode used to elicit the cortical response, but in their study it lacking the comparison with luminance VECPs. Based in the findings of the effects of the pattern mode presentation on conventional VECPs we could expect that different pseudo random VECP waveforms would be elicited by achromatic and chromatic stimulus for trichromat observers, and color-blind subjects would have decrease or absent responses for chromatic stimulation.

Some studies indicated that the use of non-linear analysis with the separation of the visual response in different states of adaptation (kernels) permit to investigate the presence of mechanisms in the cortical response with different physiological properties distributed in the different kernels (Crewther and Crewther, 2010; Araújo et al., 2013). In the present study, we applied the paradigm of Gerth et al. (2003) by using sinusoidal gratings in order to evaluate how the presentation mode affects luminance and chromatic pseudo-random VECPs. Responses obtained from normal trichromats and red-green congenital color-blinds were compared. A short communication comprising some results of this work was previously presented in the ARVO Annual Meeting (Souza et al., 2012).

MATERIALS AND METHODS

SUBJECTS

All procedures were approved by the Ethic Research Committee of the Tropical Medicine Nucleus, Federal University of Para (Protocol #023/2011). Eleven normal trichromats (21.28 ± 1.86 years old) and 17 red-green congenital color-blinds (eight protans and nine deutans) were monocularly tested. None of the subjects had previous visual or neurological diseases. We evaluated subject color vision using the Ishihara Plates (1997 38-plate edition; Kanehara & Co Ltd, Tokyo, Japan), an anomaloscope (HMC-Anomaloskop model 47715, Oculus Optikgeräte GmbH, Wetzlar, Germany), and by measuring their color discrimination thresholds (Cambridge Colour Test, Cambridge Research System Ltd, Rochester, England, UK).

STIMULATION

Visual stimulation, bioelectric recording, and data extraction were performed using a Veris Science 6.10 system (Electro-Diagnostic Imaging, Inc., Redwood City, CA, USA). We presented luminance and compound horizontal gratings, 8°of visual angle, 2 cycles/degree in a CRT display with 75 Hz frame rate and 1280 × 1204 pixels spatial resolution (FlexScan T662, Eizo, Ishikawa, Japan).

We used sine-wave gratings for the luminance test. A yellow chromaticity (CIE 1976 color space: u' = 0.276, v' = 0.545) was modulated with 99% Michelson contrast, mean luminance of 10 cd/m^2. The background was a homogeneous field with the same chromaticity and mean luminance.

We used two chromaticities for the test with compound gratings, red (u' = 0.432, v' = 0.527) and green (u' = 0.12, v' = 0.564; **Figure 1A**). For each half cycle of the stimulus the luminance changed sinusoidally from 5 to 10 cd/m^2 and back at the same time that the chromaticity changed sinusoidally from green or red to the intermediate yellow (**Figure 1B**). The chromatic contrast was modulates along a protan confusion line and at about five away from a deutan confusion line in the CIE 1976 color space. The background had the same stimulus yellow mean chromaticity but the luminance was kept at 10 cd/m^2 throughout the entire stimulus set. For monitor calibration, we used a CS-100A Colorimeter (Minolta, Osaka, Japan). Compound gratings used in this study was similar but not entirely equal to those used previously by Lee et al. (2011) and Li et al. (2014).

A binary m-sequence ($2^{14}-1$ elements) controlled stimulus temporal presentation. We used two stimulus presentation modes: pattern-reversal and pattern-onset. For pattern-reversal, each one of two m-steps had base period of 13.3 ms and we set each of them to show each frame of the grating stimulus with 180°phase difference. Most of the multifocal VECP studies used this configuration for pattern-reversal mode (e.g., Baseler and Sutter, 1997). For pattern-onset, each m-step had a base period of 26.6 ms (two frames). The first m-step presented one frame with the grating followed by another frame with the background. The second m-step showed two consecutive frames with the background. This pattern-onset configuration was used before to improve VECP signal-to-noise ratio (Hoffmann et al., 2003). Therefore, we had four stimulus conditions: luminance pattern-reversal, luminance pattern-onset,

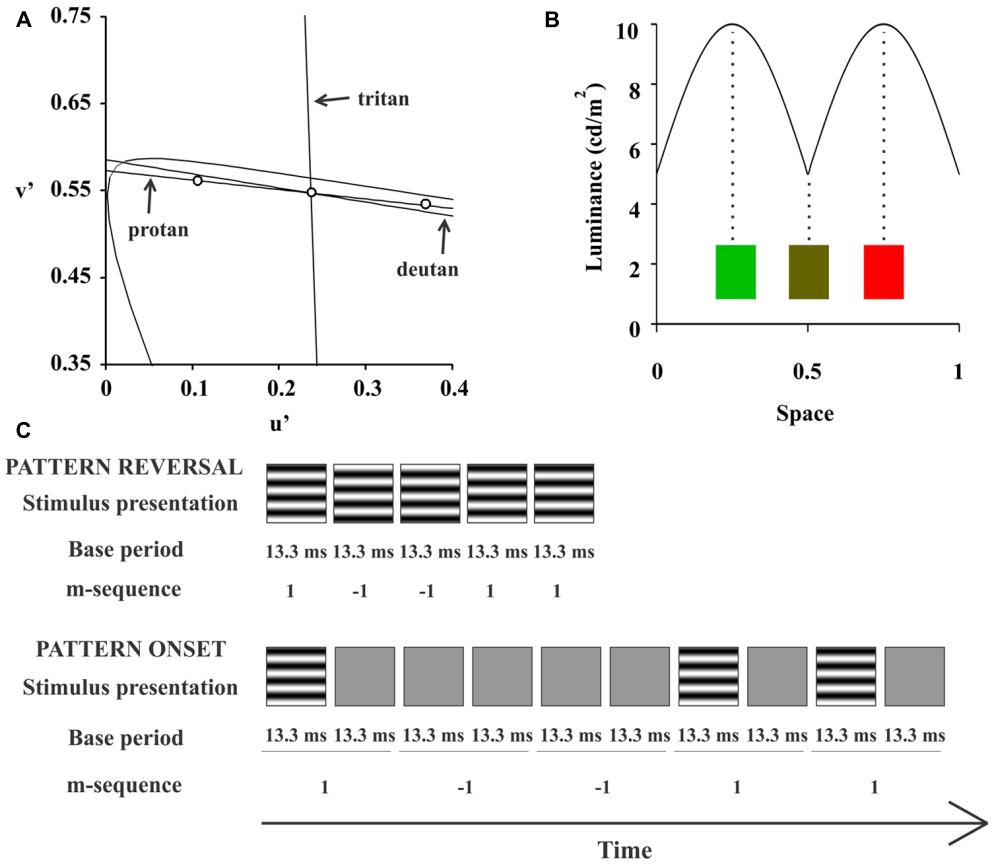

FIGURE 1 | Compound stimuli. For compound stimulation, we used two chromaticities defined in the CIE 1976 Chromaticity Diagram: red (u' = 0.432, v' = 0.527) and green (u' = 0.12, v' = 0.564; **(A)** For each half cycle of the stimulus, the luminance changed sinusoidally from 5 to 10 cd/m^2 and back, at the same time that the chromaticity changed sinusoidally from green or red to the intermediate yellow, **(B). (C)** Shows a space-time diagram of the m-sequence configuration for each presentation mode.

red-green pattern-reversal, and red-green pattern-onset. A space-time diagram of each pattern mode stimulation is shown in the **Figure 1C**.

RECORDING SETTINGS

One-channel electroencephalographic signals were recorded using 10 mm gold surface electrodes (Grass Safelead Gold Disc Electrodes, Grass Technologies, Richmond, USA). Electrode placement followed the standard of the International Society for Clinical Electrophysiology of Vision (ISCEV; Odom et al., 2010): active electrode was placed at Oz, reference electrode at Fz, and ground electrode at Fpz. Continuous recordings were amplified x50,000, on-line filtered between 0.1 and 100 Hz (P511 Amplifier, Grass Technologies), and digitized at 1.2 kHz. For each stimulus condition, we used the Veris Science version 6.010 platform to perform a cross-correlation. The kernel extraction from the VECP was set using the Veris Science software. We extracted the first order kernel (K1), second order kernel first slice (K2.1), and second order kernel second slice (K2.2). The kernel for more information about kernel significance, see Sutter (2000) and Odom (2006). After kernel extraction, the waveforms were low-pass filtered at 50 Hz.

DATA ANALYSIS

Visual evoked cortical potential kernel waveforms had several positive and negative components starting at about 70 ms after stimulus onset (**Figures 2–4**). In order to estimate the evoked response magnitude, we calculated the recording total power. The total power was taken as the numerical integration of the squared amplitude of all amplitude data in the first 500 ms of the recordings. We used Kruskal–Wallis test with Dunn's *post hoc* test ($\alpha = 0.05$) to compare the magnitude of the VECP components at different stimulus conditions. The *p*-values were corrected by Bonferroni correction.

RESULTS

VECP WAVEFORMS IN TRICHROMATS

The VECP waveforms across different kernels varied with stimulus presentation mode and presence of color contrast in the stimulus. **Figure 2** shows the VECP kernels waveforms elicited by different stimuli in trichromats. Results obtained from the 11 trichromats were averaged to provide **Figure 2** waveforms. For luminance pattern-onset stimulation, K1 had a negative peak at about 100 ms followed by a positive peak at about 150 ms. K2.1 and K2.2 also had a negative peak at 100 ms, but the positivity was

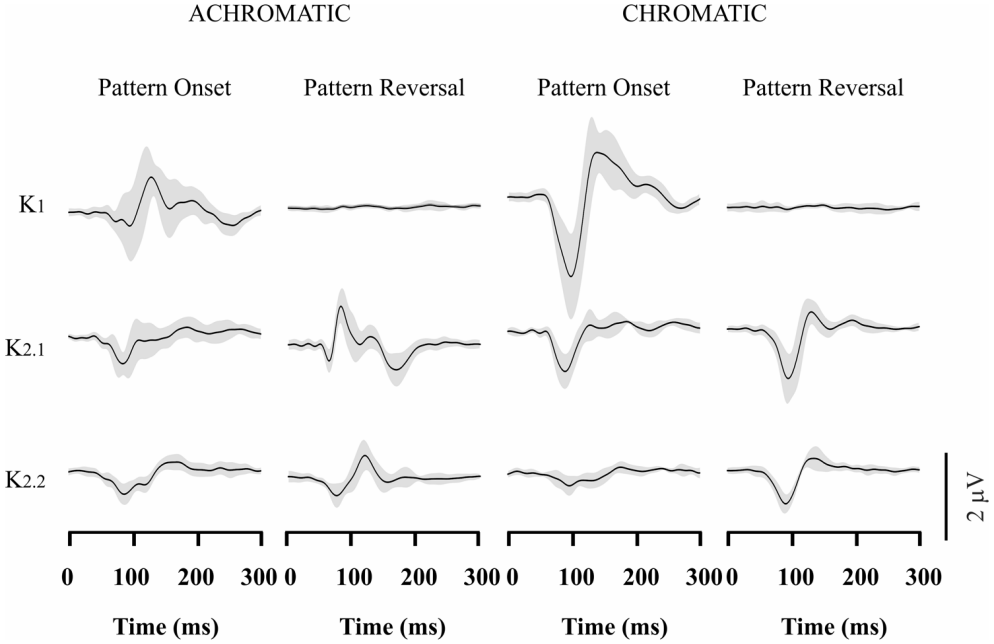

FIGURE 2 | Visual evoked cortical potential (VECP) average waveforms obtained from normal trichromats using luminance and compound stimuli, as well as pattern-onset and pattern-reversal stimulations. Waveforms were obtained by averaging results from 11 subjects. From top to bottom are depicted waveforms corresponding to the first order kernel (K1), first slice of the second order kernel (K2.1), and second slice of the second order kernel (K2.2). The average waveforms were dominated by the presence of negativity at about 100 ms for the majority of stimulus conditions and kernels. An important exception is achromatic pattern-reversal K2.1 waveform which is dominated by a positive peak at the same latency. The gray shades represent the SD of the averaged recordings. They provide an indication of interindividual variability.

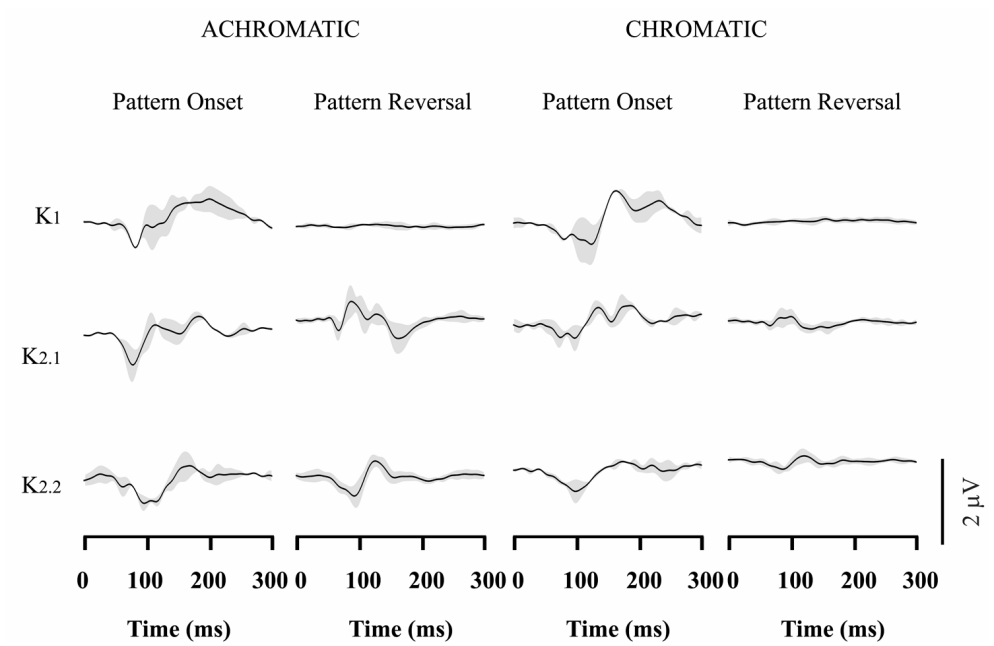

FIGURE 3 | Visual evoked cortical potential average waveforms obtained from protans using luminance and compound stimuli, as well as pattern-onset and pattern-reversal stimulations. Waveforms were obtained by averaging results from eight subjects. For luminance stimuli, VECP waveforms were similar to those obtained from trichromats. For compound stimuli, pattern-onset stimulation elicited smaller negative amplitudes than in trichromats at 100 ms, while pattern-reversal stimulation evoked no response or small positive components at the same latency. The gray shades represent the SD of the averaged recordings. They provide an indication of interindividual variability.

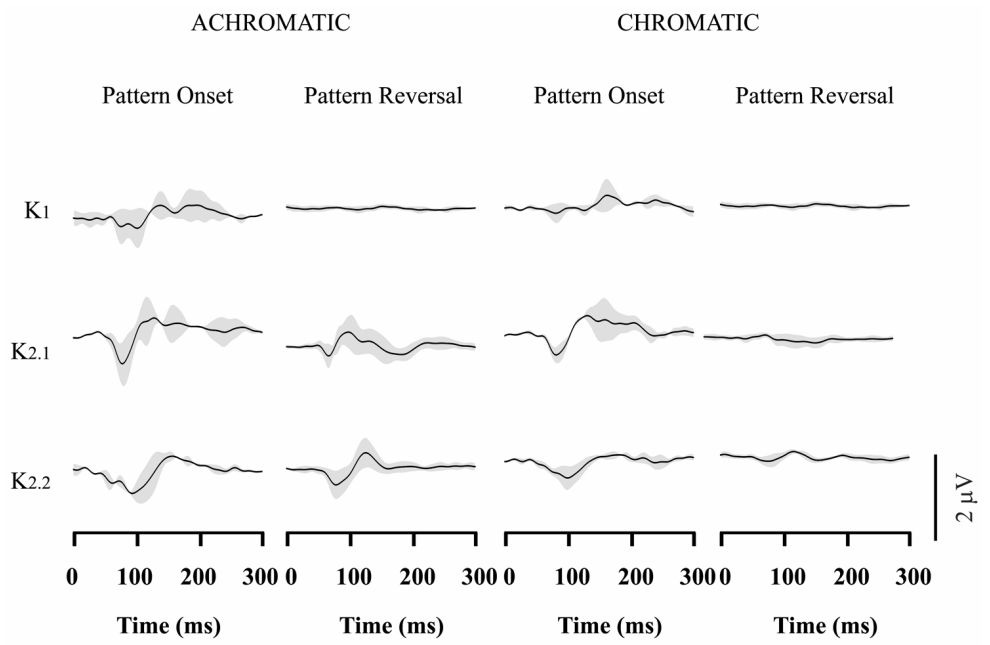

FIGURE 4 | Visual evoked cortical potential average waveforms obtained from deutans using luminance and compound stimuli, as well as pattern-onset and pattern-reversal stimulations. Waveforms were obtained by averaging results from 9 subjects. For luminance stimuli, VECP waveforms were similar to those obtained from trichromats. For compound stimuli, pattern-onset stimulation elicited smaller negative amplitudes at 100 ms than in trichromats, while pattern-reversal stimulation resulted in no response or a small positivity at the same latency. The gray shades represent the SD of the averaged recordings. They provide an indication of interindividual variability.

small or entirely missing. For luminance pattern-reversal stimulation, K1 was very small or absent, K2.1 had a negative peak at about 85 ms followed by a double-peaked positivity between 100 and 120 ms, and K2.2 had a negative peak at 100 ms followed by a positive peak at 130 ms.

For compound pattern-onset stimulation, all kernels waveforms (K1, K2.1, and K2.2) were dominated by negativity at about 100 ms. K1 also had a pronounced positive peak at 150 ms following the very pronounced main negative component. For compound pattern-reversal, similarly to luminance pattern-reversal stimulation stimulation, K1 was also very small or absent. In addition, K2.1 and K2.2 were dominated by a negativity occurring at about 100 ms. It should be noted that K2.1 showed opposite polarity for compound pattern-reversal stimulation when compared with luminance pattern-reversal stimulation. It can be interpreted as an indication of differential activation on luminance and chromatic mechanism.

VECP WAVEFORMS IN CONGENITAL RED-GREEN COLOR BLINDS

Figures 3–4 show VECP waveforms for different kernels obtained by recording from red-green congenital color blinds, either protans (**Figure 3**) or deutans (**Figure 4**). As for normal trichromats (**Figure 2**), VECP was elicited by luminance and compound stimuli as well as by pattern-onset and pattern-reversal stimulation modes. Waveforms were obtained by averaging the results obtained from eight protans and nine deutans, respectively.

Red-green color blinds responses were similar to responses obtained from normal trichromats for both kinds of luminance stimulation. For luminance pattern-onset stimulation, K1 had low-amplitude negative and positive components (slightly larger in protans when compared with deutans), while K2.1 and K2.2 were dominated by a negative peak at about 100 ms. For luminance pattern-reversal stimulation, all kernels were very similar in color blinds and normal trichromats: K1 was very small or absent, K2.1 had a negative peak at about 85 ms followed by a double-peaked positivity between 100 and 120 ms, and K2.2 had a negative peak at 100 ms followed by a positive peak at 130 ms.

For compound pattern-onset, K1 was very small or had a small negativity at about 100 ms in different color-blind subjects, was much smaller in both groups of color blinds when compared with normal trichromats, and was larger in protans when compared with deutans. K2.1 and K2.2 were dominated by a negative peak at 100 ms. K2.1 was small in deutans, slightly larger in protans, and larger in normal trichromats. K2.2 was similar in the three groups.

For compound pattern-reversal, K1 was absent while K2.1 and K2.2 were very small with a small positive component at 100 ms in both groups of color blinds. Thus, while pattern-reversal K1 was similar in normal trichromats, protans, and deutans, pattern-reversal K2.1 and K2.2 were very different between color blinds and normal trichromats.

EVALUATION OF THE VECP MAGNITUDE AND ITS COMPARISON AMONG THE KERNELS

Figures 5–6 show box-plots representing the recording total power in the first 500 ms elicited by luminance (**Figure 5**) or compound (**Figure 6**) stimuli. Results from normal trichromats are

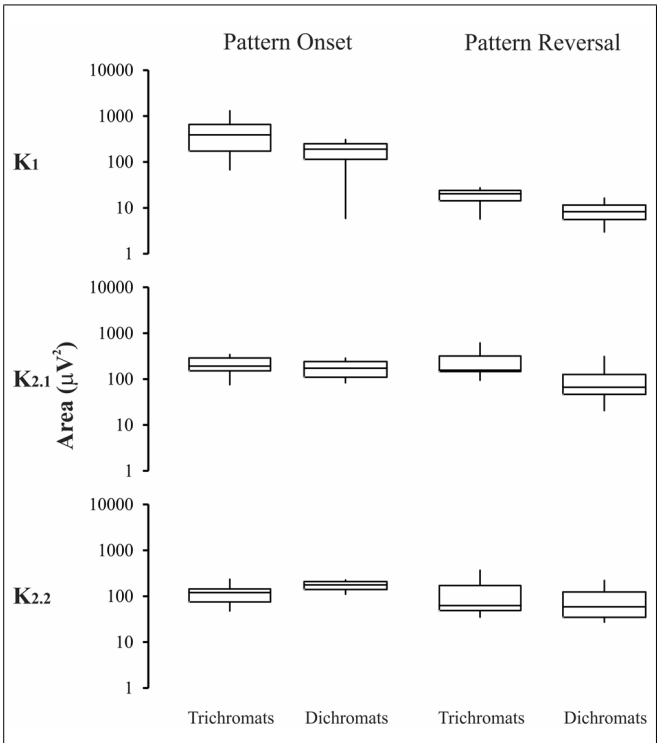

FIGURE 5 | Magnitude of the VECP elicited by luminance stimuli in trichromats and color blinds. No difference was found in the results obtained with pattern-onset and pattern-reversal for all kernels waveforms. Box-plots represent medians (middle horizontal lines), first quartiles (lower horizontal lines), third quartiles (upper horizontal lines), maximum values (upper vertical lines), and minimum values (lower vertical lines).

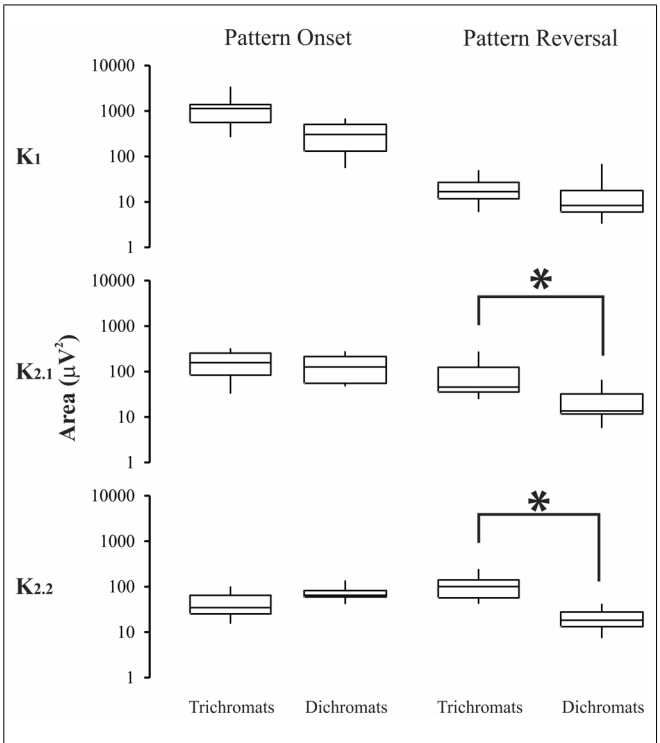

FIGURE 6 | Magnitude of the VECP elicited by compound stimuli in trichromats and color blinds. Pattern-reversal K2.1, and pattern-reversal K2.2 had higher values for trichromats than color-blinds. Asterisks (*) were used to mark statistically significant differences. Box-plots represent medians (middle horizontal lines), first quartiles (lower horizontal lines), third quartiles (upper horizontal lines), maximum values (upper vertical lines), and minimum values (lower vertical lines).

compared with those from red-green color-blinds dichromats. Protans and deutans were grouped together for this comparison with normal trichromats. For luminance stimuli (**Figure 5**) there were no significant differences ($p > 0.05$) for both pattern-onset and pattern-reversal stimulation modes and for the three kernels: pattern-onset K1, $p = 0.7$; pattern-onset K2.1, $p = 0.16$; pattern-onset K2.2, $p = 0.35$; pattern-reversal K1, $p = 0.47$; pattern-reversal K2.1, $p = 0.12$; pattern-reversal K2.2, $p = 0.98$.

For compound stimuli (**Figure 6**) trichromats had significant larger VECP magnitude than color-blinds in the pattern-reversal K2.1, and pattern-reversal K2.2 ($p < 0.05$). The results of the statistical analysis were as follows: pattern-onset K1, $p = 0.09$; pattern-onset K2.1, $p = 0.12$; pattern-onset K2.2, $p = 0.64$; pattern-reversal K1, $p = 0.57$; pattern-reversal K2.1, $p = 0.002$; pattern-reversal K2.2, $p = 0.0001$).

For the dichromats, the kernels of the chromatic waveforms were very similar to those of the achromatic waveforms with slightly reduced amplitude. However, there were no significant differences in amplitudes between the same kernel (or kernel slice).

DISCUSSION

We used pseudo-random sequences to temporally modulate luminance and compound (luminance plus red-green) sinusoidal gratings presented in pattern-onset and pattern-reversal modes. The present study introduced the use of compound gratings to study the VECP mechanisms. Previously, similar stimuli were used in psychophysical, electroretinographic, and single-unit studies (Lee et al., 2011; Parry et al., 2012; Li et al., 2014). The VECP kernels elicited by pattern-onset and pattern-reversal compound gratings was dominated by negative components at 100 ms. This kind of compound stimuli was previously used in order to simultaneously generate visual responses for luminance and chromatic contrast (Lee et al., 2011). In the present study, we suggest that the responses for compound stimuli were dominated by chromatic information, especially for pattern-reversal stimulation. Two results support this hypothesis: (i) the pattern-reversal luminance response was dominated by a positive component, while the pattern-reversal compound response was dominated by negativity at the same latency; and (ii) compound stimuli elicited small or no response in red-green congenital color blinds indicating that the cortical response for compound stimuli in the present experiment was dominated by chromatic contribution. Even compound stimuli have been composed by luminance plus chromatic contrast the responses for the present experiments seem to be dominated by chromatic information.

Carden et al. (1985), using conventional VECP, described luminance and chromatic pattern-reversal VECP dominated by positivity at 100 ms and pattern-onset VECP dominated by negativity for chromatic stimuli and positivity for luminance stimuli at

the same latency. We have observed that only pattern-reversal stimuli elicited K2.1 with opposite polarity at 100 ms for luminance or compound contrast, respectively. No difference was observed for pattern-onset in the same kernel at the same latency for these two types of contrast.

Two other previous studies were able to isolate the chromatic response elicited by patterned pseudo-random stimulation (Baseler and Sutter, 1997; Gerth et al., 2003). Baseler and Sutter (1997) observed positive-dominated K2.1 waveforms for pattern-reversal equiluminant red-green dartboards, while Gerth et al. (2003) described negative-dominated K1 for pattern-onset and negative-dominated K2.1 waveforms for pattern-reversal equiluminant red-green triangle arrays, respectively.

The polarity of pseudo-random luminance VECPs depends on stimulus configuration. K2.1 with positive polarity at 100 ms was observed with central single hexagon stimulus of high luminance contrast (Klistorner et al., 1997) as well as with high luminance contrast pattern-reversal sinusoidal gratings (Araújo et al., 2013). However, when triangle patterns were used, luminance pattern-onset K1 had negative polarity, similarly to chromatic pattern-onset K1 (Gerth et al., 2003). We found no difference between color blinds and normal trichromats in the amplitude of luminance pattern-onset and pattern-reversal VECP kernels.

Conventional chromatic VECP recorded from congenital red-green color-blinds were used to evaluate if the response would be dependent of color-opponent mechanisms (Kinney and McKay, 1974; Regan and Spekreijse, 1974; Crognale et al., 1993; Suttle and Harding, 1999; Gomes et al., 2006, 2008). All these studies have found that VECP had small amplitude or was entirely absent for color contrast modulated along color confusion axes. In this work, we observed that the amplitudes at 100 ms of VECP kernels obtained from color blinds by using compound stimuli were much smaller than from normal trichromats. Some color blind subjects exhibited small positivity at 100 ms evoked by compound pattern-reversal stimuli, probably reflecting the activation of luminance mechanisms.

Visual evoked cortical potential kernels elicited by pattern-reversal and pattern-onset stimuli might not represent the same state of adaptation of the visual system (Sutter, 2000). We used base periods of 13.3 and 26.6 ms for pattern-reversal and pattern-onset stimuli, respectively. The pattern-reversal K2.2 is equivalent to the pattern-onset K2.1, once both of them represent the interaction between two stimulus impulses separated by 26.6 ms. The statistical differences of the VECP amplitude between trichromats and color-blinds for pattern-reversal K2.1, and pattern-reversal K2.2 give support to the suggestion that these kernels are generated by similar chromatic mechanisms.

CONCLUSION

In conclusion, we suggest that compound pattern-reversal K2.1 is the best stimulus configuration to differentiate between luminance and chromatic mechanisms in VECP studies.

ACKNOWLEDGMENTS

This research was supported by the following grants: CNPq-PRONEX/FAPESPA #316799/2009; CNPq #486545/2012-1; and FINEP IBN Net #1723. Bárbara B. O. Risuenho, Eliza Maria C. B. Lacerda, Letícia Miquilini received CAPES fellowship for graduate students. Luiz Carlos L. Silveira is a CNPq research fellow.

REFERENCES

Araújo, C. S., Souza, G. S., Gomes, B. D., and Silveira, L. C. L. (2013). Visual evoked cortical potential (VECP) elicited by sinusoidal gratings controlled by pseudo-random stimulation. *PLoS ONE* 8:e70207. doi: 10.1371/journal.pone.0070207

Baseler, H. A., and Sutter, E. E. (1997). M and P components of the VEP and their visual field distribution. *Vision Res.* 37, 675–690. doi: 10.1016/S0042-6989(96)00209-X

Berninger, T. A., Arden, G. B., Hogg, C. R., and Frumkes, T. (1989). Separable evoked retinal and cortical potentials from each major visual pathway: preliminary results. *Br. J. Ophthalmol.* 73, 502–511. doi: 10.1136/bjo.73.7.502

Carden, D., Kulikowski, J. J., Murray, I. J., and Parry, N. R. A. (1985). Human occipital potentials evoked by the onset of equiluminant chromatic gratings. *J. Physiol. (Lond.)* 369:44P.

Crewther, D. P., and Crewther, S. G. (2010). Different temporal structure for form versus surface cortical color systems–evidence from chromatic non-linear VEP. *PLoS ONE* 5:e15266. doi: 10.1371/journal.pone.0015266

Crognale, M. A., Switkes, E., Rabin, J., Schneck, M. E., Hægerström-Portnoy, G., and Adams, A. J. (1993). Application of the spatiochromatic visual evoked potential to detection of congenital and acquired color-vision deficiencies. *J. Opt. Soc. Am.* 10, 1818–1825. doi: 10.1364/JOSAA.10.001818

Dreher, B., Fukada, Y., and Rodieck, R. W. (1976). Identification, classification and anatomical segregation of cells with X-like and Y-like properties in the lateral geniculate nucleus of old-world primates. *J. Physiol.* 258, 433–452. doi: 10.1113/jphysiol.1976.sp011429

Gerth, C., Delahunt, P. B., Crognale, M. A., and Werner, J. S. (2003). Topography of the chromatic pattern-onset VEP. *J. Vision* 3, 171–182. doi: 10.1167/3.2.5

Gomes, B. D., Souza, G. S., Lima, M. G., Rodrigues, A. R., Saito, C. A., da Silva Filho, M., et al. (2008). Color discrimination ellipses of trichromats measured with transient and steady-state visual evoked potentials. *Vis. Neurosci.* 25, 333–339. doi: 10.1017/S0952523808080383

Gomes, B. D., Souza, G. S., Rodrigues, A. R., Saito, C. A., Silveira, L. C. L., and da Silva Filho, M. (2006). Normal and dichromatic color discrimination measured with transient visual evoked potential. *Vis. Neurosci.* 23, 617–627. doi: 10.1017/S0952523806233194

Gomes, B. D., Souza, G. S., Saito, C. A., da Silva Filho, M., Rodrigues, A. R., Ventura, D. F., et al. (2010). Cone contrast influence on components of the pattern onset/offset VECP. *Ophthal. Physiol. Opt.* 30, 518–524. doi: 10.1111/j.1475-1313.2010.00751.x

Gouras, P. (1968). Identification of cone mechanisms in monkey ganglion cells. *J. Physiol.* 199, 533–547. doi: 10.1113/jphysiol.1968.sp008667

Hicks, T. P., Lee, B. B., and Vidyasagar, T. R. (1983). The responses of cells in macaque lateral geniculate nucleus to sinusoidal gratings. *J. Physiol.* 337, 183–200. doi: 10.1113/jphysiol.1983.sp014619

Hoffmann, M. B., Straube, S., and Bach, M. (2003). Pattern-onset stimulation boosts central multifocal VEP responses. *J. Vision* 3, 432–439. doi: 10.1167/3.6.4

Kaplan, E., and Shapley, R. M. (1982). X and Y cells in the lateral geniculate nucleus of macaque monkeys. *J. Physiol.* 330, 125–143. doi: 10.1113/jphysiol.1982.sp014333

Kaplan, E., and Shapley, R. M. (1986). The primate retina contains two types of ganglion cells, with high and low contrast sensitivity. *Proc. Natl. Acad. Sci. U.S.A.* 83, 2755–2757. doi: 10.1073/pnas.83.8.2755

Kinney, J. A. S., and McKay, C. L. (1974). Test of color-defective vision using the visual evoked response. *J. Opt. Soc. Am.* 64, 1244–1250. doi: 10.1364/JOSA.64.001244

Klistorner, A., Crewther, D. P., and Crewther, S. G. (1997). Separate magnocellular and parvocellular contributions from temporal analysis of the multifocal VEP. *Vision Res.* 37, 2161–2169. doi: 10.1016/S0042-6989(97)00003-5

Kulikowski, J. J., Murray, I. J., and Parry, N. R. A. (1989). Electrophysiological correlates of chromatic-opponent and achromatic stimulation in man. *Doc. Ophthalmol.* 52, 145–153. doi: 10.1007/978-94-009-2695-0_17

Kulikowski, J. J., and Parry, N. R. A. (1987). Human occipital potentials evoked by achromatic or chromatic checkerboards and gratings. *J. Physiol. (Lond.)* 388:45P.

Kulikowski, J. J., Robson, A. G., and McKeefry, D. J. (1996). Specificity and selectivity of chromatic visual evoked potentials. *Vision Res.* 36, 3397–3401. doi: 10.1016/0042-6989(96)00055-7

Lee, B. B., Martin, P. R., and Valberg, A. (1989). Sensitivity of macaque retinal ganglion cells to chromatic and luminance flicker. *J. Physiol. (Lond.)* 414, 223–243. doi: 10.1113/jphysiol.1989.sp017685

Lee, B. B., Sun, H., and Valberg, A. (2011). Segregation of chromatic and luminance signals using a novel grating stimulus. *J. Physiol. (Lond.)* 589, 59–73. doi: 10.1113/jphysiol.2010.188862

Li, X., Chen, Y., Lashgari, R., Bereshpolova, Y., Swadlow, H. A., Lee, B. B., et al. (2014). Mixing of chromatic and luminance retinal signals in primate Area V1. *Cereb. Cortex* doi: 10.1093/cercor/bhu002 [Epub ahead of print].

McKeefry, D. J., Russell, M. H., Murray, I. J., and Kulikowski, J. J. (1996). Amplitude and phase variations of harmonic components in human achromatic and chromatic visual evoked potentials. *Vis. Neurosci.* 13, 639–653. doi: 10.1017/S0952523800008543

Mullen, K. T. (1985). The contrast sensitivity of human colour vision to red-green and blue-yellow chromatic gratings. *J. Physiol. (Lond.)* 359, 381–400. doi: 10.1113/jphysiol.1985.sp015591

Murray, I. J., Parry, N. R. A., Carden, D., and Kulikowski, J. J. (1987). Human visual evoked potentials to chromatic and achromatic gratings. *Clin. Vision Sci.* 3, 231–244. doi: 10.1007/BF01184777

Odom, J. V. (2006). "Kernel analysis," in *Handbook of Clinical Electrophysiology of Vision Testing*, 2nd Edn, eds J. Heckenlively and G. Arden (Cambridge, MA: The MIT Press).

Odom, J. V., Bach, M., Brigell, M., Holder, G. E., McCulloch, D. L., and Tormene, A. P. (2010). ISCEV standard for clinical visual evoked potentials. *Doc. Ophthalmol.* 120, 111–119. doi: 10.1007/s10633-009-9195-4

Parry, N. R., Murray, I. J., Panorgias, A., McKeefry, D. J., Lee, B. B., and Kremers, J. (2012). Simultaneous chromatic and luminance human electroretinogram responses. *J. Physiol. (Lond.)* 590, 3141–3154. doi: 10.1113/jphysiol.2011.226951

Porciatti, V., and Sartucci, F. (1999). Normative data for onset VEPs to red-green and blue-yellow chromatic contrast. *Clin. Neurophysiol.* 110, 772–781. doi: 10.1016/S1388-2457(99)00007-3

Rabin, J., Switkes, E., Crognale, M., Schneck, M. E., and Adams, A. J. (1994). Visual evoked potentials in three-dimensional color space: correlates of spatio-chromatic processing. *Vision Res.* 34, 2657–2671. doi: 10.1016/0042-6989(94)90222-4

Regan, D., and Spekreijse, H. (1974). Evoked potential indications of colour blindness. *Vision Res.* 14, 89–95. doi: 10.1016/0042-6989(74)90120-5

Souza, G. S., da Silva, V. G. R., Araújo, C. S., Risuenho, B. B., Gomes, B. D., and Silveira, L. C. L. (2012). "Effects of the presentation mode and color contrast in visual evoked potential elicited by pseudo-random stimuli. Em: annual meeting of the association for research in vision and ophthalmology (ARVO)," in *Investigate Ophthalmology Visual Science,* Vol. 53 (Rockville: The Association for Research in Vision and Ophthalmology), 5717.

Souza, G. S., Gomes, B. D., Lacerda, E. M. C. B., Saito, C. A., da Silva Filho, M,. and Silveira, L. C. L. (2008). Amplitude of the transient visual evoked potential (tVEP) as a function of achromatic and chromatic contrast: contribution of different visual pathways. *Vis. Neurosci.* 25, 317–325. doi: 10.1017/S0952523808080243

Sutter, E. E. (2000). The interpretation of multifocal binary kernels. *Doc. Ophthalmol.* 100, 49–75. doi: 10.1023/A:1002702917233

Suttle, C. M., and Harding, G. F. A. (1999). Morphology of transient VEPs to luminance and chromatic pattern onset and offset. *Vision Res.* 39, 1577–1584. doi: 10.1016/S0042-6989(98)00223-5

Conflict of Interest Statement: The authors declare that the research was conducted in the absence of any commercial or financial relationships that could be construed as a potential conflict of interest.

Received: 13 August 2014; accepted: 12 January 2015; published online: 28 January 2015.

Citation: Risuenho BBO, Miquilini L, Lacerda EMCB, Silveira LCL and Souza GS (2015) Cortical responses elicited by luminance and compound stimuli modulated by pseudo-random sequences: comparison between normal trichromats and congenital red-green color blinds. Front. Psychol. ***6****:53. doi: 10.3389/fpsyg.2015.00053*

This article was submitted to Perception Science, a section of the journal Frontiers in Psychology.

frontiers in
PSYCHOLOGY

ORIGINAL RESEARCH ARTICLE
published: 27 November 2014
doi: 10.3389/fpsyg.2014.01376

Color-discrimination threshold determination using pseudoisochromatic test plates

Kaiva Jurasevska[1]*, Maris Ozolinsh[1,2], Sergejs Fomins[1,2], Ausma Gutmane[1], Brigita Zutere[3], Anete Pausus[1] and Varis Karitans[2]

[1] *Department of Optometry and Vision Science, Faculty of Physics and Mathematics, University of Latvia, Riga, Latvia*
[2] *Institute of Solid State Physics, University of Latvia, Riga, Latvia*
[3] *Faculty of Biology, University of Latvia, Riga, Latvia*

Edited by:
Marcelo Fernandes Costa, Universidade de São Paulo, Brazil

Reviewed by:
Mark M. Schira, University of Wollongong, Australia
Aaron Paul Johnson, Concordia University, Canada

****Correspondence:***
Kaiva Jurasevska, Department of Optometry and Vision Science, Faculty of Physics and Mathematics, University of Latvia, 8 Kengaraga Street, Riga LV-1063, Latvia
e-mail: kaiva.jurasevska@gmail.com

We produced a set of pseudoisochromatic plates for determining individual color-difference thresholds to assess test performance and test properties, and analyzed the results. We report a high test validity and classification ability for the deficiency type and severity level [comparable to that of the fourth edition of the Hardy–Rand–Rittler (HRR) test]. We discuss changes of the acceptable chromatic shifts from the protan and deutan confusion lines along the CIE *xy* diagram, and the high correlation of individual color-difference thresholds and the red–green discrimination index. Color vision was tested using an Oculus HMC anomaloscope, a Farnsworth D15, and an HRR test on 273 schoolchildren, and 57 other subjects with previously diagnosed red–green color-vision deficiency.

Keywords: color vision, psychophysics, vision system, color measurement, color-vision deficiency, color-vision defects, color perception

INTRODUCTION

Pseudoisochromatic (PIC) test plates are widely used for color-vision screening, congenital deficiency classification, and grading. Regardless of the design used in the creation of the PIC tests, they produce different grouping responses in people with normal trichromatic vision and abnormal color vision. Vanishing design PIC test plates are the easiest to produce, and all PIC tests contain these plates (Birch, 1993).

It is possible to obtain PIC tests with high performance (sensitivity and specificity approaching values of 1.00) by carefully choosing colored symbol chromatic values (Cole et al., 2006; Cole, 2007). PIC tests usually classify color-vision deficiency into three groups in terms of severity: mild, medium (moderate), and strong (severe). The total color difference (ΔE^*_{ab}) of the plate stimuli determines the level of difficulty of the plate. For red–green color-vision deficiencies, the advisable values of ΔE^*_{ab} measured according to the *Commission internationale de l'eclairage* (CIE) LAB formula are as follows:

- 15–22 units for small deficiency (screening),
- 30–40 units for medium deficiency, and
- 50–60 units for severe deficiency detection (Birch, 1993).

The gold standard for color-vision diagnostics is the anomaloscope testing procedure, which also characterizes the abnormality by assigning a quantitative value to the examination result. Other frequently used tests are usually based on error counting, which is further associated with the severity of color-vision deficiency based on measurement of chromatic detection thresholds. Although the anomaloscope is a precise instrument, it has been reported that the correlation between matching range results and the ability to perform everyday color-discrimination tasks, such as judging surface colors, is poor (Birch, 2008; Baraas et al., 2010). Nevertheless, the anomaloscope matching range of an individual is often used as a measure of the severity of the color-vision deficiency (Birch, 1993).

It would be convenient to characterize individual color-discrimination sensitivity in terms of a threshold value, such as the total color-difference value in the CIE LAB color space, for colors on confusion lines to perceive a noticeable difference. It has been suggested that scoring techniques for expressing test results in terms of sensitivity loss may be informative (Smith et al., 1993). We have developed a set of PIC plates for determining individual ΔE^*_{ab} (hereafter abbreviated as ΔE for brevity) threshold values (Luse et al., 2012, 2013). Three main points distinguish KAMS (a term comprising the names of the test developers) from other PIC tests currently used in clinics. First, it is based on matching experimental data for color deficient individuals. Second, it characterizes the severity of deficiency in numerical units associated to sensitivity loss along the color confusion line. Third, the KAMS test is psychophysical, whereas other PIC tests, including Hardy–Rand–Rittler (HRR) and Ishihara, are not. The aim of this study is to assess the clinical performance and physical properties of our test plate set and to report its scientific relevance.

METHODS

DEVELOPMENT OF TEST PLATES

The KAMS test was designed using the principles described by Birch (1993), using neutral colors (i.e., colors that are confused with gray). In our previous work, we chose the chromaticities used for the KAMS plates. Five color-vision-deficient individuals

(3 deutan, 2 protan) performed matching experiments under controlled illumination conditions (using a Qualitest CT-100W1 light booth under D65 illumination with a color temperature of $T = 6500$ K). In total, we created more than 300 chromatic and 106 gray color samples along and next to the deutan and protan color confusion lines passing through the achromatic area in the CIE *xy* color diagram. Samples had various saturation and lightness levels, and were 3 cm × 3 cm. The subjects were given two tasks: first, to sort samples into stacks of gray and chromatic, and second, to sort gray samples in piles of similar lightness. In a similar manner, via two subsequent trials subjects matched more samples, which we created, to achieve a gradual increase in ΔE in the KAMS test plates. A more detailed explanation can be found in our previous work (Luse et al., 2012).

A set of 24 PIC plates [10 for protan deficiency (5 reddish and 5 greenish) and 14 for deutan deficiency (9 reddish and 5 greenish)] was created based on psychophysical design. Each plate had two circle sets (A) and (B), where only one held a chromatic symbol. The symbols used were four different digits with a rounded shape (i.e., 6, 8, 9, and 0), giving a guessing rate for each plate of 12.5%. **Figure 1** shows an example of a plate for detecting deutan deficiency (the corresponding ΔE for the printed plate is 27 units). The observers had two tasks: detection (to determine whether circle (A) or (B) contains a symbol) and recognition (to determine which of the four numbers the circle contains). Each plate was printed on a single page. The pages were turned at 3-s intervals.

The tests were printed using a calibrated inkjet printer (Epson-Stylus Pro 7800) using nine UltraCrome K3 Epson Ink cartridges (four types of black, light cyan, light magenta, cyan, magenta, and yellow) on Premium Semimatte photopaper 260, with a resolution of 2880 dpi. It has been reported that higher quality can be achieved in terms of narrow chromatic value dispersion along the CIE *xy* color diagram by using inkjet printing (Luse et al., 2012, 2013) instead of the typography method used in the production of commercially available PIC plates (Lee and Honson, 2003; Dain, 2004; Fomins and Ozolinsh, 2011).

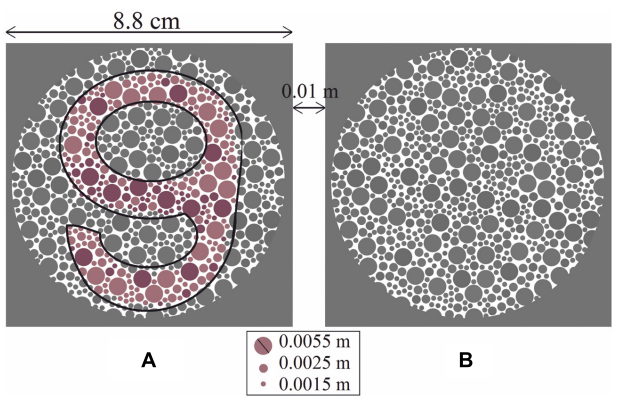

FIGURE 1 | Each large circle set (A) and (B) was composed of equal numbers of small dots, with three different sizes, some of which formed the shape of a symbol. The proportion of lighter symbol-forming dots to darker symbol-forming dots was constant for all plates. Circle **(A)** contains the chromatic symbol "9" (shown with a black outline for clarity in the black and white prints of the manuscript), and circle **(B)** is empty. In this case, the deutan classification plate with $\Delta E = 27$ is shown.

Increasing difficulty of the plates was achieved by decreasing ΔE of the test stimuli and the background. Such an approach has been reported previously (Wenzel and Samu, 2012). The symbol on test plates was composed of two stimuli–background-forming dot pairs (one lighter and one darker). The lighter pairs (making up 57% of the body of the symbol) were chosen to closely match the intensity (and accordingly the ΔE) of the darker ones; the deviation in most cases was less than a few units. The calculation of the color pair ΔE values was performed based on data obtained using a Konica Minolta CS-100A colorimeter (CIE *xy* diagram color space coordinate *x*, *y*, and *Y* values were recorded). Samples were illuminated with simulated D65 ($T = 6500$ K) illumination via a Qualitest CT-100W1 light booth. Color differences were calculated using the formula proposed by Berns (2006), taking into account the differences in sample lightness (ΔL^*), chroma (ΔC^*_{ab}), and hue (ΔH^*_{ab}), i.e.,

$$\Delta E^*_{ab} = \sqrt{(\Delta L^*)^2 + (\Delta C^*_{ab})^2 + (\Delta H^*_{ab})^2}.$$

ANALYSIS OF PLATE COLOR STABILITY

Using calibrated inkjet printing instead of typography methods to produce PIC plates showed that several aspects should be considered, such as a smaller spread of chromatic values (Luse et al., 2012); however, the main drawback is faster changes in color over time (Lee and Honson, 2003; Lee, 2006). We have reported significant changes in the plate stimuli color saturation after 7 months of use (Luse et al., 2013). Prior to and throughout the study, the fading of pigments was monitored monthly using multispectral imaging, and the colorimeter measurements described above. Multispectral imaging was performed using a CRI Nuance Vis 07 multispectral camera with a Nikon AF-S Micro-Nikkor 60-mm *f*/2.8*D* objective lens. Image acquisition was performed in an otherwise dark room; the samples were inserted in the Qualitest CT-100W1 light booth; the samples were attached to the wall at a constant height and 50 ± 5 cm away from the camera, and were illuminated from above using a standard D65 light source ($T = 6500$ K). 1290 × 920 pixel spatial images were captured at visible wavelengths (420–720 nm, in steps of 10 nm). The images were transformed into cone excitation images using cone sensitivities [the method is described in detail in (Fomins and Ozolinsh, 2011)]. Selected image areas of 89 pixels were analyzed, and CIE *xy* color space (*x*, *y*, *Y*) values were acquired for each pixel. Changes in the mean color values of the pixels and the corresponding pixel distributions were not statistically significant during the first 3 months of use, as shown in **Figure 2**. The study described below was conducted over a period of 3 months using a newly printed, chromatically identical set of test plates. The mean standard deviation of the pixel value dispersion was 0.002–0.0028 units along the *x*-axis and 0.0026–0.003 along the *y*-axis (larger for darker samples).

ANALYSIS OF SAMPLE RELATION TO COLOR CONFUSION LINES

Color pairs for the PIC plates were created via matching experiments carried out on several color-vision-deficient subjects (the experimental conditions are described in detail in Luse et al., 2012).

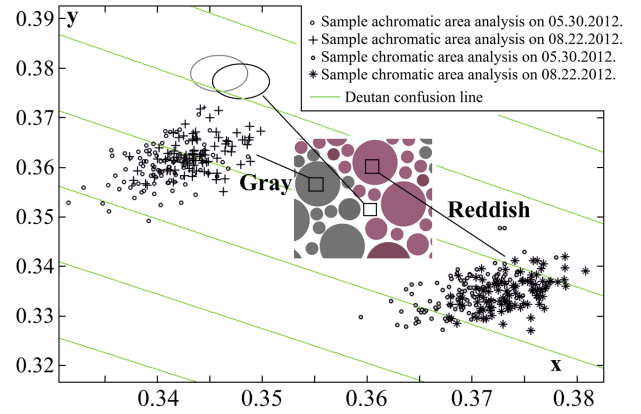

FIGURE 2 | Pseudoisochromatic (PIC) plate image pixel color dispersion changes over 3 months in the CIE *xy* color diagram (one plate stimulus is shown, and the corresponding plate is described in Figure 1). Statistically significant fading was not detected (data points in both sets for both color pairs – chromatic and achromatic –overlapped and were of equal size). The ellipses show an analysis of the yellowing of the white paper (black ellipse to gray ellipse). The paper color coordinate values were more consistent than those of the printed areas, therefore the ellipses (and data point distributions that are not shown in the graph) were smaller than the other pixel value distributions.

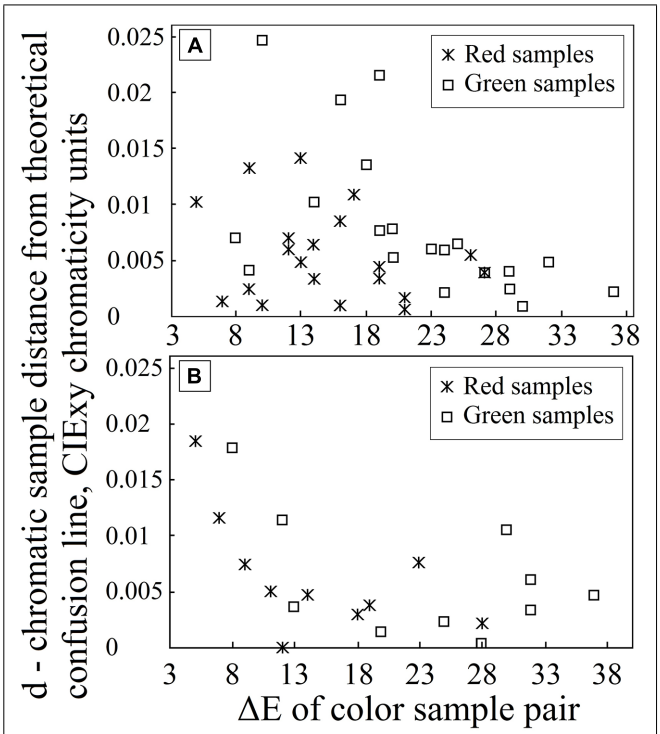

FIGURE 3 | Graph **(A)** depicts the distance *d* for each chromatic sample from the line defined by the deutan confusion line copunctal point and the corresponding achromatic pair in the CIE *xy* color diagram (on the *y*-axis) as the sample color difference increases in CIE LAB color space (on the *x*-axis). Graph **(B)** depicts the corresponding distance *d* for protan plate analysis.

Over the course of several trials, using several hundred samples, 60 valid color pairs (a reddish or greenish sample for stimuli and a corresponding gray sample for background) were obtained for construction of PIC plates. The colored dots on each plate had chromaticity coordinates that lie on or close to the protan or deutan confusion line connecting the dichromatic confusion line copunctal point and each chromaticity coordinate "cloud" center of the gray background color. The confocal points we used are given by CIE chromaticity coordinates (0.75, 0.25) for protan and (1.40, −0.40) for deutan deficiencies (Birch, 1993). All obtained chromatic sample relations (that is, the distances d) to confusion lines were analyzed to answer the following question: how far from the corresponding theoretical confusion line (for the congenital color-vision-deficient individual) may the colored stimuli chromaticity coordinate distribution center be situated and still prove to be indistinguishable from its achromatic pair? For these calculations, geometrical equations were used. If a line is given by two points (x_1, y_1; i.e., the deutan or protan confusion line copunctal point) and (x_2, y_2; i.e., the center of each achromatic sample pixel color coordinate distribution center), and the point in question is (x_0, y_0; i.e., the chromatic sample color coordinate distribution center), d can be found as follows:

$$d = |(x_2 - x_1)(y_1 - y_0) - (x_1 - x_0)(y_2 - y_1)| \div \sqrt{(x_2 - x_1)^2 + (y_2 - y_1)^2}.$$

The results for deutan and protan sample color pairs are shown in **Figures 3A,B**, respectively. We find that larger shifts from the confusion line are acceptable for the observers if the sample was less saturated. As the color difference increased, the acceptable shift decreased for greenish and reddish samples. It is not surprising that larger shifts in the greenish zone of the CIE *xy* color diagram can be tolerated because of the size increment of the McAdam ellipses in the green area compared with the red area. We propose that the tolerated sample shifts for red–green color-vision-deficient individuals in the color diagram form the pattern shown in **Figure 4**. This hypothesis requires further investigation. Matching experiments for stimuli with a larger color difference might have been unsuccessful (even for deuteranope and protanope observers) because the color coordinate distribution of the printed areas exceeded the acceptable shifts in the saturated areas in the color diagram (see **Figure 4**).

OBSERVERS

Children in two Latvian schools were tested to assess the clinical validity of the KAMS test. In total, 273 children (136 girls and 137 boys) from the Vainode region (Vainode secondary school) and the Priekule region (Gramzda elementary school) in Latvia participated. We chose these two schools in the periphery of our country to represent our population for a number of reasons: first, to join these schools, there are no specific requirements in terms of IQ, gender, or future choice of profession, which might lead to the sample being unrepresentative; second, school children form a group of individuals that is relatively homogeneous in age. The participation rate from both schools was 84.5%, and the age range was 7–19 years (with a mean age of 12.1 and a SD of 3.3 years). The study was conducted from mid-September to mid-October, 2012. Additionally, 57 volunteer individuals (with an age range of

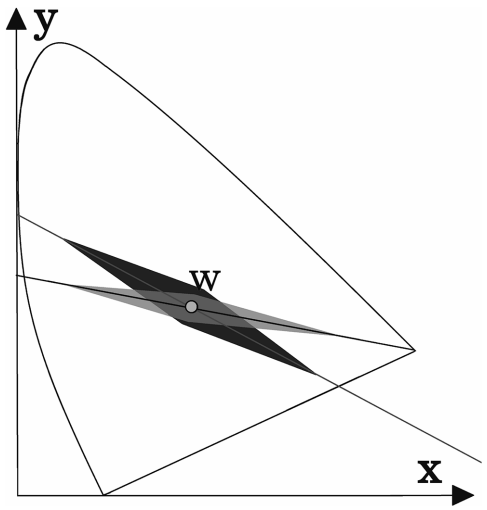

FIGURE 4 | A possible explanation for the results shown in Figure 3. The acceptable shift (darker area) from the deutan confusion line decreases as the stimuli intensity increases. The acceptable shift distance for protans is shown as the lightest shaded area. The area suitable for screening purposes (i.e., the overlap area) is highlighted in gray. (These areas are not shown to scale.)

7–67 years) with red–green deficiencies were examined from mid-September to mid-December, 2012. The study was conducted in accordance with the principles embodied in the Declaration of Helsinki Code of Ethics of the World Medical Association. All participants were unaware of the specific aims of the study.

TESTING PROCEDURE

The room was illuminated using Narva LT-T8 18-W Colourlux plus CW (cool white) light bulbs. The color-rendering index of the bulbs was >80, the correlated color temperature was $T = 4000$ K, and the mean illumination of the test plates was 400 lx. It has been shown that fluorescent light sources are acceptable for color-vision testing (Dain et al., 1993).

The visual acuity of the children was examined using a LogMAR chart with the Landolt ring optotypes. If the near visual acuity was sufficient (better than 0.2 LogMAR), each child was tested using the fourth edition of the Richmond HRR plates (Richmond Products, Albuquerque, NM, USA), which is recommended for clinical use due to the high diagnostic accuracy (Cole et al., 2006; Dain, 2006; Cole, 2007), as well as the KAMS test. In the event that a single error was made in any of the above tests, an Oculus HMC (R) anomaloscope (type 47720) was used, and the Farnsworth D15 saturated and desaturated (Cole and Orenstein, 2003) testing procedure was carried out. Children were classified as color-vision-deficient only if they failed the anomaloscope test.

The HRR and KAMS tests were also carried out on the volunteer participants. If the anomaloscope and/or the D15 testing procedures were available, they were also performed. All of the volunteers undertook at least three of the above-mentioned tests. In total, results from 65 color-vision-deficient individuals (8 school children and 57 volunteers) were recorded; 21 subjects were classified as protans and 43 were classified as deutans [forming a large enough group of color-affected individuals for hypothesis testing, compared to other studies in the field (Huna-Baron et al., 2013; Lillo et al., 2014)]. It was not possible to interpret the results obtained with a single observer; hence, these results were excluded from further analysis.

THE ΔE THRESHOLD

Following the diagnosis of each participant as deutan or protan, his or her results from the KAMS test were analyzed to determine the ΔE threshold for reddish and greenish plates separately. If, for example, the subject's answers to the plates with ΔE values of 9, 10, 12, 17, 19, 21, and 27 were, respectively, wrong, wrong, wrong, wrong, correct, correct, and correct, then the ΔE threshold would be recorded as between 17 and 19 units (with a midpoint of 18 units and an uncertainty of $\pm$ 1 unit). If all plates were answered incorrectly, it was assumed that the ΔE threshold was between 27 and 60 units. At least two correct consecutive answers were required to assume that the threshold was between 0 and 27 units.

RESULTS

SPECIFICITY AND SENSITIVITY OF KAMS

The ability of the KAMS test to diagnose red–green color-vision deficiency was calculated based on data acquired in the population study (schools in Vainode and Gramzda). With the chosen criterion (> 1 error), the sensitivity of the test was 100%, and the specificity was 99.62%. The sensitivity was defined as the percentage of people with the condition that tested positive, and the specificity was defined as the percentage of people without the condition that tested negative (Norton et al., 2002).

PROTAN/DEUTAN CLASSIFICATION AND DEFICIENCY SEVERITY LEVEL GRADING OF KAMS

Although the PIC plate results alone should not be used to diagnose type of color-vision deficiency, we performed such an analysis to determine the suitability of the test for ΔE threshold determination for protans and deutans using separate plate groups. First, each individual participant was diagnosed as protan or deutan using the test battery described earlier. From the 64 individuals, in total, the HRR test misdiagnosed 1 deutan and 2 protans, and in seven cases, the HRR test failed to classify subjects (that is, it showed an equal number of errors in each column). The KAMS test misdiagnosed 5 deutans and 1 protan, and in two cases classification failed. We compared the ability of the KAMS test to grade the severity of the deficiency with that of the HRR test. Moderately good agreement was achieved ($r = 0.74$ and $p < 0.01$) in the case of protans. Test results for deutans are shown in detail in **Figure 5**.

ΔE THRESHOLD VALUE IN CASE OF MILD DEFICIENCY AND CORRELATION WITH RGI

A convenient unit for characterizing red–green discrimination sensitivity is the red–green discrimination index (RGI), which is defined (Barbur et al., 2008) as

$$RGI = [1 - (R - MR) \div 73],$$

where R is the test subject's Nagel matching range, and MR is the mean normal subject's matching range. This definition results in

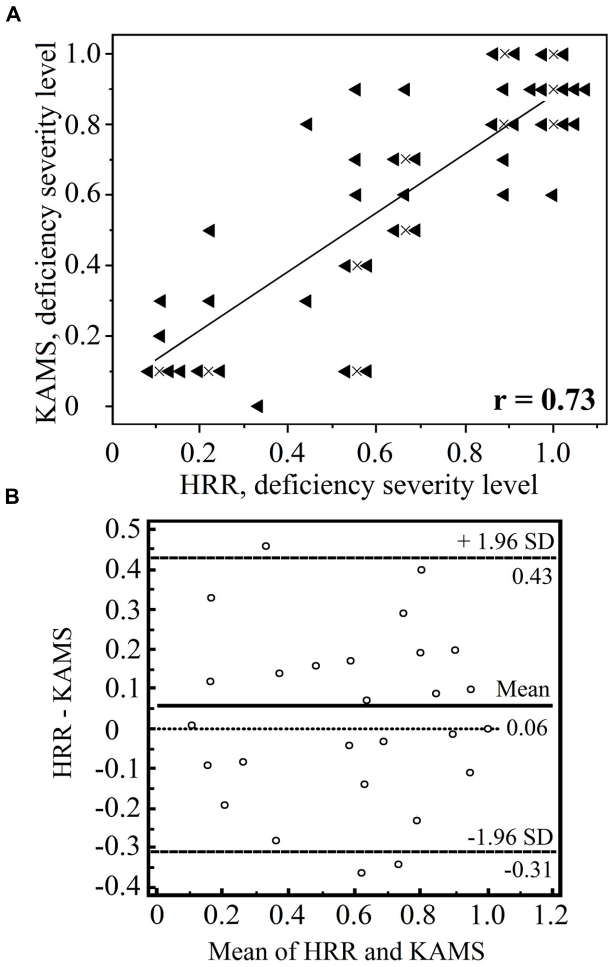

FIGURE 5 | Comparison of the Hardy–Rand–Rittler (HRR) and KAMS test results in terms of grading the severity of the deutan deficiency ($n = 43$). The results of the screening plates are omitted. Graph **(A)** shows the number of errors made in the specific deutan grading plates with each test. A result of 1.0 corresponds to mistakes in all specific deutan plates, whereas a result of 0.5 means that 50% of the grading plates were determined correctly. The results of the two tests show a moderately high correlation ($r = 0.73$ and $p < 0.001$). A linear trend inferred from the data is also shown. Data points that overlap were offset from their true locations for demonstration purposes. The actual positions of the overlapping points are marked by the crosses. Graph **(B)** shows the Bland–Altman plot for both methods (using the MedCalc software package). No consistent bias was detected, and the difference in the sample means was not statistically significant ($p = 0.05$).

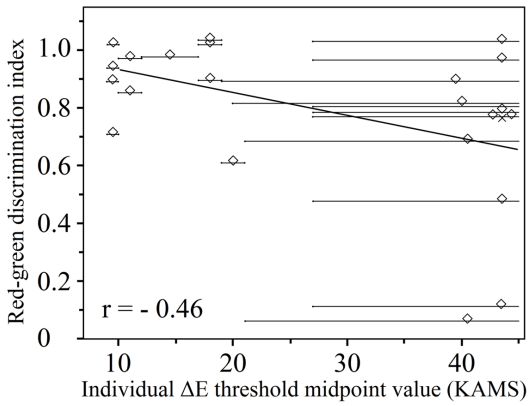

FIGURE 6 | Individual ΔE threshold midpoints obtained using the KAMS test as a function of the red–green discrimination index (deutan subjects, $n = 22$; 3 deuteranopes, 19 deuteranomalous). Overlapping data points are offset from their true location for purposes of visualization. The actual positions of the overlapped points are marked by crosses. A linear regression to the data is also shown. Lighter gray horizontal lines show the uncertainties in the thresholds.

RGI values that range from zero (in the case of dichromacy) to about one (in the case of high red–green color discrimination; Barbur et al., 2008).

As expected, there was a moderately strong negative correlation between the midpoint threshold values obtained using the KAMS test in deutan ($n = 22$) observers ($r = -0.46$ and $p = 0.042$ for thresholds obtained with reddish plates, and $r = -0.44$ and $p = 0.042$ for thresholds obtained using greenish plates). The relationship is shown in **Figure 6** in the case of deutan observers for thresholds obtained by reddish plates. Identical (positive only) correlation coefficients and p-values were obtained for the correlation of the anomaloscope matching range to the obtained threshold values. Because of the small number of protan observers ($n = 13$), a negligible correlation was obtained for threshold values obtained using the green test plates ($r = -0.09$ and $p = 0.775$), and a moderate negative correlation was obtained for threshold values from the reddish test plate results ($r = -0.33$ and $p = 0.263$).

Figure 6 shows individual ΔE threshold midpoints; two data distributions can be distinguished, which were separated by an empty area in the center of the plot. In reality, it was possible to obtain a valid threshold region with limits from both sides only for the participants corresponding to data points on the left side of this graph. For the participants marked by points on the right, it was possible (with the PIC plates available) to be certain only about the smallest threshold midpoint region. To tackle this problem, a ΔE value of 60 units was used as the largest possible threshold value in the case of each participant for the data clustered on the right-hand side of the graph. The midpoint was calculated keeping in mind that there is a large position uncertainty in the precise thresholds of the midpoints. In other words, those subjects with lower ΔE discrimination thresholds had a higher red–green discrimination index; however, subjects with higher ΔE discrimination thresholds than we could determine may have various RGIs. We can only suggest that, based on the distribution of data points on the left-hand side of the figure, these other data points might be aligned along a line with a negative gradient (as shown in **Figure 6**), if the testing method were improved. Nonetheless, we have shown that a lower ΔE discrimination threshold is consistent with smaller matching ranges in the anomaloscope testing procedure for deuteranomalous observers.

Color vision is known to change with age (Roy et al., 1991). The group of individuals with affected color vision that we studied was not coherent in terms of age. We carried out separate data analysis to eliminate the possible effects of age on the variation of the acquired KAMS thresholds (as well as the anomaloscope matching

range midpoint values). A weak correlation was found, ruling out direct causation of threshold variance due to age differences (charts attached to the supplementary material).

DISCUSSION

We have compared the KAMS test with the Richmond HRR test throughout this study because the latter is one of the best clinical PIC tests (Cole et al., 2006; Dain, 2006; Cole, 2007). The high sensitivity and specificity of KAMS suggests that although the KAMS test was created for scientific (as opposed to clinical) purposes, it is a potential supplementary test for use in both research and clinics; we do not suggest replacing currently used tests with the KAMS test. The good level of agreement in terms of the grading results obtained using KAMS and the HRR test suggests that the tests are comparable; however, our plate set has scope for use in psychophysical investigations. The main novelty of our research is the depiction of the results of a PIC test via a discrimination threshold described by a numerical value. The total color difference is a commonly used quantity in science. The results given in terms of total color difference may be useful and easy to interpret for specific job applications or for product developers (the results depict color-sensitivity loss in comparison with the color-discrimination ability of a normal observer for neutral colors). Using a limited number of plates (five for greenish and nine for reddish directions in the CIE *xy* coordinates), we were able to determine individual ΔE discrimination thresholds for deutans. Standardization and development of finer plate grading might improve the reliability of the results; for example, by reducing the uncertainty interval in the data (see **Figure 6**). By improving the test method, we could clarify whether individual thresholds are fixed or variable, as well as the amount of variability.

Our results show a correlation of the individual ΔE thresholds and the RGI for deuteranomalous individuals. Such an outcome was expected, as Cole (2007) reported similar results for HRR grading and the Nagel matching range ($r = 0.58$). However, the Nagel matching range is not correlated with the obtained red–green thresholds in the Color Assessment and Diagnosis test, which uses neutral colors for the background, similar to the HRR and KAMS test (Barbur et al., 2008). These results might be explained by differences in the perception of rapidly moving and changing images compared with that of static images. However, the following question remains: why are the results of the Farnsworth D15 test not comparable to the anomaloscope data (Birch, 2008)? A different approach to the analysis of the experimental data might provide other results. Furthermore, our results might be partly affected by the effect of normal age-related changes in color vision. A larger and more age-coherent sample size for the color-vision impaired group (especially in case of the protan observers) would be necessary to make a full assessment of the effects analyzed in this study.

CONCLUSION

(1) The KAMS test was found to be valid for the screening of congenital red–green color-vision deficiencies, and the sensitivity and specificity are comparable to those of the HRR test (2002, 4th edition).

(2) The design of psychophysical tests can be used to assess red–green color-vision deficiencies and obtain individual color saturation discrimination thresholds in the case of anomalous trichromates.

(3) The size of the anomaloscope-matching range in Nagel units for deutan observers exhibited a moderately strong positive correlation (a moderately strong negative correlation, in the case of RGI) with the acquired ΔE threshold midpoints of the psychophysical testing procedure used in this study.

ACKNOWLEDGMENT

Kaiva Jurasevska is supported by the European Social Fund within the project "Support for Doctoral Studies at the University of Latvia." Authors Maris Ozolinsh, Sergejs Fomins, Anete Pausus and Varis Karitans are supported by ESF Nr. 2013/0021/1DP/1.1.1.2.0/13/APIA/VIAA/001.

SUPPLEMENTARY MATERIAL

The Supplementary Material for this article can be found online at: http://www.frontiersin.org/journal/10.3389/fpsyg.2014.01376/abstract

REFERENCES

Baraas, R. C., Foster, D. H., Amano, L., and Nascimento, S. M. C. (2010). Color constancy of red-green dichromats and anomalous trichromats. *Invest. Ophthalmol. Vis. Sci.* 51, 2286–2293. doi: 10.1167/iovs.09-4576

Barbur, J. L., Rodrigues-Carmona, M., Harlow, J. A., Mancuso, K., Neitz, J., and Neitz, M. (2008). A study of unusual Rayleigh matches in deutan deficiency. *Vis. Neurosci.* 25, 507–516. doi: 10.1017/S0952523808080619

Berns, R. S. (2006). *Billmeyer and Saltzman's Principles of Color Technology,* 3rd Edn. New York, NY: John Wiley & Sons.

Birch, J. (1993). *Diagnosis of Defective Colour Vision.* New York, NY: Oxford University Press.

Birch, J. (2008). Failure of concordance of the Farnsworth D15 test and the Nagel anomaloscope matching range in anomalous trichromatism. *Vis. Neurosci.* 25, 451–453. doi: 10.1017/S0952523808080231

Cole, B. L. (2007). Assessment of inherited colour vision defects in clinical practice. *Clin. Exp. Optom.* 90, 157–175. doi: 10.1111/j.1444-0938.2007.00135.x

Cole, B. L., Lian, K. Y., and Lakkis, C. (2006). The new Richmond HRR pseudoisochromatic test for colour vision is better than the Ishihara test. *Clin. Exp. Optom.* 89, 73–80. doi: 10.1111/j.1444-0938.2006.00015.x

Cole, B. L., and Orenstein, J. M. (2003). Does the Farnsworth D15 test predict the ability to name colours? *Clin. Exp. Optom.* 86, 221–229. doi: 10.1111/j.1444-0938.2003.tb03109.x

Dain, S. J. (2004). Colorimetric analysis of four editions of the Hardy-Rand-Rittler pseudoisochromatic tests. *Vis. Neurosci.* 21, 437–443. doi: 10.1017/S0952523804213475

Dain, S. J. (2006). Illuminant and observer metamersim and the Hardy-Rand-Rittler color vision test editions. *Vis. Neurosci.* 23, 685–694. doi: 10.1017/S095252380623356X

Dain, S. J., Honson, V. J., and Curtis, C. T. (1993). Suitability of fluorescent tube light sources for the Ishihara test as determined by colorimetric methods. *Colour Vis. Defic.* 56, 327–333. doi: 10.1007/978-94-011-1856-9_33

Fomins, S., and Ozolinsh, M. (2011). Multispectral analysis of color vision deficiency tests. *Mater. Sci. (Medžiagotyra)* 17, 1392–1320. doi: 10.5755/j01.ms.17.1.259

Huna-Baron, R., Glovinsky, Y., and Habot-Wilner, Z. (2013). Comparison between Hardy-Rand-Rittler 4th edition and Ishihara color plate tests for detection of dyschromatopsia in optic neuropathy. *Graefes Arch. Clin. Exp. Ophthalmol.* 251, 585–589. doi: 10.1007/s00417-012-2073-x

Lee, D. Y. (2006). Color changes in the red-green plates of the 50-year-old AO HRR color vision test. *Vis. Neurosci.* 23, 681–684. doi: 10.1017/S0952523806233054

Lee, D. Y., and Honson, M. (2003). Chromatic variation of Ishihara diagnostic plates. *Color Res. Appl.* 28, 267–276. doi: 10.1002/col.10161

Lillo, J., Alvaro, L., and Moreira, H. (2014). An experimental method for the assessment of color simulation tools. *J. Vis.* 14, 15. doi: 10.1167/14.8.15

Luse, K., Fomins, S., and Ozolinsh, M. (2012). Pseudoisochromatic test plate colour representation dependence on printing technology. *IOP Conf. Ser. Mater. Sci. Eng.* 38, 012024. doi: 10.1088/1757-899X/38/1/012024

Luse, K., Ozolinsh, M., Fomins, S., and Gutmane, A. (2013). Multispectral analysis and cone signal modeling of pseudoisochromatic test plates. *IOP Conf. Ser. Mater. Sci. Eng.* 49, 012041. doi: 10.1088/1757-899X/49/1/012041

Norton, T. T., Corliss, D. A., and Bailey, J. E. (2002). *The Psychophysical Measurement of Visual Function.* Burlington, MA: Butterworth–Heinemann.

Roy, M. S., Podgor, M. J., Collier, B., and Gunkel, R. D. (1991). Color vision and age in normal North American population. *Graefes Arch. Clin. Exp. Opthalmol.* 229, 139–144. doi: 10.1007/BF00170545

Smith, V. C., Pokorny, J., and Yeh, T. (1993). Pigment tests evaluated by a model of chromatic discrimination. *J. Opt. Soc. Am. A Opt. Image Sci. Vis.* 10, 1773–1784. doi: 10.1364/JOSAA.10.001773

Wenzel, K., and Samu, K. (2012). Pseudo-isochromatic plates to measure colour discrimination. *Acta Polytechnica Hungarica* 9, 1–11.

Conflict of Interest Statement: The authors declare that the research was conducted in the absence of any commercial or financial relationships that could be construed as a potential conflict of interest.

Received: 27 August 2014; paper pending published: 09 October 2014; accepted: 11 November 2014; published online: 27 November 2014.

Citation: Jurasevska K, Ozolinsh M, Fomins S, Gutmane A, Zutere B, Pausus A and Karitans V (2014) Color-discrimination threshold determination using pseudoisochromatic test plates. Front. Psychol. ***5****:1376. doi: 10.3389/fpsyg.2014.01376*

This article was submitted to Perception Science, a section of the journal Frontiers in Psychology.

frontiers in Psychology

ORIGINAL RESEARCH
published: 30 March 2016
doi: 10.3389/fpsyg.2016.00429

Reduced Discrimination in the Tritanopic Confusion Line for Congenital Color Deficiency Adults

Marcelo F. Costa[1,2], Paulo R. K. Goulart[3], Mirella T. S. Barboni[1] and Dora F. Ventura[1,2]*

[1] Laboratório de Psicofisiologia Sensorial, Departamento de Psicologia Experimental, Instituto de Psicologia, Universidade de São Paulo, São Paulo, Brasil, [2] Núcleo de Neurociências e Comportamento e Núcleo de Neurociências Aplicadas, Universidade de São Paulo, São Paulo, Brasil, [3] Núcleo de Teoria e Pesquisa do Comportamento, Universidade Federal do Pará, Belém, Brasil

In congenital color blindness the red–green discrimination is impaired resulting in an increased confusion between those colors with yellow. Our post-receptoral physiological mechanisms are organized in two pathways for color perception, a red–green (protanopic and deuteranopic) and a blue–yellow (tritanopic). We argue that the discrimination losses in the yellow area in congenital color vision deficiency subjects could generate a subtle loss of discriminability in the tritanopic channel considering discrepancies with yellow perception. We measured color discrimination thresholds for blue and yellow of tritanopic channel in congenital color deficiency subjects. Chromaticity thresholds were measured around a white background (0.1977 u′, 0.4689 v′ in the CIE 1976) consisting of a blue–white and white–yellow thresholds in a tritanopic color confusion line of 21 congenital colorblindness subjects (mean age = 27.7; *SD* = 5.6 years; 14 deuteranomalous and 7 protanomalous) and of 82 (mean age = 25.1; *SD* = 3.7 years) normal color vision subjects. Significant increase in the whole tritanopic axis was found for both deuteranomalous and protanomalous subjects compared to controls for the blue–white ($F_{2,100} = 18.80$; $p < 0.0001$) and white–yellow ($F_{2,100} = 22.10$; $p < 0.0001$) thresholds. A Principal Component Analysis (PCA) found a weighting toward to the yellow thresholds induced by deuteranomalous subjects. In conclusion, the discrimination in the tritanopic color confusion axis is significantly reduced in congenital color vision deficiency compared to normal subjects. Since yellow discrimination was impaired the balance of the blue–yellow channels is impaired justifying the increased thresholds found for blue–white discrimination. The weighting toward the yellow region of the color space with the deuteranomalous contributing to that perceptual distortion is discussed in terms of physiological mechanisms.

Keywords: chromaticity discrimination, anomalus trichromacy, chromatic thresholds, color vision, tritanopic color confusion line, visual psychophysics

OPEN ACCESS

Edited by:
Laurence T. Maloney, Stanford University, USA

Reviewed by:
Maria Olkkonen, Durham University, UK/University of Helsinki, Finland
Maris Ozolinsh, University of Latvia, Latvia

****Correspondence:***
Marcelo F. Costa
costamf@usp.br

Specialty section:
This article was submitted to Perception Science, a section of the journal Frontiers in Psychology

Received: *13 June 2014*
Accepted: *10 March 2016*
Published: *30 March 2016*

Citation:
Costa MF, Goulart PRK, Barboni MTS and Ventura DF (2016) Reduced Discrimination in the Tritanopic Confusion Line for Congenital Color Deficiency Adults. Front. Psychol. 7:429. doi: 10.3389/fpsyg.2016.00429

INTRODUCTION

Congenital color blindness is a genetic condition in which male subjects show impairment in performing red–green discriminations increasing the confusion between those colors with yellow. The chromatic discrimination impairment can vary from a very weak loss of discrimination mediated by the L-cone or M-cone – anomalous trichromacy – to total loss of discrimination –

dichromacy (Motulsky, 1988; Neitz and Neitz, 1995; Neitz et al., 2004; Deeb, 2005). Two post-receptoral channels exclusively carrying L- and M-cone information building physiologically opponent center-surround input processing in which signals from the L- and M-cones are antagonists – often called red–green opponency (De Valois and Abramov, 1966; De Valois and Jacobs, 1968; Lee et al., 1989; Lee, 1996). The Parvocellular (PC) pathway is suggested to carry the color information to the visual cortex and the Magnocellular (MC) pathway the luminance information (Lee, 1996).

The inputs of the L- and M-cones also contribute to another post-receptoral channel in which the S-cone signal is processed opponent to the L and M-cone signals combined – subjects show impairment in performing blue–yellow color discriminations increasing the confusion between those colors with white – called blue–yellow opponency, projecting to visual cortex via Koniocellular (KC) pathway of the LGN (Silveira et al., 1999; Teufel and Wehrhahn, 2000; Szmajda et al., 2006; Roy et al., 2009; Packer et al., 2010). The lines on the CIE color diagram corresponding to the red–green (protan and deutan) and blue–yellow (tritanopic) color opponency are the color confusion axes (**Figure 1**).

A recent study characterizing the S+ and S− cells of the macaque LGN showed critical asymmetries between those S-cone cells (Tailby et al., 2008). Three main results were found in that study. The prevalence of S+ and S− cells had similar proportions which differ from previous studies reporting higher proportion of S+ cells. The chromatic proprieties of the S+ and S− cells show differences in the anatomical level. S− cones sum information over a larger retinal area than the S+ cones. Additionally, the input from L and M cones linked to the S+ cones had the same sign (summed). Differently from the S-cones in which the M cone has the same sign than the S-cone (summed) and the L cone had an opposite sign.

Considering the post-receptoral contributions of L and M cones in the blue–yellow opponency channel, the proportions of the L and M cells directed by ON or OFF bipolar cells should be the basis for different chromatic configuration of the S+ and S− cells. New electrophysiological evidences in the macaque's LGN shows that, given the S+ cells receive inputs from L and M cones over a larger region of the retina, there were more chances of the L and M inputs having the same sign [S against (L + M)] (**Figure 1B**). Since S− receives inputs from smaller retina areas, and the proportion of L cones are higher than M cones, there is a higher chance of the inputs that come from the L and M cells shows opponent signs that configure the channel [(S− +M) against L] (Tailby et al., 2008; **Figure 1C**).

The authors also found a strong alignment to tritanopic axis for the physiological responses recorded in S+ cells, unlike the S− cells in which responses recorded generates a color confusion axis varying between the S-cone axis and the L − M axis. This means that the S− cells could be much more affected by the spectral sensitivity changes in the M or L cones. Considering the S− cells more variable responses behavior we argue that the changes in the spectral sensitivity of L or M cones, such as those characteristic of congenital anomalous trichromats, will probably impact the tritanopic confusion axis.

Based on that physiological information, we could suppose that in deuteranomalous and in protanomalous subjects the spectral sensitivity shifts would affect more the responses of S− cells. In addition, the S− cells show lower contrast sensitivity and stronger habituation susceptibility. The S+ cells discrimination would be less affected by spectral sensitivity changes of L and M cones since they show more restricted discrimination to tritanopic axis in both deutanomalous and protanomalous subjects. Thus, for the S− cells pathway we expect a more drastic effect in discrimination since this subtype is less specific to the tritanopic axis.

Behavioral studies of chromatic discrimination on the tritanopic color confusion axis in congenital color blindness are nevertheless scarce. Tritanopic discrimination was studied in patients with glaucoma, using Farnsworth 100-hue and the Besacon anomalometer. The results showed a significant shift to the blue part of the anomalous coefficient at the anomalometer equation and a higher total error score in the FMH100 with a lower discrimination at the blue region caps suggesting impairment in the S-cone pathway (Huang et al., 1993; Mantyjarvi and Tuppurainen, 1994). That result also could support the findings of another study showing a greater spectral shift in the blue region than in the yellow region of the tritanopic color confusion axis (De Valois et al., 1997). However, the whole picture is not too clear. Under high light levels the S-cone pathway could mediate some red–green discrimination in dichromatic subjects (Mcmahon and MacLeod, 1998).

In this paper, we investigate the chromaticity discrimination in the tritanopic color confusion axis in anomalous trichromats and dichromats subjects, assuming that their impaired L or M cone spectral sensitivity should impair their tritanopic discrimination. Our hypotheses are: (1) Protanomalous and deuteranomalous subjects have similar tritanopic discrimination as normal color vision subjects since on a S+ channel the restricted responses to S cone axis would preserve the discrimination despite the yellow region shifts to more reddish or greenish regions away from the axis, respectively; (2) Protanomalous and deuteranomalous subjects exhibit different from normal color discrimination on tritanopic axis since the S− cells had increased sensitivity to spectral shifts. Both hypotheses are possible since the proportion of S+ and S− pathways were found similar in the macaque LGN (Tailby et al., 2008).

MATERIALS AND METHODS

Subjects

We evaluated 82 subjects with normal color vision recruited among the Institute of Psychology of the University of São Paulo students and staff with mean age of 25.1 years ($SD = 3.56$, 40 males). Anomalous trichromats ($n = 21$, mean age 27.7, $SD = 5.6$, all male) were also from the University of São Paulo students and staff. Demographic data is presented in **Table 1**. All subjects underwent a complete ophthalmological examination, including best-corrected visual acuity measurement, slit-lamp biomicroscopy and optic disk evaluation with the pupils dilated,

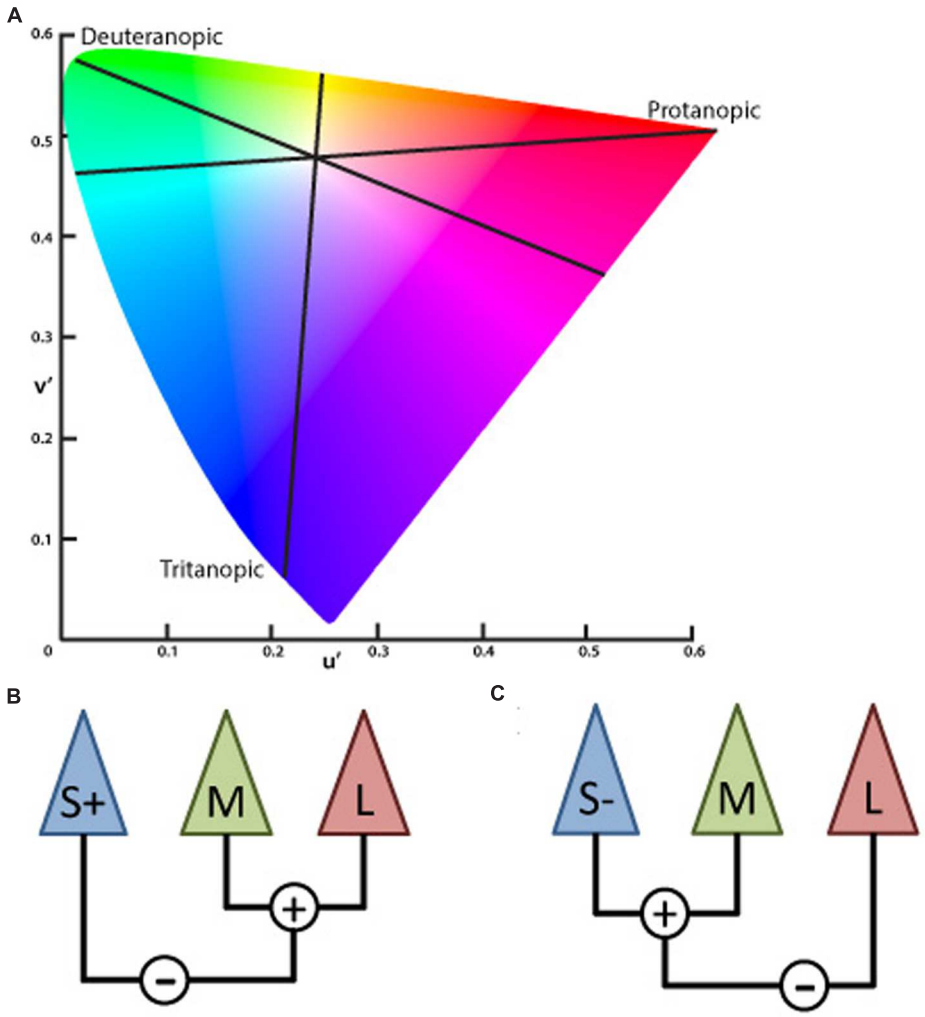

FIGURE 1 | (A) Graphic representation adapted from the CIE 1976 L*u*v* Color Space and u′, v′ Uniform Chromaticity Scale Diagram (www.cie.co.at/index.php/Publications/Standards). This spatial representation of colors is a non-linear transformation from the CIE 1931 L*x*y* color space to attempt a perceptual uniformity. The black lines represent the three – protanopic (L-cone), deuteranopic (M-cone), and tritanopic (S-cone) – color confusion axis in which colors of both sides along each of those lines could be mixed to be confused with the white center. **(B)** Schematic view of the S, M, and L cones contribution to the chromatic information of the koniocellular pathway, based on the physiological recordings of cone inputs to the lateral geniculate nucleus (LGN) of *Macaca fascicularis* performed by Tailby et al. (2008). Cone input configuration of the S+ cells in which the S-cone signal is opposed to the sum of the L- and M-cones. **(C)** Cone input of the S− cells in which the S-cone signal is summed with the M- cone and opposed to the L- cone.

with a 78-diopter lens. Inclusion criteria were best-corrected visual acuity of 20/20 or better measured monocularly at 4 m using an ETDRS chart – tumbling E (Xenonio, Sao Paulo, Brazil), refraction of $\leq$3.0 diopters considering the spherical equivalent of astigmatism values, absence of ophthalmological diseases and absence of known neurological and systemic diseases.

The study was approved by the Ethics Committee of the Institute of Psychology, University of Sao Paulo, and all subjects gave a signed informed consent to participate in the experiment. All were unaware to the specific experimental question. This study is also in accordance with the ethical standards laid out in the 1964 Declaration of Helsinki.

Equipment and Procedures

The evaluation of the color discrimination was performed using the commercial version of the Cambridge Color Test, CCT (v2.0 [Cambridge Research Instruments]) installed in a personal computer (Dell Dimension XTC-600) with a graphic card VSG 2/5 (Cambridge Research Instruments). The stimuli were generated in a high-resolution color monitor, Sony FD Trinitron model GDM-F500T9 (Sony). Testing was conducted in a dark room with the patients positioned 3 m away from the screen.

The stimulus provided by the CCT was similar to those used in the pseudoisochromatic plate tests, such as the Ishihara test (Kanehara Traiding Co.) or the AO H-R-R (v.4 Richmond Products, Albuquerque, NM, USA 2006). The target consisted of

TABLE 1 | Demographic data of the controls.

Age	CCT trivector			CCT ellipse			Anomalous quotient	Matching point (amplitude in anomaloscope units)	CCT†	Anomalous%
	Protan	Deutan	Tritan	Length	Axis	Angle				
Controls										
25.0	36.3	36.5	56.1	0.0103	1.45	76.3	0.97	37 (1.0)		
(3.6)*	(11.0)	(10.1)	(15.9)	(0.003)	(0.25)	(17.8)	(0.10)			
Anomalous trichromats										
23	315	312	141	0.0474	1.86	170.2	1.56	45 (11.0)	PN	PN
32	907	131	46	29.267	309.55	4.6	1.47	44 (19.0)	PN	PN
22	640	251	62	0.1658	9.11	3.5	1.61	45.5 (20.0)	PN	PN
34	268	1100	85	0.1391	10.49	167.0	0.83	33.5 (17.5)	DT	DN
25	265	332	85	0.0973	9.13	5.1	0.85	34 (15.0)	DN	DN
36	265	1100	96	0.2311	9.42	168.0	0.72	31 (20.0)	DT	DN
35	1100	261	70	0.1745	11.45	2.6	1.39	43 (19.0)	PT	PN
24	240	1100	80	132.882	1266.18	166.7	0.55	26.5 (68.0)	DT	DN
25	156	642	70	0.0324	2.98	167.5	0.80	33 (13.5)	DN	DN
27	33	140	88	0.583	4.36	169.1	0.85	34 (23.0)	DN	DN
25	216	638	78	0.0384	4.1	174.8	0.85	34 (19.5)	DN	DN
30	284	1100	83	0.0286	3.55	177.7	0.60	28 (23.5)	DT	DN
39	392	1100	129	0.2614	12.41	167.8	0.57	27 (12.5)	DT	DN
38	255	908	79	0.0949	4.45	172.8	0.62	28.5 (22.0)	DN	DN
23	69	131	70	0.0216	2.22	173.5	0.79	32 (13.5)	DN	DN
23	322	218	63	0.0451	4.7	4.3	1.48	44 (16.5)	PN	DN
26	319	845	102	0.1634	9.86	160.7	0.89	35 (19.5)	DN	DN
25	1006	354	109	0.2152	12.8	4.00	1.66	46 (12.5)	PN	PN
22	639	250	65	0 1657	9.12	3.9	1.81	47.5 (16.5)	PN	PN
23	310	316	139	0.0476	2.06	173.3	0.90	35 (13.0)	DN	DN
25	210	642	75	0.0383	4.5	176.2	0.66	29.5 (24.0)	DN	DN

Dlchromat and Anomalous Trichromat Subjects.
†*Diagnosis Based on CCT Trivector; *standard deviation.*
%*Diagnosis based on Anomalous cope.*
PT, Protanope/PN, Protanomalous; DT, Deuteranope/DN, deuteranomalous.

a Landolt "C" that differed in chromaticity from the single neutral background [coordinates 0.1977, 0.4689 of the International Commission on Illumination (CIE) u′v′ 1976 color space] (**Figure 2A**). The size of the Landolt C gap corresponded to 1.25° of visual angle, with the outer diameter 5.40° and the inner diameter 2.75° at the test distance of 3 m. Both the target and the background were composed of small patches of varying sizes (0.5–2 cm in diameter) and six luminance levels [8, 10, 12, 14, 16, and 18 candela (cd)/m2] randomly distributed on the screen. This visual layout creates spatial and luminance noise aiming to avoid the influence of cues derived from luminance differences and/or simultaneous contrast from target contours in the intended hue discrimination.

The target was randomly presented with its opening in one of four positions: up, bottom, right, and left (4-Alternative Forced Choice strategy). The patient's task was to press one of the four buttons of the response box [CT3 (Cambridge Research Instruments)], to indicate the position of the "C" opening. The patients had up to 5 s to give the response. A psychophysical staircase procedure was used for threshold determination. Each staircase began with a saturated chromaticity (strong color very different from the background), which was changed along the vector connecting it to the background chromaticity. The change depended on the patient's response: the target chromaticity approached the background chromaticity every time there was a correct response and moved away from it every time there was an incorrect response or no response. The chromaticity excursion along the vectors ranged from 0.1100 to 0.0020 u′v′ units of CIE 1976 color space. After six staircase reversals, the program automatically calculated the threshold for that vector as the average of the chromaticities corresponding to the last four reversals. The step size used in the staircase followed a dynamic rule; basically the size considered in the performance of the last responses to calculate the next values to present [for more details on the CCT methodology, see the work of (Regan et al., 1994) and, for CCT norms, see the work of (Ventura et al., 2002, 2003b; Costa et al., 2006; Paramei, 2012)].

In order to measure the thresholds along the tritanopic color confusion line, we used the CCT protocol for the construction of a discrimination ellipse (MacAdam ellipse) for the type of color impairment and their respective severity classification (**Figure 2B**). However, some methodological adjustments were performed since we were measuring only one of eight axes. The ellipses adjustment is performed using the Least Squares Method and our empirical experiment reveal that in many congenital color deficit subjects the ellipses fitting generate

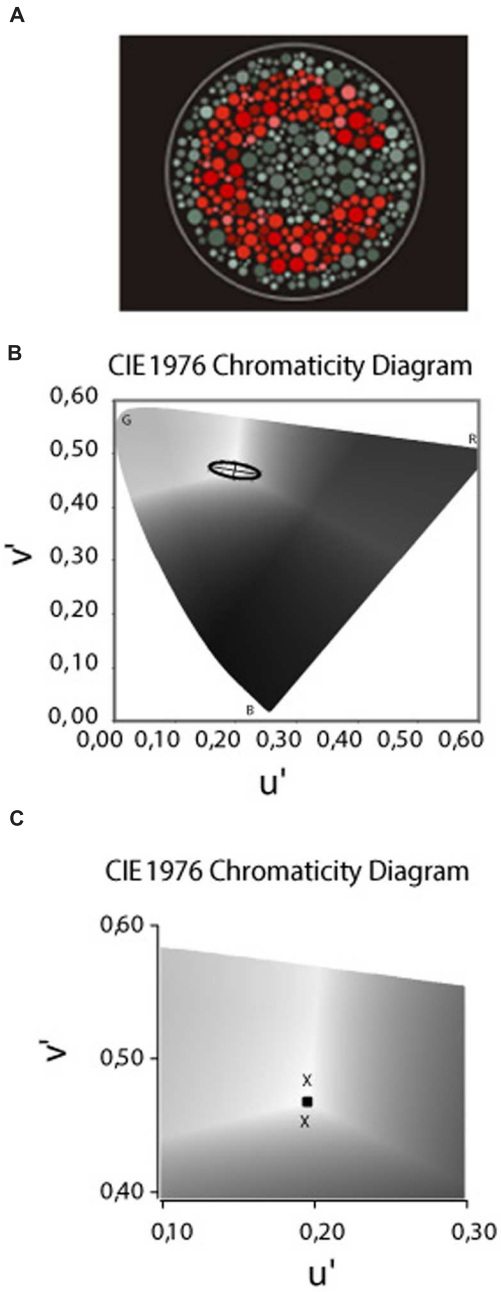

FIGURE 2 | (A) The target – a Landolt "C" – that differed in chromaticity from the single neutral background [coordinates 0.1977, 0.4689 of the (CIE) u′v′ 1976 color space]. The target and background composed of small patches of varying sizes and luminance levels randomly distributed in the display. **(B)** The CIE 1976 u′ v′ Chromaticity Diagram used to draw the MacAdam ellipses or the non-discriminable area. The letters B, G, and R represent the spatial position of the blue, green, and red primaries, respectively. The bright central area (coordenates 0.1977 u′, 0.4689 v′) was the stimulus background and the "Xs" represents the thresholds measured in the each of the eight color confusion vectors. The ellipses drawn is regarding to one of our deuteranomalous subjects based on the method of the least squares. **(C)** Magnification of the Chromaticity Diagram in which we present a sample of thresholds measured in the tritanopic axes to the yellow (upper cross) and blue (lower cross) directions. The central square represents the backgroud chromaticity coordinates.

distortions in the tritanopic axes in which the ellipses contour passes away from the threshold measured. The distortion in the tritanopic axis, probably, occurs in the congenital color deficient subjects since, different from the subjects with normal color vision, they had significantly worse thresholds in the red–green axes compared to the blue–yellow axis which are perpendicular. The ellipses adjustment considers the Laplace distribution of the error which uses a symmetric two-sided exponential distribution to model the error distribution, and the sum of absolute deviation as estimation error; in our case, applied in an asymmetrical distribution of the thresholds data around background.

Since we were exclusively interested in the tritanopic discrimination, and to avoid the distortions in the ellipses fitting, as previously described, we considered the value of the thresholds measured at 90° and at 270° directions from the background described in u′ v′ coordinates of the CIE 1976 color space, and not the ellipses fitting to that color confusion axis (**Figure 2C**).

The staircases corresponding to these vectors were run in interleaved pairs randomly chosen by the software. We used the thresholds measured in the tritanopic axes as an indicator of the subject's performance in color discrimination for "yellow" and "blue" sides against the white background.

Statistical Analysis

Statistical analysis was performed with the software Statistica (v.12 StatSoft Inc. CA, USA, 2012). A full descriptive analysis was performed. Statistical differences among the groups were verified with the One-Way ANOVA. We use the Fisher least square differences (LSD) *post hoc* comparison, to determine the significant differences between group means in the ANOVA test. We used the method of PCA, for the purpose of variables diagnostics, computing factor coordinates and factor score coefficients as a classification technique, highlighting the relations among variables (thresholds for the blue–white and white–yellow directions of the tritanopic color confusion line in subjects with protan, deutan color vision defects and normal color vision) and cases (subjects). Adhesion to the normal distribution was checked with the Kolmogorov–Smirnov test.

RESULTS

Thresholds measurements were performed in both control and congenital color vision impairment groups. The mean value obtained for the tritanopic axis was 0.0096 u′v′ units ($SD = 0.00244$) for controls and 0.0160 u′v′ units ($SD = 0.0070$) for the congenital color impairment group. The longer diameters measured in the color congenital impairment group had a statistical difference ($F_{2,100} = 46.95$; $p < 0.0001$) compared with those of the Control group. The breakdown analysis performed in the congenital color impairment group tested for differences between the subjects with protan (mean diameter 0.0150 u′v′ units; $SD = 0.0055$) and deutan (0.0166 u′v′ units; $SD = 0.0078$) color defects. No statistical differences were found between these two groups, but both of them differ statistically from the control group subjects ($F_{1,101} = 25.32$; $p < 0.0001$; **Figure 3**).

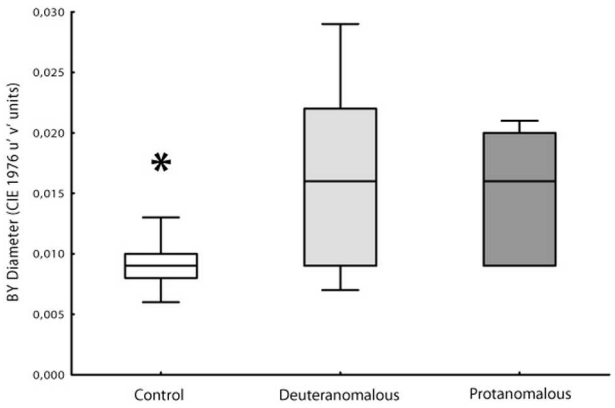

FIGURE 3 | Box Plot showing the median and interqurtile ranges with brackets showing the 95% of blue–yellow discrimination diameter. Normal color vision subjects had significant better discrimination than deuteranomalous or protanomalous subjects. Control's are statistically significant better than others (*$p > 0.001$).

In order to investigate if the increase in tritanopic thresholds was symmetric to blue and yellow regions of the color space, we calculate a blue–yellow difference index, in which for each subject we subtracted the thresholds of blue from the yellow. Values around zero suggest symmetry between those thresholds at the color space. Positive values suggest higher thresholds for the yellow region and negative values suggest higher thresholds toward the blue region of the tritanopic axis (**Figure 4**). Statistical differences were found for protan (mean difference 0.0150 u′v′ units; $SD = 0.0014$) and deutan (0.0165 u′v′ units; $SD = 0.0048$) color defect subjects with normal color vision subjects (−0.0005 u′v′ units; $SD = 0.0015$; $F_{1,101} = 199.71$; $p < 0.0001$) for both blue and yellow distances.

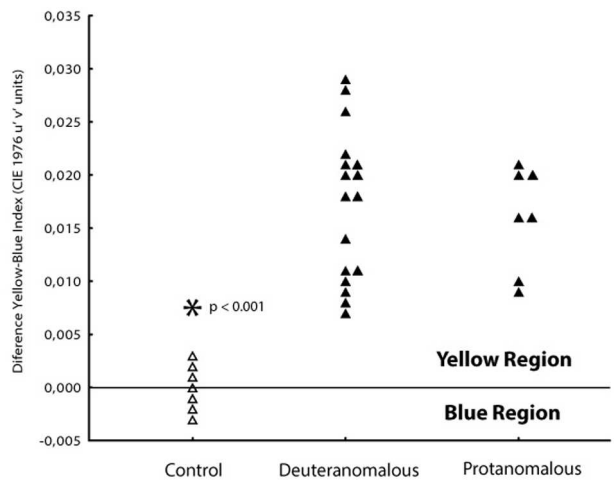

FIGURE 4 | Differences between thresholds obtained at 90 and 270° axes in order to analyses the yellow–blue symmetry. Normal color vision subjects (△) had thresholds spread symmetrically between the orthogonal axes with a mean blue–yellow index around zero. Both protanomalous and deuteranomalous subjects (▲) had a asymmetrical shift toward the yellow direction (positive values) showing worse discrimination to that direction.

Since the higher dispersion of the thresholds values in color congenital deficiency subjects could be masking possible weighting for yellow or blue regions of the tritanopic axis, we performed a PCA to investigate if there were asymmetries supporting differences in those axis' regions. As we could see, we found a statistically significant discrimination between the blue and yellow thresholds related to the total distance in which the yellow distance is an isolated component suggesting it as a more affected region of the tritanopic axis. The PCA results are shown in **Table 2** and **Figure 5**.

Two factors were obtained in the PCA analysis. The first factor represents the subject groups (controls and congenital color deficiency), and the second factor represents the thresholds of the yellow and blue regions of the tritanopic axis. In **Table 2** we can see a high degree of similarity, based on correlation analysis, suggesting a strong association between the variables for the first factor (control vs. color deficient). However, the second factor (blue vs. yellow thresholds in the tritanopic axis) shows a different projection of the individual cases of congenital color deficiency subjects to the yellow region of the chromaticity diagram, when compared with the blue region. Negative values of the first factor indicate a strong effect of color deficiency subjects and the second factor indicates that those effects are related to the yellow direction of the diagram. This result is seen in the PCA graphical analysis (**Figure 5A**).

Another interesting result can be observed in the graphical analysis of each single case (**Figure 5B**). Control subjects (labeled 1) were located in the right side of the factor 1 and were symmetrically spread around zero value of the factor 2. The deuteranomalous subjects (labeled 3) were more distant in factor 1, which means that they present stronger defects and also they were located in the positive values of factor 2 associated with the yellow projection, suggesting a high correlation between them.

DISCUSSION

In our paper, we showed consistent tritanopic color vision impairment in subjects with congenital color deficiency. Protanomalous and deuteranomalous subjects had higher thresholds of color discrimination compared with subjects with normal color vision. We were able to measure separated thresholds for the yellow and the blue regions of tritanopic axis. We also have strong information that supports the evidence that an abnormal L or M cone contributes to a statistically significant higher threshold on the yellow region.

Few studies were careful to analyze the yellow and blue regions of the tritanopic color confusion axis. In this sense, our paper corroborates previous studies showing separated channels for blue and yellow in which they reported longer reaction times to blue than green and yellow stimuli in normal color vision subjects (Medina and Diaz, 2006, 2010; Medina and Mullen, 2009). Additional evidence came from the study of Devos et al. (1996) in which the authors found bigger axis length in the MacAdam ellipses axis for blue–yellow discrimination in color

TABLE 2 | Principal component analysis (PCA) factors.

	Factor 1	Factor 2
BY yellow region	−0,944736	0,327832
BY blue region	−0,954880	−0,296992
BY diameter	−0,999658	−0.026132

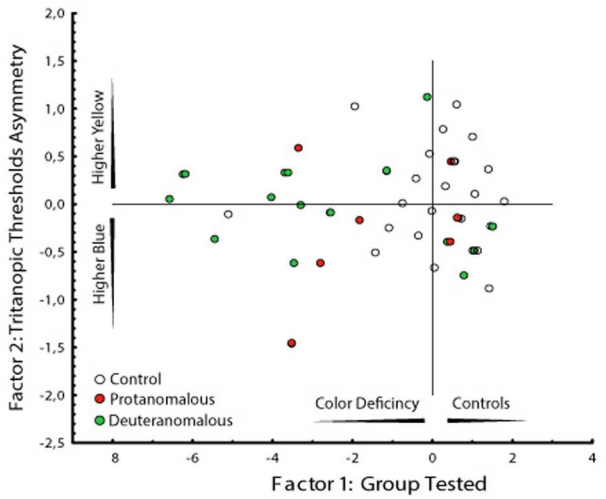

FIGURE 5 | Graphical analysis of the two factors computed by the PCA. Factor 1 represent the subject groups (controls and congenital color deficiency) and factor 2 the thresholds to the yellow and blue regions of the tritanopic axes. It is interesting that the deuteranomalous subjects (labeled 3) had longer distances from the central than protanomalous (labeled 2) and controls (labeled 1), which means that they were the more affected group (more to the left side) and they showed the worse yellow color discrimination (more to upper side).

congenital than normal subjects. Those results are in line with ours and could be considered an indirect result of our threshold measurements.

The main purpose of this research was to investigate possible tritanopic deficits in color discrimination of congenital color deficiency subjects and we were able to prove them. We had two main hypotheses about the tritanopic color discrimination impairment. The post-receptoral color vision mechanism is based on an opponency system of photoreceptors inputs to ganglion cells via bipolar cells. Two color pathways and one achromatic pathway leave the retina toward the higher subcortical and cortical processing levels. The Parvocellular pathway carries the color opponency of the L and M cones, and the Koniocellular pathway carries the S and (L + M cones; Cole et al., 1993; Dacey and Lee, 1994; Dacey, 1999; Packer et al., 2010). Since in congenital color deficiencies, the subjects express abnormal M or L pigments with a consequent shifting at the spectral absorption peak (Nathans et al., 1992; Deeb et al., 1994; Neitz and Neitz, 2000; Deeb, 2004, 2005; Neitz et al., 2004), it is quite reasonable to suppose that their color discrimination will be impaired for the colors in the tritanopic color confusion axis as well as for the evident red–green color confusion axes. However, the thresholds and scores found for most of the studies done on congenital color impairment subjects reveal that in the tritanopic color confusion axis, so far were found to be similar to those of normal color vision subjects (Pinckers et al., 1985; Birch, 1989; Ing et al., 1994; Kon and De, 1996; Hovis et al., 2004). The chromaticity discrimination in tritanopic color confusion axis in anomalous trichromats and dichromats subjects should impair their S cell's discrimination as previously discussed. In our study, protanomalous and deuteranomalous subjects exhibit different color discrimination on tritanopic axis when compared to subjects with normal color vision which lead us to suggest that S cells had increased sensitivity to spectral shifts.

A recent study characterized the S+ and S− cells measured at the macaque LGN showed critical asymmetries between those S-cone cells (Tailby et al., 2008). The S− cells receive inputs from L and M cones over a larger region of retina, increasing the chances of L and M inputs having the same sign [S against (L + M)]. The S+ cells, however, receive inputs from smaller retina areas and given that the proportion of L cones is frequently higher than M cones, there is a higher chance that L and M cones inputs show opponent signs configuring the channel S− against L cells. Our results show that protanomalous subjects presented better color discrimination in the tritanopic color confusion axis than deuteranomalous subjects. We believe that S+ channel could support our findings. Considering the S+ channel of deuteranomalous subjects, the shift in the M cone spectral sensitivity closer to L cone should decrease the discrimination than the spectral sensitivity shift of L cone in direction to M cone presented in the protanomalous. This result supports the idea that deuteranomalous and protanomalous subjects had more complex perceptual differences for chromatic stimuli than we predicted.

We believe that the recent computerized method makes this kind of analysis easier to be implemented, due to its impressive methodological refinement. Chromaticity modifications are faster and reliable using computers and monitor screens. Computerized methods of study color discrimination for red–green and blue–yellow opponency, are far more superior to classical arrangement tests such as: FMH100, and pseudoisochromatic plates that have been reported in the literature (Ing et al., 1994; Birch, 1997; Ventura et al., 2003a,b, 2004, 2005a,b, 2007; Costa et al., 2005, 2006, 2007; Seshadri et al., 2005; Melamud et al., 2006; Paramei, 2012).

According to the PCA the increase of color discrimination thresholds at the tritanopic color confusion axis was due to the loss of discrimination generated by the yellow (or L + M cone) region of the axis. This is expected because the gene alteration in congenital color deficiency occurs in the chromosome that encodes both of those opsins (Nathans et al., 1992; Neitz and Neitz, 1995; Deeb, 2004, 2005). This idea is supported by the psychophysical findings in measurements of reaction time for chromatic stimulus that both red–green and blue–yellow post-receptoral channels had different mechanisms for each region (Medina and Diaz, 2006, 2010; Medina and Mullen, 2009). Nevertheless, our study found similar results using not only the hue dimension, but chromaticity coordinates; which are a more complex stimuli since it changes with hue and saturation simultaneously.

Asymmetries for thresholds measured by equiluminous spots for the blue, green, and yellow, but not the red sides of the color confusion axes were also found in subjects with optic nerve hypoplasia (Billock et al., 1994). This is an intriguing result and suggests a post-receptoral independence for each branch of the color opponent channel. The study of Devos et al. (1996) found that the thresholds along the red–green direction of the MacAdam ellipses minor axis (tritanopic axis) of the congenital color deficient subjects were significantly lower than those along the tritanopic axis measured for subjects with normal color vision. This result corroborates our findings suggesting additional tritanopic axis differences in congenital colorblindness. However, when the authors computed the tritanopic axis length (total distance between the ellipses borders) no difference was found leading them to conclude that there was no difference between the groups. Here, we have an important methodological point that could justify the absence of differences. The MacAdam ellipses adjustment was performed using the Least Squares Method which minimizes vast discrepancies by squaring the summed errors. In congenital color deficient subjects that method generates fitting distortions in the tritanopic color confusion axis in which the ellipses contour fitting frequently passes distant from the threshold measured. Additionally, our result shows a weighted contribution of the deuteranomalous for the yellow asymmetry. Hence, we suggest that the increase in the yellow region of the tritanopic color confusion axis is probably more related to the M than to the L cone contribution for the yellow color (L + M cone). Considering that our paper presents the first report on this matter, we consider that future works addressing these analyses in subjects with color congenital deficiencies are needed to confirm the hypothetical weighted M cone to yellow discrimination and to explore the L + M cone contributions in the tritanopic color discrimination reported in previous studies (Dacey and Lee, 1994; Dacey, 1996, 1999; Stromeyer et al., 1998; Horwitz et al., 2005; Diaconu and Faubert, 2006; Packer et al., 2010).

CONCLUSION

The paper emphasizing our main findings: that the tritanopic color confusion axis impairment is present in subjects with congenital color deficiencies. The yellow region of the tritanopic color confusion axis was more evidently affected when compared with the blue region. Additionally, we found that deuteranomalous subjects were more affected than the protanomalous subjects; suggesting different and more complex color discrimination performances between them that we traditionally expect.

AUTHOR CONTRIBUTIONS

All authors listed, have made substantial intellectual contribution to the work, and approved it for publication. MC performed all statistical analysis, figures and wrote the first versions of the MS. PG collected almost of the CCT data. MB and DV performed substantial modifications in the MS and also collected some data.

FUNDING

This study was supported by CNPq Edital Ciências Humanas (401153/2009-6), Edital Universal (472093/2010-0) and FAPESP Projeto Temático (2008/58731-2).

ACKNOWLEDGMENTS

We would like to thank Agatha Rodrigues and Luiz Silva dos Santos for some support in statistical analysis. We also would like to thank Luiz Claudiel dos Santos for the administrative support. MC and DV are CNPq Fellow Researchers.

REFERENCES

Billock, V. A., Vingrys, A. J., and King-Smith, P. E. (1994). Opponent-color detection threshold asymmetries may result from reduction of ganglion cell subpopulations. *Vis. Neurosci.* 11, 99–109. doi: 10.1017/S0952523800011147

Birch, J. (1989). Use of the Farnsworth-Munsell 100-Hue test in the examination of congenital colour vision defects. *Ophthalmic Physiol. Opt.* 9, 156–162. doi: 10.1111/j.1475-1313.1989.tb00836.x

Birch, J. (1997). Clinical use of the City University Test (2nd Edition). *Ophthalmic Physiol. Opt.* 17, 466–472. doi: 10.1111/j.1475-1313.1997.tb00084.x

Cole, G. R., Hine, T., and McIlhagga, W. (1993). Detection mechanisms in L-, M-, and S-cone contrast space. *J. Opt. Soc. Am. A* 10, 38–51. doi: 10.1364/JOSAA.10.000038

Costa, M. F., Oliveira, A. G. F., Feitosa-Santana, C., Zatz, M., and Ventura, D. F. (2007). Red-green color vision impairment in Duchenne muscular dystrophy. *Am. J. Hum. Genet.* 80, 1064–1075. doi: 10.1086/518127

Costa, M. F., Oliveira, A. G. F., Santana, C. F., Lago, M., Zatz, M., and Ventura, D. F. (2005). Red-green color vision and luminance contrast sensitivity losses in Duchenne Muscular Dystrophy. *Invest. Ophthalmol. Vis. Sci.* 46, 4576.

Costa, M. F., Ventura, D. F., Perazzolo, F., Murakoshi, M., and Silveira, L. C. D. (2006). Absence of binocular summation, eye dominance, and learning effects in color discrimination. *Vis. Neurosci.* 23, 461–469. doi: 10.1017/S095252380623311X

Dacey, D. M. (1996). Circuitry for color coding in the primate retina. *Proc. Natl. Acad. Sci. U.S.A.* 93, 582–588. doi: 10.1073/pnas.93.2.582

Dacey, D. M. (1999). Primate retina: cell types, circuits and color opponency. *Prog. Retin. Eye Res.* 18, 737–763. doi: 10.1016/S1350-9462(98)00013-5

Dacey, D. M., and Lee, B. B. (1994). The 'blue-on' opponent pathway in primate retina originates from a distinct bistratified ganglion cell type. *Nature* 367, 731–735. doi: 10.1038/367731a0

De Valois, R. L., and Abramov, I. (1966). Color vision. *Annu. Rev. Psychol.* 17, 337–362. doi: 10.1146/annurev.ps.17.020166.002005

De Valois, R. L., De Valois, K. K., Switkes, E., and Mahon, L. (1997). Hue scaling of isoluminant and cone-specific lights. *Vision Res.* 37, 885–897. doi: 10.1016/S0042-6989(96)00234-9

De Valois, R. L., and Jacobs, G. H. (1968). Primate color vision. *Science* 162, 533–540. doi: 10.1126/science.162.3853.533

Deeb, S. S. (2004). Molecular genetics of color-vision deficiencies. *Vis. Neurosci.* 21, 191–196. doi: 10.1017/S0952523804213244

Deeb, S. S. (2005). The molecular basis of variation in human color vision. *Clin. Genet.* 67, 369–377. doi: 10.1111/j.1399-0004.2004.00343.x

Deeb, S. S., Jorgensen, A. L., Battisti, L., Iwasaki, L., and Motulsky, A. G. (1994). Sequence divergence of the red and green visual pigments in

great apes and humans. *Proc. Natl. Acad. Sci. U.S.A.* 91, 7262–7266. doi: 10.1073/pnas.91.15.7262

Devos, M., Spileers, W., and Arden, G. (1996). Colour contrast thresholds in congenital colour defectives. *Vision Res.* 36, 1055–1065. doi: 10.1016/0042-6989(95)00188-3

Diaconu, V., and Faubert, J. (2006). Chromatic parameters derived from increment spectral sensitivity functions. *J. Opt. Soc. Am. A Opt. Image Sci. Vis.* 23, 2677–2685. doi: 10.1364/JOSAA.23.002677

Horwitz, G. D., Chichilnisky, E. J., and Albright, T. D. (2005). Blue-yellow signals are enhanced by spatiotemporal luminance contrast in macaque V1. *J. Neurophysiol.* 93, 2263–2278. doi: 10.1152/jn.00743.2004

Hovis, J. K., Ramaswamy, S., and Anderson, M. (2004). Repeatability indices for the Adams D-15 test for colour-normal and colour-defective adults. *Clin. Exp. Optom.* 87, 326–333. doi: 10.1111/j.1444-0938.2004.tb05062.x

Huang, S., Wu, L., and Wu, D. Z. (1993). The normal color vision evaluated with FM 100-hue test. *Yan Ke Xue Bao* 9, 158–160.

Ing, E. B., Parker, J. A., and Emerton, L. A. (1994). Computerized color-vision testing. *Can. J. Ophthalmol. J. Can. D Ophtalmol.* 29, 125–128.

Kon, C. H., and De, A. D. (1996). A new colour vision test for clinical use. *Eye (Lond.)* 10(Pt 1), 65–74. doi: 10.1038/eye.1996.10

Lee, B. B. (1996). Receptive field structure in the primate retina. *Vision Res.* 36, 631–644. doi: 10.1016/0042-6989(95)00167-0

Lee, B. B., Martin, P. R., and Valberg, A. (1989). Nonlinear summation of M- and L-cone inputs to phasic retinal ganglion cells of the macaque. *J. Neurosci.* 9, 1433–1442.

Mantyjarvi, M., and Tuppurainen, K. (1994). Changes of color-vision in ocular hypertension. *Int. Ophthalmol.* 18, 345–349. doi: 10.1007/BF00930312

Mcmahon, M. J., and MacLeod, D. I. (1998). Dichromatic color vision at high light levels: red/green discrimination using the blue-sensitive mechanism. *Vision Res.* 38, 973–983. doi: 10.1016/S0042-6989(97)00280-0

Medina, J. M., and Diaz, J. A. (2006). Postreceptoral chromatic-adaptation mechanisms in the red-green and blue-yellow systems using simple reaction times. *J. Opt. Soc. Am. A Opt. Image Sci. Vis.* 23, 993–1007. doi: 10.1364/JOSAA.23.000993

Medina, J. M., and Diaz, J. A. (2010). S-cone excitation ratios for reaction times to blue-yellow suprathreshold changes at isoluminance. *Ophthalmic Physiol. Opt.* 30, 511–517. doi: 10.1111/j.1475-1313.2010.00745.x

Medina, J. M., and Mullen, K. T. (2009). Cross-orientation masking in human color vision. *J. Vis.* 9, 20.1–20.16. doi: 10.1167/9.3.20

Melamud, A., Simpson, E., and Traboulsi, E. I. (2006). Introducing a new computer-based test for the clinical evaluation of color discrimination. *Am. J. Ophthalmol.* 142, 953–960. doi: 10.1016/j.ajo.2006.07.027

Motulsky, A. G. (1988). Normal and abnormal color-vision genes. *Am. J. Hum. Genet.* 42, 405–407.

Nathans, J., Merbs, S. L., Sung, C. H., Weitz, C. J., and Wang, Y. (1992). Molecular genetics of human visual pigments. *Annu. Rev. Genet.* 26, 403–424. doi: 10.1146/annurev.ge.26.120192.002155

Neitz, M., Carroll, J., Renner, A., Knau, H., Werner, J. S., and Neitz, J. (2004). Variety of genotypes in males diagnosed as dichromatic on a conventional clinical anomaloscope. *Vis. Neurosci.* 21, 205–216. doi: 10.1017/S0952523804213293

Neitz, M., and Neitz, J. (1995). Numbers and ratios of visual pigment genes for normal red-green color vision. *Science* 267, 1013–1016. doi: 10.1126/science.7863325

Neitz, M., and Neitz, J. (2000). Molecular genetics of color vision and color vision defects. *Arch. Ophthalmol.* 118, 691–700. doi: 10.1001/archopht.118.5.691

Packer, O. S., Verweij, J., Li, P. H., Schnapf, J. L., and Dacey, D. M. (2010). Blue-yellow opponency in primate S cone photoreceptors. *J. Neurosci.* 30, 568–572. doi: 10.1523/JNEUROSCI.4738-09.2010

Paramei, G. V. (2012). Color discrimination across four life decades assessed by the Cambridge Colour Test. *J. Opt. Soc. Am. A Opt. Image Sci. Vis.* 29, A290–A297. doi: 10.1364/JOSAA.29.00A290

Pinckers, A., Nabbe, B., and Vossen, H. (1985). Standard pseudoisochromatic plates part 2. *Ophthalmologica* 190, 118–124. doi: 10.1159/000309504

Regan, B. C., Reffin, J. P., and Mollon, J. D. (1994). Luminance noise and the rapid determination of discrimination ellipses in colour deficiency. *Vision Res.* 34, 1279–1299. doi: 10.1016/0042-6989(94)90203-8

Roy, S., Jayakumar, J., Martin, P. R., Dreher, B., Saalmann, Y. B., Hu, D., et al. (2009). Segregation of short-wavelength-sensitive (S) cone signals in the macaque dorsal lateral geniculate nucleus. *Eur. J. Neurosci.* 30, 1517–1526. doi: 10.1111/j.1460-9568.2009.06939.x

Seshadri, J., Christensen, J., Lakshminarayanan, V., and Bassi, C. J. (2005). Evaluation of the new web-based "Colour Assessment and Diagnosis" test. *Optom. Vis. Sci.* 82, 882–885. doi: 10.1097/01.opx.0000182211.48498.4e

Silveira, L. C., Lee, B. B., Yamada, E. S., Kremers, J., Hunt, D. M., Martin, P. R., et al. (1999). Ganglion cells of a short-wavelength-sensitive cone pathway in New World monkeys: morphology and physiology. *Vis. Neurosci.* 16, 333–343. doi: 10.1017/S0952523899162138

Stromeyer, C. F. I, Chaparro, A., Rodriguez, C., Chen, D., Hu, E., and Kronauer, R. E. (1998). Short-wave cone signal in the red-green detection mechanism. *Vision Res.* 38, 813–826. doi: 10.1016/S0042-6989(97)00231-9

Szmajda, B. A., Buzas, P., Fitzgibbon, T., and Martin, P. R. (2006). Geniculocortical relay of blue-off signals in the primate visual system. *Proc. Natl. Acad. Sci. U.S.A.* 103, 19512–19517. doi: 10.1073/pnas.0606970103

Tailby, C., Solomon, S. G., and Lennie, P. (2008). Functional asymmetries in visual pathways carrying S-cone signals in macaque. *J. Neurosci.* 28, 4078–4087. doi: 10.1523/JNEUROSCI.5338-07.2008

Teufel, H. J., and Wehrhahn, C. (2000). Evidence for the contribution of S cones to the detection of flicker brightness and red-green. *J. Opt. Soc. Am. A Opt. Image Sci. Vis.* 17, 994–1006. doi: 10.1364/JOSAA.17.000994

Ventura, D. F., Costa, M. F., Gualtieri, M., Nishi, M., Bernick, M., Bonci, D. M., et al. (2003a). "Early vision loss in diabetic patients assessed by the Cambridge Colour Test," in *Normal and Defective Colour Vision*, eds J. D. Mollon, J. Pokorny, and K. Knoblauch (New York, NY: Oxford University Press Inc.), 395–403.

Ventura, D. F., Costa, M. T. V., Costa, M. F., Berezovsky, A., Salomao, S. R., Simoes, A. L., et al. (2004). Multifocal and full-field electroretinogram changes associated with color-vision loss in mercury vapor exposure. *Vis. Neurosci.* 21, 421–429. doi: 10.1017/S0952523804213372

Ventura, D. F., Gualtieri, M., Oliveira, A. G., Costa, M. F., Quiros, P., Sadun, F., et al. (2007). Male prevalence of acquired color vision defects in asymptomatic carriers of Leber's hereditary optic neuropathy. *Invest. Ophthalmol. Vis. Sci.* 48, 2362–2370. doi: 10.1167/iovs.06-0331

Ventura, D. F., Quiros, P., Carelli, V., Salomao, S. R., Gualtieri, M., Oliveira, A. G., et al. (2005a). Chromatic and luminance contrast sensitivities in asymptomatic carriers from a large Brazilian pedigree of 11778 Leber hereditary optic neuropathy. *Invest. Ophthalmol. Vis. Sci.* 46, 4809–4814. doi: 10.1167/iovs.05-0455

Ventura, D. F., Rodrigues, A. R., Moura, A. A., Vargas, A. C., Costa, M. F., de Souza, J. M., et al. (2002). Color discrimination measured by the cambridge colour vision test (CCNT) in children and adults. *Invest. Ophthalmol. Vis. Sci.* 43, U1046.

Ventura, D. F., Silveira, L. C., Rodrigues, A. R., de Souza, J., Gualtieri, M., Bonci, D. M., et al. (2003b). "Preliminary norms for the Cambridge Colour Test," in *Colour and Defective Colour Vision*, eds J. D. Mollon, J. Pokorny, and K. Knoblauch (New York, NY: Oxford University Press Inc.), 331–339.

Ventura, D. F., Simoes, A. L., Tomaz, S., Costa, M. F., Lago, M., Costa, M. T. V., et al. (2005b). Colour vision and contrast sensitivity losses of mercury intoxicated industry workers in Brazil. *Environ. Toxicol. Pharmacol.* 19, 523–529. doi: 10.1016/j.etap.2004.12.016

Conflict of Interest Statement: The authors declare that the research was conducted in the absence of any commercial or financial relationships that could be construed as a potential conflict of interest.

frontiers in PSYCHOLOGY

ORIGINAL RESEARCH ARTICLE
published: 07 October 2014
doi: 10.3389/fpsyg.2014.01136

Effects of saturation and contrast polarity on the figure-ground organization of color on gray

***Birgitta Dresp-Langley*[1]* and *Adam Reeves*[2]**

[1] ICube UMR 7357 CNRS/Université de Strasbourg, Strasbourg, France
[2] Psychology Department, Northeastern University, Boston, MA, USA

Edited by:
Marcelo Fernandes Costa, Universidade de São Paulo, Brazil

Reviewed by:
Andrew M. Haun, Harvard Medical School, USA
Ko Sakai, University of Tsukuba, Japan

***Correspondence:**
Birgitta Dresp-Langley, ICube UMR 7357 CNRS/Université de Strasbourg, 2 rue Boussingault, 67000 Strasbourg, France
e-mail: birgitta.dresp@icube.unistra.fr

Poorly saturated colors are closer to a pure gray than strongly saturated ones and, therefore, appear less "colorful." Color saturation is effectively manipulated in the visual arts for balancing conflicting sensations and moods and for inducing the perception of relative distance in the pictorial plane. While perceptual science has proven quite clearly that the luminance contrast of any hue acts as a self-sufficient cue to relative depth in visual images, the role of color saturation in such figure-ground organization has remained unclear. We presented configurations of colored inducers on gray "test" backgrounds to human observers. Luminance and saturation of the inducers was uniform on each trial, but varied across trials. We ran two separate experimental tasks. In the relative background brightness task, perceptual judgments indicated whether the apparent brightness of the gray test background contrasted with, assimilated to, or appeared equal (no effect) to that of a comparison background with the same luminance contrast. Contrast polarity and its interaction with color saturation affected response proportions for contrast, assimilation and no effect. In the figure-ground task, perceptual judgments indicated whether the inducers appeared to lie in front of, behind, or in the same depth with the background. Strongly saturated inducers produced significantly larger proportions of foreground effects indicating that these inducers stand out as figure against the background. Weakly saturated inducers produced significantly larger proportions of background effects, indicating that these inducers are perceived as lying behind the backgrounds. We infer that color saturation modulates figure-ground organization, both directly by determining relative inducer depth, and indirectly, and in interaction with contrast polarity, by affecting apparent background brightness. The results point toward a hitherto undocumented functional role of color saturation in the genesis of form, and in particular figure-ground percepts in the absence of chromatostereopsis.

Keywords: color perception, luminance contrast sensitivity, depth perception, achromatic contrast discrimination, colorimetry

INTRODUCTION

Poorly saturated colors, since they are closer to a pure gray than intense hues, appear less "colorful" than strongly saturated colors, yet, they still contain hue information. In the visual arts, color saturation is widely exploited as a measure for balancing opponent or conflicting sensations and moods. In the nineteenth century, at the dawn of abstract expressionism, painters such as Turner (especially in his later works) effectively used color to suggest what should be nearer or further away to the observer in the painting, relying on chromatic brightness, and saturation to express and balance figure and ground, moods, and other qualia (**Figure 1**). The earlier Renaissance painters had preferentially resorted to chiaroscuro and geometric cues to aerial perspective using a limited chromatic range to create landscape depth and figure-ground effects. Later in the evolution of visual art, modern architects and designers like Vasarély effectively manipulated color saturation in combination with planar shape geometry to play with foreground and background effects in a complex and abstract manner (**Figure 2**), illustrating how chromatic luminance, saturation, and shape can be combined to elicit powerful visual sensations suggesting three-dimensional structure. While contemporary visual artists tend to share the strong belief that saturation is a key medium for creating perceptual structure, perceptual science has not yet clarified the functional contribution of color saturation to perceptual organization. Imagine the simplest possible two-dimensional image with no more than two adjacent surface regions. When there is a difference in brightness between the two adjacent regions, they can constitute a figure-ground reversible pattern, where the region seen as figure is perceived in front of the region seen as ground. This difference in perceived depth between the two regions increases as their difference in brightness increases. The observation originally stems from an experiment by Egusa (1977), who presented two different achromatic surfaces, viewed through a small aperture, on a black screen. The surface on the right was of one of three different shades of gray, and the one on the left was either white or black. Observers made

FIGURE 1 | In the nineteenth century, painters like Turner effectively exploited color, saturation, and luminance effects to suggest figure and ground, as here in "Sunset on Rouen."

judgments regarding the apparent depth of these surfaces in terms of which of the two appeared nearer. The results of this study were the first to reveal a systematic relation between perceived relative depth and brightness differences between adjacent surface regions, in that increasing the brightness difference increased the perceived depth separation in every observer. Whether the brighter or the darker of the two test surfaces appeared nearer differed from observer to observer. Subsequently, Egusa (1983) examined the effects of brightness, hue, and saturation on the perceived depth between two adjacent regions. Again, the stimuli consisted of two hemifields, either both achromatic, one achromatic the other chromatic, or of two different colors. Subjects were asked to state which hemifield appeared nearer, and to put a number on the perceived depth between (depth magnitude estimation). When both hemifields were achromatic, the perceived depth was found to increase with increasing brightness difference. Again, some subjects tended to judge the brighter side nearer, others the darker side. With the achromatic-chromatic combination, there were no differences in perceived depth among three hue conditions, whilst with the chromatic-chromatic combination the perceived depth depended on the hue combination. In terms of decreasing frequency of "nearer" judgments, the hue order was red, green, and blue. When two chromatic hemifields differed in saturation only, the perceived depth increased with increasing difference in saturation, and whether the more saturated or the less saturated side was judged nearer depended on hue. Thus, the figure-ground differentiation between two adjacent chromatic regions in the visual field is jointly determined by brightness, hue and saturation, affecting the perceived distance of a given region from the observer.

Since Leonardo Da Vinci's *Trattato della Pittura* (Da Vinci, 1651) mentioning luminance contrast as a cue to pictorial depth, perceptual science has confirmed that it directly determines what will be seen as nearer or further away in two-dimensional visual configurations and images (Mount et al., 1956; Farnè, 1977; Rohaly and Wilson, 1993; O'Shea et al., 1994; Dresp et al., 2002; Guibal and Dresp, 2004; Dresp-Langley and Reeves, 2012). These observations, however, do not cover possible interactions between hue, luminance contrast, and saturation on the figure-ground organization of color adjacent to, or surrounded by, achromatic fields, or gray tones of varying luminance intensity. Reasons why such effects were not actively searched for may relate to the fact that chromatic and achromatic pathways in the visual brain are widely believed to be independent (e.g., Page and Crognale, 2005), presuming no functional interaction between chromatic and achromatic neural signals.

To clarify whether or not saturation influences figure-ground perception of color patterns on achromatic backgrounds, we used stimuli from a previous study (Dresp-Langley and Reeves, 2012), which had already shown that colors of any hue could alter the

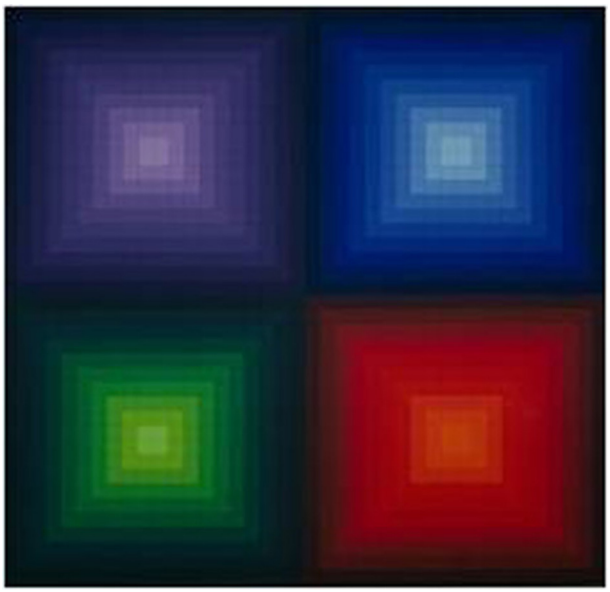

FIGURE 2 | In the twentieth century, designers like Vasarély, as here in "Arcturus II," demonstrated how the manipulation of color, saturation, and luminance contrast cooperates with planar shape geometries for the generation of compelling figure-ground effects.

perceived intensity of their achromatic backgrounds, pointing toward hitherto unsuspected interactions between color signals and achromatic contrast signals. Also, colors on gray produce depth effects that can directly be explained by variations in their luminance contrast irrespective of hue. Here in this study, we varied the saturation levels, luminance contrast, and contrast polarity of colored and/or achromatic inducers on gray backgrounds in planar configurations that may be similar to complex patterns in natural images. We tested test how these variations affect perceived background brightness and figure-ground organization. In a relative background brightness task, observers were asked to indicate whether a gray background containing colored or achromatic inducers appeared "brighter" than, "darker" than, or the "same" as a comparison background, which contained no inducers. In a relative depth (figure-ground) task, observers were asked to indicate whether colored, or achromatic inducers appeared to stand "in front of" or "behind" their gray background surface, or whether all surfaces appeared to lie in the "same" plane.

MATERIALS AND METHODS

Experiments were run under Windows XP on a Dell PC computer equipped with a mouse device and a high resolution color monitor (EIZO LCD "Color Edge CG275W") with an in-built color calibration device (colorimeter), which uses the Color Navigator 5.4.5 interface for Windows. The colors of the stimuli were generated in Photoshop using selective combinations of Adobe RGB increments. The color coordinates (see **Table 1**) for each RGB triple are retrieved from the look-up table of the colorimeter after calibration. All luminance values for calculating the stimulus contrasts (see the Michelson contrasts, with negative and positive contrast polarities, here in **Table 2**) were determined on the basis of standard photometry using an external photometer and adequate interface software (Cambridge Research Instruments).

SUBJECTS

Ten unpracticed observers, mostly graduate students in computational and/or design engineering and unaware of the hypotheses of the study, participated in the experiments. We obtained informed consent from all of them, in compliance with international ethical standards for experimentation on human observers. All subjects had normal or corrected-to-normal visual acuity and normal color vision (assessed on the basis of the Ishihara plates).

STIMULI

The stimuli (see **Figure 3** upper panel) consisted of configurations of 20 colored square-shaped surfaces, as from now called inducers, placed on a gray square-shaped surface which formed the surrounding background, and displayed on a black (0 cd/m^2) computer screen. The hue of the inducers could be red, green, blue, yellow, or achromatic (gray). The saturation of the inducer colors was varied to produce configurations with fully saturated and configurations with weakly saturated hues (see **Table 1**). Inducer luminance (in cd/m^2) was 22.1 and 9.9 for strongly saturated red, 53.2 and 16.7 for weakly saturated red; 54.0 and 7.1 for strongly saturated green, 53.9 and 11.5 for weakly saturated green; 5.1 and 1.4 for strongly saturated blue, 34.6 and 11.6 for weakly saturated blue; 79.0 and 3.2 for strongly saturated yellow, 12.3, 58.8, and 12.3 for weakly saturated yellow. The luminance of achromatic inducers was 9.95 and 82.70 cd/m^2. The luminance of the gray backgrounds was 2.6 and 25 cd/m^2. Inducer-background combinations produced eight contrast levels, one for each hue of a given saturation on each background, four per saturation level of a given hue, and four contrast levels for achromatic combinations. These Michelson contrasts, calculated on the basis of $(L_{max} - L_{min})/(L_{max} + L_{min})$, are given in **Table 2**. There was at least one negative contrast polarity for each level of hue and saturation. Color coordinates (X, Y, Z) for inducer colors are given in **Table 1** as a function of color appearance and the two saturation levels. In the task where observers had to judge relative background brightness, two background configurations were presented simultaneously: a configuration with inducers on the test background, and a comparison background without inducers (see lower panel in **Figure 3**). The location of test and comparison backgrounds on the screen varied randomly between left and right. A small fixation cross of low intensity was presented between trials to help subjects fixate the center of the screen. The horizontal distance between two backgrounds on the screen was 4 cm, and a given configuration on each side was 1.5 cm away from the central fixation mark that appeared between trials. The height of each background square was 9.7 cm and the width 10 cm. The smallest horizontal distance between colored inducers was 0.4 cm, the smallest vertical distance 0.5 cm. All colored inducers had identical height (0.9 cm) and width (1 cm). In the task where observers had to judge relative inducer depth, a single inducer-background configuration was displayed centrally on the screen on each trial.

Table 1 | Color coordinates (X, Y, Z) and RGB (Adobe) triplets associated with the different hues (shown on their gray backgrounds here in Figure 3).

	Color coordinates							
	"Weakly" saturated hues				"Fully" saturated hues			
	x	*y*	*z*	RGB	*x*	*y*	*z*	RGB
COLOR APPEARANCE								
≪Light≫ RED	0.33	0.33	0.34	[235, 197, 197]	0.68	0.31	0.01	[250, 0, 0]
≪Dark≫ RED	0.33	0.33	0.34	[127, 99, 99]	0.68	0.31	0.01	[100, 0, 0]
≪Light≫ GREEN	0.31	0.35	0.34	[183, 221, 183]	0.20	0.70	0.10	[0, 250, 0]
≪Dark≫ GREEN	0.31	0.35	0.34	[91, 110, 91]	0.20	0.70	0.10	[0, 100, 0]
≪Light≫ BLUE	0.29	0.30	0.41	[180, 201, 255]	0.15	0.05	0.80	[0, 0, 150]
≪Dark≫ BLUE	0.29	0.30	0.41	[90, 104, 160]	0.15	0.05	0.80	[0, 0, 125]
≪Light≫ YELLOW	0.32	0.36	0.32	[220, 220, 175]	0.42	0.51	0.07	[255, 255, 0]
≪Dark≫ YELLOW	0.32	0.36	0.32	[130, 123, 85]	0.42	0.51	0.07	[100, 100, 0]

Table 2 | Michelson contrasts (four per hue and saturation level and four additional achromatic conditions) of the inducer-background configurations.

Hues	"Fully" saturated				"Weakly" saturated			
RED inducers	−0.44	−0.08	0.58	0.79	−0.21	0.30	0.73	0.91
GREEN inducers	−0.57	0.35	0.47	0.91	−0.38	0.35	0.63	0.91
BLUE inducers	−0.90	−0.67	−0.29	0.32	−0.38	0.14	0.63	0.86
YELLOW inducers	−0.78	0.11	0.51	0.94	−0.36	0.30	0.65	0.92
ACHROMATIC inducers	−0.45	0.52	0.59	0.94				

TASK INSTRUCTIONS

Both experimental tasks used three-alternative forced choice to measure perceptual decisions. In the background contrast task, observers were asked to indicate whether the gray background containing inducers appeared "brighter" than, "darker" than, or the "same" as the comparison background, which contained no inducers. It was made clear that all subjects had understood that they were to compare the relative brightness of the two gray backgrounds on either side of the screen. In the relative depth or figure-ground task, observers were asked to indicate whether the colored inducer surfaces appeared to stand "in front of" or "behind" their gray background surface, or whether all surfaces appeared to lie in the "same" plane. It was made sure that all observers understood the instructions correctly before an experiment was initiated.

PROCEDURE

Subjects were seated at a distance of 1.5 m from the screen, their heads comfortably resting on a head-and-chin support. The experiments were run in a dimmed room, with blinds closed on all windows (mesopic range). Previous research had established that rod vision is not required for the generation of either apparent brightness or depth with the type of stimuli used here (Dresp-Langley and Reeves, 2012). Five of the ten observers were run in the relative background brightness task first and then in the relative depth task, the other five were run in reverse order. In the task where observers had to judge relative background brightness, two background configurations were presented simultaneously, a test background with inducers on one side of the screen (randomly on the left or right) and a comparison background without inducers on the other side. In the task where observers had to judge relative inducer depth, a single inducer-background configuration was displayed centrally on the screen on each trial. In each task or session, the configurations were presented in random order for about 1 s each and each configuration was presented twice. Inter-stimulus intervals typically varied from 1 to 3 s and were placed under the control of the subject to allow for any after-images to vanish before the next trial was initiated. Between stimuli, subjects were exposed to a uniformly black screen, with a small, slightly brighter, fixation cross displayed in the center, which was to help them control the direction of gaze. Each individual session consisted of 72 trials per subject, of which 64 with colored inducers on the gray backgrounds and eight with achromatic inducers on the gray backgrounds.

RESULTS AND DISCUSSION

The data from each task were analyzed separately. Response proportions were determined on the basis of the frequency with which a given effect was observed in each of the two tasks. Relative background brightness (task 1) was assessed on the basis of frequencies of contrast effects, assimilation effects, and responses signaling no effect. Relative inducer depth or figure-ground (task 2) was assessed on the basis of frequencies of foreground effects ("in front"), background effects ("behind"), and responses signaling no effect.

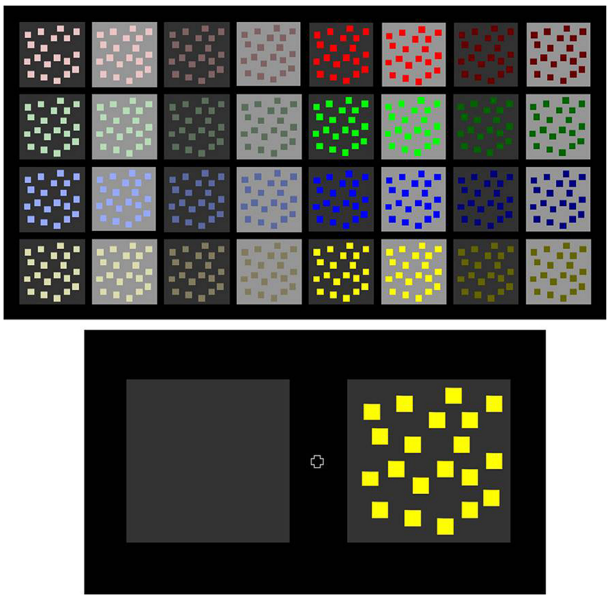

FIGURE 3 | We varied the luminance contrast and saturation (as shown in the upper panel here) of colored inducers presented on gray backgrounds. In the relative background brightness task, observers had to judge the relative brightness (brighter, darker, or same) of a gray test background with inducers in comparison with a simultaneously presented background field, of identical luminance but without inducers (as shown in the lower panel here). In this pair of configurations, 90% of subjects perceive the gray background with inducers on the right as darker than the plain comparison background on the left, a typical subjective contrast effect. In the relative inducer depth task, observers had to indicate the relative depth of the inducers in *single* inducer-background configurations (there was no comparison field). They had to decide whether inducers are seen as standing in front or behind the gray background, or whether inducers, and background appeared to lie in the same plane. In the configuration shown on the right of the lower panel here, 95% of subjects perceive the colored inducers as standing in front of their gray background, a typical foreground effect.

CONTRAST AND ASSIMILATION OF THE GRAY BACKGROUNDS

We determined frequencies (F) of contrast effects reflecting responses where a test background containing brighter inducers was judged "darker" than the comparison field, or a test background containing darker inducers was judged "brighter" than the comparison field. Frequencies of assimilation effects reflect responses where a test background containing brighter inducers was judged "brighter" than the comparison field, or where a test background containing darker inducers was judged "darker" than the comparison field. Frequencies of no effect reflect responses where the test background appeared of the same brightness as the comparison field (Experiment 1). These frequencies were then transformed into response proportions $P = F/N$ where N is the number of observations in a given condition.

Since inter-individual differences are not uncommon in this type of task (Egusa, 1977, 1983), we checked the raw data in the spreadsheet first for inter-observer consistency, which was good (10 two-by-two comparisons returned 80–85% matches between observers). Several statistical analyses were then performed on average values for P per experimental condition using a recent version of *Systat*, which systematically checks that conditions of normality and equality of variance are satisfied before generating further output. All comparisons given here below (analyses 1–4) had passed both tests.

Analysis 1: Two-Way ANOVA for a 2 × 4 factorial design was performed first, with two levels of the saturation factor (weak saturation, strong saturation) and the four levels of the hue factor (red, green, blue, yellow). The results of this first analysis signaled no statistically significant effects of hue or saturation on the response proportions for contrast, assimilation or, redundantly, no effect. For the next analysis (analysis 2), the four different hues were grouped with regard to luminance (Michelson) contrast and split into two polarity groups. The eight strongest positive contrasts (shown in **Table 2** on the right of each panel of values for a given saturation level) formed one group, and the remaining eight (on the left of each panel for a given saturation level in **Table 2**), of which most were negative, the second group.

Analysis 2: A Two-Way ANOVA for a 2 × 2 factorial design was performed, with the two levels of saturation and the two levels of contrast polarity, as defined here above. These statistics signaled significant effects of contrast polarity on response proportions for contrast [$F_{(1,\ 1)} = 39.36$, $p < 0.001$], assimilation [$F_{(1,\ 1)} = 66.83$, $p < 0.001$], and no effect [$F_{(1,\ 1)} = 22.20$, $p < 0.001$], and statistically significant interactions between saturation, and contrast polarity on these response proportions [$F_{(1,\ 1)} = 6.18$, $p < 0.05$ for contrast, $F_{(1,\ 1)} = 8.37$, $p < 0.01$ for assimilation, and $F_{(1,\ 1)} = 8.29$, $p < 0.01$ for no effect].

Average response proportions (P) for contrast, assimilation, and no effect are plotted in **Figures 4**, **5** as a function of the hue, Michelson contrast, and saturation level of the inducers (analysis 1). The graphs show that fully saturated inducers have a tendency to yield higher proportions of background contrast than weakly saturated inducers, while weakly saturated inducers have a tendency to yield higher proportions of background assimilation than fully saturated inducers although the main effect of saturation is not statistically significant, but significantly interacts with the effect of contrast polarity. The effect of saturation depends on contrast polarity. This significant interaction between saturation and contrast polarity is reflected by several observations. Strongly saturated inducers with the highest positive luminance contrast produced the largest proportions of contrast effects, while the weakly saturated inducers with the highest negative luminance contrast produce the smallest proportion of contrast effects (**Figure 4**). Although, at a first glance, weakly, and strongly saturated inducers seem to produce more or less evenly distributed proportions of assimilation at all luminance contrasts, the largest proportion of assimilation effects is observed with the weakly saturated inducers of the highest negative Michelson contrast, while the smallest proportion of assimilation arises from the strongly saturated inducers with the highest positive Michelson contrast (**Figure 5**).

The significant interaction between saturation and contrast polarity on the effects in this experiment is highlighted by the data show in **Figure 6**, which regroups the means of observations within each of the two contrast polarity categories (analysis 2). Response proportions for trials with the achromatic inducers are included in this graph for comparison. The strongest contrast

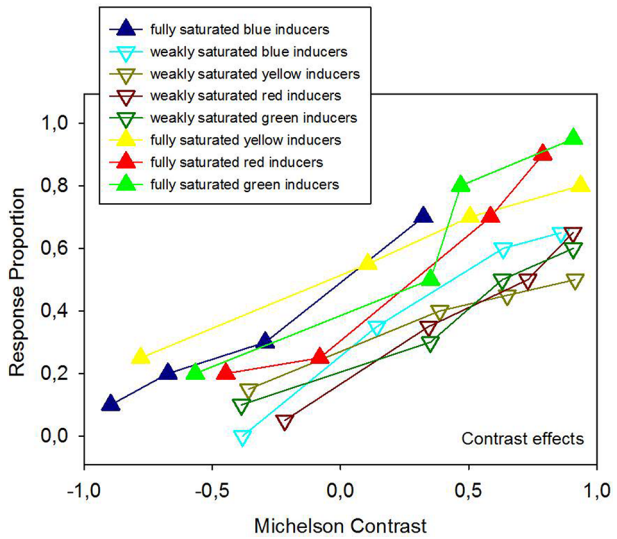

FIGURE 4 | Average response proportions for contrast effects as a function of hue, Michelson contrast, and saturation levels of the colored inducers. Although 2 × 2 ANOVA on these means (analysis 1) did not signal statistically significant effects of hue and saturation, there is a systematic trend for fully saturated hues to produce stronger contrast effects compared with weakly saturated hues.

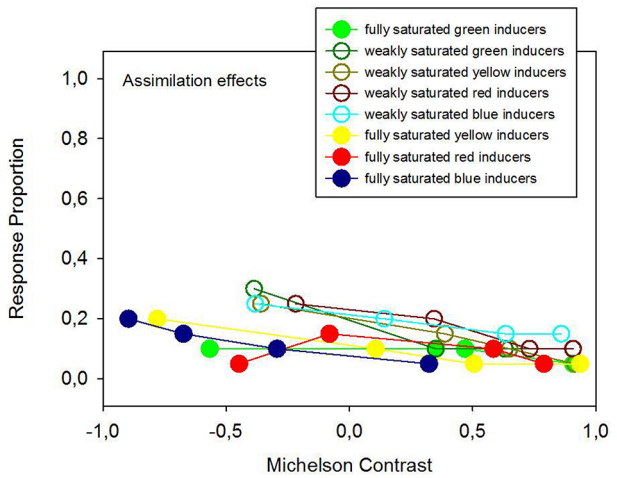

FIGURE 5 | Average response proportions for assimilation effects as a function of hue, Michelson contrast, and saturation levels of the colored inducers. Although 2 × 2 ANOVA (analysis 1) did not signal statistically significant effects of hue and saturation, there is a systematic trend for weakly saturated hues to produce stronger assimilation effects compared with fully saturated hues.

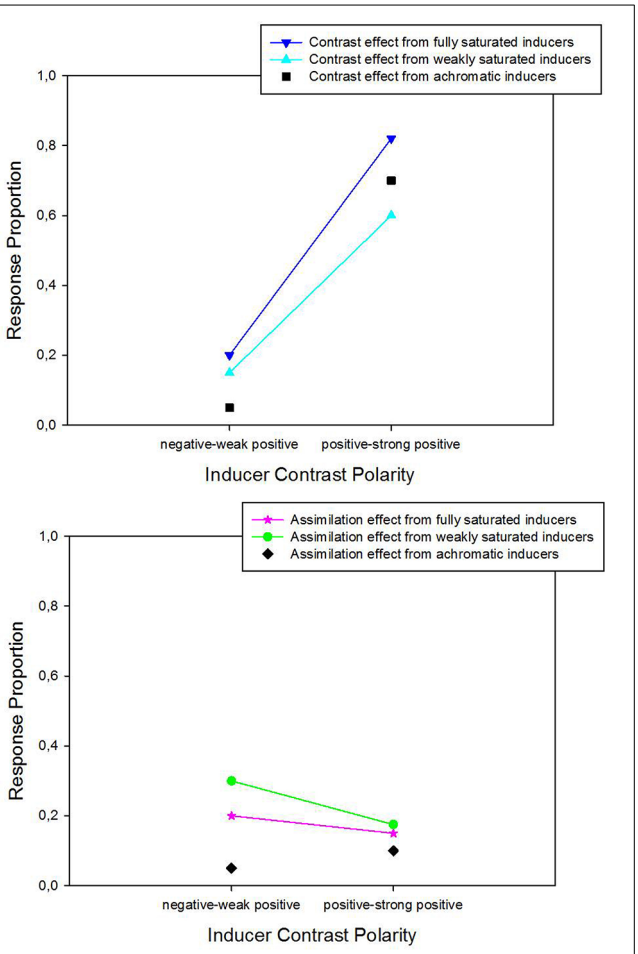

FIGURE 6 | Average response proportions for contrast (upper panel) and assimilation (lower panel) as a function of the contrast polarity and saturation levels of the colored inducers. Data from the different hues were grouped and divided into two balanced categories (negative-to-weak-positive and positive-to-strong positive) to test for effects of contrast polarity (analysis 2). 2 × 2 ANOVA on means signaled statistically significant effects of contrast polarity and significant interactions between contrast polarity and saturation, on contrast (shown here in the upper graph) and assimilation (shown in the lower graph). Average data from the conditions with achromatic inducer-background configurations are shown for comparison.

effects (upper panel in **Figure 6**) are generated by fully saturated colored inducers with positive contrast polarity. Inducers with negative contrast sign produce very little. The assimilation effects (lower panel in **Figure 6**) are markedly smaller than the contrast effects. The comparison of data with colored inducers with the data from the achromatic inducers shows that all induction effects, including the achromatic ones, depend on contrast polarity. Simple explanations or models in terms of summative effects of differences in contrast, where brightness would be a fixed weighted sum of these latter (e.g., Burns et al., 1982), do not hold in the light of this dependency on contrast polarity.

FIGURE-GROUND ORGANIZATION

The following analyses concern individual frequencies (F) of responses signaling figure and ground, reflecting observations where inducers were judged as standing "in front" or "behind" the gray background (Experiment 1). Frequencies of responses signaling no effect reflected individual observations where the inducers were judged to lie in the "same" plane as their gray background. The subjects' responses were analyzed for each experimental condition and individual. The responses frequencies (F)

were transformed into response proportions $P = F/N$ where N is the number of observations in a given condition.

Analysis 3: Two-Way ANOVA for a 2 × 2 factorial design with the two levels of the saturation factor and the four levels of the hue factor signaled no significant effects for hue (see also Dresp-Langley and Reeves, 2012). The effects of saturation on response proportions for foreground effects, background effects, and no effect were all statistically significant [$F_{(1,\ 1)} = 7.49$, $p < 0.01$ for "in front," $F_{(1,\ 1)} = 4.761$, $p < 0.05$ for "behind").

Analysis 4: ANOVA for a 2 × 2 factorial design with the two levels of the saturation factor and two levels of the polarity factor was performed. As before, the luminance contrasts associated with the four hues were split into two polarity groups according to the same principle. In addition to the significant effect of saturation (see above), this analysis revealed a significant effect of contrast polarity on the proportion of responses signaling foreground effects [$F_{(1,\ 1)} = 62.20$, $p < 0.001$], background effects [$F_{(1,\ 1)} = 14.90$, $p < 0.01$], and no effect [$F_{(1,\ 1)} = 32.21$, $p < 0.001$]. A significant interaction between saturation and contrast polarity was found to influence the response proportions for background effects [$F_{(1,\ 1)} = 18.33$, $p < 0.01$].

Average response proportions (P) for figure and ground, expressed in terms of foreground effects ("in front") and background effects ("behind"), and response proportions relative to no effect are given in **Figures 7**, **8** as a function of hue, Michelson contrast, and saturation levels (analysis 3). Strongly saturated inducers produce significantly larger response proportions for foreground effects than weakly saturated inducers (**Figure 7**). Strongly saturated inducers with the strongest positive luminance contrasts produce the largest response proportions relative to foreground effects, where the inducers are seen as standing in front of the configuration. Weakly saturated inducers yield significantly larger response proportions for background effects than strongly saturated ones (**Figure 8**).

Average response proportions (P) for figure and ground in terms of foreground and background effects are summarized as a function of the two contrast polarity categories (analysis 4) in **Figure 9**. Response proportions for trials with the achromatic inducers are included in this graph for comparison. Achromatic inducers with negative-to-weak positive luminance contrast and weakly saturated colored inducers with negative-to-weak-positive polarity yield the largest average response proportion for background effects (upper panel in **Figure 9**), while achromatic and fully saturated colored inducers with medium-to-strong positive luminance contrast yield the largest average response proportion for foreground effects lower panel in **Figure 9**). Proportions of foreground effects indicating that inducers are seen as figure tend to increase between negative and positive contrast polarities, while background effects indicating that inducers are seen as ground tend to decrease. The average data as plotted in **Figure 9** highlight the statistically significant effects (analysis 4) of saturation and contrast polarity on the relative depth judgments (Experiment 2) even more, showing that fully saturated and weakly saturated inducers of similar luminance contrast produce markedly different effects within a given range of contrast polarities.

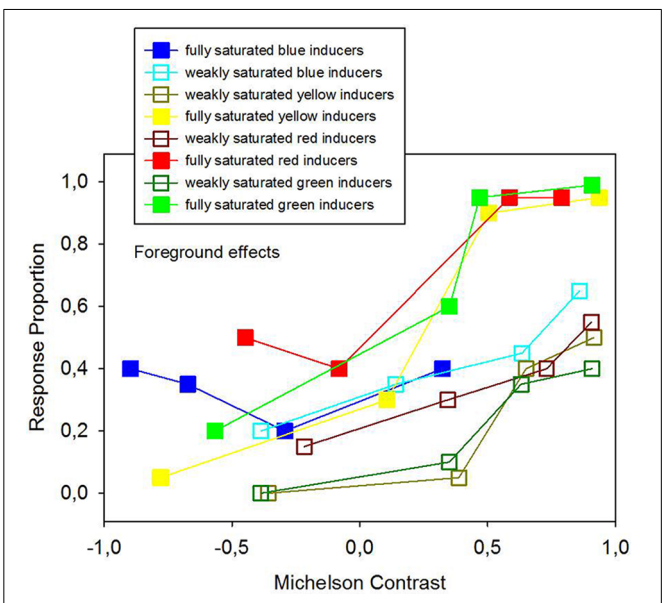

FIGURE 7 | Average response proportions of foreground effects, indicating that the colored inducers were seen as figure, as a function of hue, Michelson contrast and saturation levels of the colored inducers. 2 × 2 ANOVA signaled a statistically significant effect of saturation (analysis 3) on foreground effects, where fully saturated inducers produce stronger figure percepts than weakly saturated inducers, as shown here in the graph.

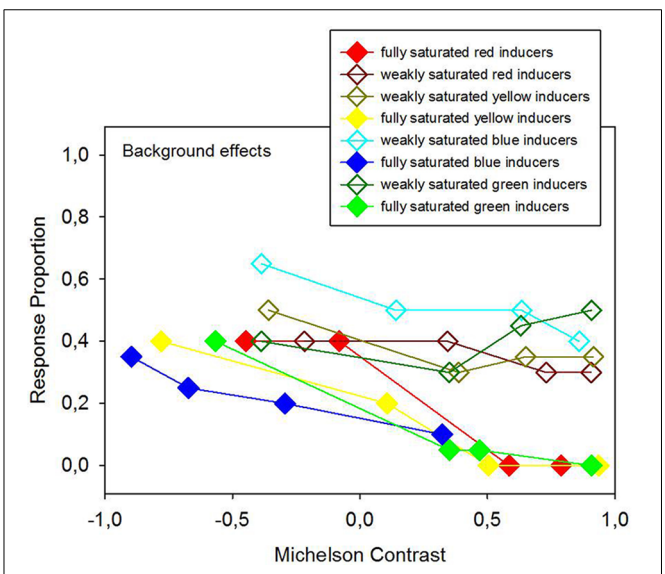

FIGURE 8 | Average response proportions of background effects, indicating that the colored inducers were seen as ground, as a function of hue, Michelson contrast, and saturation levels of the colored inducers. 2 × 2 ANOVA signaled a statistically significant effect of saturation (analysis 3) on background effects, where weakly saturated inducers produce stronger ground percepts than fully saturated inducers, as shown here in the graph.

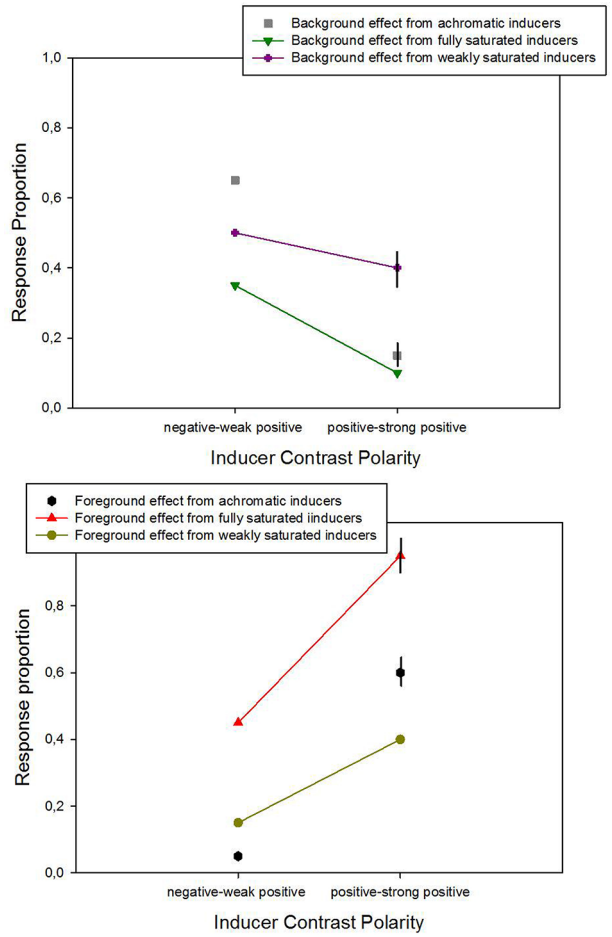

FIGURE 9 | Average response proportions for background (upper panel) and foreground effects (lower panel) as a function of the two contrast polarity categories (analysis 4). 2 × 2 ANOVA signaled statistically significant effects of contrast polarity on background (top) and foreground (bottom) effects. *Post-hoc* paired comparisons between individual means from achromatic inducer-background configurations and data from configurations with color on gray signaled a significant difference between achromatic and weakly saturated inducers for background effects in the positive contrast polarity range (top, with error bars for the two conditions of that comparison), and a significant difference between achromatic and fully saturated inducers for foreground effects (bottom, with error bars for the two conditions relative to that comparison).

DISCUSSION

Hue as such does not significantly affect relative background brightness or figure-ground organization in displays consisting of colored inducers on gray backgrounds under the conditions tested here. This result replicates a finding from an earlier study with similar configurations and tasks (Dresp-Langley and Reeves, 2012). To examine the possibility of a contribution of hue further, it would be interesting to pursue these experiments by testing the effects of iso-luminant inducer-background configurations with different hues in both type on relative background brightness (induction effects) and relative depth judgments.

The influence of saturation on relative background brightness (induction effects) is shown here to depend on contrast polarity. The significant interaction between saturation and contrast polarity found here may be summarized as follows. Strongly saturated inducers with the medium-to-strong positive luminance contrast produced the largest proportions of contrast effects, while weakly saturated inducers with the negative luminance contrast produce the largest proportion of assimilation effects. We infer that color saturation modulates figure-ground organization indirectly, in interaction with contrast polarity, by affecting apparent background brightness.

Color saturation significantly contributes to the figure-ground organization of the colored inducers on the achromatic backgrounds. Strongly saturated surface colors associated with a positive luminance contrast are the most likely to promote foreground effects, i.e., to be seen as standing in front of their achromatic backgrounds. Weakly saturated surface colors associated with a negative luminance contrast are the most likely to generate background effects, i.e., to be seen as standing behind their achromatic backgrounds.

It has been suggested that the figure-ground organization of colored surfaces on achromatic backgrounds is more ambiguous compared with that of achromatic inducers on achromatic backgrounds. This seems to hold especially in the range of strong negative luminance contrasts, where achromatic inducers were found to engender clear foreground percepts while colored inducer produced more ambiguous percepts (Guibal and Dresp, 2004). This may be one of the deeper reasons why renaissance painters tended to exploit chiaroscuro and geometric cues to pictorial depth using preferably achromatic contrasts and resorting to color only within a very limited chromatic range. Yet, some differences between colored and achromatic inducers in effects on background brightness and depth seem to shed a new light on this question. These can be are appreciated here by looking at the average data in **Figure 9** here (data from analysis 4).

It is shown that the effects of achromatic inducers on figure-ground percepts depend, like the effects of colored inducers, on contrast polarity (ANOVA could not be performed for this comparison), with similar asymmetries between negative and positive polarity ranges. Also, these data suggest some meaningful differences in effects of achromatic and colored inducers with regard to both foreground and background effects. Two additional *post-hoc* comparisons (*t*-tests on individual data, $N = 2 \times 10$ for each paired comparison) signaled a significant difference between achromatic and weakly saturated chromatic inducers in their influence on background effects (upper panel in **Figure 9**) in the positive-to-strong positive polarity range $[t_{(1,\ 18)} = 5.44;\ p < 0.001]$, and between achromatic and fully saturated chromatic inducers in their influence on foreground effects (lower panel in **Figure 9**) in the positive-to-strong-positive polarity range $[t_{(1,\ 18)} = 4.38;\ p < 0.001]$. It is therefore likely that weakly saturated chromatic inducers generate more powerful background effects than achromatic inducers, and that fully saturated inducers generate more powerful foreground effects than achromatic inducers within the medium-to-strong-positive polarity range. These results encourage to pursue testing for such differences with a wider range of chromatic achromatic contrasts in different polarity ranges.

The results from this study suggest that induction polarity (assimilation vs. contrast) and depth order (foreground vs. background) cannot be linked by any straightforward causal explanation. While color saturation systematically and significantly determines depth order, this is not so for the case of background brightness induction in terms of contrast or assimilation. Also, one cannot conclude that variables which support contrast systematically bring a contrasted surface to the foreground. In the case of colored inducers, it all depends on their saturation and contrast polarity, and in the case of achromatic inducers, on their contrast polarity. This is consistent with conclusions from earlier studies (e.g., Egusa, 1977, 1983; Guibal and Dresp, 2004; Dresp-Langley and Reeves, 2012) and contradicts the intuition that perceived pictorial depth may be directly linked to subjective brightness effects and color appearance (e.g., Katz, 1911; Long and Purves, 2003). In a review chapter, we (Dresp-Langley and Reeves, 2013) discussed the possibility that a probability based selection of neural signals may drive perceptual grouping (see also Grossberg, 1994; Dresp and Langley, 2005), or Gestalt formation (Dresp, 1997; Pinna, 2011, 2012), and guide the brain in working out the most likely hypothesis of visual structure from elementary characteristics of current visual input.

At some stage, bottom-up attention becomes critically important as some input characteristics readily attract attention away from others in the visual field. Image parts with a stronger and more salient contrast or color may benefit from selection for attention when presented together with objects of a less salient contrast or color. Color saturation may have a decisive influence here. Data from recent visual studies indeed suggest that feature-based selection for attention can be based on any aspect of color contrast. Hue alone may be used independently of lightness in displays with multiple colors, and saturation may be used in displays where color is held constant (Stuart et al., 2014), as was the case in our displays here.

CONCLUSION

We conclude that color saturation modulates figure-ground organization, both directly by determining relative inducer depth, and indirectly, and in interaction with contrast polarity by affecting apparent background brightness. The results point toward a hitherto undocumented functional role of color saturation in the genesis of form, and in particular figure-ground percepts. They cannot be accounted for in terms of chromatostereopsis, or summative effects of luminance contrasts. Some interesting differences between effects of achromatic inducers and effects of chromatic inducers highlighted herein deserve further attention. Brightness induction effects (assimilation vs. contrast) and the depth order (foreground vs. background) of surfaces in complex image patterns cannot be linked by any straightforward causal explanation.

ACKNOWLEDGMENTS

Financial support from CNRS (PICS 05971, Qualia) is gratefully acknowledged.

REFERENCES

Burns, S. A., Smith, V. C., Pokorny, J., and Elsner, A. E. (1982). Brightness of equal-luminance lights. *J. Opt. Soc. Am.* 72, 1225–1232.

Da Vinci, L. (1651). *Trattato Della Pittura Di Leonardo Da Vinci. Scritta da Raffaelle du Fresne.* Paris: Langlois.

Dresp, B. (1997). On illusory contours and their functional significance. *Curr. Psychol. Cogn.* 16, 489–518.

Dresp, B., Durand, S., and Grossberg, S. (2002). Depth perception from pairs of overlapping cues in pictorial displays. *Spat. Vis.* 15, 255–276. doi: 10.1163/15685680260174038

Dresp, B., and Langley, O. K. (2005). Long-range spatial integration across contrast signs: a probabilistic mechanism? *Vision Res.* 45, 275–284. doi: 10.1016/j.visres.2004.08.018

Dresp-Langley, B., and Reeves, A. (2012). Simultaneous brightness and apparent depth from true colors on grey: Chevreul revisited. *Seeing Perceiving* 25, 597–618. doi: 10.1163/18784763-00002401

Dresp-Langley, B., and Reeves, A. (2013). "Color and figure-ground: from signals to qualia," in *Perception Beyond Gestalt: Progress in Vision Research*, eds S. Magnussen, M. Greenlee, J. Werner, and A. Geremek (Abingdon: Psychology Press), 159–171.

Egusa, H. (1977). On the color stereoscopic phenomenon. *Jpn. Psychol. Rev.* 20, 369–386.

Egusa, H. (1983). Effects of brightness, hue, and saturation on the perceived depth between adjacent regions in the visual field. *Perception* 12, 167–175.

Farnè, M. (1977). Brightness as an indicator to distance: relative brightness *per se* or contrast with the background? *Perception* 6, 287–293.

Grossberg, S. (1994). 3D vision and figure-ground separation by visual cortex. *Percept. Psychophys.* 55, 48–120.

Guibal, C. R. C., and Dresp, B. (2004). Interaction of color and geometric cues in depth perception: when does "red" mean "near"? *Psychol. Res.* 10, 167–178. doi: 10.1007/s00426-003-0167-0

Katz, D. (1911). Die Erscheinungsweisen der Farben und ihre Beeinflussung durch die individuelle Erfahrung. *Z. Psychol.* 7, 6–31.

Long, F., and Purves, D. (2003). Natural scene statistics as the universal basis for color context effects. *Proc. Natl. Acad. Sci. U.S.A.* 100, 1519–15193. doi: 10.1073/pnas.2036361100

Mount, G. E., Case, H. W., Sanderson, J. W., and Brenner, R. (1956). Distance judgment of colored objects. *J. Gen. Psychol.* 55, 207–214.

O'Shea, R. P., Blackburn, S. G., and Ono, H. (1994). Contrast as a depth cue. *Vision Res.* 34, 1595–1604.

Page, J. W., and Crognale, M. A. (2005). Differential ageing of chromatic and achromatic visual pathways: behavior and electrophysiology. *Vision Res.* 45, 1481–1489. doi: 10.1016/j.visres.2004.09.041

Pinna, B. (2011). The organization of shape and color in vision and art. *Front. Hum. Neurosci.* 5:A104. doi: 10.3389/fnhum.2011.00104

Pinna, B. (2012). Perceptual organization of shape, color, shade, and lighting in visual and pictorial objects. *Iperception* 3, 257–281. doi: 10.1068/i0460aap

Rohaly, A. M., and Wilson, H. R. (1993). The role of contrast in depth perception. *Invest. Ophthalmol. Vis. Sci.* 34:1437.

Stuart, G. W., Barsdell, W. N., and Day, R. H. (2014). The role of lightness, hue and saturation in feature-based visual attention. *Vision Res.* 96, 25–32. doi: 10.1016/j.visres.2013.12.013

Conflict of Interest Statement: The authors declare that the research was conducted in the absence of any commercial or financial relationships that could be construed as a potential conflict of interest.

Received: 02 June 2014; accepted: 18 September 2014; published online: 07 October 2014.

*Citation: Dresp-Langley B and Reeves A (2014) Effects of saturation and contrast polarity on the figure-ground organization of color on gray. Front. Psychol. **5**:1136. doi: 10.3389/fpsyg.2014.01136*

This article was submitted to Perception Science, a section of the journal Frontiers in Psychology.

frontiers in PSYCHOLOGY

ORIGINAL RESEARCH ARTICLE
published: 10 February 2015
doi: 10.3389/fpsyg.2015.00067

Lightness dependence of achromatic loci in color-appearance coordinates

Ichiro Kuriki*

Research Institute of Electrical Communication, Tohoku University, Sendai, Japan

Edited by:
Marcelo Fernandes Costa, Universidade de São Paulo, Brazil

Reviewed by:
Sophie Wuerger, The University of Liverpool, UK
Balazs Vince Nagy, Budapest University of Technology and Economics, Hungary

****Correspondence:***
Ichiro Kuriki, Research Institute of Electrical Communication, Tohoku University, 2-1-1 Katahira, Aoba-ku, Sendai, 980-8577, Japan
e-mail: ikuriki@riec.tohoku.ac.jp

Shifts in the appearance of color under different illuminant chromaticity are known to be incomplete, and fit nicely with a simple linear transformation of cone responses that aligns the achromatic points under two illuminants. Most chromaticity-transfer functions with von-Kries-like transformations use only one set of values to fit the color shifts from one illuminant to another. However, an achromatic point shifts its chromaticity depending on the lightness of the test stimulus. This lightness dependence of the achromatic-point locus is qualitatively similar to a phenomenon known as the Helson-Judd effect. The present study suggests that the lightness dependency of achromatic points appears to be a general trend, which is supported by the results from deriving the optimal von-Kries coefficients for different lightness levels that best fit the color shifts under a different illuminant chromaticity. Further, we report that such a lightness dependence of the achromatic-point loci can be represented simply as a straight line in coordinates defined using color-appearance models such as CIECAM when normalized for daylight.

Keywords: color vision, color constancy, achromatic point, lightness dependence, corresponding colors

INTRODUCTION

Several studies on color-constancy have reported that shifts in color appearance under changes in illuminant chromaticity are often incomplete. Shifts in an achromatic point have been used as a measure to investigate changes in the sensitivity of color vision, which may result in shifts in color appearance. Some previous studies have reported that shifts in color appearance can be fitted using a simple linear scaling of the cone excitations, such that the chromaticity of light perceived as achromatic (i.e., achromatic points) under two illuminants will be aligned in the cone-response space (Speigle and Brainard, 1999; Kuriki et al., 2000). Linear transformations of cone excitations using a 3×3 diagonal matrix are termed a *von-Kries type* or *von-Kries transformation*, after the discovery by Johannes von Kries (1970) The diagonal entries of a 3×3 matrix are often called *von-Kries coefficients*, which only vary the gain of three photoreceptors, i.e., the L, M, and S cones. Our previous study reported that shifts in the appearance of color chips under a different illuminant chromaticity are nicely fitted using a scaling of the cone responses (Kuriki et al., 2000), with the von-Kries coefficients derived by shifts in the achromatic point.

On the other hand, several studies have reported that the locus of an achromatic point depends on the lightness level of the test stimulus. The so-called Helson-Judd effect is a phenomenon in which spectrally non-selective (i.e., achromatic) surfaces under monochromatic light appear different in hue for lighter and darker samples (Helson, 1938; Judd, 1940; Helson and Michels, 1948). Helson (1938) first reported that lighter samples appear to have the same hue as that predicted by the wavelength of a monochromatic illuminant, whereas darker samples appear to have a hue opposite to what is predicted. Because monochromatic light has only a single wavelength component, the only factor that changes in a space illuminated with monochromatic light is the energy of the reflected light. Therefore, if the color appearance is a consequence of linear transformations of the cone responses, the apparent hue of the object, illuminated under a monochromatic light, should not vary with the intensity of the reflected light. Therefore, the Helson-Judd effect implies that *an achromatic point should be lightness dependent*; in other words, an achromatic point should be less saturated than the illuminant chromaticity for higher-reflectance samples, and more saturated than the illuminant chromaticity for lower-reflectance samples. Helson and Michels (1948) reported a phenomenon of systematic dependence of the locus of an achromatic point on the lightness of the test sample, and some recent studies have also reported the dependence of an achromatic point on the intensity of the test stimulus in relation to the surrounding surfaces (e.g., Bäuml, 2001; Kuriki, 2006).

If the alignment of the achromatic points under a different illuminant chromaticity predicts a shift in the color appearance of color chips with the same lightness, different von-Kries coefficients should be derived for the different lightness levels. However, the von-Kries coefficients applied in previous studies were derived using only a single pair of achromatic points under two different illuminant conditions (Speigle and Brainard, 1999; Kuriki et al., 2000), and did not take the lightness dependence into account. Thus, a simple question arises: *is there a contradiction between our two studies?*

The first half of this paper demonstrates that the loci of achromatic points are lightness dependent. As a part of this demonstration, we use data from two studies (Kuriki et al., 2000; Kuriki, 2006) to show that these two reports are not subject

to discrepancies. We first evaluate the lightness dependency by deriving the optimal von-Kries coefficients for each lightness level in the data for the asymmetric color-matching experiment (Kuriki et al., 2000). We then compare these results with our later study reporting the lightness dependence of an achromatic point (Kuriki, 2006). In the second half of this paper, we provide a supplementary exploration by plotting the achromatic-point loci used in the previous study (Kuriki, 2006) at various coordinates defined using color-appearance models. We report that the achromatic loci, measured under various illuminant colors, appear nearly parallel with each other along the lightness axis when the color space is normalized to a pure-white (i.e., spectrally non-selective) surface with 100% reflectance in daylight.

It must be carefully stated that the *achromatic points* used in this and previous studies (Speigle and Brainard, 1999; Kuriki et al., 2000; Kuriki, 2006) represent a chromaticity of light that gives a colorless appearance to the subjects. On the other hand, a color of light that yields zero chromatic components (i.e., lightness axis) in the color-appearance models implies that the color *matches* the apparent color of the achromatic chips under the tested illuminant; in other words, they do not always represent the points of an achromatic (i.e., colorless) *subjective* appearance because the color appearance models were developed to predict shifts in the benchmark data of the "corresponding colors," and were clearly not optimized for the prediction of achromatic loci (Fairchild, 2013).

In addition, the definitions of the terms *intensity*, *luminance*, and *lightness* used in the present study should be clarified. Herein, "intensity" indicates the strength of light in a general sense, and can include the notions of both luminance and lightness. The word "luminance" is a psychophysical scale indicating the intensity of light, and can be derived physically by integrating the spectrum of light incident to the eye, multiplied by the luminosity efficiency function, $V(\lambda)$, across the visible wavelength spectrum using an appropriate scaling factor. The luminance is a physically measurable value and is proportional to the energy of light. The terms "lightness" refers to the perceived strength of light from an object surface with respect to the perceived strength of light of another area that shows a high-reflectance of *white* under the same illumination. The lightness is proportional to the luminance (or energy) of light to the 1/3rd power, which is referred to as the *1/3 power-law*, and is adopted as the intensity axis in the CIE LAB space (1976) defined by the International Commission on Illumination (CIE). For more formal definitions of these words, see CIE's list of terms (http://eilv.cie.co.at/).

Models for a color-appearance transformation have been rigorously tested by technical committees at CIE. CIE has proposed several numerical models that satisfactorily match the shifts in the appearance of color chips, observed under standard illuminants, mainly between standard illuminants A and D_{65} (Fairchild, 2013). However, the present study does not debate quantifying the color appearance, such as the lightness, hue, and chromatic saturation, of color chips. Rather, the present study focuses on introducing some suggestions for a particularly general view of how the *neutral point of color appearance* changes with the illuminant colors. To do so, we take a much wider range of illuminant colors into account, including red-green directions (Kuriki, 2006). As a part of such a general view on the sensitivity changes in color vision, the achromatic loci used in our previous study were tested in spaces defined by color-appearance models such as CIELAB (1976), CIECAM97s (revised version by Fairchild, 2001), CIECAM02 (2002), Nayatani's model (Nayatani et al., 1990), Hunt's model (Hunt, 1994), and RLAB (Fairchild, 2013), the results of which are described in the latter half of this study.

CONFIRMATION OF THE LIGHTNESS DEPENDENCE FOR ACHROMATIC LOCI

RATIONALE

If the alignment of achromatic-point shifts in the cone excitations (Speigle and Brainard, 1999; Kuriki et al., 2000) successfully predicts shifts in the color appearance under different illuminants, the von-Kries coefficients that minimize the differences between the appearance and the predicted colors will represent shifts in the achromatic points. A search for the optimal von-Kries coefficient was conducted using our previous data (Kuriki et al., 2000) at each of three lightness levels (Munsell *Values* of 3, 5, or 7). The prediction of the color appearance for the corresponding color chips under a particular illuminant was derived from the color appearance, matched under a standard white (D_{65}) illuminant, by applying the von-Kries coefficients. **Figure 1** illustrates the concept of a color-shift model under this configuration.

Figure 1 shows an example of an achromatic point and the appearance of a color chip *C* by taking the logarithm of the cone response as the axes. In this space, a von-Kries-like transformation can be represented as a parallel shift, and the degree of shift along each axis corresponds to the coefficients for each cone response. For simplicity, only two of the three dimensions are shown. The origin of the axes are normalized to the achromatic point under illuminant *K*. **Figures 1A,B** represent the color appearance under illuminants *K* and *L*, respectively. The open and filled symbols indicate the achromatic point and appearance

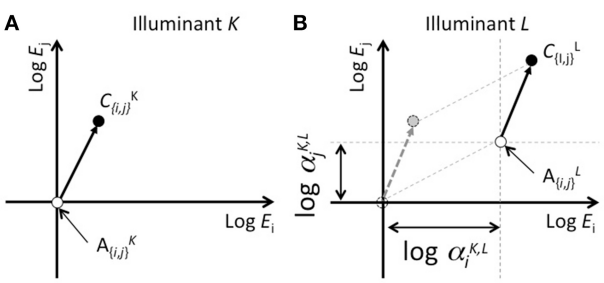

FIGURE 1 | Schematic of the concept of color-shift predictions from scaling cone responses in accordance with the achromatic point. (A,B) represent color appearance in cone response space under illuminants *K* and *L*, respectively. The vertical and horizontal axes represent logarithms of the responses for two cone classes. The scaling of the cone response is represented by a parallel shift in this plane. The difference between the achromatic points under two illuminant conditions ($alpha_{\{i,j\}}^{K,L}$, where *i* and *j* represent cone classes, and *K* and *L* represent illuminant differences) represents logarithms for the von-Kries coefficients.

of the color chip C, respectively, under each illuminant. In Panel **Figure 1B**, the dotted lines parallel to the axes indicate a shift in the achromatic point from illuminants K to L. Given that $W_{\{i,j\}}^{\{K,L\}}$ represents the coordinates (either i or j) for the achromatic point under illuminants K or L, the scaling coefficient that aligns the achromatic points is defined as follows:

$$\alpha_{\{i,j\}}^{K,L} = W_{\{i,j\}}^{L} / W_{\{i,j\}}^{K} \tag{1}$$

The application of this coefficient to the coordinates of the color chip can be represented as follows:

$$\widehat{C}_{i,j}^{L} = \alpha_{\{i,j\}}^{K,L} C_{\{i,j\}}^{K}, \tag{2}$$

where $\widehat{C}_{\{i,j\}}^{L}$ represents the calculated coordinates for cone class i or j under illuminant L after scaling the cone responses.

In our previous study, the subjects matched the color appearance under different chromatic illuminants by adjusting the chromaticity of a color stimulus on a CRT surface, shown through a hole in a mid-level gray wall under a standard illuminant, D_{65}(see Kuriki et al., 2000 for details). The matched colors under D_{65} represent the appearance of color chips under the chromatic illuminants tested.

We calculated the *optimal* von-Kries coefficients for each of the three lightness levels such that the color differences between the matched and calculated colors were minimized in CIE delta-E^*. To confirm the consistency with our previous study, the coefficients obtained in the results were plotted in the same way as in **Figures 4**, **5** of our previous study on the loci of the achromatic points (Kuriki, 2006).

PROCEDURE

The following procedure was adopted. First, an illuminant was selected for testing using a set of 20 color chips from our previous study (Kuriki et al., 2000). We chose the cone excitations that match the chromaticity for each color chip under the tested illuminant, and the cone excitations for the control match (D_{65} to D_{65}) of the color chip. The following simple von-Kries-like transformation was applied:

$$\begin{bmatrix} \hat{L}_i^j \\ \hat{M}_i^j \\ \hat{S}_i^j \end{bmatrix} = \begin{bmatrix} \alpha_k^{D_{65},j} & 0 & 0 \\ 0 & \beta_k^{D_{65},j} & 0 \\ 0 & 0 & \gamma_k^{D_{65},j} \end{bmatrix} = \begin{bmatrix} L_i^{D_{65}} \\ M_i^{D_{65}} \\ S_i^{D_{65}} \end{bmatrix}, \tag{3}$$

where subscript i for cone excitations L, M, and S represents the color chip, instead of the cone classes in Equation (2), and superscript j represents the test illuminant. Subscript k for the coefficients (alpha, beta, and gamma) represents the lightness levels (3, 5, or 7) of the color chip. These coefficients were commonly used among the color chips of the same lightness k under illuminant j. The errors were defined based on the Euclidean distance between the estimated color and the matches of the subjects in the a^*b^* plane of the CIE LAB space:

$$\begin{aligned} &\left[\Delta E_{i,j}^{*}\left(\alpha_k^{D_{65},j}, \beta_k^{D_{65},j}, \gamma_k^{D_{65},j}\right)\right]^2 \\ &\quad = \left[a_{i,j,new}^{*}\left(\alpha_k^{D_{65},j}, \beta_k^{D_{65},j}, \gamma_k^{D_{65},j}\right)\right. \\ &\quad \left. - a_{i,j,match}^{*}\left(\alpha_k^{D_{65},j}, \beta_k^{D_{65},j}, \gamma_k^{D_{65},j}\right)\right]^2 \\ &\quad + \left[b_{i,j,new}^{*}\left(\alpha_k^{D_{65},j}, \beta_k^{D_{65},j}, \gamma_k^{D_{65},j}\right)\right. \\ &\quad \left. - b_{i,j,match}^{*}\left(\alpha_k^{D_{65},j}, \beta_k^{D_{65},j}, \gamma_k^{D_{65},j}\right)\right]^2 \end{aligned} \tag{4}$$

where $a^{\star}_{i,j,new}$ *and* $b^{\star}_{i,j,new}$ represent the estimated chromaticity, derived from the estimated cone excitations $\widehat{L}_i^j$, $\widehat{M}_i^j$,and $\widehat{S}_i^j$, as a function of the von-Kries coefficients (*alpha*, *beta*, and *gamma*) for color chips i under illuminant j. Likewise, $a^{\star}_{i,j,match}$ and $b^{\star}_{i,j,match}$ represent the matches of the subjects for color chips i under illuminant j in our previous study (Kuriki et al., 2000). Finally, three pairs of alpha, beta, and gamma values were obtained for the three lightness levels under illuminant j that minimizes the sum of the errors across the 20 color chips (Equation 5).

$$\Delta E_j^* = \left(\sum_i \Delta E_{i,j}^{*2}\right)^{1/2} \tag{5}$$

For comparison, similar errors were calculated between the estimated value and the actual matches from the results of our original study (Kuriki et al., 2000).

The increase or decrease of the coefficients by a common factor for all three photoreceptors (*alpha*, *beta*, and *gamma*) will result in changes in intensity, not chromaticity. To elucidate the effects of von-Kries-coefficient changes on the color appearance, the coefficients were normalized with respect to the beta value, i.e., the coefficient for the M-cone response, in the same way as in our previous study on the achromatic locus (Kuriki, 2006). The *beta*/*alpha* and *beta*/*gamma* values were used for changes to the achromatic point in the L-M and S directions of the cone-opponent space, respectively.

RESULTS

To determine the general trend through a comparison of our two studies (Kuriki et al., 2000; Kuriki, 2006), **Figure 2** shows the results of the optimized coefficients for a subject who participated in both studies.

Because the illuminant chromaticity in the color-matching study (Kuriki et al., 2000) changed in the blue-yellow direction, the changes were only evident in the results for the S-cone excitations. As a reference, the achromatic loci measured in our previous study (Kuriki, 2006) are shown by the dotted lines. The overall trend for the optimal von-Kries coefficient in our color-matching data (Kuriki et al., 2000) and the relative M-cone weights for the achromatic loci (Kuriki, 2006) are similar. This implies that the introduction of changes to the chromaticity of an achromatic point based on lightness may better explain the color shifts with regard to the von-Kries-like transformation, as reported in our achromatic-loci study (Kuriki, 2006).

To examine the efficiency of introducing achromatic point changes based on lightness, the residual errors in CIE delta-E^*

were analyzed by comparing the von-Kries coefficient with and without the introduction of a lightness dependence. The results from the three subjects are shown in **Figure 3**. The absolute value of delta-E^* was reduced by approximately 40% on average. According to the analysis of variance, they differed with a statistical significance [$F_{(1,\ 829)} = 88.5, p < 0.0001$].

Our analysis described thus far has demonstrated that the lightness-level dependence of the relative changes in von-Kries coefficients (i.e., *relative M-cone weights*, *beta/alpha* and *beta/gamma*) better explains the results of asymmetric color matches measured using two different apparatuses for two entirely different purposes. In a recent study, another group tested and partially confirmed the dependence of achromatic points on the lightness of a target (Chauhan et al., 2014) using the relative M-cone weights defined in our previous study (Kuriki, 2006). Their results were slightly different from ours under one of their illuminant conditions, probably owing to the difference in the lightness level of the wall of the illuminated room, which acted as the largest adapting field for the subject, which was "dark" gray in Chauhan's et al. (2014) apparatus, and N5 in our own. These

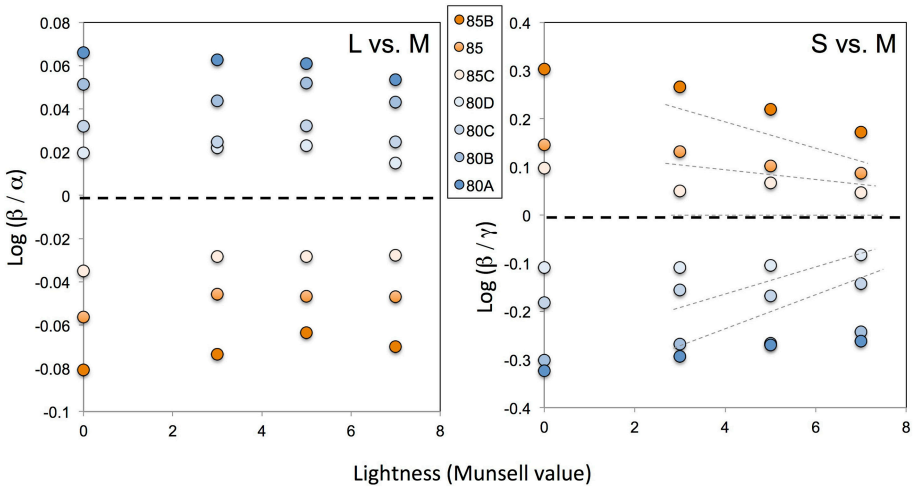

FIGURE 2 | Optimal von-Kries coefficients derived from our previous study (Kuriki et al., 2000), plotted in the space used for an evaluation of the relative cone responses (Kuriki, 2006). The horizontal axis indicates the lightness (in a Munsell value) of the color chips tested. The symbols on the vertical axis represent the chromaticity of the illuminant at this scale. The different symbols represent different illuminant conditions as indicated by the filter codes from Kodak (see Kuriki et al., 2000 for further details). Note that the panel on the left, comparing the relative contributions between the L- and M-cones, has a much smaller range than in our previous study (Kuriki, 2006) and between the S- and M-cones in the panel shown on the right. The thin dotted lines in the right panel show the achromatic-point loci re-plotted from our previous data (Kuriki, 2006) for the sake of comparison. Because the illuminant varied exclusively in the blue-amber direction, the relative contributions of the S- vs. M-cone responses show a similar trend as in the previous study.

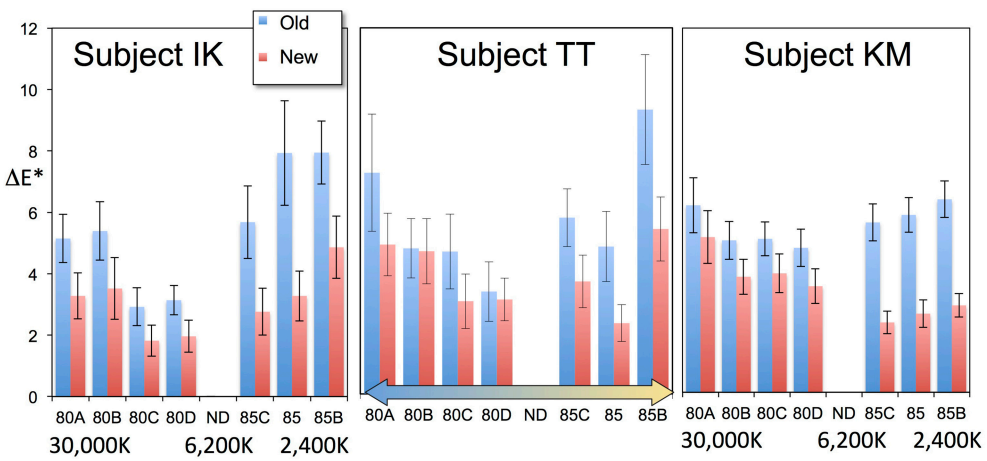

FIGURE 3 | Comparison of errors in our previous data ("Old") against errors after optimizing for different lightness levels ("New"). Each bar represents the mean errors of 20 color chips, and the error bars represent the standard errors. The introduction of optimization for different lightness levels clearly improved the fitting. The two conditions show a statistically significant difference. See the text for further details.

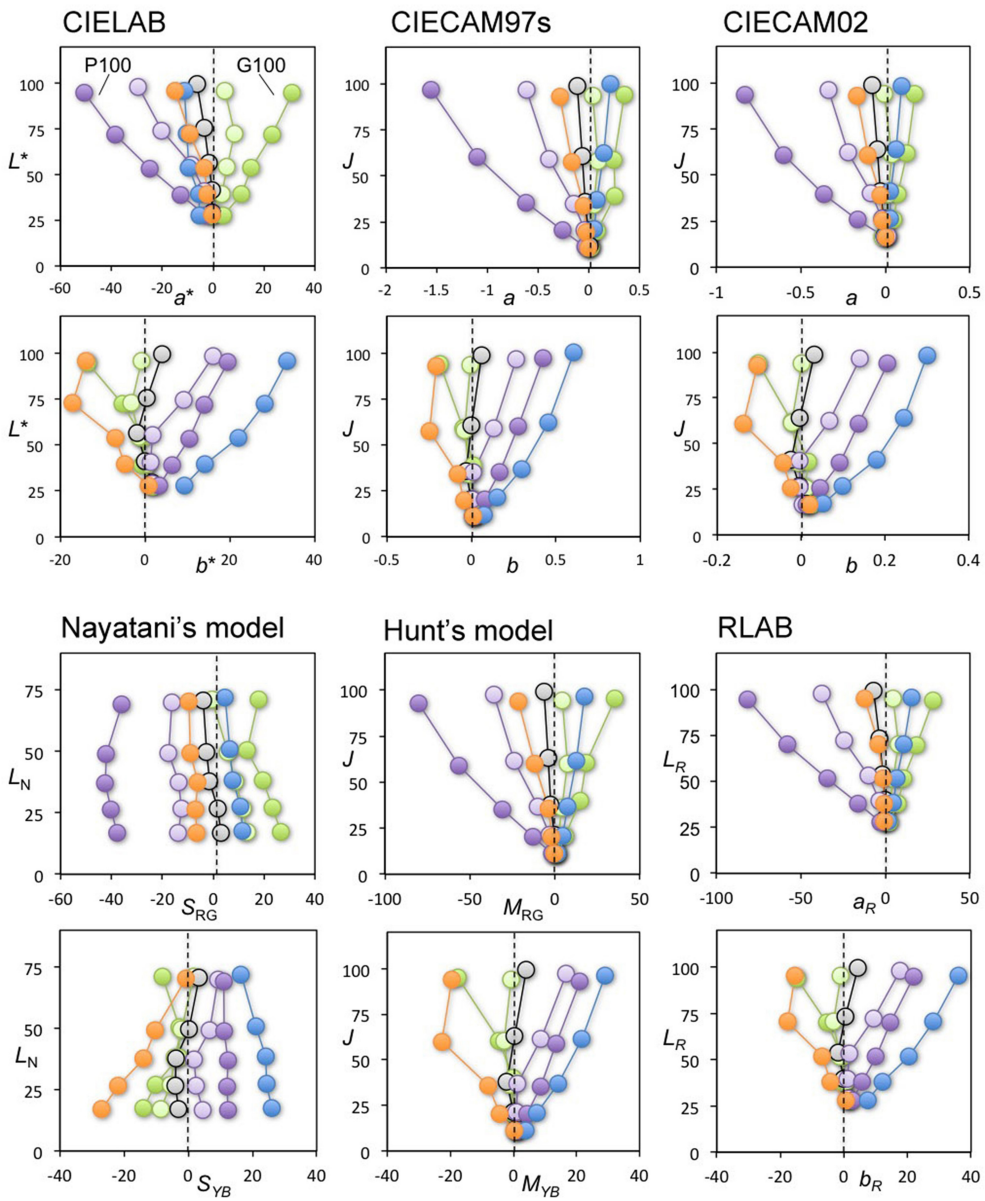

FIGURE 4 | Achromatic-point loci from our previous study (Kuriki, 2006) plotted in various spaces for color appearance. Top-two rows, from the left: CIE LAB, CIE CAM97s revised version, and CIE CAM02. Bottom-two rows, from the left: Nayatani's model, Hunt's model, and RLAB. The symbols connected by a line represent the achromatic points under each illuminant condition, coded with a symbol color. For each color space, the horizontal and vertical axes in the panels in the upper row represent redness-greenness and lightness axes, respectively. Similarly, the horizontal and vertical axes in the panels in the lower row represent blueness-yellowness and lightness axes, respectively. With the exception of Nayatani's model, all plots show traces radiating from the zero point on the horizontal axis.

facts imply that a von-Kries transformation is an appropriate first-order approximation for color shifts under a different illuminant chromaticity, and improves significantly when the lightness dependence of the coefficients is introduced.

ACHROMATIC LOCI IN COLOR-APPEARANCE COORDINATES

PURPOSE

As demonstrated in the previous section, progressive changes in the achromatic point with the lightness level were consistently observed in an asymmetric color-matching study conducted using a different apparatus, which was not designed to observe the achromatic-point shifts based on the lightness level. This implies that the shift in achromatic points with the lightness level may be a general trend. In a previous study, the achromatic loci were plotted in the axes based on the ratio of von-Kries coefficients among the cone types. This ratio (*relative M-cone weights* in Kuriki, 2006) was used to emphasize the lightness dependency of the von-Kries coefficients. If the von-Kries coefficients are independent from the lightness, the ratios of the cone excitations between different types will remain constant regardless of the lightness.

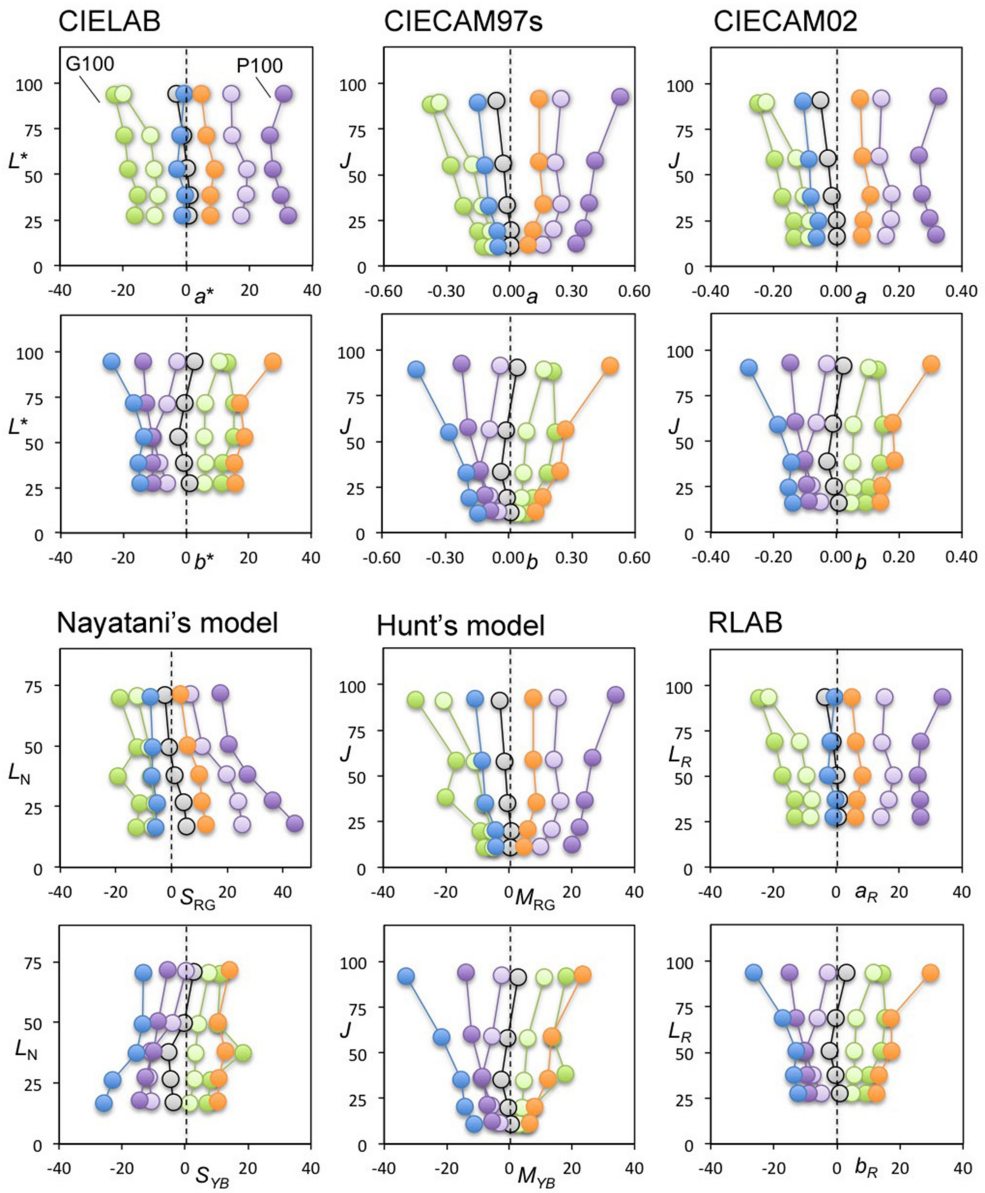

FIGURE 5 | The same achromatic-point loci shown in Figure 4 plotted in the color-appearance space, normalized to daylight (D_{65}). The profiles show trajectories that are considerably more parallel than in **Figure 4**. See the text for further details.

Thus, the results shown in **Figure 2** and those from our previous study (Kuriki, 2006) clearly demonstrate that they are lightness dependent.

As the next attempt, the achromatic loci were plotted in nonlinear spaces designed to represent the appearance of the color because they often introduce a lightness dependency in the formula (Fairchild, 2013). Among them, CIE LAB (1976) is a color coordinate with the simplest formula, which adopts the 1/3 power-law in terms of both lightness (L^*) and chromaticity axes (a^*, b^*). If such a simple nonlinearity can account for the nonlinearity of an achromatic-point locus, it will appear in a simpler form in these color spaces.

METHODS

Data on the achromatic points from three subjects, measured in a previous study (Kuriki, 2006), were used in the plots. The achromatic loci were plotted in the following color spaces designed to take changes in the illuminant color into account: CIE LAB (1976), CIE CAM97s (revised version by Fairchild, 2001), CIE CAM02, Nayatani's model (Nayatani et al., 1990), Hunt's model (Hunt, 1994), and RLAB (Fairchild, 2013). These were used in two ways, i.e., based on their original method, and with normalization to daylight (D_{65}).

The color appearance models use a standard "white point" to take illuminant-color changes into account. Basically, color

appearance models use the tristimulus value of light reflected on a white (i.e., spectrally non-selective) surface with 100% reflectance under the environment illuminant of the test field as the normalization term. For example, the CIE XYZ (1931) tristimulus value of a spectrally non-selective (white) surface of 100% reflectance under the test illuminant is used as the normalization term [X_n, Y_n, Z_n] for the derivation of the CIE LAB (1976) coordinates, which is an example of the original method mentioned above. The other method, normalization to daylight (D_{65}), was realized by fixing the normalization term to the tristimulus value of 100% white under a D_{65} illuminant regardless of the actual illuminant conditions of the test field.

The achromatic-point loci from a previous study were plotted in various color spaces under both normalization methods to test whether achromatic loci in any of the color-appearance spaces show a much simpler locus representation.

RESULTS

All panels in **Figure 4** show the achromatic loci from one of the subjects in our previous study (Kuriki, 2006). A pair of two panels in a vertical arrangement show the results for each color space with lightness as the vertical axis, and red-green and yellow-blue as the horizontal axes in the upper and lower panels, respectively. The illuminant conditions for the achromatic loci measurements are indicated for the two most-saturated conditions (i.e., P100 and G100 in Kuriki, 2006) in the upper panel. They indicate that the achromatic loci for *reddish* and *greenish* illuminant conditions, counter intuitively, reside on the *negative* and *positive* sides of this plot, respectively. In most models, the loci spread out from the origin. Interestingly, the exception is Nayatani's model, which is the only color-appearance model known to implement changes to the color appearance based on lightness, i.e., the Helson-Judd effect. The loci in Nayatani's model space appear nearly parallel around the vertical axis. However, the loci do not coincide with the vertical axis in either the upper or lower panels, representing zero red-greenness and zero yellow-blueness, respectively. Rather, they tend to be located in a direction *opposite* from the illuminant color. For example, the achromatic loci for the purple illuminant are at the left-most part of the upper panel and on the right side in the lower panel, indicating that the achromatic surfaces (i.e., chromaticity along the vertical axis) should have appeared reddish and bluish. However, it should be repeated that the achromatic-point loci are the chromaticity of light that actually *appeared achromatic*. The purple illuminant clearly appeared reddish and bluish, even after 15 min of adapting to the illuminated room (see Kuriki, 2006 for details).

This result indicates that the illuminant color, which is almost at the horizontal position of the origin in this plot, appears as its illuminant color because the achromatic point indicates the chromaticity of light that appears colorless under the measurement conditions (Kuriki, 2006). The color spaces, however, were derived for an optimal description of the typical correspondence of color chips between illuminants A and D_{65} (Fairchild, 2013), and its origin does not guarantee a colorless appearance. This point is discussed further in Section General Discussions.

Figure 5 shows the same loci in color spaces after normalization using a daylight (D_{65}) illuminant without taking the illuminant conditions into consideration when plotting the achromatic loci. Interestingly, the loci in most of the color spaces resulted in a parallel arrangement similar to Nayatani's model shown in **Figure 4**. This result implies that the color appearance of the achromatic loci from the viewpoint of a color space normalized to D_{65} may be nearly constant in terms of chromatic saturation along with the lightness when the lightness dependence of the color appearance is taken into account.

To define the straightness of this plot (**Figure 5**), in comparison with a radial plot (**Figure 4**), the ratios of distance at the lightest and darkest points were calculated between the left- and right-most loci. Where the loci are parallel, and where for different illuminants they vary both systematically and in terms of smoothness, the distances along the horizontal axis at the lowest and highest lightness levels are nearly identical between the left- and right-most loci. Therefore, the most parallel plot will have the ratio closest to 1.0, as shown in the results listed in **Table 1**.

On average, the color space with the ratio closest to 1.0 was CIE LAB. Nayatani's space reached nearly the same ratio, but its profile shrank slightly as the lightness increased (**Table 1**, **Figure 5**). The most important point illustrated in **Figures 4**, **5** is the general trend of the achromatic loci, which are nearly parallel in the color-appearance spaces normalized to daylight (D_{65}), and in Nayatani's space after being normalized to the illuminant color. However, Nayatani's space normalized to the illuminant is the only exception among the color-appearance models, which are normalized to each ambient illuminant. Thus, it is natural to consider that the nearly straight locus of the achromatic points observed in the color-appearance space normalized to daylight may be a more general property.

We next plotted the achromatic loci for all three subjects from our previous study (Kuriki, 2006) in the CIE LAB space. CIE LAB space was selected as a representative color space among those used in **Figures 4**, **5** because it is the space with the simplest transformation and the simplest (i.e., parallel) phenomenal structure of achromatic loci, as shown in **Figure 5**. The CIE LAB coordinates used in **Figure 5** were calculated through normalization using a diffuse white surface with 100% reflectance under a D_{65} illuminant as [X_n, Y_n, Z_n]. Again, the achromatic-point loci for different illuminants were *not* normalized to a surface with 100% reflectance under each illuminant. Instead, the CIE LAB space normalized for D_{65} in **Figure 5** was used for all illuminant conditions.

Figure 6 shows the results of the achromatic-point loci from three subjects (Kuriki, 2006) plotted in a CIE LAB space normalized for D_{65}. The loci of the averaged achromatic points

Table 1 | Parallelism of achromatic loci in various color spaces.

	CIELAB	CIECAM97s revised	CIECAM02	Nayatani	Hunt	RLAB
Top/bottom: red-green	1.11	2.04	1.27	0.64	2.29	1.45
Top/bottom: yellow-blue	1.69	3.37	2.08	0.76	1.63	2.25
Average	1.40	2.70	1.68	0.70	1.63	2.25

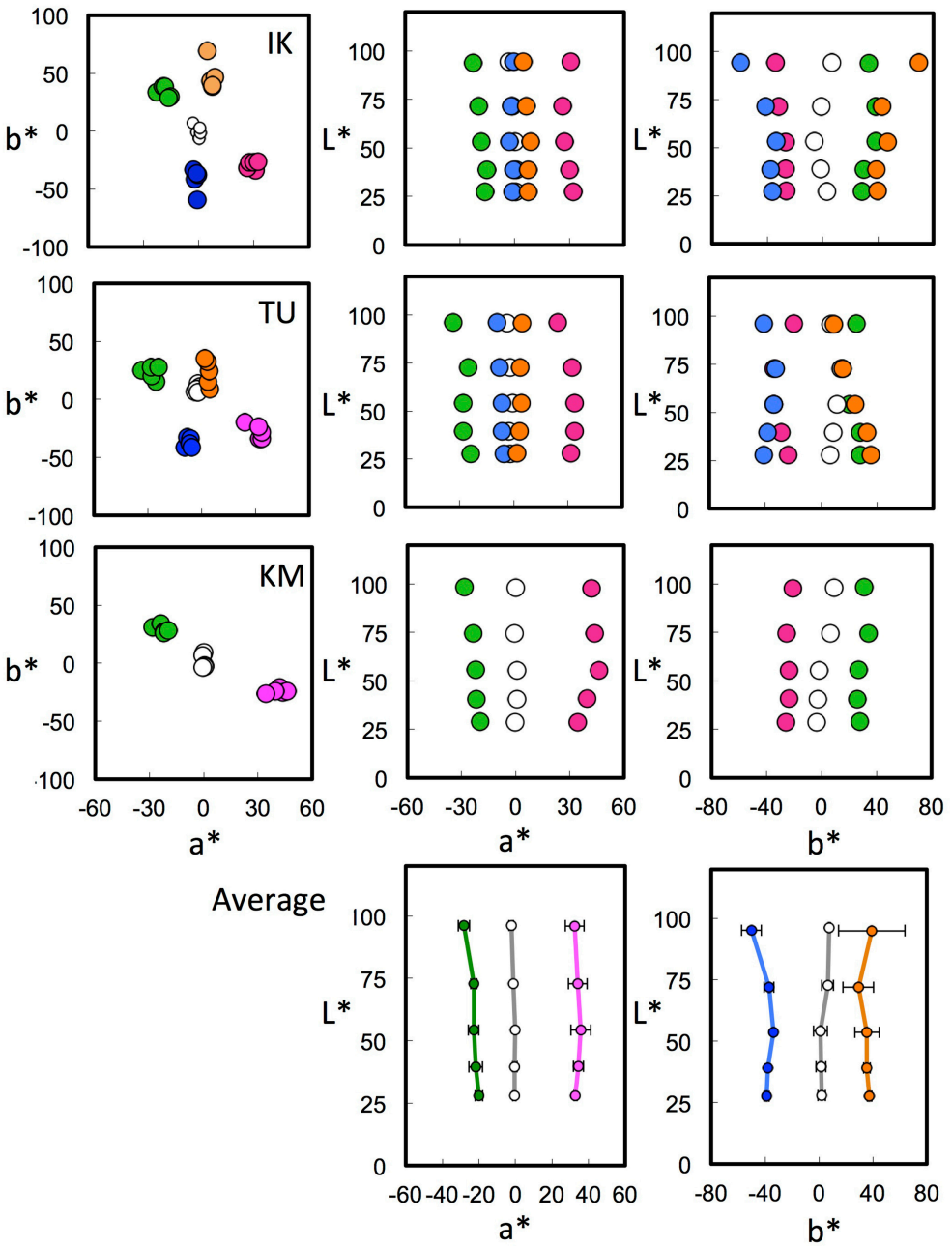

FIGURE 6 | Achromatic loci in CIE LAB space normalized to D_{65}. The top three rows show the chromatic loci for three subjects in the CIE LAB space normalized to daylight. The columns show different profiles, from left: a^*-vs-b^*, a^*-vs-L^*, and b^*-vs-L^* planes. The various colors of the symbols represent a different illuminant chromaticity. For simplicity, the 50% green and 50% purple illuminant conditions (G50 and P50 in Kuriki, 2006) in IK were omitted. The bottom row shows the averaged achromatic loci in the a^*-vs-L^* and b^*-vs-L^* planes. The loci for different illuminant chromaticities are almost parallel to the vertical axis. See the text for further details.

are shown in the a^*-vs-L^* or b^*-vs-L^* plane. These planes reveal a clear parallelism between the achromatic-point loci and the L^* axis; the achromatic loci are nicely fitted as parallel shifts in the vertical lines. Furthermore, we informally tested the achromatic loci in the CIE LUV (1976) space, which also adopts the 1/3 power-law for lightness (L^*) but not for chromaticity (u*, v*); however, a parallelism of the achromatic loci was not observed.

Nevertheless, the amount to which the point will shift away from the L^* axis is not easy to predict from the illuminant chromaticity, as shown in **Figures 5**, **6**. The chromaticity loci for achromatic surfaces under each illuminant are radial lines from the origin in the a^*-vs-L^* and b^*-vs-L^* planes. A perceptual achromatic point, which appears non-chromatic, is clearly different from the chromaticity of the achromatic color chips except at around the lower L^* level.

A recent study reported that the iso-hue loci of four unique hues under chromatic illuminant conditions did not converge at a point, i.e., an achromatic point, and the estimated converging point was slightly offset from the lightness axis of CIE CAM02 (Xiao et al., 2014). One of the possible interpretations of the deviations of the achromatic point loci from the lightness axis, including our results in **Figures 4**, **5**, are a failure in the prediction of an achromatic point by the color appearance models. However, the color appearance models are aimed to fit the apparent correspondence of color chips between different illuminants, by definition, and they do not use achromatic loci for the model optimization (Fairchild, 2013). Therefore, a discrepancy between the achromatic loci and the lightness axis of the color appearance models may be inevitable. In addition, it must be noted that the purpose of the present study is not to argue the "failure and/or success" of the color appearance models in terms of their prediction of the achromatic loci.

GENERAL DISCUSSIONS

The first comparison between our two previous studies demonstrated that the dependence of the achromatic point on the lightness better explains the shifts in color appearance under different levels of illuminant chromaticity measured for entirely different purposes. This suggests that the color-appearance mechanisms may not be as simple as a cone-response scaling using a common coefficient for each cone class across all lightness levels. The fitting may be improved if the lightness dependency of the achromatic point (i.e., the scaling factor for each cone) is taken into account. This is because the lightness dependence of the achromatic-point loci is systematic, as discussed at length in our previous work (see Section 3.1 in Kuriki, 2006), with regard to comparisons with previous studies measuring unique yellows or achromatic points. However, a unified model that explains the achromatic loci under all illuminant conditions remains complicated (for examples of this, see Equations 7a and 7b and Figure 10 in Kuriki, 2006).

The second attempt demonstrated that the achromatic loci can be described in a relatively simple fashion (namely, a straight line) for color spaces that were designed to equate the perceptual differences based on the color appearance across a color space, such as CIE LAB (1976), which was defined to follow the 1/3 power-law for both lightness (L^*) and chromaticity (a^* and b^*). The achromatic-point loci were parallel to the L^* axis in the CIE LAB space when normalized to daylight. A similar trend was observed in other spaces designed to predict color shifts under different levels of illuminant chromaticity when normalized to daylight. Nayatani's model was the only exception, showing somewhat parallel lines in a space normalized under each illuminant chromaticity. However, the other spaces also show nearly parallel loci for the achromatic points when normalized to daylight. Thus, it is natural to interpret the parallelism under daylight normalization being a more general characteristic.

What does it mean if a line parallel to a lightness axis *normalized to daylight* can best represent an achromatic locus? A locus in a color-appearance space parallel to the lightness axis represents an iso-chromatic line, i.e., a line of coordinates with *constant hue and saturation components across the lightness*. The color space normalized to daylight implies that the achromatic locus is defined in a color space for which the chromaticity of the illuminant is irrelevant. However, the direction and offset from the lightness axis are defined based on the environmental illuminant. This implies that a system invariant to changes in the environmental illuminant defines the color space normalized to daylight, but not the color appearance.

This implication applies when the visual system holds a color axis invariant to the environmental illuminant. Such a high degree of color constancy was observed when tested using a real object and categorical judgment (Uchikawa et al., 1998; Olkkonen et al., 2009). In general, however, color-matching results exhibited a color constancy that remained incomplete (see Foster, 2011 for a systematic review along with the original derivation of the constancy index for each study). Further, this can be confirmed from the observation of a sheet of white paper being identifiable under candlelight despite the fact that it does not appear as white as it would in daylight. From a computational point of view, a nearly color-constant property is present in the scene, i.e., the contrast of the cone responses among the surfaces is nearly invariant across changes in illuminant color (e.g., Land and McCann, 1971; Lucassen and Walraven, 1993). A color-appearance space normalized to daylight may be defined for the human visual system if such information is fully utilized.

Given that a color-appearance space normalized to daylight was obtained, an open question remains regarding how to determine the position of the achromatic locus. A clue to answering this question may be found in the achromatic point under a *low level of lightness*. Whereas, many studies have reported that color-appearance mechanisms are incomplete with regard to color constancy, there are no clear answers to how this incompleteness is determined. A clue to this can be found in the results of the present study under a low level of lightness. **Figure 7**

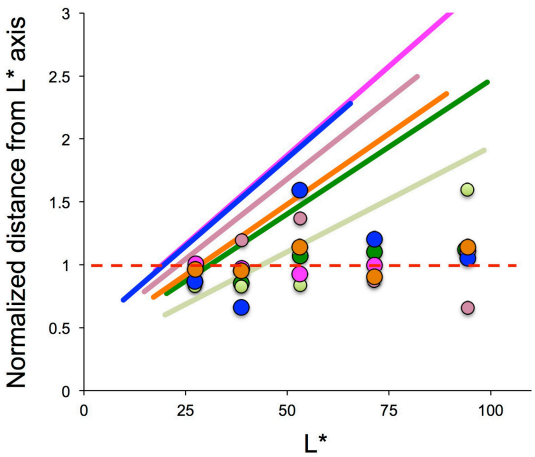

FIGURE 7 | Illuminant chromaticity profile as a function of lightness (*L).** The vertical axis shows the Euclidean distance of the illuminant chromaticity from the lightness axis (a^*, b^*) = (0,0) for each a^*-vs-b^* plane normalized to the Euclidean distance for the achromatic points averaged across five lightness levels. The slanted lines indicate the illuminant chromaticity, and the intersection at 1.0 is found at approximately $L^* = 25$. See the text for further details.

provides a profile of the illuminant chromaticity in relation to the achromatic point-locus in a CIE LAB space. The loci of the achromatic point and the illuminant chromaticity are projected onto a plane that includes the L^* axis and the illuminant-chromaticity locus. The deviation along the vertical axis indicates the chromaticity normalized to the achromatic points averaged across the various lightness levels under each illuminant condition.

These lines intersect at a value of 1.0 on the vertical axis around the darkest level of lightness. If the color-appearance space, normalized to daylight, is acquired before judging the color appearance, the neutral point in the hue-saturation space can be defined by the illuminant chromaticity at the lower end of the lightness. The slanted lines for the illuminant chromaticity have a value of 1.0 or less only with a very dark range of lightness. Because a value of 1.0 in the vertical axis represents an achromatic point, and a larger value represents greater saturation in the illuminant hue, an achromatic sample that reflects the same illuminant chromaticity with a value of less than 1.0, as shown in **Figure 7**, would appear in the opposite hue of the illuminant. The original work by Helson (1938) reported the appearance of the opposite hue for darker samples observed within a much wider range of lightness. However, subsequent work by Helson and Michels (1948) reported that the achromatic point for the darkest level of lightness appeared to be nearly the same as the illuminant color. This was described in terms of *adaptation ratio r* (Figure 2 in their work), and is qualitatively similar to the results from our previous study (Figure 10 in Kuriki, 2006). The adaptation ratio *r* rarely took a value higher than 100%, implying that the samples appearing in the opposite hue were rare in the study by Helson and Michels (1948). Therefore, further studies are required to investigate the means by which the achromatic points are to be determined.

One clear weak point of the present study is the small number of subjects used, i.e., three. It is also true that there are some minor deviations from the ideal parallelism, which is different among the subjects. However, the general trend after normalization is similar across the subjects and illuminant chromaticity (**Figures 6**, **7**). In addition, despite the minor differences, the general tendency of the "approximately parallel form" of achromatic loci in the CIELAB space, normalized to daylight, is mostly consistent across the subjects under most illuminant conditions, i.e., 15 loci in total from the three subjects. Because the aim of the latter half of this manuscript is to share this phenomenon and the conceptual idea regarding the cause of this achromatic loci, the results of the present study, although from a small number of subjects, can be considered a useful hint toward areas of future study on achromatic point loci.

ACKNOWLEDGMENTS

The present study was supported by the Grant-in-Aid for Scientific Research (KAKENHI) by Japan Society for the Promotion of Science, #24330205 and # 25245065 to Ichiro Kuriki.

REFERENCES

Bäuml, K. H. (2001). Increments and decrements in color constancy. *J. Opt. Soc. Am. A Opt. Image Sci. Vis.* 18, 2419–2429. doi: 10.1364/JOSAA.18.002419

Chauhan, T., Perales, E., Xiao, K., Hird, E., Karatzas, D., and Wuerger, S. (2014). The achromatic locus: effect of navigation direction in color space. *J. Vis.* 14, 25. doi: 10.1167/14.1.25

Fairchild, M. D. (2001). A revision of CIECAM97s for practical applications. *Color Res. Appl.* 26, 418–427. doi: 10.1002/col.1061

Fairchild, M. D. (2013). *Color Appearance Models.* Chester: John Wiley & Sons. doi: 10.1002/9781118653128

Foster, D. H. (2011). Color constancy. *Vision Res.* 51, 674–700. doi: 10.1016/j.visres.2010.09.006

Helson, H. (1938). Fundamental problems in color vision. I. The principle governing changes in hue, saturation, and lightness of non-selective samples in chromatic illumination. *J. Exp. Psychol.* 23, 439. doi: 10.1037/h0060971

Helson, H., and Michels, W. C. (1948). The effect of chromatic adaptation on achromaticity. *J. Opt. Soc. Am.* 38, 1025–1031. doi: 10.1364/JOSA.38.001025

Hunt, R. W. G. (1994). An improved predictor of colourfulness in a model of colour vision. *Color Res. Appl.* 19, 23–26.

Judd, D. B. (1940). Hue, saturation, and lightness of surface colors with chromatic illumination. *J. Opt. Soc. Am.* 30, 2–32. doi: 10.1364/JOSA.30.000002

Kuriki, I. (2006). The loci of achromatic points in a real environment under various illuminant chromaticities. *Vision Res.* 46, 3055–3066. doi: 10.1016/j.visres.2006.03.012

Kuriki, I., Oguma, Y., and Uchikawa, K. (2000). Dynamics of asymmetric color matching. *Opt. Rev.* 7, 249–259. doi: 10.1007/s10043-000-0249-9

Land, E. H., and McCann, J. (1971). Lightness and retinex theory. *J. Opt. Soc. Am.* 61, 1–11. doi: 10.1364/JOSA.61.000001

Lucassen, M. P., and Walraven, J. (1993). Quantifying color constancy: evidence for nonlinear processing of cone-specific contrast. *Vision Res.* 33, 739–757. doi: 10.1016/0042-6989(93)90194-2

Nayatani, Y. K., Takahama, K., Sobagaki, H., and Hashimoto, K. (1990). Color-appearance model and chromatic adaptation transform, *Color Res. Appl.* 15, 210–221. doi: 10.1002/col.5080150407

Olkkonen, M., Hansen, T., and Gegenfurtner, K. R. (2009). Categorical color constancy for simulated surfaces. *J. Vis.* 9, 6. doi: 10.1167/9.12.6

Speigle, J. M., and Brainard, D. H. (1999). Predicting color from gray: the relationship between achromatic adjustment and asymmetric matching. *J. Opt. Soc. Am. A Opt. Image Sci. Vis.* 16, 2370–2376. doi: 10.1364/JOSAA.16.002370

Uchikawa, K., Kuriki, I., and Tone, Y. (1998). Measurement of color constancy by color memory matching. *Opt. Rev.* 5, 59–63. doi: 10.1007/s10043-998-0059-z

von Kries, J. (1970). "Chromatic adaptation," in *Sources of Color Vision,* ed D. L. MacAdam (Cambridge, MA: MIT Press), 145–148. Originally published in Festschrift der Albrecht-Ludwigs-Universitat (1902).

Xiao, K., Pointer, M., Cui, G., Chauhan, T., and Wuerger, S. (2014). Unique hue data for colour appearance models. Part III: Comparison with NCS unique hues. *Color Res. Appl.* doi: 10.1002/col.21898. [Epub ahead of print].

Conflict of Interest Statement: The author declares that the research was conducted in the absence of any commercial or financial relationships that could be construed as a potential conflict of interest.

Received: 15 October 2014; accepted: 13 January 2015; published online: 10 February 2015.

Citation: Kuriki I (2015) Lightness dependence of achromatic loci in color-appearance coordinates. Front. Psychol. ***6****:67. doi: 10.3389/fpsyg.2015.00067*

This article was submitted to Perception Science, a section of the journal Frontiers in Psychology.

frontiers in Psychology

ORIGINAL RESEARCH
published: 02 April 2015
doi: 10.3389/fpsyg.2015.00337

Color difference threshold of chromostereopsis induced by flat display emission

Maris Ozolinsh[1,2]* *and Kristine Muizniece*[2]

[1] *Institute of Solid State Physics, University of Latvia, Riga, Latvia,* [2] *Department of Optometry and Vision Science, University of Latvia, Riga, Latvia*

The study of chromostereopsis has gained attention in the backdrop of the use of computer displays in daily life. In this context, we analyze the illusory depth sense using planar color images presented on a computer screen. We determine the color difference threshold required to induce an illusory sense of depth psychometrically using a constant stimuli paradigm. Isoluminant stimuli are presented on a computer screen, which stimuli are aligned along the blue–red line in the computer display CIE xyY color space. Stereo disparity is generated by increasing the color difference between the central and surrounding areas of the stimuli with both areas consisting of random dots on a black background. The observed altering of illusory depth sense, thus also stereo disparity is validated using the "center-of-gravity" model. The induced illusory sense of the depth effect undergoes color reversal upon varying the binocular lateral eye pupil covering conditions (lateral or medial). Analysis of the retinal image point spread function for the display red and blue pixel radiation validates the altering of chromostereopsis retinal disparity achieved by increasing the color difference, and also the chromostereopsis color reversal caused by varying the eye pupil covering conditions.

Keywords: chromostereopsis, eye chromatic aberrations, fusion of retinal images, stereo disparity, perception threshold

OPEN ACCESS

Edited by:
Marcelo Fernandes Costa, Universidade de São Paulo, Brazil

Reviewed by:
Balazs Vince Nagy, Budapest University of Technology and Economics, Hungary
Andrey V. Larichev, Moscow State University, Russia

***Correspondence:**
Maris Ozolinsh, Department of Optometry and Vision Science, University of Latvia, 8 Kengaraga Street, Riga LV1063, Latvia
ozoma@latnet.lv; k.muizniece@gmail.com

Specialty section:
This article was submitted to Perception Science, a section of the journal Frontiers in Psychology

Received: *15 October 2014*
Accepted: *09 March 2015*
Published: *02 April 2015*

Citation:
Ozolinsh M and Muizniece K (2015) Color difference threshold of chromostereopsis induced by flat display emission. Front. Psychol. 6:337. doi: 10.3389/fpsyg.2015.00337

Introduction

The ability of the human eye to visualize its surrounding environment is excellent despite the fact that its optics is distinctly non-ideal. Over an extended evolution process, the human brain has adapted to the non-ideality of the human visual system. The various neural pathways of visual inputs correct our visual perception in the most economical manner. In this context, over the past few decades, life has changed relatively suddenly in terms of living conditions and habits, and many new problems have begun to affect visual perception. This is partly due to the fact that nowadays people spend long hours looking at colorful but flat visual stimuli. Thus, new considerations have to be made regarding the eye and its perception. Consequently, the study and impact of colored stimulus on the human eye via different display devices forms a primary concern.

In the above mentioned context, we first note that the optical structure of the eye possesses imperfect form factors and presents refractive index heterogeneity at different wavelengths (Gross et al., 2008; Howard and Rogers, 2012). The eye segments like other optical systems exhibit monochromatic and chromatic aberrations as well as transversal and longitudinal aberrations (Thibos et al., 1990). Chromatic aberrations result in a person's perception of a colorful flat surface as an image consisting of several layers. Each of these layers is characterized by its inherent light

wavelength or color (Thompson et al., 1993; Hong et al., 2011). The resulting effect is readily observed in many daily situations, for e.g., a subject will have the impression that a blue river or a black highway on a map appears to float slightly above the map surface instead of remaining located on the plane of the map. Further, this phenomenon manifests itself more clearly at night when the pupil diameter is increased. This phenomenon is known as (induced) color stereovision or chromostereopsis (Vos, 1960, 2008; Kishto, 1965; Ye et al., 1992; Thompson et al., 1993; Westheimer, 2008, 2013a).

Human beings also possess the ability to perceive the depth of a visual stimulus while analyzing image content This depth processing is performed by processing cues regarding the size or placement of the stimulus (Gross et al., 2008; Howard and Rogers, 2012; Dresp and Reeves, 2014). The perception of the depth (stereovision or stereopsis) occurs on the basis of the neural processing of input from both the left and right eyes.

The human brain can merge the slightly differential inputs from both eyes into one image. If the source of the inputs is flat, then stereo disparity (the horizontal difference in retinal images or image elements) can be induced by presenting slightly different images to the left and right eyes. These images can be separated optically by using anaglyphs or by use of stereo goggles while watching films on stereo projectors. Retinal stereo disparity can also occur because of light rays following different paths in the eye media, particularly when the image has a wide wavelength spectrum.

The merging of binocular retinal images has been described elsewhere for disparities originating from different kind of sources: planar or 3D, random dot or continuous, and black–white or color sources (Julesz, 1981; Simmons and Kingdom, 2002; Howard and Rogers, 2012; Ozolinsh et al., 2012). Further, induced stereopsis and stereodisparity evaluation have also recently been reported in people who spend a large percentage of time viewing computer screens (Hayashi et al., 2012).

The most commonly induced color stereovision can be observed if the stimulus contains elements of discrete spatial divisions, and further contains colors that lie far from each other on the spectrum, e.g., blue lettering on a red background. The special features of this visual effect form a primary concern in the fields of visual information design and computer displays (Vos, 2008; Chen et al., 2012).

With regard to the study of chromostereopsis, further analysis looks at longitudinal and transversal/lateral aberrations. Because of longitudinal aberrations in the eye, rays of different colors are focused at different planes in the eye, and not all these planes coincide with the retinal plane.

In the case of lateral aberrations, parallel rays of different wavelengths focus at non-corresponding retinal positions of each eye during binocular viewing. This lateral shift of focus depends on the dispersion of the eye's refractive indices and on the angle between the incident rays and line of sight. These chromatic aberrations are observable for the case of oblique incidence. Lateral aberrations cause illusory stereo effects.

In studying chromostereopsis, many investigators have analyzed the Stiles–Crawford effect, which is the directional sensitivity of the cone photoreceptors; light entering the eye near the pupil's periphery produces a lower photoreceptor response when compared with that produced with light of equal intensity entering near the pupil center. The Stiles–Crawford effect can be analyzed from the perspective of the origin of binocular disparity of illusory stereopsis (Ye et al., 1992; Applegate and Lakshminarayanan, 1993; Westheimer, 2013b). The Stiles–Crawford effect is considered a reason for chromostereopsis sign reversal (Winn et al., 1995).

Most studies have thus far focused on the investigation of chromostereopsis when visual stimuli consist of colors with a large span of spectral content. The aim of the present study is: (a) to investigate the binocular perception of color images and the generation of the illusory effect of stereopsis when the scene contains stimuli with small differences in the colors' dominant wavelengths; (b) to evaluate the threshold of the minimum color difference necessary to induce chromostereopsis.

Experimental Setup

Stimuli

In our study on the color difference threshold of chromostereopsis induced by flat display emissions, we used visual stimuli consisting of two sections. Both these sections, which comprised central and surrounding areas (**Figure 1**), were generated as random dots. These dots formed colored elementary areas on a black background, and these elementary areas (whose color was generated by monitor luminophores) in the central area were of a slightly different color from that of the surrounding dots. The colors of these dots lay along the blue–red line of the color primaries of the display in the CIE xy diagram.

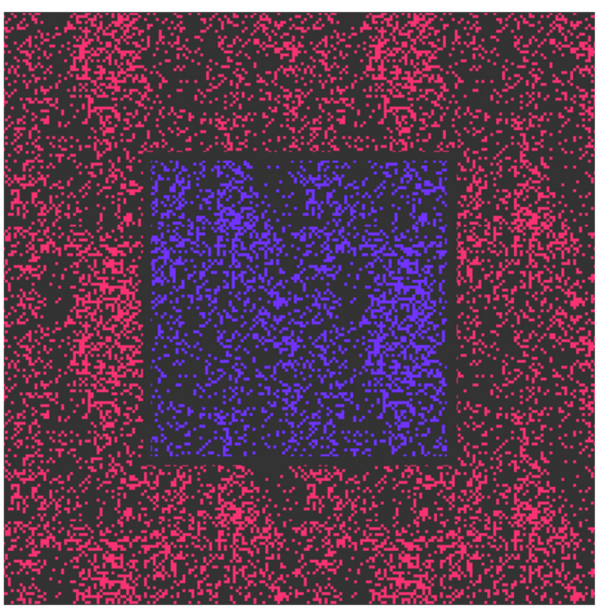

FIGURE 1 | Stimulus presented on a planar light-emitting diode (LED) display. The area of the central section is 300 × 300 pixel and the viewing area is 600 × 600 pixel.

We used such visual stimuli to ensure that there were a sufficient number of vertically oriented borders in the stimulus area. We assume that this fact facilitated binocular depth sense generation. Moreover, the use of a black-colored (instead of white-colored) stimuli structure strengthened the stimulus viewing luminance, contrast, and thus the stereo disparity formation.

The colors of the stimuli corresponded to the magenta region, and dots were generated using two colored light sources (red and blue luminophores) on a DELL U2412M display with a pixel pitch of 0.27 mm (**Figure 2**). The observation distance was 0.8 m. Therefore, displaying 1 pixel corresponded to an angle around the visual limit of 1′. The central section of the stimulus comprised a square containing pixels of the central color, and the square size was 300 × 300 pixel. The surrounding section covered an area of 600 × 600 pixel and comprised a dot structure of another (surrounding) color. The minimum area of the elementary point dot was 3 × 3 pixel. Due to eye transversal chromatic aberrations rays emitted from one monitor pixel with different color excite photoreceptors at slightly shifted retinal positions, if the rays are not aligned along the eye achromatic axis. For the oblique rays observing the stimuli with angular size inside of 10° the maximum angular dispersion of polychromatic beam inside the eye with central wavelengths of 497 nm (blue luminophore of CRT monitor) and 605 nm (red luminophore) can reach 3 arc min (Thibos et al., 1990; Rynders et al., 1995). That is more than the size of point spread function (PSF) of the focused eye in normal vision conditions.

The average density of colored dots within the stimuli area (duty cycle) of the colored pixels was r ≈ 0.26 and the average dot area was ∼32 pixel area units. Vertical colors' border count per one horizontal scan of the central area equaled to ≈40. The angular size of the central part was slightly greater than 5°, which is larger than the angle comprising the eye fixation direction, i.e., line of sight and the eye optical ("achromatic") axis. The chromatic characteristics of the stimuli were measured by means of an OceanOptics 4000 Fiberoptic spectrometer and a Minolta CS-100A Luminance and Color Meter. The Minolta CS-100A measures CIE xy coordinates according to the CIE chromaticity 1931 xyY color space (the uncertainty of the device luminance measurements at the measured stimuli range was ±2%).

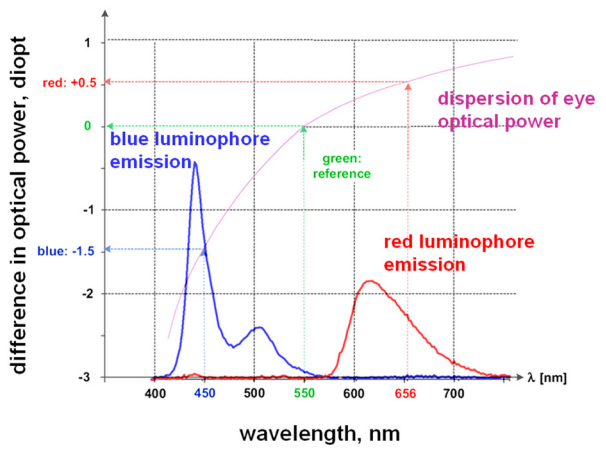

FIGURE 2 | Blue and red pixel emission spectra (used on the LED screen in the trials) together with the variation in the eye's refractive power with emission wavelength (latter data from Gross et al., 2008).

The saturation of the stimuli was always set at the maximum allowed by the display. The display area outside the stimulus corresponded to an angle of ≈20°, and it consisted of a neutral gray background corresponding to CIE values of $x_o = 0.316$, $y_o = 0.336$, and $Y_o = 16.4$ cd/m^2 (this value is close to the luminance of the color dots on the monitor screen). Experiments were carried out in semi-darkness under fluorescent-lamp global and incandescent-lamp local lighting conditions. The experimental room illumination was adjusted such that the luminance of the almost neutral wall (the chromaticity CIE values of $x_{SR} = 0.393$ and $y_{SR} = 0.379$) behind the monitor coincided with the monitor background area luminance.

Procedure

The abovementioned stimuli were presented in trials in which the central and surrounding color pair differences were varied randomly. Each trial stimuli color content was centered around the trial symmetry center, where stimuli central and peripheral dots had the same blue/red content. The difference between the stimuli colors, i.e., for the central area dots more blue vs. red (when compared with stimulus color blue/red content in the trial stimuli symmetry center) in both the central and peripheral sections were symmetrically varied while attempting to maintain the stimuli isoluminance when moving away from the trial symmetry center. Up to 30 presentations were made per trial for each color-difference pair. The multi-choice task paradigm was used to evaluate the psychophysical testing of the observers' vision. The observers' task was to respond to the question: "Central part or peripheral part: Which part is closer?" The central part response was assigned a value of "1" and that for the peripheral part was assigned "0," and the responses were summed. The psychometric curves R(N) were fitted to a sigmoid function (wherein the trial sample set number N# was used as the ordinate), and the slope parameter σ was used to define the effect threshold in stimuli numbering metrics (N_{Th}).

The sets of trial colored-image pairs were measured, and their colors were located in the CIE xy diagram. The threshold value N_{Th} was recalculated to determine the color difference threshold $\Delta\lambda_{Th}$ (the central and surrounding color coordinates of the N-th sample were projected from the initiating point towards the color gamut opposite border, i.e., crossing the white point O in the CIE xy diagram).

The participants comprised two male and eight female observers. Nine subjects were school students studying optometry (age span 18–22), and one of the other participants was a 63-year-old presbyopic male observer who used the corresponding optical power goggles enabling him to see clearly red stimuli. Basic measurements were performed for "trained" observers (both the authors of the present study, a younger student who did not use viewing aids and an elderly presbyopic patient).

In order to vary the experimental conditions, we employed partial bilateral covering of the eye pupils, which produces an

additional type of retinal stereo disparity. During these experiments, the observer was asked to place his head in a special mounting to avoid lateral head movements.

The study was conducted in accordance with the principles embodied in the Declaration of Helsinki Code of Ethics of the World Medical Association. All participants were unaware of the specific aims and methods of the study.

Results

Our experiments with non-covered eye pupils allowed the determination of the minimum color difference causing chromostereopsis for stimuli created by red–blue luminophores. We attempted to ensure that the stimuli luminance was constant during each trial (as allowed by digital control of the computer's video output). The measured stimuli color range varied within the CIE xyY coordinates of x = 0.226–0.245 and y = 0.140–0.153, and the color spot luminance varied within the mentioned color range as Y = 15.7–17.2 cd/m^2. Adaptation to illumination and luminance levels closer to mesopic conditions can lead to a shift in the eye's red/blue color sensitivity (position and height of eye spectral sensitivity V_λ curve). In this context, we remark that adaptation to the background illumination level and the individual eye spectral sensitivity of observers were not examined in our study. To stabilize the perception and to obtain data for a smooth psychophysical curve, the measurements for trained observers were obtained at least 30 min after adaptation to the experimental illumination conditions.

The filling of color spots was randomly distributed over the stimulus area. The actual luminance of the stimuli area had a standard deviation of $SD_Y \approx 1$ cd/m^2, and the mean luminance was Y = 4.3 cd/m^2. The monitor white point O CIE xy chromaticity coordinates were determined as $x_o = 0.316$ and $y_o = 0.336$.

Participants experienced illusory depth perception while viewing planar color images when they were observing the stimuli binocularly. Monocular viewing did not lead to any 3D perception. Binocular stereovision, i.e., stereopsis is detectable if the color difference between the central and surrounding sections of the trial stimulus is sufficient and if the image texture is optimum with a sufficient number of vertically oriented structure transients.

We hypothesized lateral aberrations as the main cause of the illusory depth effect experienced by the observer upon viewing the color stimuli on a plane display. The perceived stereopsis and the stability of observation depend on the accommodation and fixation habits concerning the viewing of such composite images, the geometry, and decentralization of the pupil, its distraction degree, and the pupil aperture shape. The trial results of naïve patients confirmed their perception of color stereopsis; however, their observation results did not aid in building a satisfactory set of psychometric curves for threshold evaluation. The relatively low mean luminance of the stimulus area could also facilitate instability of the effect polarity (Kishto, 1965).

Figure 3 (curve 1) shows the psychometric plot of the stable perception of color stereopsis when observing a trial set similar

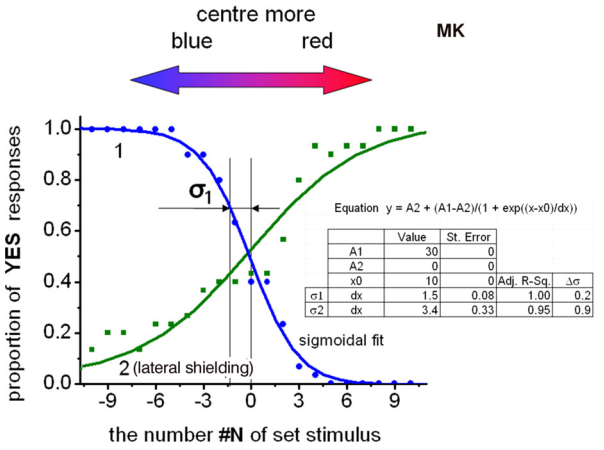

FIGURE 3 | Psychometric curves to determine the threshold of color difference to detect the induced color stereo effect. The curves are – corresponding to viewing with uncovered pupils (curve 1) and curve corresponding to viewing with lateral shielding (curve 2). Parameters of sigmoidal fit of experimental points and of statistical data analysis are depicted in inset.

to the stimulus shown in **Figure 1**. Subjects were asked to concentrate only on their sense of depth and ignore any cues arising from their perception of color. The arrows at the top of figure show the direction of corresponding color increase in the central part of the image.

Next, we prepared 21 trial stimuli [from N#(−10) to N#(10)] that exhibited a gradual increase in the central redness. In a synchronous manner, the increase of redness (see the inset of **Figure 4**) was offset by a decrease of bluishness in the central part, and with the opposite varying of colors in the peripheral part of the stimuli. The surrounding and central areas of the stimuli N#(0) consisted of randomly distributed active elements emitting the same color. In addition, the ratio of the blue to red of the stimuli color was opposite for stimuli with positive vs. negative indexing, for e.g., for N#(−5) and N#(5), in the left and the right sides of the central stimuli N#(0) in **Figure 3**.

Thus, each trial had stimuli with 10 difference values between the colored dots of the central and peripheral parts. The resulting psychophysical curves allowed the determination of the threshold of the color difference. The inset of **Figure 4** schematically depicts the stimuli chromatic x coordinates (curve 1) for the central part and the variation in the color difference $\Delta xy = \sqrt{(x_c - x_p)^2 + (y_c - y_p)^2}$ (wherein the subscripts indicate the indexing points: central or peripheral) between the central and peripheral parts in CIE xy metrics (curve 2) along the trial stimuli set.

Another key point of our study involved the presentation of the results in terms of reasonable metrics for color research. As the color of the stimuli lay on the line connecting the display's blue and red luminophore CIE xy chart coordinates, we proposed also the stimuli's complementary color dominant wavelength as a potential measure of the stimuli (schematically shown in **Figure 4**).

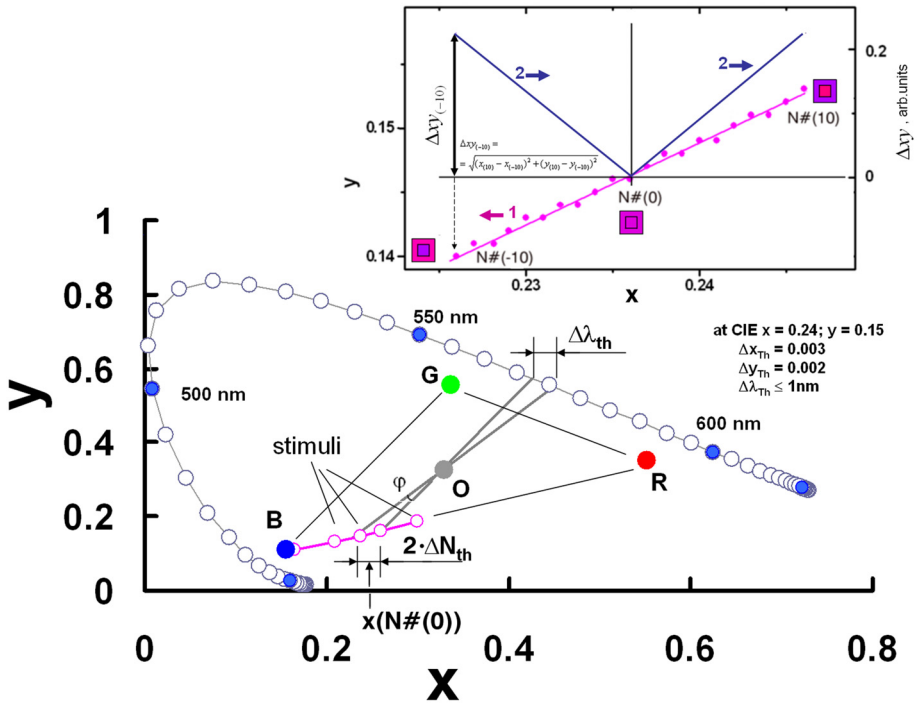

FIGURE 4 | Schematical presentation of the trial stimuli in CIE xy chart – its central part chromaticity coordinates, and the principles of recalculation of the color difference threshold in the complimentary wavelength metrics. In the upper right corner the trial stimuli central-area dot chromaticity CIE xy coordinates are depicted – curve 1, and varying of the color difference between stimuli central and peripheral parts Δxy for trial stimuli N#(−10) to N#(10) – curve 2, shown.

The colorimetric coordinates in the CIE xy chart of the following points were first determined. First, we determined x_i and y_i for the set of trial stimuli on both sides of the trial equilibrium point N#(0). For equilibrium point N#(0) the central and surrounding colors are identical with coordinates corresponding to – x_0 and y_0. Secondly, we determined the virtual points N#(−σ) and N#(+σ) with coordinates $x_{0-\sigma}$, $y_{0-\sigma}$ and $x_{0+\sigma}$, $y_{0+\sigma}$. These points were shifted along the monitor's blue–red line in the CIE xy chart from both sides of the equilibrium point N#(0) at the distance that corresponds to the threshold distance σ in the metrics of stimuli numbering. The values of $x_{0-\sigma}$, $y_{0-\sigma}$ and $x_{0+\sigma}$, $y_{0+\sigma}$ were determined by performing a linear interpolation of data along the stimuli line in corresponding CIE xy chart area. The triangle with vertices of the O-point, $x_{0-\sigma}$, $y_{0-\sigma}$, and $x_{0+\sigma}$, $y_{0+\sigma}$ determined the angle of the O-point vertex value φ (**Figure 4**). The projection of this angle on the color locus green–yellow area allowed the use of CIE complementary wavelength metrics for the stimuli color difference threshold. The data in **Figure 3** can be used to determine the color stereopsis threshold of $N_{Th} = \sigma_1 = 1.5$ for the uncovered pupil conditions at the color equilibrium point specified by x = 0.24, y = 0.15 in the CIE xy chart. Average luminance of the display screen in these trials was Y = 4.3 cd/m^2. Statistical analysis yielded the uncertainty of the sigmoid function data in **Figure 3** – $\Delta\sigma = \pm 0.2$ for $p = 0.95$. The average CIE chart parameter thresholds for chromostereopsis on the display's red–blue line of the group for two trained observers were $\Delta x_{Th} = 0.003$ and $\Delta y_{Th} = 0.004$. The data for the older presbyopic observer's color stereopsis when compared with that of the younger observer revealed higher data scattering, however, the sigmoid fit yielded σ values that were not significantly larger.

Our recalculations according to the abovementioned algorithm yielded the threshold value for the uncovered pupil color stereopsis as $\varphi_{Th} = 0.7°$, and the corresponding threshold in terms of the complementary wavelength metrics was $\Delta\lambda_{Th} \leq 1$ nm. We note that the last set of metrics can be universally applied to trichromatic stimuli along other axes in the CIE xy diagram, and for stimuli along the blue–red display line, the metric set can be very resolvable.

Figure 3 (curve 2) also shows the psychometric plot under conditions wherein the eye pupil areas were partially covered. The observers in this case used a trial frame with semi-circle apertures, which allowed centering of the apertures and the realizing of synchronous horizontal flips of the covered pupil area for the left and right eyes. Variation in the covered pupil areas (medial or lateral) switched the stereopsis polarity. Curve 2 shows the psychometric curve slope and the slope parameters (**Figure 3**) for observation conditions with lateral shielding.

Discussion

The angular size of the central area in our study was slightly larger than the eye angles between the fixation and optical axes (Thibos

et al., 1990). In the experiments, we asked observers to make their decision about the perceived mutual displacement of a larger area that lay outside the range comprising these visual axes, including the direction along the eye's "achromatic" axis.

The light rays emitted from the stimuli area are subject to chromatic aberrations in the eye. Furthermore, binocular viewing leads to disparity based on the color content of the stimuli, and the summary effect should be considered taking into account integration over all viewing angles. When permission was given to the naïve observers to freely move the eye fixation line over the entire central area, the "noise" of their decisions increased. This type of instability in decision-making and increase in the noise can be due to various reasons, all of which are eventually due to the large viewing angle of all stimuli.

The results for the observers can be grouped in the following manner. Subjects in the first group experience stereopsis (the stimuli center is in front of stimuli periphery or vice versa) in the range of demonstrated trial stimuli. However, the observations are not stable; i.e., we can state "stereopsis is present; however, it does not have a measureable threshold," which was true for eight naïve observers. As regards the second observation group, the subjects experience stable stereopsis; however, their responses are not clearly distinct. The shape and width of the fitted psychometric curve are definite, but the data points are noisy, and they do not lie along the fitting curve. This result was valid for two trained observers. In the third observation group, subjects are well concentrated for such experiments and they experience stable stereopsis. In this case, the psychometric curves are less noisy and the threshold can be clearly detected for the same two trained observers as measured in another test series with the same parameters. Actually, all participants including the naïve observers experienced the depth effect in the range of demonstrated trial stimuli, however, the responses of the naïve subjects were not stable. We did not statistically consider the oscillating responses in evaluating the color stereopsis for the group of naïve observers. The impossibility of obtaining consistent psychophysical curves for these observers with non-stable stereopsis prevents us from combining their data without violating the description (including mathematical description) of the effect.

Previous reports (Rozkova et al., 2012) have indicated eye strabismus as a possible cause that can alter positive ("Red-in-front") color stereopsis to negative ("Blue-in-front") color stereopsis. Binocular features such as eye tropias and phorias, fixation disparity, and the possibility of fixating on an imaginary stereo plane can all influence the color stereopsis sign and observation stability.

In previous studies, the stimuli mostly were monochromatic (Ye et al., 1991; Thompson et al., 1993) or generated on a computer screen by display color primaries (Simmons and Kingdom, 2002; Kitaoka et al., 2006; Hayashi et al., 2012). In our study, we

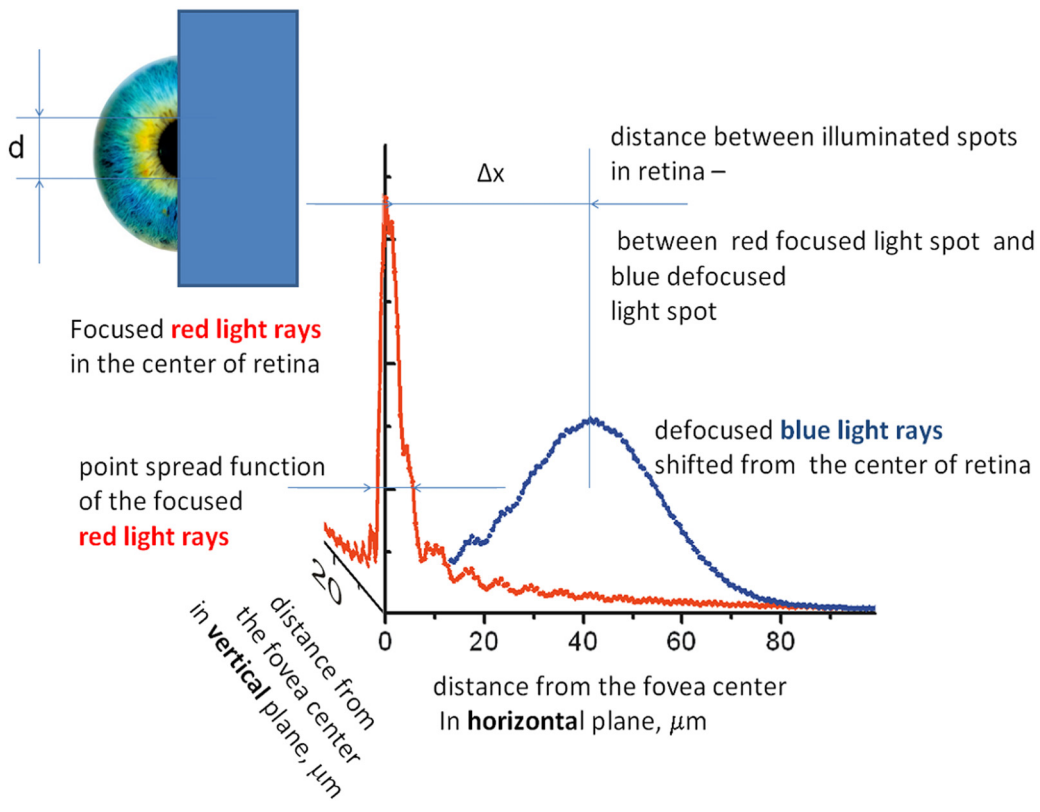

FIGURE 5 | Retinal illumination at the eye's horizontal and vertical planes from a single-display R + B pixel calculated from the point spread function (PSF) and its defocusing for blue emission. Calculations are performed for eye with half the pupil covered. Inset shows the covering of the eye pupils.

used a series of magenta stimuli around the "equilibrium point" (wherein the colors in stimuli's central and surrounding areas have equal chromaticity coordinates). Each of the stimuli dots sends emission from the blue and red luminophores toward the eye retinal plane at two distinct retina areas: one for blue pixel and other for red one. These areas coincide only if the emission rays pass along the eye achromatic axis. Due to longitudinal chromatic aberrations of the eye, these projections are not well focused at the retinal plane. We use the term "center-of-gravity," which was introduced by Kitaoka et al. (2006) to characterize this situation.

For the stimulus at the trial equilibrium point, when center and peripheral dots are of the same color, each of the stimulus dots of both the center and surrounding areas projects an identical spatial distribution of the chromatic emission on the eye's retinal plane. The centers-of-gravity for both primary and secondary color contributions are situated in the same retinal position. No stereo disparity can be generated in this case. When colors of central and surrounding areas move away from the trial equilibrium point in opposite directions, the central and surrounding dots due to their dissimilar color project different spatial distribution of emission on the retina. This difference creates stereo disparity of the illusory depth sense via binocular observation in such cases, when eyes' pupils are not circular, for e.g., semicircular with opposite geometry regarding to the face symmetry.

The center-of-gravity model can be used to explain the results (**Figure 3**, curve 2) of studies on chromostereopsis when observations are made through shielded eye pupils. We used the Fourier transformation of the aperture for radiation through the eye pupil of the half-covered eye for red emission, and we evaluated the circle of confusion for non-focused and wavelength-diffused blue emission to subsequently calculate the retinal illumination. **Figure 5** shows the determined PSF of the half-covered eye at the focus point for the displayed red emission and defocused illumination for blue emission (the color caused an optical power shift of $\Delta P \approx 1.3$ in the eye, according to **Figure 2**).

The medial or lateral covering of pupils distinctly switches the polarity of the induced depth sense, i.e., the blue image plane is perceived in front of the red image plane and vice versa. The right and left eyes exhibit mirror symmetry of retinal illumination, and further, non-oblique rays (due to their lateral aberrations) can contribute to the induced stereo disparity. In addition, the effect polarity or positive vs. negative switching, i.e., the perception of blue being closer than red and vice versa, occurs upon altering the geometry of eye pupil covering. Our observations confirm this phenomenon, i.e., the pronounced switching of the depth effect polarity by altering the shielding of half of the pupils from medial to lateral. However, the experimental points on the psychophysical curve in the case of shielding exhibited a larger deviation at first, and the color difference threshold at least doubled subsequently. Such variance can perhaps be explained by the minimization and decentralization of the pupil area and decrease in retinal illumination.

Conclusion

We studied chromostereopsis by continuously increasing the color difference of the central area and the surrounding dots. The simultaneous increase in stereo disparity was substantiated by application of the center-of-gravity model.

We determined that chromostereopsis becomes detectable for the color difference of image elements above the threshold with values of $\Delta x_{Th} = 0.003$ and $\Delta y_{Th} = 0.004$ according to CIE chromaticity coordinates that can be transposed to stimuli complimentary wavelength metrics as $\Delta\lambda_{Th} \leq 1$ nm. Such color difference threshold parameters are valid for the case of red–blue computer display radiation determined at the color difference equilibrium point of $x = 0.24$, $y = 0.15$ in the CIE xy chart for stimuli with an averaged luminance of $Y = 4.3$ cd/m^2. These values were determined under viewing conditions in which no eye-pupil-shielding obstacles were used. Symmetrical bilateral medial or lateral screening of both eye pupils led to reversal of the illusory effect, i.e., from the perception of blue in front of red to that of red in front of blue. Our findings are important in terms of evaluating induced stereopsis effects on images produced on planar screens when the digital chromatic output consists of more or less saturated short- and long-wavelength colors. The use of colors with a large wavelength span can cause an essential distortion of visual information.

Acknowledgments

This study was supported by Latvian Research Funding grant ESF 2013/0021/1DP/1.1.1.2.0/13/APIA/VIAA/001. We thank Gunta Krumina for helpful assistance in software design and suggestions during experimental work and valuable comments discussing preparation of manuscript.

References

Applegate, R. A., and Lakshminarayanan, V. (1993). Parametric representation of Stiles-Crawford functions: normal variation of peak location and directionality. *J. Opt. Soc. Am. A* 10, 1611–1623. doi: 10.1364/JOSAA.10.001611

Chen, Z., Shi, J., Tai, Y., and Yun, L. (2012). Stereoscopic depth perception varies with hues. *Opt. Eng.* 51, 1–6. doi: 10.1117/1.OE.51.9.097401

Dresp, B., and Reeves, A. (2014). Effects of saturation and contrast polarity on the figure-ground organization of color on gray. *Front. Psychol.* 5:1136. doi: 10.3389/fpsyg.2014.01136

Gross, H., Blechinger, F., and Achtner, B. (2008). "Human eye," Chap. 36, in *Handbook of Optical Systems: Survey of Optical Instruments,* Vol. 4, ed. H. Gross (Weinheim: WILEY-VCH Verlag GmbH & Co), 1092.

Hayashi, T., Kawai, Y., and Sakata, Y. (2012). Individual differences in chromostereopsis under natural viewing conditions. *Iperception* 3, 617.

Hong, J. Y., Lee, H. Y., Park, D. S., and Kim, C. Y. (2011). "Depth perception enhancement based on chromostereopsis," in *Proceeding of the SPIE Human Vision and Electronic Imaging XVI 7865, 786513,* San Francisco, CA. doi: 10.1117/12.872290

Howard, I. P., and Rogers, B. J. (2012). *Perceiving in Depth*, Vol. 2, *Stereoscopic Vision*. Oxford: Oxford University Press. doi: 10.1093/acprof:oso/9780199764143.001.0001

Julesz, B. (1981). Textons, the elements of texture perception, and their interactions. *Nature* 290, 91–97. doi: 10.1038/290091a0

Kishto, B. N. (1965). The colour stereoscopic effect. *Vision Res.* 5, 313–329. doi: 10.1016/0042-6989(65)90007-6

Kitaoka, A., Kuriki, I., and Ashida, H. (2006). The Center-of-gravity model of chromostereopsis. *Ritsumeikan J. Hum. Sci. 27*, 59–64.

Ozolinsh, M., Martín, I., Lauva, D., and Karitans, V. (2012). Howard-Dolman stereo-vision test at different opponent colour stimuli. *J. Mod. Opt.* 58, 1749–1754. doi: 10.1080/09500340.2011.559313

Rozkova, G. I., Rozkov, S. N., and Richkova, S. I. (2012). "Chromostereopsis at optical correction of refractive anomalies and strabismus," in *Proceedings of the Conference on Applied Optics-2012*, St. Petersburg, 235–239. Available at: http://www.oop-ros.org/maket2012/part7/7.2.pdf [in Russian]

Rynders, M., Lidkea, B., Chisholm, W., and Thibos, L. N. (1995). Statistical distribution of foveal transverse chromatic aberration, pupil centration, and angle psi in a population of young adult eyes. *J. Opt. Soc. Am. A Opt. Image Sci. Vis. 1* 2, 2348–2357. doi: 10.1364/JOSAA.12.002348

Simmons, D. R., and Kingdom, F. A. (2002). Interactions between chromatic- and luminance-contrast-sensitive stereopsis mechanisms. *Vision Res.* 42, 1535–1545. doi: 10.1016/S0042-6989(02)00080-9

Thibos, L. N., Bradley, A., Still, D. L., Zhang, X., and Howarth, P. A. (1990). Theory and measurement of ocular chromatic aberration. *Vision Res.* 30, 33–49. doi: 10.1016/0042-6989(90)90126-6

Thompson, P., May, K., and Stone, R. (1993). Chromostereopsis: a multicomponent depth effect? *Displays* 14, 227–233. doi: 10.1016/0141-9382(93)90093-K

Vos, J. J. (1960). Some new aspects of color stereoscopy. *J. Opt. Soc. Am.* 50, 785–790. doi: 10.1364/JOSA.50.000785

Vos, J. J. (2008). Depth in colour, a history of a chapter in physiologie optique amusante. *Clin. Exp. Optom.* 91, 139–147. doi: 10.1111/j.1444-0938.2007.00212.x

Westheimer, G. (2008). Illusions in the spatial sense of the eye: geometrical–optical illusions and the neural representation of space. *Vision Res.* 48, 2128–2142. doi: 10.1016/j.visres.2008.05.016

Westheimer, G. (2013a). Clinical evaluation of stereopsis. *Vision Res.* 90, 38–42. doi: 10.1016/j.visres.2012.10.005

Westheimer, G. (2013b). Retinal light distributions, the Stiles–Crawford effect and apodization. *J. Opt. Soc. Am. A Opt. Image Sci. Vis.* 30, 1417–1421. doi: 10.1364/JOSAA.30.001417

Winn, D. B., Bradley, A., Strang, N. C., McGraw, P. V., and Thibos, L. N. (1995). Reversal of colourdepth illusion explained by ocular chromatic aberration. *Vision Res.* 35, 2675–2684. doi: 10.1016/0042-6989(95)00035-X

Ye, M., Bradley, A., Thibos, L. N., and Zhang, X. (1991). Interocular differencies in transverse chromatic aberration determine chromostereopsis for small pupils. *Vision Res.* 31, 1787–1796. doi: 10.1016/0042-6989(91)90026-2

Ye, M., Bradley, A., Thibos, L. N., and Zhang, X. (1992). The effect of pupil size on chromostereopsis and chromatic diplopia: interaction between the Stiles-Crawford effect and chromatic aberrations. *Vision Res.* 32, 2121–2128. doi: 10.1016/0042-6989(92)90073-R

Conflict of Interest Statement: The authors declare that the research was conducted in the absence of any commercial or financial relationships that could be construed as a potential conflict of interest.

frontiers in
PSYCHOLOGY

ORIGINAL RESEARCH ARTICLE
published: 09 December 2014
doi: 10.3389/fpsyg.2014.01416

Variability and systematic differences in normal, protan, and deutan color naming

Balázs V. Nagy[1,2]*, Zoltán Németh[2], Krisztián Samu[2] and György Ábrahám[2]

[1] Vision Laboratory, Institute of Psychology, University of São Paulo, São Paulo, Brazil
[2] Department of Mechatronics, Optics and Engineering Informatics, Budapest University of Technology and Economics, Budapest, Hungary

Edited by:
Laurence T. Maloney, Stanford University, USA

Reviewed by:
David Bimler, Massey University, New Zealand
Jessie J. Peissig, California State University Fullerton, USA

***Correspondence:**
Balázs V. Nagy, Department of Mechatronics, Optics and Engineering Informatics, Budapest University of Technology and Economics, Bertalan Lajos u. 2-4, Budapest 1111, Hungary
e-mail: nagyb@mogi.bme.hu

The congenital color vision deficient (CVD) generally demonstrates difficulties in color naming tasks. In our study we investigated color naming properties and uncertainties of a relatively large group of red–green CVDs using quasi monochromatic stimuli and seven basic color terms. The results show a large variability in color naming for the CVD when contrasted to normal color vision and similar alterations when comparing protans to deutans. Statistically significant differences were found in specific wavelength ranges between the tested groups. In general, protans and deutans have shown better color naming ability than expected, which suggests the use of non-chromatic visual cues.

Keywords: color vision deficiency, color naming, monochromatic visual stimulation, protan and deutan vision, visual psychophysics

INTRODUCTION

In classical literature a great amount of studies can be found on how the neural system in the eye responds to color stimuli and how chromatic information is processed (Young, 1802; Helmholtz, 1852; Hering, 1905; Hurvich and Jameson, 1957; Kaiser and Boynton, 1996; Wyszecki and Stiles, 2000). Congenital color deficiency has already been studied by several authors (Hurvich and Jameson, 1957; Nathans et al., 1986) and today the genetic background is also well understood (Neitz and Neitz, 2000). The most common type is red–green color deficiency which can be divided into four main subtypes: protanomaly, deuteranomaly, protanopy, and deuteranopy. The former two are the anomalous trichromat types where the trichromatic color vision is preserved but with spectral sensitivity change generally in one of the cone photoreceptors. The latter two are the dichromats which generally means that there are only two functioning cone photoreceptor types (Deeb and Motulsky, 2005).

The functioning of higher order neural color processing mechanisms has also been studied by many research groups. Yet, these issues still raise many questions and require further research work. One of these areas is the color identification and its verbal expression: color naming. This complex process involves all stages in human color perception beginning with the color stimulus up to its association with linguistic terms, i.e., color names. Several researchers have already approached this topic from different points of view, whereas linguistic and geographical distribution of color terms have been broadly studied (Berlin and Kay, 1969; Rosch-Heider, 1972; Kay and MacDaniel, 1978; Kay and Regier, 2003). In their summarizing work on linguistic and geographical aspects of color, Kay and Regier (2003) found eleven basic color terms when comparing different languages and locations. Their corresponding English names are the following: Red, Yellow, Green, Blue, Purple, Brown, Orange, Pink, Black, White, and Gray. However, Saunders and van Brakel (1997) questioned the generality of these 11 terms. Further researchers applied them when testing color naming; taking into account hue, saturation, and brightness at the same time (Boynton and Olson, 1987; le Rochelles and Viénot, 1995; Pitchford and Mullen, 2003). Other studies applied specific samples from color systems (such as the Munsell color chart) when performing color naming tests (Guest and van Laar, 2000; Lillo et al., 2001; Franklin et al., 2005; Bonnardel, 2006; Cole et al., 2006). Moreover, researchers dealt with the spectral dependence of color names (Boynton and Gordon, 1965; Beare and Siegel, 1967; Luria, 1967; Byrne and Hilber, 2003; Troup et al., 2005) including the comparison of normal subjects' results with those of the color vision deficient (CVD; Scheibner and Boynton, 1968; Smith et al., 1973; Paramei, 1996; Paramei et al., 1998; Diaconu et al., 2010). Most spectral color naming studies restrict the use of color terms to the four basic colors (i.e. blue, green, yellow, and red) with notable exceptions such as Beare and Siegel (1967) who conducted multiple color naming studies applying up to six color names and their compounds. Moreira et al. (2014) have created models based on the CIE u'v' chromaticity coordinates and compared them to measurement data. In summary, there is an extensive classical and modern literature on the topic of color naming.

The current study set out to contribute to the existing knowledge on CVD color naming, using the seven basic color terms (the "rainbow colors") that are monochromatically distinguishable by people with normal color vision. The colors "violet," "turquoise," and "orange" were added to the "blue," "green," "yellow," and "red" set ("ibolya," "türkiz," "narancs," "kék," "zöld," "sárga," and "piros" in Hungarian). These were applied within a relatively large group of human subjects, including red–green CVDs and normals. In a previous study (Nagy et al., 2008) using the CVD color naming

dataset we have introduced a possible method to categorize CVDs into arbitrary groups. In our current work we intended to provide a more justifiable categorization (comparing with anomaloscope categories) and a more detailed analysis than in previous studies. Mathematical modeling and statistical evaluation was applied to show the spectral differences within and between the tested groups, including color normals, protan and deutan CVDs. Moreover, the relatively large number of CVDs tested enabled us to statistically evaluate the uncertainty of color naming at each test wavelength, which can be characteristic for a given group of CVDs. Hence, it can be used as diagnostic information of the specific color vision deficiency type.

MATERIALS AND METHODS

EQUIPMENT

A computer controlled test instrument was applied in order to evaluate color naming ability in the human visual spectrum (from 400 to 700 nm). The stimulus consisted of a central 2° field of view target and a 16° surround viewed through the instrument's eyepiece. The 2° stimulus field targets foveal vision only and eliminates the possibility of rod influence on the results (Nagy and Boynton, 1979; Montag and Boynton, 1987). We used a continuous spectrum constant white background with a spectrally adjustable target stimulus in the center. The target stimulus was realized with a continuous interference filter (IF) of approximately 15 nm FWHM (full width at half maximum). The target luminance, generated by the combination of the light source and the IF filter varied throughout the spectrum within the photopic range (>5 cd/m^2). Luminance calculations were based on normal color vision, avoiding mesopic luminance levels where significant changes in color naming might occur (Paramei et al., 1998). The radiance of the stimuli was between 1 and 9 W/(m^2·sr) (**Figure 1**). The background luminance had a uniform spectral distribution and was maintained at 120 cd/m^2 (0.6 W/(m^2·sr)), calculated with the spectral luminous efficiency function of normal color vision.

TEST SEQUENCE

Prior to the color naming examination, subjects underwent classical color vision tests of Ishihara plates under natural daylight illumination and anomaloscopy using a Heidelberg instrument (Nagel, 1907; Birch, 1993). During the pretesting phase subjects were instructed to adjust the eyepiece of the color naming test instrument. Furthermore, they were able to sweep through the whole spectral range manually, in order to gain a first impression on the expected targets. In real test situations subjects were presented with quasi monochromatic target stimuli in random sequence throughout the visible spectrum with a 10 nm spectral resolution (31 test wavelengths in total). To reduce learning effects and to compensate the non-equiluminance of the target stimuli a spectral shift of approximately 50 nm between consecutive stimuli was applied. Subjects were instructed to name the stimuli using the seven color terms within 2 s to avoid adaptation. If it was necessary, two terms could be ascribed to a stimulus, in which case subjects were asked to indicate the dominant one. The reported color names were recorded. An additional test sequence was applied for the CVD subjects to search for an achromatic neutral target stimulus around 500 nm. During this test the stimulus wavelength was adjusted continuously by the subject and the neutral point's wavelength was recorded in case of a positive response. Subjects also had to adjust the wavelength at the long wavelength end of the spectrum where the stimulus color faded into the background. Here the threshold wavelength (the so called red-end) has been recorded.

SUBJECTS

The control group consisted of 31 normal subjects without impairment in color vision (25 men and 6 women), all within the age range of 17–55 with a dominance of the age group 19–23. The CVD group comprised 107 male subjects among whom 22 were diagnosed as protanomals, 26 as protanopes, 30 as deuteranomals, and 29 as deuteranopes. All subjects were of Hungarian nationality and signed a written consent, agreeing to participate in the tests, which adhered the requirements of the institutional regulations.

RESULTS

Individual subjects were assigned into five categories, i.e., normal, protanomal, protanope, deuteranomal, and deuteranope.

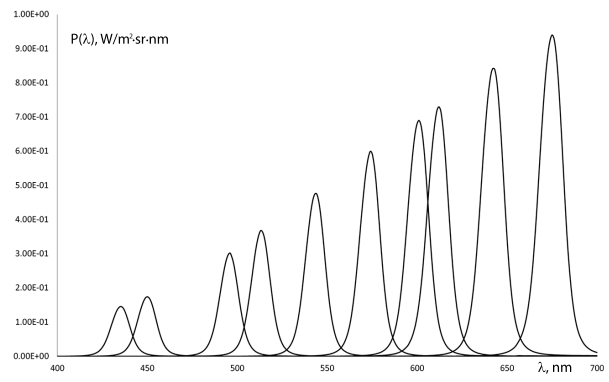

FIGURE 1 | Spectral radiance distribution variation of some of the stimuli used in the color naming tests.

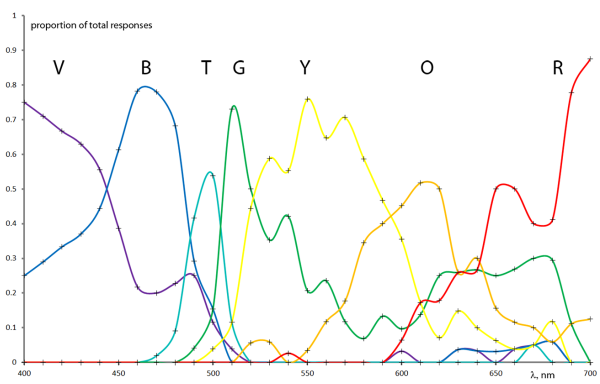

FIGURE 2 | Interpolation of raw color naming group results normalized to the total number of color names at each wavelength from the deuteranope CVD group (the measured points are indicated with crosses). Note that the color name distributions can be well approximated with Gaussian types of distributions.

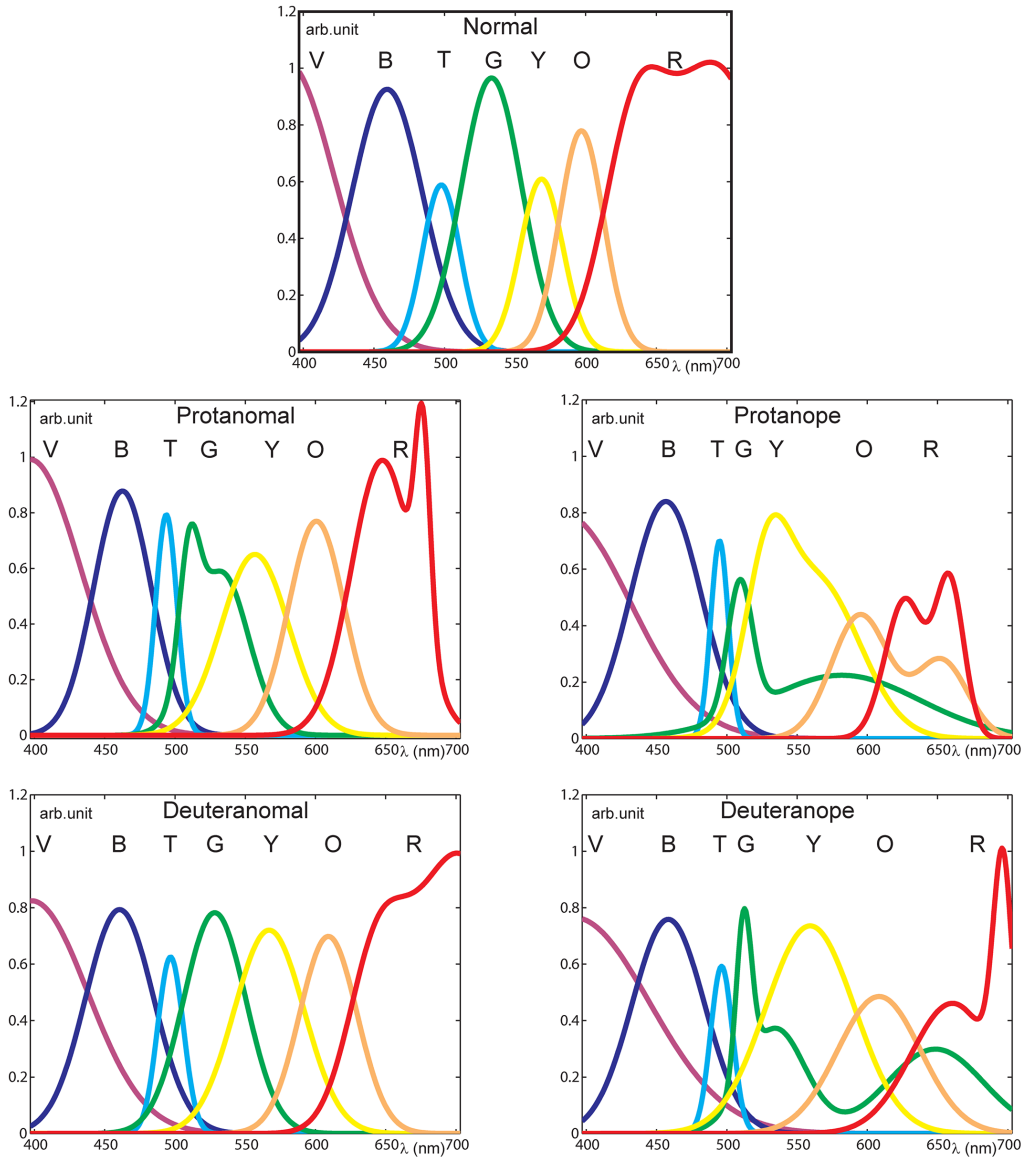

FIGURE 3 | Normalized pooled color naming results for all categories fitted with Gaussian functions with acceptable goodness of fit. (Initials of the color names are shown at the peaks of the distributions for the black and white version.) The distributions of color names indicate larger variability in the range from green to red with increasing severity of the deficiency. Note that in protan cases the red distribution ends below 700 nm as their perception in this range is spectrally limited.

Normals were distinguished with the Ishihara plates (Birch, 1993) while CVD groups were assigned when the anomaloscope tests agreed with both the monochromatic neutral point (Wyszecki and Stiles, 2000) and the red end (Kaiser and Boynton, 1996) results. The anomaloscope indicates protanomal, protanope, deuteranomal, and deuteranope categories. Protan results were accepted when indicated by the anomaloscope and if a red-end threshold lower than 700 nm was found. Similarly anope type anomaloscope results were justified by the existence of the neutral point around 500 nm.

The seven color terms' spectral distributions were normalized at each specific wavelength resulting in the fraction of the total responses for each color term. (See an example of normalized raw data of the deuteranope group in **Figure 2**.) In order to estimate color naming information with higher spectral resolution and to produce specific analysis parameters we applied mathematical models for the measurement results. First and second order Gaussian fits (**Figure 3**) were used to approximate the measured points and to provide analytical functions for each color term in each subject category. The distribution of the results for each color name indicated Gaussian like shapes for the mathematical fitting whereas our measurement data from a relatively large population generally did not show plateaus (Beare and Siegel, 1967) in the color naming spectral distributions (the only exception was

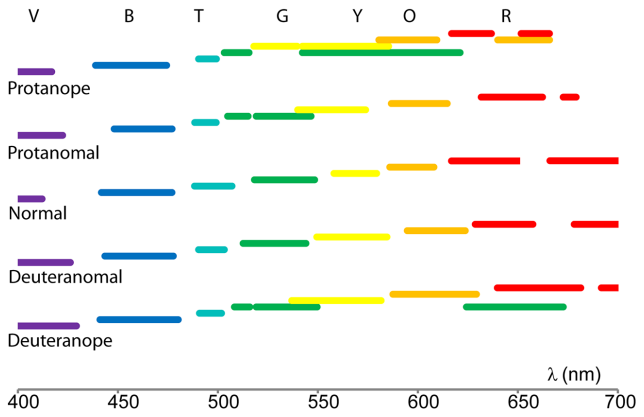

FIGURE 4 | Color naming ranges of the five tested groups indicated with their colors. (The color names' initials are positioned in the middle of the normal ranges.) The overlapping ranges show increase in uncertainty when naming the stimulus color.

the 'red' naming of the color normals above 670 nm where the Gaussian fit slightly distorted the plateau without effecting further analysis). Note that some of the distributions could only be approximated with second order Gaussian functions due to the asymmetry of some color name distributions especially in anope cases. The goodness of fit was adjusted for all cases to achieve a sum squared error (SSE) less than 0.10 and a high correlation between the model and the data ($R^2 > 0.85$).

Color naming ranges for each color term and subject category were calculated by applying the mathematical fit functions. Results shown in **Figure 3** were processed by using fit parameters (calculating the range of a specific color name using the full width at half maximum centered onto the peak) in order to compare the color naming ranges. **Figure 4** represents how color naming differs in the case of normals and in the four CVD groups. The overlapping ranges show increasing uncertainty of color name use especially in the anope groups.

To analyze the variability of the interpersonal results numerical scores were applied (Nagy et al., 2008) to the ordinal scale of color names ranging from violet to red (1 – violet; 2 – blue; 3 – turquoise/cyan; 4 – green; 5 – yellow; 6 – orange; 7 – red). The numerical scale enabled us to calculate an average score and its SD for each wavelength. These latter values demonstrate the variability of the color naming results in the spectrum. **Figure 5** shows the average scores compared between the groups along with the SD at 95% confidence level.

Color vision deficients generally have larger scores in the "green" range (500 nm $< \lambda <$ 550 nm) and lower scores in the orange–red range (600 nm $< \lambda$) than normals. The difference from normals increases from anomal to anope types. The SD results show a general increase in all groups tested for all wavelengths when compared to normals. However, anopes show larger increase in SD at wavelengths above 600 nm confirming an even higher uncertainty to name colors in this spectral range. Both the average and standard deviation results indicate similarities between the two anomal and the two anope groups, respectively.

To compare the results of the five groups a statistical analysis was carried out, using the non-parametric Mann-Whitney *U* test at each tested wavelength. The table in **Figure 6** displays the results of the analysis showing no statistically significant differences in the shorter wavelength range. The results are significantly different between normals and all groups in the "green" color naming range while in the "orange/red" range the anopes show significant differences at more wavelengths both from the normals and the anomals. Few significant differences have been detected between the two anomal and the two anope groups, which suggest great similarities in color naming between these groups.

DISCUSSION

Fundamental literature (Smith et al., 1973; Kaiser and Boynton, 1996; Wyszecki and Stiles, 2000) summarizes the basic color identification abilities of CVDs. Our results coincide well with existing literature data (Beare and Siegel, 1967; Luria, 1967; Scheibner and Boynton, 1968; Paramei, 1996) even at different luminance levels. Moreover, they support most of the previous statements, i.e., that CVD subjects have reduced ability in color naming and that they have significantly more yellowish and generally less red experience when identifying hues.

The difference in stimulus brightness is a key issue when considering the test results as this information can be used as a cue for discriminating between colors and also can affect color naming to some extent (Jameson and Hurvich, 1978; Paramei et al., 1998). As the luminous efficiency function varies among normals and CVD groups (Stockman et al., 1993) luminance values will be different for each stimulus for each test subject when using the same stimulus radiance spectral distribution. For this reason the generation of equiluminant stimulation without knowing the exact spectral luminous efficiency function of each subject can be rather complicated and spectral equiluminance based on normal color vision might generate significantly different perceived brightness for CVD subjects at each wavelength. We also need to emphasize the possible, although minor differences in luminance calculations based on the spectral luminous efficiency function – V(λ) – and perceived brightness (Schanda et al., 2002). As the V(λ) function has been determined based on monochromatic tests considering Abney's Law (Abney, 1913) for polychromatic stimuli, our quasi-monochromatic stimuli might be affected by it resulting in a different perceived brightness from what is predicted by the luminance calculations. These arguments indicate for further research that to equilibrate perceived brightness for color tests one might need an individual brightness calibration for all presented stimuli. Consequently, the stimulation used in our study could not provide the same brightness for all tested groups and individuals; however, the luminance calculated for normal color vision was above the upper mesopic luminance limit. The unequal brightness of the stimulus spectrum can have an effect on the results of color naming; however minor they might be at photopic luminance levels. These should be considered when comparing our results spectrally, thus a better CVD color naming can arise using brightness differences when judging the stimuli at different consecutive wavelengths. Since the same stimulus radiance distribution has been applied for all test subjects, the results

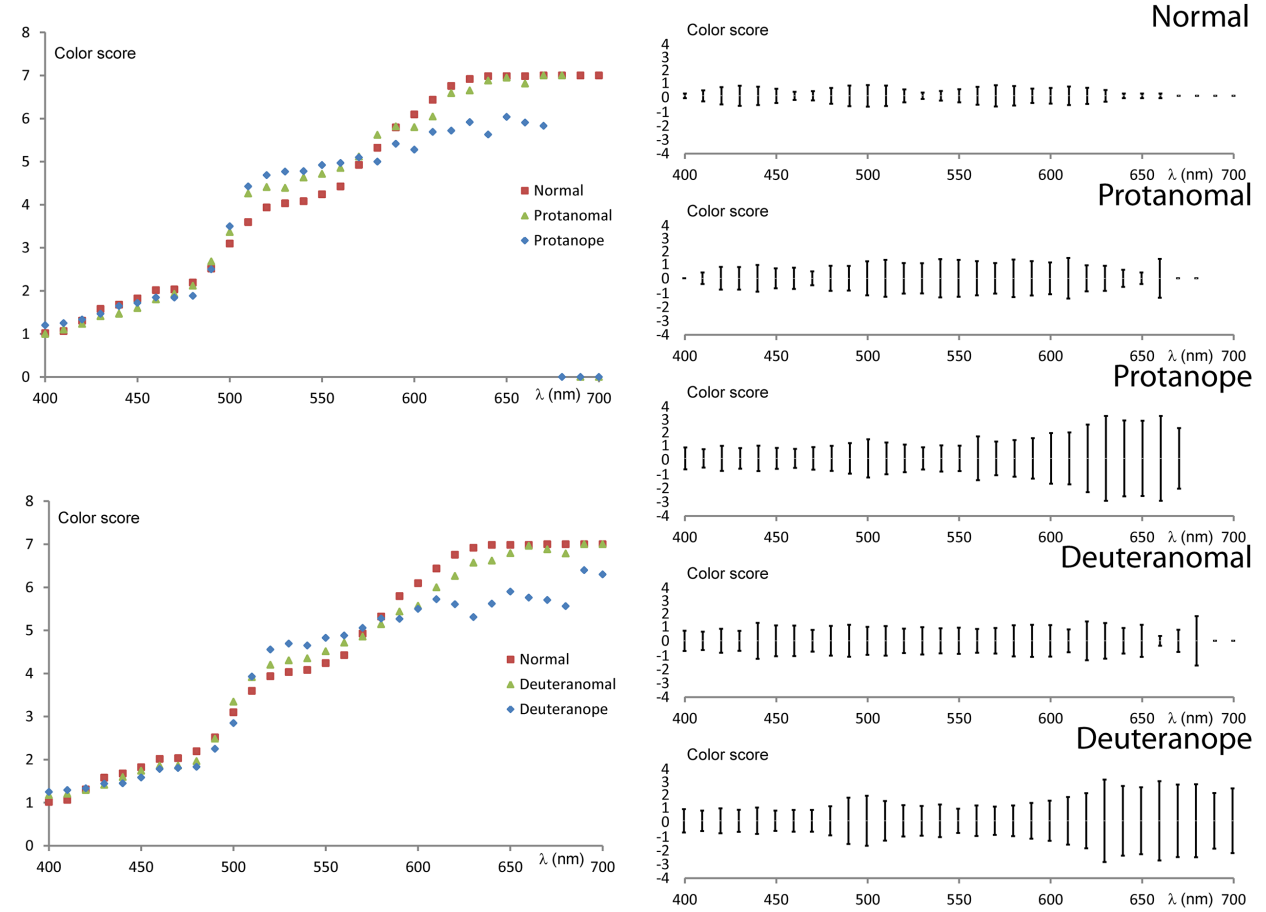

FIGURE 5 | Numerical evaluation of color naming results. The two figures on the left show the average scores for each wavelength comparing protans and deutans to normals. (Basic scores are the following: 1 – violet, 2 – blue, 3 – turquoise, 4 – green, 5 – yellow, 6 – orange, 7 – red.) The five figures on the right show the SD of the scores at 95% confidence level.

demonstrate the between groups spectral comparison of color naming.

Our statistically analyzed results show several differences and also some similarities comparing the five groups tested (including normals). We have found that violet and blue color naming ability seems to be similar for the CVDs when compared to normal. However, the variability of the color name use is increased even for these colors. As expected from protan and deutan types, the larger variation appears at wavelengths above 500 nm. Here we can observe a significant enlargement of the "green," "yellow," and "orange" ranges with reduction of the "red" range. Interestingly there are two specific wavelengths where no statistical differences have been detected (490 and 570 nm) when comparing the different CVD groups to normals. These are the regions of the turquoise and the yellow perception peaks. It seems that these two color perception ranges are specifically preserved in the case of red-green color vision deficiency. The numerical transformation describes the variability of the color naming results for the five tested groups. Clearly anopes have more uncertainty when naming color stimuli especially in the spectrum range above 600 nm. However all red–green CVD types have larger uncertainty in color naming for all wavelengths when compared to normals. Another interesting fact deriving from the numerical analysis is that protanope and deuteranope groups have similar color naming when not taking the protans' spectrally reduced red-end perception into account. Such similarities (or more precisely the lack of statistically significant differences) are observed between protanomals and deuteranomals as well. Thus when considering color naming tasks and applications where the perceptual identification of a color stimulus is necessary (for example in single color identification tasks with no discrimination possibility with other colors) the majority of anomalous trichromats and dichromats (red–green types) could be considered without any specificity to be protans or deutans.

Another interesting finding arose when looking at the color naming of CVD groups, comprising a relatively large number of subjects. The "green" color name's range in the pooled anope cases has an additional range at longer wavelengths (around the "orange" wavelength range in the protan case and around the "red" range in the deutan case). This issue of the anopes' "reappearing green" at the longer wavelengths is still an effect to be

	n-pl	n-pe	n-dl	n-de	pl-pe	pl-dl	pl-de	pe-dl	pe-de	dl-de
400	.93	.43	.08	.27	.59	.60	.44	.94	.87	.74
410	.76	.16	.08	.11	.51	.70	.44	.71	.87	.59
420	.27	.78	.47	.77	.65	.77	.62	.78	1.00	.77
430	.28	.39	.13	.28	.72	.94	.85	.70	.85	.87
440	.19	.87	.34	.11	.39	.67	.93	.51	.31	.57
450	.04	.50	.14	.03	.38	.60	.93	.66	.31	.46
460	.02	.04	.04	.01	.69	.91	.89	.79	.57	.80
470	.10	.11	.08	.01	.92	.81	.49	.97	.64	.60
480	.32	.01	.04	.00	.31	.36	.10	.64	.74	.41
490	.10	.82	.79	.40	.30	.18	.08	.81	.32	.36
500	.19	.05	.09	.22	.53	.99	.04	.46	.01	.02
510	.00	.00	.01	.00	.14	.05	.18	.00	.01	.57
520	.00	.00	.01	.00	.05	.20	.33	.00	.28	.01
530	.00	.00	.02	.00	.01	.55	.04	.00	.48	.00
540	.00	.00	.02	.00	.18	.13	.72	.00	.24	.03
550	.00	.00	.03	.00	.11	.31	.25	.00	.49	.01
560	.00	.00	.00	.00	.72	.51	.69	.31	.98	.24
570	.27	.25	.62	.32	.91	.08	.86	.10	.77	.11
580	.02	.03	.09	.58	.00	.00	.04	.40	.13	.38
590	.30	.08	.03	.00	.05	.03	.01	.97	.42	.33
600	.03	.00	.00	.00	.05	.12	.11	.24	.41	.73
610	.01	.00	.00	.00	.17	.34	.16	.20	.87	.27
620	.35	.00	.00	.00	.02	.10	.00	.19	.52	.01
630	.03	.00	.02	.00	.13	.87	.00	.16	.07	.00
640	.23	.00	.00	.00	.00	.03	.00	.06	.82	.01
650	.73	.00	.07	.00	.00	.21	.00	.02	.62	.01
660	.61	.03	.15	.00	.10	.46	.03	.16	.79	.01
670	1.00	.01	.06	.00	.11	.76	.12	.04	.97	.00
680	1.00	N/A	.07	.00	N/A	.84	.26	N/A	N/A	.00
690	N/A	N/A	.27	.16	N/A	N/A	N/A	N/A	N/A	.27
700	N/A	N/A	1.00	.16	N/A	N/A	N/A	N/A	N/A	.18

FIGURE 6 | Statistical analysis of the numerically transformed color naming result. The numbers in the cells show the *p*-values. The cells are painted light green when the *p*-value is below 0.05 and dark green when it is below 0.01 showing the higher significance level of statistical difference. Red cells indicate *p*-values where no statistically significant differences were detected. n, normal; pl, protanomal; dl, deuteranomal; pe, protanope; de, deuteranope.

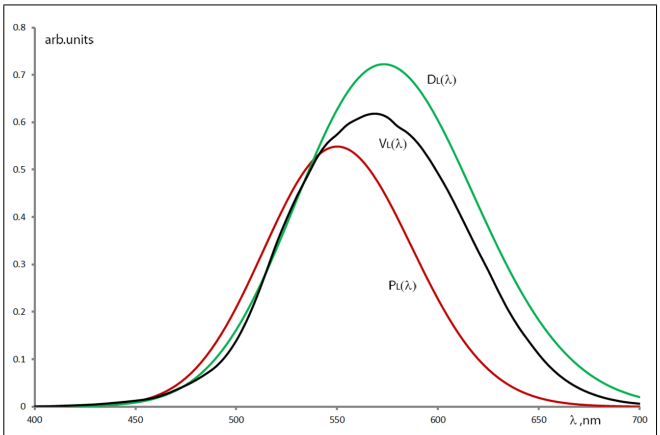

FIGURE 7 | Relative luminous efficiency functions of protanopes – $P_L(\lambda)$, deuteranopes – $D_L(\lambda)$ and normal – $V_L(\lambda)$ calculated from the data of Stockman et al. (1993) using Gaussian fit onto their measured results and weighted with the spectral radiance distribution of the applied stimuli.

discussed. At first instance, it would be considered as an effect of the spectral non-equiluminance of the stimulation. Although as mentioned before, an equiluminant stimulation considering the spectral luminous efficiency of normal color vision would generate different perceived brightness for the CVD groups. Therefore, we used the spectral radiance distribution of our stimulation as a weight function onto the luminous efficiency functions of normals, protans, and deutans (Stockman et al., 1993) to estimate their spectral brightness perception (**Figure 7**). When looking at the color naming ranges in our test results, protans tend to use "green" instead of "orange" while deutans confuse mainly the "red" with the "green." (Respectively 65 and 51% of the protan and deutan subjects have used the "green" term for naming stimuli at long wavelengths in the "orange" or "red" ranges.) Diaconu et al. (2010) also reported on green naming confusion at 625 nm in the case of protanope subjects, while Bonnardel (2006) showed the appearance of green naming for purple Munsell samples with significant long wavelength spectral content (spectral mixture of the short and long wavelength ends of the visible spectrum) in the case of deutan subjects. However, for "pure" red Munsell samples she did not find such confusions. Bonnardel (2006) provides the hypothesis for the unexpectedly larger diversity of color term use of CVDs: their significantly reduced hue discrimination ability (Kaiser and Boynton, 1996; Wyszecki and Stiles, 2000) in the red–green wavelength region might be enhanced by learning to use other visual cues. The results of the present study seem to support this as even anopes have applied all the seven basic terms allowed in our test with stimuli of spectrally varying brightness. (Nevertheless this latter fact could also be due to a bias in our method as we informed the subjects about the possibility to use all seven color terms.) The hypothesis for such visual cues is that anopes involve the brightness properties (Scheibner and Boynton, 1968; Jameson and Hurvich, 1978; Diaconu et al., 2010) of the different spectral stimuli when judging their chromatic content. In several cases (not only in color naming tests) we have also experienced that anopes (also some anomalous trichromats) tend to describe a chromatic stimulus, first by naming its brightness properties, followed by specifying a hue as if its determination required the preceding brightness judgment (Boynton and Scheibner, 1967; Paramei et al., 1998). Applying the anope color naming results onto the perceived brightness estimation curves in **Figure 7** we can see that the original "green" region (around 510 nm) and the longer wavelength "green" region (around 580 and 640 nm for protans and deutans, respectively) have approximately similar brightness levels. This might be considered as a use of brightness cue when applying quasi monochromatic stimuli for anopes who have reduced chromatic perception for the identification of green and orange/red hues. Obviously the question can arise why this does not happen with other color names especially with a "reappearing orange" at shorter wavelengths? Similarly to the case of CVD color discrimination (Thomson and Trezona, 1951), our hypothesis declares that at the shorter wavelengths the signal of the intact tritos photoreceptor dominates the decision making in color naming tasks even for the anopes.

ACKNOWLEDGMENT

Author Balázs V. Nagy was supported by CNPq fellowship (162576/2013-7).

REFERENCES

Abney, W. W. (1913). *Researches in Colour Vision and the Trichromatic Theory.* London: Longman, Green & Co.

Beare, A. C., and Siegel, M. H. (1967). Color name as function of wavelength and instruction. *Percept. Psychophys.* 2, 521–527. doi: 10.3758/BF03210259

Berlin, B., and Kay, P. (1969). *Basic Color Terms: Their Universality and Evolution.* Oakland, CA: University of California Press.

Birch, J. (1993). *Diagnosis of Defective Colour Vision.* Oxford: Oxford University Press .

Bonnardel, V. (2006). Color naming and categorization in inherited color vision deficiencies. *Visual Neurosci.* 23, 637–643. doi: 10.1017/S0952523806233558

Boynton, R. M., and Gordon, J. (1965). Bezold-Brücke hue shift measured by color naming technique. *J. Opt. Soc. Am. A* 55, 78–86. doi: 10.1364/JOSA.55.000078

Boynton, R. M., and Olson, C. X. (1987). Locating basic colors in the OSA space. *Col. Res. App.* 12, 94–105. doi: 10.1002/col.5080120209

Boynton, R. M., and Scheibner, H. (1967). On the perception of red by 'redblind' observers. *Ada Chromatica* 1, 205–220.

Byrne, A., and Hilber, D. (2003). Color realism and color science. *Behav. Brain Sci.* 26, 3–64. doi: 10.1557/S0883769400046649

Cole, B. L., Faao, L., Kayee, B., Sharpe, K., and Lakkis, C. (2006). Categorical color naming of surface color codes by people with abnormal color vision. *Optom. Vis. Sci.* 83, 879–886. doi: 10.1097/01.opx.0000249974.22205.2a

Deeb, S. S., and Motulsky, A. G. (2005). *Red-Green Color Vision Defects. GeneReviews.* Seattle, WA: University of Washington.

Diaconu, V., Sullivan, D., Bouchard, J. F., and Vucea, V. (2010). Discriminating colors through a red filter by protanopes and colour normals. *Ophthalmic Physiol. Opt.* 30, 66–75. doi: 10.1111/j.1475-1313.2009.00695.x

Franklin, A., Clifford, A., Williamson, E., and Davies, I. (2005). Color term knowledge does not affect categorical perception of color in toddlers. *J. Exp. Child Psychol.* 90, 114–141. doi: 10.1016/j.jecp.2004.10.001

Guest, S., D., and van Laar, D. (2000). The structure of colour naming space. *Vision Res.* 40, 723–734. doi: 10.1016/S0042-6989(99)00221-7

Helmholtz, H. L. F. (1852). Über die theorie der zusammengesetzten farben. *Ann. Phys.* 887, 45–66. doi: 10.1002/andp.18521630904

Hering, E. (1905). *Outline of a Theory of the Light Sense.* Cambridge: Harvard University Press .

Hurvich, L. M., and Jameson, D. (1957). An opponent process theory of color vision. *Psychol. Rev.* 64, 384–404. doi: 10.1037/h0041403

Jameson, D., and Hurvich, L. M. (1978). Dichromatic color language: 'reds' and 'greens' don't look alike but their colors do. *Sens. Process* 2, 146–155.

Kaiser, P. K., and Boynton, R. M. (1996). *Human Color Vision.* Washington, DC: Optical Society of America.

Kay, P., and MacDaniel, C. K. (1978). The linguistic significance of the meanings of basic color terms. *Language* 54, 610–646. doi: 10.1353/lan.1978.0035

Kay, P., and Regier, T. (2003). Resolving the question of color naming universals. *PNAS* 100, 9085–9089. doi: 10.1073/pnas.1532837100

le Rochelles, J., and Viénot, F. (1995). Contribution of two colour opponent mechanism to Fechner-Benham subjective colours. Colour Vision Deficiencies XIII. *Doc. Ophthalmol. Proc. Ser.* 57, 251–258. doi: 10.1007/978-94-011-0507-1_30

Lillo, J., Davies, I., Collado, J., Ponte, E., and Vitini, I. (2001). Colour narning by colour blind children. *Anu. Psicol.* 32, 5–24.

Luria, S. M. (1967). Color-name as a function of stimulus-intensity and duration. *Am. J. Psychol.* 80, 14–27. doi: 10.2307/1420537

Montag, E. D., and Boynton, R. M. (1987). Rod influence in dichromatic surface color perception. *Vision Res.* 27, 2153–2162. doi: 10.1016/0042-6989(87)90129-5

Moreira, H., Lillo, J., Alvaro, L., and Davies, I. (2014). Use of basic color terms by red-green dichromats. II. Models. *Col. Res. Appl.* 39, 372–386. doi: 10.1002/col.21802

Nagel, W. A. (1907). Neue erfahrungen über das farbensehen der dichromaten auf grossen felde. *Z. Sinnesphysiol.* 41, 319–337.

Nagy, A. L., and Boynton, R. M. (1979). Large-field color naming of dichromats with rods bleached. *J. Opt. Soc. Am. A* 69, 1259–1265. doi: 10.1364/JOSA.69.001259

Nagy, B. V., Nemeth, Z., and Abraham, G. (2008). Human wavelength identification, numerical analysis and statistical evaluation. *Periodica Polytechnica Mech. Eng.* 52, 77–81. doi: 10.3311/pp.me.2008-2.07

Nathans, J., Piantanida, T. P., Eddy, R. L., Shows, T. B., and Hogness, D. S. (1986). Molecular genetics of inherited variation in human color vision. *Science* 232, 203–210. doi: 10.1126/science.3485310

Neitz, M., and Neitz, J. (2000). Molecular genetics of color vision and color vision defects. *Arch. Ophthalmol.* 118, 691–700. doi: 10.1001/archopht.118.5.691

Paramei, G. V. (1996). Color space of normally sighted and color-deficient observers reconstructed from color naming. *Psychol. Sci.* 7, 311–317. doi: 10.1111/j.1467-9280.1996.tb00380.x

Paramei, G. V., Bimler, D. L., and Cavonius, C. R. (1998). Effect of luminance on color perception of protanopes. *Vision Res.* 38, 3397–3401. doi: 10.1016/S0042-6989(97)00454-9

Pitchford, N. J., and Mullen, K. T. (2003). The development of conceptual colour categories in pre-school children: influence of perceptual categorization. *Vis. Cogn.* 10, 51–77. doi: 10.1080/713756669

Rosch-Heider, E. R. (1972). Universals in color naming and memory. *J. Exp. Psychol.* 93, 10–20. doi: 10.1037/h0032606

Saunders, B. A. C., and van Brakel, J. (1997). Are there nontrivial constraints on colour categorization? *Behav. Brain Sci.* 20, 167–228.

Schanda, J., Morren, L., Rea, M., Rositani-Ronchi, L., and Walraven, P. (2002). Does lighting need more photopic luminous efficiency functions? *Light. Res. Technol.* 34, 1.69–1.78. doi: 10.1191/1365782802li031oa

Scheibner, H. M., and Boynton, R. M. (1968). Residual red-green discrimination in dichromats. *J. Opt. Soc. Am. A* 58, 1151–1158. doi: 10.1364/JOSA.58.001151

Smith, V. C., Pokorni, J., and Swartley, R. (1973). Continuous hue estimation of brief flashes by deuteranomlaous observers. *Am. J. Psychol.* 86, 115–131. doi: 10.2307/1421852

Stockman, A., MacLeod, D. I. A., and Johnson, N. E. (1993). Spectral sensitivities of human cones. *J. Opt. Soc. Am. A* 10, 2491–2521. doi: 10.1364/JOSAA.10.002491

Thomson, L. C., and Trezona, P. W. (1951). The variations of hue discrimination with the change of luminance level. *J. Physiol.* 114, 98–106.

Troup, L., Pitts, M., Volbrecht, V., and Nerger, J. (2005). Effect of stimulus intensity on the sizes of chromatic perceptive fields. *J. Opt. Soc. Am. A* 22, 2137–2142. doi: 10.1364/JOSAA.22.002137

Wyszecki, G., and Stiles, W. S. (2000). *Color Science: Concepts and Methods, Quantitative Data and Formulae.* New York: Wiley-Interscience Publication.

Young, T. (1802). The Bakerian lecture: on the theory of light and colours. *Philos. T. R. Soc. Lond.* 92, 12–48. doi: 10.1098/rstl.1802.0004

Conflict of Interest Statement: The authors declare that the research was conducted in the absence of any commercial or financial relationships that could be construed as a potential conflict of interest.

Received: 20 August 2014; accepted: 19 November 2014; published online: 09 December 2014.

Citation: Nagy BV, Németh Z, Samu K and Ábrahám G (2014) Variability and systematic differences in normal, protan, and deutan color naming. Front. Psychol. ***5****:1416. doi: 10.3389/fpsyg.2014.01416*

This article was submitted to Perception Science, a section of the journal Frontiers in Psychology.

frontiers in PSYCHOLOGY

HYPOTHESIS AND THEORY ARTICLE
published: 30 January 2015
doi: 10.3389/fpsyg.2015.00030

An experimental study of gender and cultural differences in hue preference

Abdulrahman S. Al-Rasheed*

Department of Psychology, King Saud University, Riyadh, Saudi Arabia

Edited by:
Marcelo F. Costa, Universidade de São Paulo, Brazil

Reviewed by:
Natalia Komarova, University of California at Irvine, USA
Gregory West, University of Montreal, Canada

***Correspondence:**
Abdulrahman S. Al-Rasheed, Department of Psychology, King Saud University, P.O. Box 2458, Riyadh 11451, Saudi Arabia
e-mail: asalrasheed@ksu.edu.sa

This paper investigates the influence of both gender and culture on color preference. Inspection of previous studies of color preference reveals that many of these studies have poor control over the colors that are shown—the chromatic co-ordinates of colors are either not noted or the illuminant that colors are shown under is not controlled. This means that conclusions about color preference are made using subjective terms for hue with little knowledge about the precise colors that were shown. However, recently, a new quantitative approach to investigating color preference has been proposed, where there is no need to summarize color preference using subjective terms for hue (Hurlbert and Ling, 2007; Ling and Hurlbert, 2007). This approach aims to quantitatively summarize hue preference in terms of weights on the two channels or "cardinal axes" underlying color vision. Here I further extend Hurlbert and Ling's (2007) approach to investigating color preference, by replicating their study but with Arabic and English participants, and to answer several questions: First, are there cultural differences in the shape of the overall preference curve for English and Arabic participants? Second, are there gender differences in the shape of the overall preference curve for English and Arabic participants? Thirty eight British and 71 Saudi Arabian (Arabic) participants were compared. Results revealed that Arabic and English preference curves were found to differ, yet there was greater similarity for Arabic and English males than Arabic and English females. There was also a sex difference that was present for both Arabic and English participants. The male curve is fairly similar for both samples: peak-preference is in the blue-green region, and a preference minimum is in the red-pink/purple region. For Arabic females the preference peak appears to be in the red-pink region, whilst for English females it is shifted toward purple/blue-green.

Keywords: color preference, hue preference, gender differences, culture differences

INTRODUCTION

Color usually evokes an aesthetic, expressed, for instance, in terms of preference for some colors over others. According to Chandler (1934), studies of color preference date back to at least 1800, addressing questions such as: do people tend to prefer the same colors; do the sexes differ in patterns of preference? Embedded in both questions, is the issue of what determines preference; to what extent is it Universal, or in contrast, to what extent is it peculiar to the individual? If there are Universal patterns, are these determined by our genes, or by common experience? If experience is important, then there could be consistent cultural differences as people from the same culture are more likely to have similar experiences than people from different cultures.

Early studies were marred by lack of control over the specification of the colors and of the illuminant they were viewed under. However, half a century ago it was established that, preferences were highest for the blue-green region and lowest for the yellow and yellow-green regions (Guilford and Smith, 1959). Moreover, the preference order reported by Eysenck (1941)—blue, red, green, purple, orange, and yellow—has generally been supported by more recent studies (see Ling et al., 2006 for a summary). Note however, the majority of these studies were conducted on Western European or American informants, and the consensus does not extend to the issue of cross-cultural variation.

GENDER DIFFERENCES IN COLOR PREFERENCE

The debate about whether gender plays a role in hue preference has raged since as long ago as 1800 (Chandler, 1934). Eysenck (1941) found gender differences only for orange and yellow, while Granger (1955) concluded from his controlled ranking study of more than 400 Munsell colors covering the entire color solid, that there was no evidence of any marked difference between the preference ranking of men and women. A child hue preference study by Zentner (2001) tested 127 Swiss preschool children (mean age = 54 months) with nine color patches (black, light blue, dark blue, brown, light green, dark green, pink, red, and yellow), and children handed the experimenter the colors in order of their preference. Results showed no significant effect of gender

on color preference. Also, studies by Child et al. (1968), Camgoz et al. (2002), Ou et al. (2003), and Rosenbloom (2006) have shown no significant gender difference in hue preference.

On the other hand, other studies report substantial gender differences, and have shown that males and females differ when it comes to their favorite colors. An early major finding was that females showed a greater preference for warm colors than males and males showed a greater preference for cool colors than females (Helson and Lansford, 1970). McManus et al. (1981) have also concluded from a controlled paired comparison task, that males and females differ significantly in their hue preference, as females showed a greater preference for red and less preference for yellow compared to males. Further evidence comes from a developmental study by Burkitt et al. (2003) who tested the color preference of 330 UK children, aged between 4 and 11 years old. Children were asked to point to their preferred color from a set of 10 colors (black, blue, brown, green, orange, pink, purple, red, white, and yellow), and continued pointing until all colors were chosen. It was found that girls significantly preferred pink, purple, and red more than boys. In contrast boys showed a greater preference than girls for black, blue, brown, green, and white. More recent work by Ling and Hurlbert (2007), tested 94 males and females from China and England, aged between 20 and 26, and they were asked as quickly as possible to choose their preferred color from each of a series of paired colored rectangles. The findings from this study showed that females prefer reddish hues and dislike greenish-yellowish hues significantly more than males. These sex differences in hue preference could be due to culture (Langenbeck, 1913). For example, Paoletti (1983, 1987, 1997) documented that sex difference in color preference is culturally influenced and noted that general acceptance of pink for girls and blue for boys was inverted since 1920 in the North American culture. Cultural color stereotypes which influence color preference are found in Eichstedt's (1997) study where the awareness of gender incongruity led 24 months old to look longer at a pink hue than blue hue when it was preceded by a male than a female voice. Sex differences in color preference could also be due to biological factors (Humphrey, 1976) or due to sex differences in the evolution of color vision (e.g., Hurlbert and Ling, 2007). This issue is returned to later on.

CULTURAL DIFFERENCES IN COLOR PREFERENCE

Colors have different meanings in different cultures. For instant, red symbolizes good luck in China, Denmark, and Argentina, while it means bad luck in Germany, Nigeria, and Chad (Schmitt, 1995; Neal et al., 2002). White is a color of happiness and purity in the USA, Australia, and New Zealand, but symbolizes death in East Asia (Ricks, 1983; Neal et al., 2002). Green represents envy in the USA and Belgium, while in Malaysia it represents danger or disease (Ricks, 1983; Hupka et al., 1997). This variation in the symbolism of color could lead to variation on color preference between cultures. Choungourian (1969) compared 148 American and Lebanese children age between 5 and 10 using eight colored stimuli (red, orange, yellow, yellow-green, green, turquoise, blue, and purple) and the eight colors were paired against each other. Color preference varied between the two samples, American children showed a significant preference for red and lack of preference for green, whereas Lebanese children showed preference for blue and lack of preference for green, and their top and bottom of preference did not differ significantly from each other.

A previous comparative adult study by Choungourian (1968) which compared 160 male and female American, Lebanese, Iranian, and Kuwaiti university students, also found cultural variation in color preference. By using the same stimuli and method, results showed variation in the over-all order of color preference across the four cultures. Saito (1994) compared Japanese, Korean, and Taipei samples. Participants were asked to select from a color chart the three colors they preferred most and the three they disliked the most and, to give their reasons for their choices. Results of these studies showed that although a high preference for white was common to all three samples, each sample had a specific preference for colors not shown by the others. Saito (1996) also expanded their study using the same stimuli and procedure but testing 175 Japanese, 158 Chinese, and 157 Indonesian participants. The finding of this study confirmed the conclusion of the previous study that culture influenced color preference. More recently, Ling et al. (2006) and Hurlbert and Ling (2007) reported that cultural factors played a role in differences in the color preference of English and Chinese participants. The Chinese sample had a stronger preference for reddish hues than the English sample, and it was argued that this variation is due to a red symbolizing good luck in the Chinese culture.

AIMS OF THE STUDY

The main aim of this study was to extend Ling and Hurlbert (2007) and Hurlbert and Ling's (2007) work, by replicating their study with Arabic participants. One aim was to investigate whether the sex difference found for English and Chinese samples would also be found in a Saudi Arabian Arab sample. If so, this would be support for sex difference in the weighting of this biological component being universal and possibly linked to evolutionary processes. In addition, the study aimed to contribute to the debate about how color preference is constrained, whilst also testing whether differential weighting of the cardinal axes of color vision could explain variation in color preference for cultures other than English and Chinese.

METHOD

PARTICIPANTS

Seventy-one native Arabic-speaking undergraduates from King Saud University in Riyadh and 38 native English-speaking undergraduates from Surrey University participated in this experiment. All their ages ranged from 18 to 29 years. For the Arabic sample, there were 32 males with a mean age of 21.35 years (SD = 1.47), and 36 females with a mean age of 20.28 years (SD = 0.54). For the English sample, there were 17 males with a mean age of 21.35 years (SD = 3.32), and 31 females with a mean age of 19.32 years (SD = 2.06). All participants had normal red-green color vision as assessed by Ishihara's Tests for Color Vision Deficiency (Ishihara, 1987). Most of the participants participated for course credit and a few volunteered. No participant was aware of the predictions of the experiment at the time of testing.

Table 1 | CIE (1931), Y,x,y co-ordinates of the eight stimuli and the hue angle and the hue labels for all the stimuli: YR, yellow-red; R, red; RP, red-pink; P, pink; BG, blue-green; G, green; GY, green-yellow.

Stimulus	Y	x	y	Hue angle	Hue label
1	28.29	0.376	0.342	1.29	YR
2	28.28	0.362	0.316	1.69	R
3	28.32	0.346	0.299	2.03	RP
4	28.29	0.295	0.278	3.01	P
5	28.32	0.264	0.332	4.42	BG
6	28.32	0.274	0.360	4.84	G
7	28.29	0.291	0.382	5.17	G
8	28.32	0.353	0.410	6.15	GY

Stimuli were constant saturation (S = 0.5) and constant lightness (L = 80).

STIMULI AND APPARATUS

As in Ling and Hurlbert (2007), there were eight stimuli that varied only in hue angle (saturation = 0.5 and lightness = 80 in CIE Lu'v' HSL space). **Table 1** shows the coordinates in CIE (1931) Y,x,y space for the eight stimuli, against the uniform gray background (Y = 50 cd/m^2, x = 0.321, y = 0.337). A Cambridge Research Instruments ColorCal was used to obtain CIE co-ordinates. The color stimuli were displayed on a calibrated 17 inch CRT Sony Trinitron monitor.

DESIGN

The stimuli were presented as pairs of rectangular patches (3 cm × 2 cm) above and below central fixation (4 cm between the two patches) on the gray background. Each possible pair was shown twice, in random order, with the position of each color reversed on the second occurrence.

PROCEDURE

The experiment was conducted in a dark room. Participants were seated at a distance of 57 cm from the monitor, at eye-level to the center of the monitor, with head restrained using a chin rest. Participants were instructed to move the cursor as quickly as possible to select their preferred color in each pair. The next pair appeared immediately after each response until the end of task. Participants were told that, there was no time limit for their responding, and not to think about possible uses of the color.

RESULTS

The number of times each hue chosen as the preferred color across all the 56 trials was calculated for each participant and the mean across participants percentage preference scores for each color are shown in **Figure 1A** which gives the hue preference curves for the Arabic and English samples. It can be seen that there appear to be differences in the preference curves for Arabic and English samples. For the Arabic sample, the preference peak is in the red-pink region, with a preference minimum in the green-yellow region. For the English sample, peak preference is in the purple/blue-green region, with a preference minimum in the yellow-red region. The preference peak differs across the two samples, but the samples share a dislike of yellowish colors.

Figures 1B,C illustrate the hue preference curves by plotting the percentage preferred, for the eight stimuli for males vs. females for each of the Arabic and English samples. **Figure 1B** gives male and female preference curves for the Arabic sample while **Figure 1C** gives male and female preference curves for the English sample. From **Figure 1**, it can be seen that there appear to be sex differences in color preference for both groups. The male curve is fairly similar for both samples: peak-preference is in the blue-green region, and a preference minimum is in the red-pink/purple region. For Arabic females the preference peak appears to be in the red-pink region, whilst for English females it is shifted toward purple/blue-green. Both Arabic and English females however, appear to dislike the green-yellow hue.

The variance of each participant's preference curve was calculated. This represents how strong the variation in preference there is across the hues tested—smaller numbers indicate less variation in preference across the spectrum than larger numbers. **Figure 2** gives the variance in preference across the spectrum for males and females, for Arabic and English samples.

A two-way analysis of variance (ANOVA) with the independent group factors of Gender (Male/female) and Culture (Arabic/English) was conducted on the variance scores to investigate differences in how much variation there is in preference across the spectrum for the different sub-groups. There was a significant difference in the amount of variation in the preference curve of Arabic (mean = 1004.54, SD = 264.91) and English (mean = 903.46, SD = 286.76) samples, $F(1,112) = 9.43$, MSE = 48563, $p < 0.005$. There was also more variation in

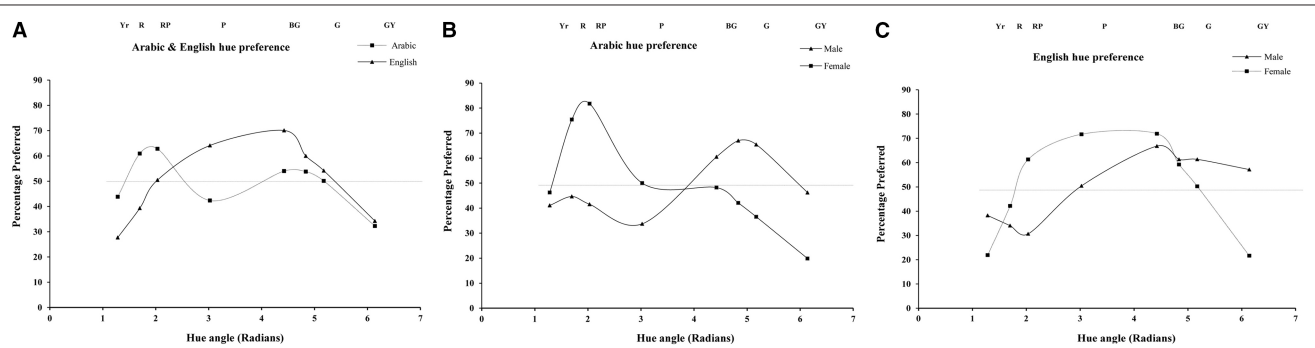

FIGURE 1 | The hue preference curve (% preferred for each stimulus) for males and females, for the Arabic and English samples. The Munsell hue labels for the stimulus range are given. The dashed line at 50% indicates no preference.

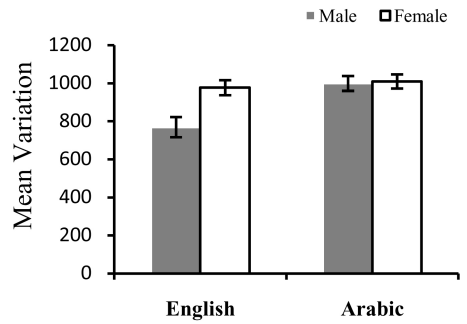

FIGURE 2 | Mean variation (±1 SE) for males and females of Arabic and English samples.

preference across the spectrum for females (mean = 994.51, SD = 201.30) than males (mean = 919.25, SD = 264.91), $F(1,112) = 6.55$, MSE = 48563, $p < 0.05$. There was also a significant interaction of Culture and Gender, $F(1,112) = 5.35$, MSE = 48563. The ANOVA was followed by independent t-tests (two-tailed) to further investigate the reason for the interaction. For English, there was a significant difference between males and females, $t(24.2) = 2.27$, $p < 0.01$, but there was no gender difference for the Arabic sample, $t(66) = 25$, $p = 0.81$.

DISCUSSION

The main aim of this study was to investigate color preference, by replicating Ling and Hurlbert (2007) and Hurlbert and Ling's (2007) study but with Arabic participants. The study aimed to answer several questions. First, are there cultural differences in the shape of the overall preference curve for English and Arabic participants? Second, does the sex difference in color preference that was previously found for English and Chinese samples extend to an Arabic sample? If so, this would be support for Hurlbert and Ling's claims that the sex difference in the weighting of this biological component is universal and possibly linked to evolutionary processes. It was hoped that addressing these questions would contribute to debates about how color preference is constrained, whilst also testing whether a model which summarizes color preference in terms of biological constructs can successfully explain variation in color preference for cultures other than English and Chinese.

DIFFERENCES IN HUE PREFERENCE ACROSS THE SPECTRUM FOR ENGLISH AND ARABIC

The results indicate that there are differences in hue preference for Arabic and English samples. Collapsing across males and females, the preference curves for the Arabic and English samples have peaks in different locations. For the Arabic sample, preference is highest for the reddish hues, whilst for the English sample, preference is highest for the blue-green region. There are also striking similarities in the preference curves of the two groups. In the green and green-yellow region, the preference ratings are almost identical for Arabic and English, with preference dropping at green-yellow. When males and females are considered separately, it becomes clear that Arabic and English males are more similar in their preference than Arabic and English females. The preference curve for Arabic and English males is highly similar, yet the shape of the curve is dissimilar for Arabic and English females. Arabic females have a strong preference peak for two of the reddish hues—other colors were either at 50% (no preference) or, in the case of greenish hues, were below 50% (an aversion to the color) on the preference scale. English females on the other hand had a preference curve that had minima at green-yellow and yellow-red, but that gradually peaked in between these hues at purple to blue-green. There therefore appears to be a cultural difference in the color preference of Arabic and English females.

The Arabic sample overall also had stronger preferences than the English sample as there was more variation in their preference curve than the English sample. The weaker variation in the preference curve for the English sample compared to the Arabic sample, was due to less variation for English males than females. Therefore, English males appear to be less strong in their hue preferences than English females, yet this sex difference is not found for the Arabic sample.

IMPLICATIONS FOR THEORIES OF COLOR PREFERENCE

The current study provides evidence for both sex differences and culturl differences in hue preference. As outlined in the introduction, there is a long history of research that has aimed to establish whether color preference varies across different groups and whether there are any universal patterns of color preference. Some of the findings of the current study appear similar to previous color preference studies. For example, McManus et al. (1981) found that females show less preference for yellow than males, and here we also find less preference for yellowish hues for females than males. However, comparisons across color preference studies that have simply summarized color preference using the subjective names for color are difficult to make as colors with the same color term can vary dramatically. The approach used in the Ling and Hurlbert studies summarizes color preference in terms of how stimulus-background cone-contrast is weighted summarizing color preference quantitatively rather than using subjective color names. Hurlbert and Ling (2007) and Ling and Hurlbert (2007) argue that this approach is better as color preference is identified in terms of biologically meaningful constructs (the cone-opponent mechanisms) whilst also quantifying how well these biological components account for variation in preference. They argue that this method enables comparisons across groups (such as by sex and culture) to be made efficiently with reference to the underlying mechanisms of preference. Here it is shown that their approach can be extended to other cultures and we show that Arabic color preference can also be identified in terms of the cone-opponent mechanisms and comparisons between Arabic and English can be made by comparing the weights on these mechanisms.

The findings have implications for theories on color preference. Some have argued that there is a universal order of color preference (e.g., Eysenck, 1941) and others have argued for universal sex differences in color preference (e.g., Ling and Hurlbert (2007)). However, the findings of the current study suggest that color preference varies with both sex and culture and that sex differences in color preference also vary culturally.

Studies of color preference need to move away from simply summarizing, quantifying and comparing color preference across cultures, sexes and ages and start to consider the factors that lead to variation. The extent to which color preferences driven by interactions with the chromatic environment, such as colors being associated with positive or negative objects, also needs to be established. For now, the strongest contribution from the current study to the literature on color preference, is that Hurlbert and Ling (2007) and Ling et al.'s (2007) suggestion that there are evolutionarily driven universal sex differences in the weighting of L-M for color preference is not supported.

CONCLUSION

The current study considered whether there is cultural variation between Arabic and English in color preference. The study used Ling and Hurlbert (2007) and Hurlbert and Ling's (2007) approach which summarizes color preference in terms of weights on the two cone-opponent processes. A substantial amount of variation in color preference color be explained for both Arabic and English speakers using this approach. Arabic and English preference curves were found to differ, yet there was greater similarity for Arabic and English males than Arabic and English females. There was also a sex difference that was present for both Arabic and English participants. Support for Ling and Hurlbert (2007) and Hurlbert and Ling's (2007) claim for a universal sex difference, meaning that females universally prefer hues redder than the background, was not provided by the findings.

ACKNOWLEDGMENTS

The authors extend their appreciation to the College of Education Research Centre at King Saud University, Riyadh, for supporting this work.

REFERENCES

Burkitt, E., Barrett, M., and Davis, A. (2003). Children's color choices for completing drawings of affectively characterized topics. *J. Child Psychol. Psychiatry* 44, 445–455. doi: 10.1111/1469-7610.00134

Camgoz, N., Yener, C., and Guvenc, D. (2002). Effect of hue, saturation, and brightness on preference. *Color Res. Appl.* 27, 199–207. doi: 10.1002/col.10051

Chandler, A. R. (1934). *Beauty and Human Nature*. New York: Appleton–Century-Crofts.

Child, I. L., Hansen, J. A., and Hornbeck, F. W. (1968). Age and sex differences in children's color preference. *Child Dev.* 39, 237–247. doi: 10.2307/1127374

Choungourian, A. (1968). Color preference and cultural variation. *Percept. Mot. Skills* 26, 1203–1206. doi: 10.2466/pms.1968.26.3c.1203

Choungourian, A. (1969). Color preference: a cross-cultural and cross-sectional study. *Percept. Mot. Skills* 28, 801–802. doi: 10.2466/pms.1969.28.3.801

Eichstedt, J. A. (1997). *Infants' Metaphorical Knowledge About Gender*. Ph.D. thesis, Concordia University, Montreal, Quebec.

Eysenck, H. (1941). A critical and experimental study of colour preference. *Am. J. Psychol.* 54, 385–391. doi: 10.2307/1417683

Granger, G. W. (1955). An experimental study of color preference. *J. Gen. Psychol.* 52, 3–20. doi: 10.1080/00221309.1955.9918340

Guilford, J. P., and Smith, P. C. (1959). A system of color preference. *Am. J. Psychol.* 72, 487–502. doi: 10.2307/1419491

Helson, H., and Lansford, T. (1970). The role of spectral of energy of source and background color in the pleasantness of object colors. *Appl. Opt.* 9, 1513–1562. doi: 10.1364/AO.9.001513

Humphrey, N. K. (1976). "The colour currency of nature," in *Colour for Architecture*, eds T. Porter and B. Mikellides (London: Studio Vista), 95–98.

Hupka, R. B., Zaleski, Z., Otto, J., Reidl, L., and Tarabrina, N. V. (1997). The colors of anger, envy, fear, and jealousy: a cross-cultural study. *J. Cross Cult. Psychol.* 28, 156–171. doi: 10.1177/0022022197282002

Hurlbert, A., and Ling, Y. (2007). Biological components of sex differences in color preference. *Curr. Biol.* 17, R623–R625. doi: 10.1016/j.cub.2007.06.022

Ishihara, S. M. (1987). *Ishihara's Tests for Colour-Blindness*. Tokyo: Kanehara & Co.

Langenbeck, K. (1913). Die akustische-chromatischen Synopsien. *Z. Sinnephysiol.* 47, 159–181.

Ling, Y. and Hurlbert, A. (2007). "A new model for color preference: universality and individuality," in *Proceeding of the 15th Color Imaging Conference* (Albuquerque, NM: Society for Imaging Science and Technology), 8–11.

Ling, Y., Hurlbert, A., and Robinson, L. (2006). "Sex differences in colour preference," in *Progress in Colour Studies 2: Cognition*, eds N. J. Pitchford and C. P. Biggam (Amsterdam: John Benjamins).

McManus, I. C., Jones, A. L., and Cottrell, J. (1981). The aesthetics of color. *Perception* 10, 651–666. doi: 10.1068/p100651

Neal, C. M., Quester, P. G., and Hawkins, D. I. (2002). *Consumer Behaviour: Implications for Marketing Strategy*. 3rd Edn. Roseville, NSW: McCraw-Hill.

Ou, L. C., Luo, M. R., Woodcock, A., and Wright, A. (2003). A study of colour emotion and colour preference Part1: colour emotion for single colours. *Color Res. Appl.* 29, 232–240. doi: 10.1002/col.20010

Paoletti, J. B. (1983). Clothes make the boy, 1860–1920. *Dress* 9, 16–20. doi: 10.1179/036121183803657763

Paoletti, J. B. (1987). Clothing and gender in America: children's fashions, 1890–1920. *Signs* 13, 136–143. doi: 10.1086/494390

Paoletti, J. B. (1997). "The gendering of infants' and toddlers' clothing in America," in *The Material Culture of Gender/The Gender of Material Culture*, eds K. A. Martinez and K. L. Ames (Hanover, NH: University Press of New England), 27–35.

Ricks, D. A. (1983). *Big Business Blunders: Mistakes in Multinational Marketing*. Homewood, IL: Dow Jones-Irwin.

Rosenbloom, T. (2006). Color Preference of High and Low Sensation Seekers. *Creativity Res. J.* 18, 229–235. doi: 10.1207/s15326934crj1802_8

Saito, M. (1994). A cross-cultural study on color preference in three Asian cities: Comparison between Tokyo, Taipei and Tianjin. *Jpn. Psychol. Res.* 36, 219–232.

Saito, M. (1996). A comparative study of color preference in Japan, China and Indonesia, with emphasis on the preference for white. *Percept. Mot. Skills* 83, 115–128.

Schmitt, B. H. (1995). Language and visual imagery: issues in corporate identities in East Asia. *Columbia J. world Bus.* 30, 28–36.

Zentner, M. R. (2001). Preferences for colors and color-emotion combination in early childhood. *Dev. Sci.* 4, 389–398. doi: 10.1111/1467-7687.00180

Conflict of Interest Statement: The author declares that the research was conducted in the absence of any commercial or financial relationships that could be construed as a potential conflict of interest.

Received: 11 August 2014; accepted: 07 January 2015; published online: 30 January 2015.

Citation: Al-Rasheed AS (2015) An experimental study of gender and cultural differences in hue preference. Front. Psychol. ***6****:30. doi: 10.3389/fpsyg.2015.00030*

This article was submitted to Perception Science, a section of the journal Frontiers in Psychology.

Advantages of publishing in Frontiers

OPEN ACCESS
Articles are free to read, for greatest visibility

COLLABORATIVE PEER-REVIEW
Designed to be rigorous – yet also collaborative, fair and constructive

FAST PUBLICATION
Average 85 days from submission to publication (across all journals)

COPYRIGHT TO AUTHORS
No limit to article distribution and re-use

TRANSPARENT
Editors and reviewers acknowledged by name on published articles

SUPPORT
By our Swiss-based editorial team

IMPACT METRICS
Advanced metrics track your article's impact

GLOBAL SPREAD
5'100'000+ monthly article views and downloads

LOOP RESEARCH NETWORK
Our network increases readership for your article

Frontiers
EPFL Innovation Park, Building I • 1015 Lausanne • Switzerland
Tel +41 21 510 17 00 • Fax +41 21 510 17 01 • info@frontiersin.org
www.frontiersin.org

Find us on